CHEMICAL TRANSFORMATION OF SHORT CHAIN SATURATED CARBOXYLIC ACIDS UNDER UV IRRADIATION IN AQUEOUS SOLUTIONS

by

Gonca F. Talu

A dissertation submitted to the Graduate Faculty in Civil Engineering in partial fulfillment of the requirements for the degree of Doctor of Philosophy, The City University of New York.

2003

UMI Number: 3103177

ProQuest Information and Learning Company
300 North Zeeb Road
P.O. Box 1346
Ann Arbor, MI 48106-1346

This manuscript has been read and has been accepted by the Graduate Faculty in Civil Engineering in satisfaction of the dissertation requirements for the degree of Doctor of Philosophy.

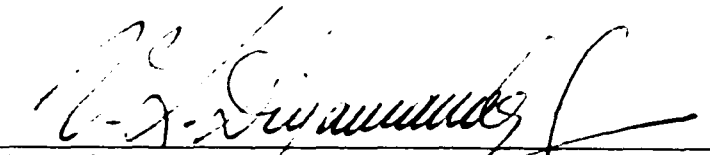

September 10, 2003
Date

Chair of Examining Committee: Prof. Vasil Diyamandoglu.
Department of Civil Engineering. The City College of The City University of New York

September 10, 2003
Date

Executive Officer: Prof. Mumtaz K. Kassir.
School of Engineering. The City College of The City University of New York

Prof. John Fillos	Department of Civil Engineering. The City College of The City University of New York
Prof. Reza Khanbilvardi	Department of Civil Engineering. The City College of The City University of New York
Prof. Haralambos V. Vasiliadis	Department of Civil Engineering. The City College of The City University of New York
Prof. Urs Jans	Department of Chemistry. The City College of The City University of New York

Supervisory Committee

ABSTRACT

Chemical Transformation of Short Chain Saturated Carboxylic Acids under UV Irradiation in Aqueous Solutions

by

Gonca F. Talu

Advisor: Vasil Diyamandoglu

Low molecular weight carboxylic acids are likely to be encountered in water supplies, and decompose during disinfection of water with UV irradiation. The photodecomposition kinetics of five short chain saturated carboxylic acids (formic, oxalic, glycolic, glyoxalic and pyruvic acids) and some selected mixtures have been studied under UV irradiation at 253.7 nm. The irradiation experiments were performed in a 5-L glass reactor equipped with eight low-pressure quartz immersion lamps. The effects of UV light intensity (I_a) (1.38×10^{-6} to 5.27×10^{-6} E/Ls), temperature (T) (15-35°C), initial concentration (C_0) (0.2 – 5.2 mg C/L), initial pH (pH_0) (5.0 - 9.0) and alkalinity (0 – 50 mgL^{-1} $NaHCO_3$ as $CaCO_3$) on the photodecomposition of acid solutions were investigated. Total carbon (TC) and non-purgable organic carbon (NPOC) profiles were also determined during some of the photodecomposition experiments to quantify the dissolved organic carbon remaining in solution. All studied acids decayed following split rate reaction. Formate and oxalate readily decayed at different rates without any observed intermediates while they were both consistent intermediates of glyoxalate decomposition. Glycolate irradiation produced glyoxalate that further decayed to form formate and

oxalate during the decomposition reaction. Glycolate and oxalate were observed as product of pyruvate along with two unidentified anionic reaction products. Oxalate was the common intermediate product of decomposition of glyoxalate, glycolate and pyruvate and decayed after the decay of all other observed intermediates. Formate, glyoxalate and glycolate decay followed pseudo-zero order kinetics while pseudo-first order kinetic was observed for oxalate and pyruvate decay. NPOC and TC data revealed that all carbon in formate and oxalate is eventually converted to CO_2, while decay of either glyoxalate, glycolate and pyruvate may result in the formation of volatile products. Dissolved oxygen (DO) utilization during the decay of single solutes in deionized water were found to be 0.5 mol of O_2/mol formate, (0.8 - 0.3) mol of O_2/mol oxalate, 0.6 mol O_2/mol glyoxalate, 1.1 mol O_2/mol glycolate and 1.4 mol O_2/mol pyruvate. The reaction pH profile for formate and oxalate photodecomposition without prior pH_0 adjustment was predicted using closed system equilibrium analysis. The kinetic data clearly showed time dependent variation in the composition of the irradiated water. It is, therefore, to be expected that the disinfection by-product formation potential (DBPFP) of any water subjected to UV irradiation will be a function of the combined effect of absorbed photon flux and the process contact time.

ACKNOWLEDGEMENTS

This thesis would not have been completed without the help and support of several people. First I would like to thank my advisor, Dr. Vasil Diyamandoglu for not only supporting and guiding me through this study but also for being patient with me through all the times of frustration and uncertainty. I am grateful to him for all his help and encouragement.

I am very thankful to Dr. John Fillos for his concern in my educational development and his valuable suggestions throughout my graduate studies.

I would like to express great thanks to Dr. Frieda Orshausky, the manager of the Environmental Engineering Laboratory, whose vast laboratory experience was extremely important in many aspects of my experimental studies.

I would like to thank Dr. Urs Jans, Dr. Reza Khanbilvardi and Dr. Vasiliadis Haralambos for their valuable comments and input to the final manuscript as members of my thesis committee.

I thank the Graduate Center of the City University of New York and the Department of Civil Engineering at City College for the financial support provided to me as a four-year fellowship that provided me with the freedom necessary for creative work.

I am indebted to my family, my father İlyas Coşkun, my mother Gürsel Coşkun, my sister Gül Yağlıoğlu and my brother Osman Coşkun for their love, endless support and encouragements.

I am grateful to my husband İlkay Talu. I would not have been able to complete this study without his love, patience and support. He also took over many of my duties at home and encouraged me to finish this study. My son, Mert, was my sunshine during the last two years of my graduate studies. He helped me forget the difficulties I had to face and motivated me to complete my studies rapidly.

TABLE OF CONTENTS

LIST OF TABLES

Page No.

Page No.

Page No.

Page No.

Page No.

Page No.

Page No.

Page No.

LIST OF FIGURES

Page No.

Page No.

Page No.

Page No.

Page No.

Page No.

CHAPTER 1

INTRODUCTION

UV irradiation (253.7 nm) is a viable primary disinfection process, as evidenced by its effectiveness to deactivate *Cryptosporidium* and *Giardia* (Clancy et al., 2000). It induces formation of photoproducts in cellular DNA which often remain damaged, thus altering DNA replication and gene expression and resulting in lower cell survival (Bolton, 2000). As UV irradiation at 253.7 nm is selected by utilities as the "primary disinfection" process of choice in place of ozonation, it is imperative to develop extensive understanding of all photo-chemical transformations that could occur to organic and inorganic constituents commonly encountered in raw potable water supplies during UV irradiation, as they would impact on the disinfection by-products (DBP) formation potential of the radiated water following free or combined chlorination as the "secondary" or residual providing disinfection process.

Most surface water supplies contain aqueous organic constituents that are derived from either natural or man-made sources. Fulvic, humic and amino acids, carbohydrates and carboxylic acids are part of NOM (natural organic matter) that is found in natural raw water supplies and constitute precursors to DBP formation.

Carboxylic acids occur abundantly in surface waters as shown in Table 1.1.

Table 1.1. Typical Concentrations of Carboxylic Acids in Natural Waters in the United States (AWWARF, 1991)

Carboxylic Acids	Typical Level in River Water (mg C/L)	Typical Level in Groundwater (mg C/L)
Nonvolatile Fatty Acids	50-500	5-50
Volatile Fatty acids	100	50
Hydroxy Acids	50	NA
Dicarboxylic Acids	3-100	NA
Aromatic Acids	3-100	NA

NA: Not available

Glyoxalate and pyruvate were observed as part of low molecular weight (LMW) carbon compounds formed during irradiation of dissolved organic matter (DOM) in natural waters (Miller, 1994). Bertilsson and Tranvik (2000) under simulated solar UV irradiation of lake waters identified formic, acetic, malonic and oxalic acids (42.2 ± 11.4, 28.1 ± 19.4, 14.1 ± 6.6 and 15.6 ± 11.7 % of total identified carboxylic acids, respectively) as process products with a combined production rate of four compounds ranging between 0.5 to 158.5 μg C $L^{-1}h^{-1}$.

Miller et al. (1963) and Fogg and Horne (1968) (cited by Hosmani et al. (1999)) showed that glycolic acid was liberated as a major component of the excreted carbon in natural environments during algal blooms. Hosmani et al. (1999) studied the biochemical aspects of water pollution based on the analysis of glycolic acid, chlorophylis, phycobiliproteins and total dissolved solids in twenty lakes around

Mysore City, India. The reported glycolic acid concentrations in some of these lakes are given in Table 1.2.

Table 1.2. Glycolic Acid Concentrations in Some Lakes around Mysore City (Hosmani et al. (1999))

Name of Lake	Glycolic Acid Concentration (mg C/L)
Chakanakere	41.03
Chikkakere	63.12
Dalvoikere	100.99
Devikere	78.9
Goblikere	220.92
Karakanakere	126.24
Kadlegerekere	22.09
Lingambudikere	113.62

In addition to natural occurrence in source waters, carboxylic acids along with aldehydes are reported as the largest portion of major ozonation by products (Glaze and Weinberg (1993)). Short chain carboxylic acids are produced from organic compounds during ozonation and they are identified as "refractory" compounds due to their resistance to further oxidation by ozone. Acetic acid, oxalic acid and glyoxalic acid are reported as major end products of ozonation of organic compounds (Krasnov et al. (1974), Hoigné and Bader (1983)) and it is reported that hydroxyl radicals ($OH^{\bullet}$) must be used to oxidize these compounds (Hoigné and Bader (1983)). Glyoxalic acid was reported to be mutagenic to *Salmonella typhimurium* Strains TA98 and TA100 (Sayato, Nakamuro and Ueno (1989)).

Carboxylic acids are also reported as important chemical constituents in the troposphere and have been detected in ambient air, precipitation and cloud water (Talbot et al. 1992, Kumar et al. 1993, Li and Winchester 1993, Sempéré and Kawamura 1994, Khwaja 1995, Souza et al. 1999, Baboukas et al. 2000). Baboukas et al. (2000) measured the concentrations of acetic, formic, pyruvic and oxalic acids both in gas and particulate phases in the marine boundary layer over the Atlantic Ocean in October/November, 1996. The average gas phase concentrations were reported as 291.2 ± 151.9, 448.7 ± 182.1, 1.1 ± 1.0 and 6.1 ± 5.4 parts per trillion by volume (pptv) for acetic, formic, pyruvic and oxalic acids, respectively. The same authors reported aerosol concentrations for acetate, formate, pyruvate and oxalate as 69.7 ± 47.5, 32.5 ± 39.4, 1.0 ± 1.0 and 5.1 ± 3.7 pptv, respectively. Souza et al. (1999) measured low molecular weight carboxylic acids in atmospheric gas and particulate-phase in São Paulo City, Brazil during July 1996. They determined oxalic, pyruvic, β–hydroxy-butyric and glycolic acids as 36.2 ± 21.4%, 15.0 ± 7.9%, 9.15 ± 9.00% and 3.55 ± 2.26%, respectively in aerosol particles, and formic and acetic acids in both gaseous (4.36 ± 2.70 and 3.66 ± 2.63 ppbv, respectively) and particulate phases (17.8 ± 12.4 and 18.2 ± 9.8 %, respectively). Sempéré and Kawamura (1994) in nine wet precipitation (snow, sleet and rain) and four aerosol samples they collected in Tokyo, detected a homologous series of dicarboxylic acids (C2-C9) in both wet precipitation (12-540 mg/L) and aerosol (1.1-3.0 mg/m^3) samples. Oxalic acid constituted 34 ± 8% of the total dicarboxylic acids in wet precipitation and 51 ± 5% of the total dicarboxylic acids in aerosol samples. Sakugawa et al. (1993) determined H_2O_2 (4.4 mM), aldehydes (3.9 mM) and

combined formic and acetic acid concentration of 16.5 mM in rainwater samples collected in Los Angeles during 1985-1991.

Li et al. (1996) reported that UV irradiation (253.7 nm) lowered TOC in aqueous solutions of humic acid (HA) (0.2-2.0%) isolated from hard coal, at pH = 6.5 – 7.0. Observed changes in the absorption maxima, loss of true HA color and stable TOC levels at long contact time were attributed to changes in the chromophore structures of HA. Decarboxylation was considered the major HA decomposition mechanism and most of the organic matter (including -COOH and $-COO^-$ groups) was oxidized to CO_2 and H_2O. Chlorination of irradiated HA solution showed that THMs increased with increasing irradiation time until 30 min then it decreased. They concluded that THM precursors decomposed and formed other compounds that were not precursors at longer irradiation times.

Kusakabe et al. (1990) reported formation and decay of formic and oxalic acids, and slow formation of acetic acid during O_3 and O_3/UV (253.7 nm) of commercial HA (TOC = 100 mg/L) in aqueous solutions buffered at pH of 6.9. As TOC decayed during application of both O_3 and O_3/UV, oxalic acid, which formed as a major product with acetic and formic acids, decayed very slowly during O_3, but rapidly decayed during O_3/UV process. Furthermore, UV irradiation increased the decay rate of DOC at least by one order of magnitude when compared with O_3 alone. Post chlorination did not result in any increase in the THM formation potential observed

during O_3/UV treatment when compared to O_3, while chloroform and organic chloride concentrations for the O_3/UV system were lower than those in O_3.

Degradation of organics in water has been studied under UV/H_2O_2 or O_3/H_2O_2. Although a number of studies have been reported on the inactivation of pathogens by UV irradiation, there is limited information on the impact of UV (253.7 nm) on organic acids encountered in natural waters. This study focused on the photodecomposition kinetics of selected saturated carboxylic acids by UV irradiation only at 253.7 nm in aqueous solutions.

1.1. Research Objectives

(i) Determine photodecomposition kinetics and reaction products of formic, oxalic, glyoxalic, glycolic, pyruvic acids and selected acid mixtures under UV irradiation.

(ii) Investigate effects of temperature, initial concentration of acids, initial pH and light intensity, and DO on the kinetics of photodecomposition.

CHAPTER 2

PHOTODECOMPOSITION OF FORMIC, OXALIC, GLYOXALIC, GLYCOLIC AND PYRUVIC ACIDS

2.1. Physicochemical Properties of Organic Acids

Selected properties of formic, oxalic, glyoxalic, glycolic and pyruvic acids are given in Table 2.1.1 (Buckingham and Donaghy, 1982; Heilbron and Bunbury, 1953).

Table 2.1.1. Physicochemical Properties of Organic Acids

Properties	Formic Acid*	Oxalic Acid*	Glyoxalic Acid*	Glycolic Acid*	Pyruvic Acid**
Structure	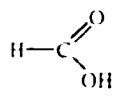	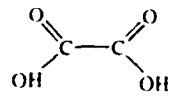	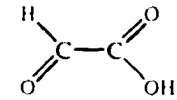	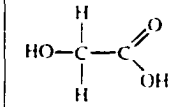	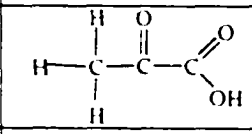
Molecular Weight	46	90	74	76	88
Melting Point (°C)	8.4	101.5	98	80	13.6
Boiling Point (°C)	100.5	Decomposes	Decomposes	Decomposes	165
pK_a (25 °)	3.62	pKa_1=1.27 pKa_2=4.28	3.32	3.82	2.49
Molar Absorption Coefficient (ε) at 253.7 nm ($M^{-1}cm^{-1}$) *** (pH)	0.3 (6.09-6.92)	25.1 (5.95-6.58)	2.7 (2.36-3.60)	0.3 (2.60-3.76)	80.7 (5.80-6.31)

* Buckingham and Donaghy, 1982.
** Heilbron and Bunbury, 1953.
*** Molar absorption coefficients were determined using UV-vis spectrophotometer.

2.2. Principles of Photochemistry

Photochemistry involves chemical reactions initiated by light. There are two basic laws of photochemistry: Grotthuss-Draper Law and Stark-Einstein Law (Coyle, 1986). Grotthuss-Draper Law states that *only the light absorbed by a molecule can be effective in bringing about chemical change*. Stark-Einstein Law's re-statement in current terminology is that *the primary photochemical act involves absorption of just one photon by a molecule*. Thus, a photochemical reaction is initiated by the absorption of a photon resulting in an electronically excited state, which then initiates the subsequent photochemical reaction steps. In the ground state, the pairs of electrons occupy the lowest energy orbital and the molecule has the lowest possible energy. The overall molecular energy is higher than the ground state in an electronically exited state and one electron occupies a higher-energy orbital, rather than the lowest–energy orbital available to it. The electronically exited state has a finite lifetime and it differs from ground state (Coyle, 1986), in that the former (a) has more energy than the ground state so it is more reactive on thermodynamic basis, (b) has very different electron distributions then the ground state which affects observed chemical changes, and (c) it is a better electron donor and a better electron acceptor than its corresponding ground state.

Light is quantized, emitted, transmitted and absorbed in discrete units, photons or quanta (Coyle, 1986). The energy (E) of a photon or quantum (the unit of light on a molecular level) is given as,

$$E = h\nu = \frac{hc}{\lambda} \qquad (2.2.1)$$

where, E is the energy of a photon (J), h is Planck's constant (6.63×10^{-34} Js), ν is the frequency of the absorbed light (s^{-1}), c is the speed of light (2.998×10^{8} ms^{-1}) and λ is the wavelength of the absorbed light (m).

Table 2.2.1 shows typical energies of some important bonds in organic molecules and approximate wavelength of light corresponding to this energy (calculated from Equation 2.2.1) (Schwarzenbach et al., 1993). If the energy of UV light is the same order of magnitude as the energy of a covalent bond, this bond could be broken as a result of light absorption. Thus, the possibility of the photochemical reaction(s) taking place depends on the likelihood of the compounds absorbing light at a given wavelength and the reactivity of the excited species. Although double bonds require more energy than the single bonds listed, the energy required to break a single bond in the carbonyl group is actually much smaller than that of a single bond, thus rendering the carbonyl group photochemically more reactive.

Table 2.2.1.Typical Energies of Some Important Bonds in Organic Molecules and Approximate Wavelength of Light Corresponding to This Energy (Schwarzenbach et al., 1993).

Bond Type	Energy (kJ mol^{-1})	Wavelength (nm)*
C-C	348	344
C-O	360	332
C-H	415	288
H-O	465	257
C=O (for aldehydes)	737	162
C=O (for ketones)	750	160

* Calculated from equation 2.1

The Beer-Lambert Law represents absorption properties at a certain wavelength (Coyle, 1986):

$$\log(I_0/I) = D = \varepsilon C d \qquad (2.2.2)$$

where, I_0 is the incident light intensity, I is the transmitted light intensity, D is the absorbance, d is the path-length of the radiation through the sample (cm) and C is the concentration of the compound (mol L^{-1}), ε is the molar absorption coefficient (L mol^{-1} cm^{-1}). This law is empirical and is not valid for very high intensities of radiation.

2.3. Photodecomposition of Aqueous Organic Acid Solutions

Earlier investigators proposed that decomposition of formic acid proceeded via intramoleculer rearrangements (Equations 2.3.1 and 2.3.2), which produce CO, CO_2, H_2 and H_2O (Ramsperger and Porter (1926)).

$$HCOOH + h\nu \rightarrow H_2 + CO_2 \quad (36\%) \qquad (2.3.1)$$

$$HCOOH + h\nu \rightarrow H_2O + CO \quad (64\%) \qquad (2.3.2)$$

Subsequent research revealed the direct photolysis, mercury photosensitization and γ-radiolysis of formic acid and aqueous formic acid solutions by formation of free radicals (Smithies and Hart (1960), Gorden and Ausloos (1961), Neta et al. (1969)). During radiolysis, reactive species (e_{aq}^-, $OH^\bullet$, H, H_2 and H_2O_2) are formed as a result of radiolysis of water, and these species decompose formic acid. Smithies and Hart (1960) studied the radiation chemistry of formic acid solutions by Co^{60} γ-rays. They also reported

photochemical decomposition results of formic acid solutions at wavelengths of 186.0, 253.7 and 266.9 nm. The reaction products were reported as CO_2, CO and H_2 for both radiolysis and photochemical decomposition of formic acid solution. The authors determined the effect of intensity, concentration and wavelength on the product yield during photochemical decomposition. At 186.0 nm and high intensity (1×10^{-22} E L^{-1} min^{-1}) CO_2 was the major product with the quantum yield of 1.0. At lower intensities (0.0032×10^{-20} – 0.0268×10^{-20} E L^{-1} min^{-1}) and wavelength of 253.7 and 266.9 the quantum yield for CO_2 became ≥2. Also, CO yield was reported as dependent on wavelength and formic acid concentration. Shorter wavelengths and higher formic acid concentrations yielded higher CO yields. At 0.0002 M formic acid concentration CO was not reported as decomposition product. H_2 was reported as minor product and its yield was increased with decreasing formic acid concentration.

Gorden and Ausloos (1961) investigated vapor-phase photolysis of formic acid at 30°C to establish the importance of free radical production. They performed direct photolysis experiments and $Hg(^3P_1)$ sensitized experiments, and used oxygen and ethylene as free radical scavengers. The measured products were H_2, CO and CO_2 as Smithies and Hart (1960) reported. They observed that these scavengers reduced H_2 yield in direct photolysis, while slightly affected the CO yield. In the case of $Hg(^3P_1)$ sensitized decomposition they obtained strong reduction in H_2 and CO yields by O_2. They concluded that in contrast to earlier investigations (Ramsperger and Porter (1926)), radical producing primary processes must also be considered. They showed that in direct photolysis of formic acid the most important free radical producing process is:

$$HCOOH \xrightarrow{h\nu} HCO + OH^{\bullet} \qquad (2.3.3)$$

Neta et al. (1969) investigated the transient absorption spectra due to radicals formed during pulse radiolysis of some aliphatic acids, including formic acid in aqueous solutions. The radicals were produced by reactions of H atoms and $OH^{\bullet}$ with carboxylic acids and/or their ions (Equations 2.3.4 and 2.3.5).

$$R_2CHCOOH + OH^{\bullet} \rightarrow R_2C^{\bullet}COOH + H_2O \qquad (2.3.4)$$

$$R_2CHCOOH + H \rightarrow R_2C^{\bullet}COOH + H_2 \qquad (2.3.5)$$

They carried out the experiments in N_2O-saturated (1 atm) solutions in order to convert all e_{aq}^- into $OH^{\bullet}$ (Equation 2.3.6).

$$e_{aq}^- + N_2O \rightarrow N_2 + OH^- + OH^{\bullet} \qquad (2.3.6)$$

For low pH, experiments were carried out under conditions that all e_{aq}^- reacted with H_3O^+ and produce H atoms (Equation 2.3.7).

$$e_{aq}^- + H_3O^+ \rightarrow H_2O + H \qquad (2.3.7)$$

For solutions containing $\{HCOO^- + N_2O\}$ or $\{HCOO^- + CO_2\}$, Neta et al. (1969) obtained the same absorption spectra (the maximum absorption at 235 nm with the extinction coefficient $\varepsilon_{235} = 3000\ M^{-1}\ cm^{-1}$) and decay rates of transients in the pH range

of 3 and 13. They concluded that this result shows the equivalence of the carboxyl radical formed by reactions with $OH^{\bullet}$ or e_{aq}^- (Equations 2.3.8 and 2.3.9).

$$HCOO^- + OH^{\bullet} \rightarrow {}^{\bullet}COO^- + H_2O \quad (2.3.8)$$

$$CO_2 + e_{aq}^- \rightarrow {}^{\bullet}COO^- \quad (2.3.9)$$

Ogata et al. (1981) observed formic (HCO_2H), glycolic ($HOCH_2CO_2H$) and tartaric acids (trace) as well as methane and CO_2 as products during photo-oxidation of acetic acid solution with hydrogen peroxide. They showed that glycolic acid and formic acid were oxidized more readily than acetic acid. Glycolic acid yielded glyoxalic acid ($HCOCO_2H$) as the hydrated form that further formed formic acid and CO_2 reacting with H_2O_2 in the dark. Formic acid also decomposed to CO_2 and H_2O under UV irradiation in the presence of H_2O_2. The proposed mechanism for decomposition of glycolic acid and formic acid are given by the following reactions:

$$H_2O_2 + h\nu \rightarrow 2HO^{\bullet} \quad (2.3.10)$$

$$HO^{\bullet} + H_2O_2 \rightarrow HOO^{\bullet} + H_2O \quad (2.3.11)$$

$$HOO^{\bullet} + H_2O_2 \rightarrow HO^{\bullet} + H_2O + O_2 \quad (2.3.12)$$

$$2HOO^{\bullet} \rightarrow H_2O_2 + O_2 \quad (2.3.13)$$

$$HOCH_2CO_2H + HO^{\bullet} \rightarrow HOC^{\bullet}HCO_2H + H_2O \quad (2.3.14)$$

$$HOC^{\bullet}HCO_2H + HO^{\bullet} \rightarrow (HO)_2CHCO_2H \quad (2.3.15a)$$

$$2HOC^{\bullet}HCO_2H \rightarrow HO_2CCH(OH)CH(OH)CO_2H \quad (2.3.15b)$$

$$(HO)_2CHCO_2H \rightarrow HCOCO_2H + H_2O \quad (2.3.16)$$

$$HCOCO_2H + H_2O_2 \xrightarrow{dark} HCO_2H + CO_2 + H_2O \quad (2.3.17)$$

$$HCO_2H + 2HO^{\bullet} \rightarrow CO_2 + 2H_2O \quad (2.3.18)$$

Yamamato and Back (1985) studied UV photolysis of oxalic acid in the gas phase at wavelengths from 257 to 313 nm and at pressures between 0.1 and 8 torr. All experiments were carried out at 115°C. CO_2, CO, H_2O and HCOOH were the observed products of the UV photolysis of oxalic acid. Formations of all products were linear in time. The ratios of CO_2/CO, H_2O/CO and $HCOOH/CO_2$ during photolysis were independent of reaction time, pressure and wavelength and were reported as 3.6 ± 0.5, ~1 and ~0.5, respectively. They same authors also studied $Hg(^3P_1)$-photosensitized decomposition and infrared multiphoton decomposition of oxalic acid vapor, and they observed the same products as they observed during UV photolysis. They concluded that during UV and infrared radiation, there were two primary processes:

$$C_2O_4H_2 \rightarrow CO_2 + HCOOH \qquad (2.3.19)$$

$$C_2O_4H_2 \rightarrow CO_2 + CO + H_2O \qquad (2.3.20)$$

with the yield of the first being 2.6 times higher than the second.

Since short chain carboxylic acids are resistant to ozonation, other oxidation processes are considered for removal of these acids from water. Processes based on hydroxyl radical ($OH^{\bullet}$) formation are commonly applied in such cases. Ikemizu et al. (1987) used O_3/UV (254 nm) system to remove organic refractory compounds that included acetic acid and oxalic acid from water. They observed $10\text{-}10^4$ times faster initial decomposition rates for organic compounds with the O_3/UV system over ozonation. During decomposition of acetic acid with O_3/UV system in the pH range of 5-8, they observed

oxalic acid as the major product. They investigated the effect of initial concentration on initial decomposition rate for acetic and oxalic acids at different pH values. Initial acid concentration increased both acetic and oxalic acid decomposition rates linearly in both O_3/UV system and ozonation. Decomposition rates increased with increasing pH for both acids in O_3/UV system. They also showed that the initial decomposition rate was dependent on the degree of dissociation and concluded that only second-stage dissociated ions reacted with $OH^{\bullet}$. This result was attributed to the decrease of nucleophilicity of reactive sites by the attraction of electrons of carboxylate group towards the undissociated carboxyl group and/or intramolecular hydrogen bonding, which reduces reactivity of partially dissociated oxalic acid.

Zuo and Hoigné (1994) investigated iron(III) catalyzed photodecomposition of oxalic, glycolic and pyruvic acids in atmospheric waters under sunlight irradiation (313 nm monochromatic light). In an earlier study the same authors reported that oxalate was stable for at least 1 hour in the absence of iron under 313 nm monochromatic light or sunlight (Zuo and Hoigné (1992)). They reported that oxalate decomposed quickly under both light sources in the presence of Fe(III). They concluded that a fast equilibrium was reached between the acids, ferric ions and corresponding Fe(III)-complexes (such as Fe(III)-mono- di- and tri-oxalato complexes) and these complexes absorbed sunlight easily. Photo-excitation of these complexes produced Fe(II) and an organic radical that reduced dissolved O_2 to superoxide ion ($O_2^{\bullet -}$), and its conjugate acid, hydroperoxide radical ($HO_2^{\bullet}$) which reduced the Fe(II) ions. This generated H_2O_2 and

reformed Fe(III). The authors also showed that the degradation rate of the acids increased with sunlight intensity, concentration of Fe(III) and concentration of acids.

Karpel Vel Leitner and Doré (1994) used the UV/H_2O_2 system, another process that produces $OH^{\bullet}$, to investigate the effect of dissolved oxygen on formic acid decomposition. They carried out experiments in a batch reactor equipped with a low-pressure mercury lamp, which emitted light at 254 nm. In the presence of DO, formic acid decomposition followed zero order kinetics while H_2O_2 remained unchanged. The authors suggested that $OH^{\bullet}$, produced from H_2O_2 by UV irradiation, reacted with formic acid and formed $^{\bullet}COO^-/^{\bullet}COOH$ which then reacted with DO to form $HO_2^{\bullet}/O_2^{\bullet-}$ and CO_2. H_2O_2 is then produced from $HO_2^{\bullet}$ radicals. In the absence of DO, both formic acid and H_2O_2 decomposed at very similar rates. In this case, $^{\bullet}COO^-/^{\bullet}COOH$ radicals reacted with H_2O_2 instead of oxygen, producing CO_2 and $OH^{\bullet}$. The mechanism they proposed for formic acid decomposition under UV irradiation in the presence of H_2O_2 is given by Equations 2.3.21 through 2.3.31:

$$2H_2O_2 \xrightarrow{2h\nu} 2OH^{\bullet} + H_2O_2 \qquad (2.3.21)$$

$$HCOOH \leftrightarrows HCOO^- + H^+ \qquad (2.3.22)$$

$$HCOO^- + OH^{\bullet} \rightarrow CO_2^{\bullet-} + H_2O \qquad (2.3.23a)$$

$$HCOOH + OH^{\bullet} \rightarrow COOH^{\bullet} + H_2O \qquad (2.3.23b)$$

$$COOH^{\bullet} \leftrightarrows CO_2^{\bullet-} + H^+ \qquad (2.3.24)$$

$$CO_2^{\bullet-} + O_2 \rightarrow CO_2 + O_2^{\bullet-} \qquad (2.3.25a)$$

$$COOH^{\bullet} + O_2 \rightarrow CO_2 + HO_2^{\bullet-} \qquad (2.3.25b)$$

$$HO_2^{\bullet-} \leftrightarrows O_2^{\bullet-} + H^+ \qquad (2.3.26)$$

$$2\,HO_2^{\bullet} \rightarrow H_2O_2 + O_2 \qquad (2.3.27)$$

$$H_2O_2 + OH^{\bullet} \rightarrow HO_2^{\bullet} + H_2O \qquad (2.3.28)$$

$$CO_2^{\bullet -} + H_2O_2 \rightarrow CO_2 + OH^{\bullet} + OH^- \qquad (2.3.29a)$$

$$COOH^{\bullet} + H_2O_2 \rightarrow CO_2 + OH^{\bullet} + H_2O \qquad (2.3.29b)$$

$$HCO_3^- + OH^{\bullet} \rightarrow CO_3^{\bullet -} + H_2O \qquad (2.3.30)$$

$$CO_2^{\bullet -} + HCO_3^- \rightarrow CO_3^{\bullet -} + HCO_2^- \qquad (2.3.31)$$

In a separate study Karpel Vel Leitner and Doré (1997) investigated the reaction mechanism between $OH^{\bullet}$ and glycolic, glyoxalic, acetic and oxalic acids in aqueous solutions. They used a 4-liter photochemical reactor equipped with a low-pressure mercury lamp (monochromatic light at a wavelength of 254 nm, photon flux $I_0=4.7\times10^{-6}$ E s^{-1}) to evaluate the H_2O_2 /UV system for the decomposition of organic acids in the presence and absence of DO. Glyoxalic and oxalic acids were the products of glycolic acid decomposition both in the presence and absence of DO, with the concentrations in the later being much lower than those in the former. They also reported formation of formic acid during the decomposition of glycolic acid in the presence of DO at $pH_0 = 6.8$. Glyoxalic acid decomposed to form oxalic acid during irradiation. Both glycolic and glyoxalic acids decomposed more rapidly in the presence of DO. The DO utilization during glycolate and glyoxalate decays was reported as 0.5 and 0.44 mol O_2/mol acid, respectively. Oxalate also decomposed in the H_2O_2 /UV system with very limited DO effect. They reported that DO utilization during oxalate decay was 0.065 mol O_2 / mol oxalic acid. Karpel Vel Leitner and Doré (1997) concluded that during the decomposition of glycolic and glyoxalic acids with H_2O_2 /UV, in the presence of oxygen, superoxide

radicals were formed. The proposed reaction mechanisms for glycolic and glyoxalic acids are given in Equations 2.3.32 through 2.3.37. Karpel Vel Leitner and Doré (1997) also suggested that during the decomposition of oxalic acid one hydrogen atom was abstracted by $OH^{\bullet}$, which was produced by H_2O_2 /UV. Then two $HOOCCOO^{\bullet}$ radicals reacted to form one oxalic acid and two CO_2 molecules. The mechanism they proposed for oxalate decomposition is given in the Equation 2.3.38 through 2.3.41.

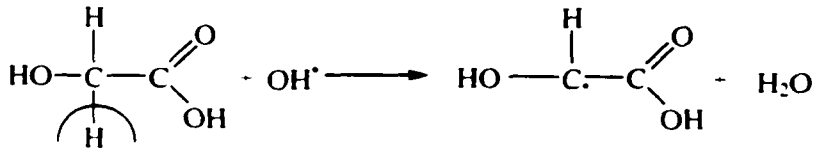

(2.3.32)

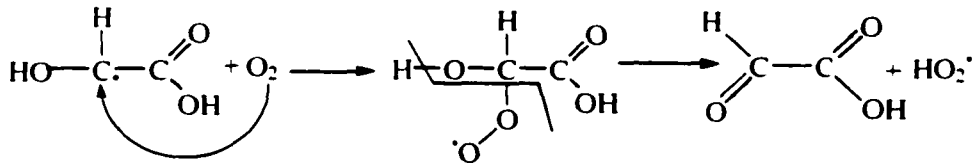

(2.3.33)

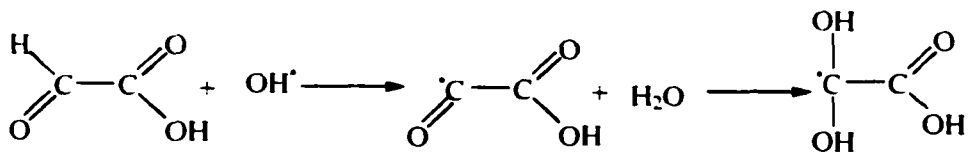

(2.3.34)

(2.3.35)

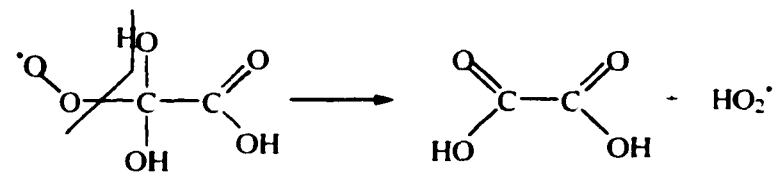

(2.3.36)

(2.3.37)

(2.3.38)

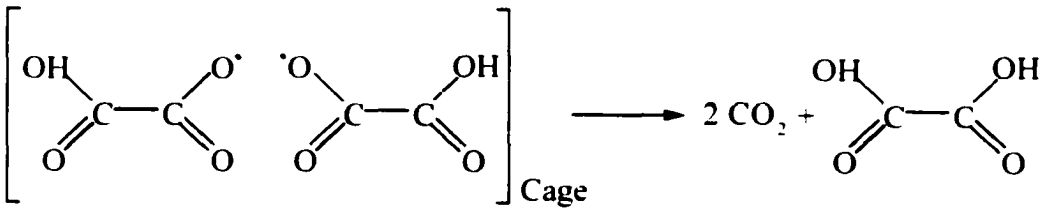

(2.3.39)

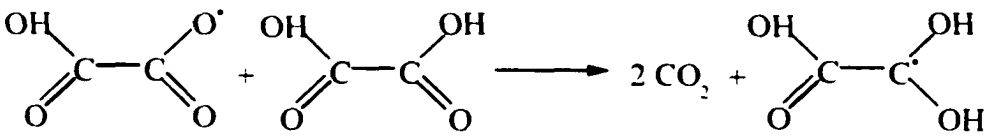

(2.3.40)

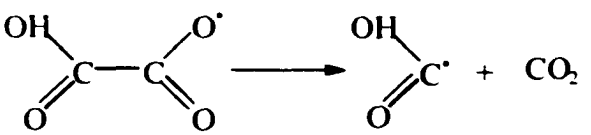

(2.3.41)

Several researchers studied photo-catalytic decomposition of carboxylic acids in aqueous solutions. Wang and Adesina (1997) investigated photo-catalytic degradation of sodium oxalate solution. They used a cylindrical photo-reactor with a fitted UV lamp (radiation range is 254-310 nm) and commercial TiO_2 powder (99% anatase) as catalyst. They showed that there was no oxalate decomposition under natural light and in the dark in the presence of oxygen. Addition of catalyst and oxygen purging in dark also did not cause any measurable oxalate decomposition. Blank experiments showed 10% conversion of

sodium oxalate under UV irradiation without any catalyst at pH 2. "The photo-catalytic causticization" of sodium oxalate was given as:

$$Na_2C_2O_4 + \frac{1}{2} O_2 + H_2O \rightarrow 2NaOH + 2CO_2\ (2NaHCO_3) \qquad (2.3.42)$$

with $\Delta H_{298} = 168$ kJ mol^{-1}. They found weak temperature dependence of oxalate photo-catalytic decomposition in the range of 303-323 K. When initial pH increased from 2 to 9, conversion decreased from 100% to 10% and initial rates were low at the pHs higher than 7. They also observed that pH of the reactor increased while oxalate concentration decreased. They reported that this observation was consistent with the findings that NaOH (or $NaHCO_3$) species concentrations increased before reaching a constant value.

Bangun and Adesina (1998) investigated photo-catalytic degradation kinetics of aqueous sodium oxalate solutions using TiO_2 as a catalyst. They used an annular photo-reactor equipped with a UV arc lamp, which was enclosed in a quartz tube. Lamp power supply had three-level setting (low = 200 W, medium = 300 W, high = 400 W) and significant fraction of the radiation was in the range of 250-310 nm. The decomposition rates they reported were the slopes of the first 30 minutes of the concentration-time profiles for each experiment. They found that initial solution pH, light intensity, catalyst loading and oxalate concentration strongly affected the decomposition rate. The initial oxalate degradation rate decreased exponentially with increasing initial pH. They concluded that at pH < 6, (the isoelectric point of titania in water occurs at pH ≈ 6) degradation rates were high because of the electrostatic attraction between oxalate ions and positively

charged catalyst surface sites. At pH > 6, degradation rates were low since the catalyst surface was negatively charged. They also remarked that free oxalate ion concentration was higher at low pH values because of decreasing solubility of sodium oxalate at increased alkalinity. The initial oxalate concentrations ranged between 0 to 3 mM. The degradation rate increased linearly with light intensity.

Krýsa et al. (1999) studied photocatalytic degradation of oxalic acid on a semi conductive layer of *n*-TiO_2 particles at 355 nm. They found that oxalate decay followed near zero-order kinetics and the rate of photocatalysis was controlled simultaneously by the flux of oxygen and photons at $[H_2C_2O_4]$ >0.005 M and photon flux intensity range of 3.26×10^{-10} to 1.07×10^{-8} $E/cm^2 \cdot s$. They proposed the following mechanism to describe the decomposition of oxalate to the presence of $OH^{\bullet}$:

$$(COOH)_2 + OH^{\bullet} \rightarrow HOOC—COO^{\bullet} + H_2O \quad (2.3.43)$$

$$HOOC—COO^{\bullet} \rightarrow CO_2 + {}^{\bullet}COOH \quad (2.3.44)$$

$$2\ {}^{\bullet}COOH \rightarrow (COOH)_2 \quad (2.3.45a)$$

or

$$2\ {}^{\bullet}COOH \rightarrow CO_2 + HCOOH \quad (2.3.45b)$$

$$HCOOH + OH^{\bullet} \rightarrow {}^{\bullet}COOH + H_2O \quad (2.3.46)$$

And the overall decomposition stoichiometry was presented as:

$$(COOH)_2 + 2\ OH^{\bullet} \rightarrow 2\ CO_2 + 2\ H_2O \quad (2.3.47)$$

Mazzarino et al. (1999) studied photo-catalytic degradation of glycolic acid in aqueous solutions using continuous flow and batch reactors. The batch reactor equipped with a 15

W low-pressure mercury lamp (254 nm) and fine particles of commercial Titania (concentration of suspended catalyst was varied in the range 10-1000 mg/L) dispersed in the liquid phase. For all of the experiments the initial glycolic acid concentration was 200 mg/L. The authors observed that decrease of the total organic carbon (TOC) concentration much slower than the glycolic acid decomposition. They reported that this difference between acid and TOC decay indicated formation of significant amount of intermediates during the degradation process. The only intermediate they identified was formic acid. They also performed experiments with H_2O_2 addition in the reactor with and without the suspended catalyst (with an initial concentration H_2O_2 two times the stoichiometric value). They observed that there was no significant difference between UV-TiO_2-H_2O_2 and UV-TiO_2 systems in terms of glycolic acid and TOC decay rates while, they both decayed faster in UV-H_2O_2 system than in UV-TiO_2-H_2O_2 system.

CHAPTER 3

METHODS AND MATERIALS

3.1. Experimental Methods

The experimental system, shown in Figure 3.1.1, was a Bioreactor (Bioflo 3000, New Brunswick Scientific, Edison, NJ) reconfigured for UV irradiation experiments. The 5-L glass reactor (17 cm inner diameter and 35 cm depth) was equipped with eight low-pressure quartz immersion lamps (3.5 W output at 254 nm, arc length of 16.5 cm, L = 27 cm, and OD = 1.3 cm). The lamps (Model No. 12128 Photochemical Immersion Lamps, ACE Glass, Vineland, NJ) were suspended in quartz tubes (ID = 2.15 cm, L = 34 cm, wall thickness of 1.35 mm) that were snugly fitted through and extending by about 3.0 cm above the 2.54 cm thick teflon cover that was tightly secured on the reactor. Each lamp was equipped with a separate power supply, thus allowing for any number of lamps to be employed simultaneously. Mixing was provided by a 130 mm arc-shaped teflon stirrer blade (Model No. 8085-19, ACE Glass, Vineland, NJ) positioned at the bottom of the reactor, under the quartz tubes, and connected with a teflon coated glass rod to the mixing motor above the teflon reactor cover. The reaction temperature and mixing intensity were controlled while the pH and dissolved oxygen (DO) were only monitored by the system microprocessor in the course of an experiment. The reactor was wrapped with aluminum foil during the reaction to prevent potential UV exposure from the lamps. Ozone that was produced in the air between the UV lamps and the quartz tubes was

continuously pumped out and bubbled through multiple stages of potassium iodide solution (10 g/L KI and 3 ml/L concentrated H_2SO_4).

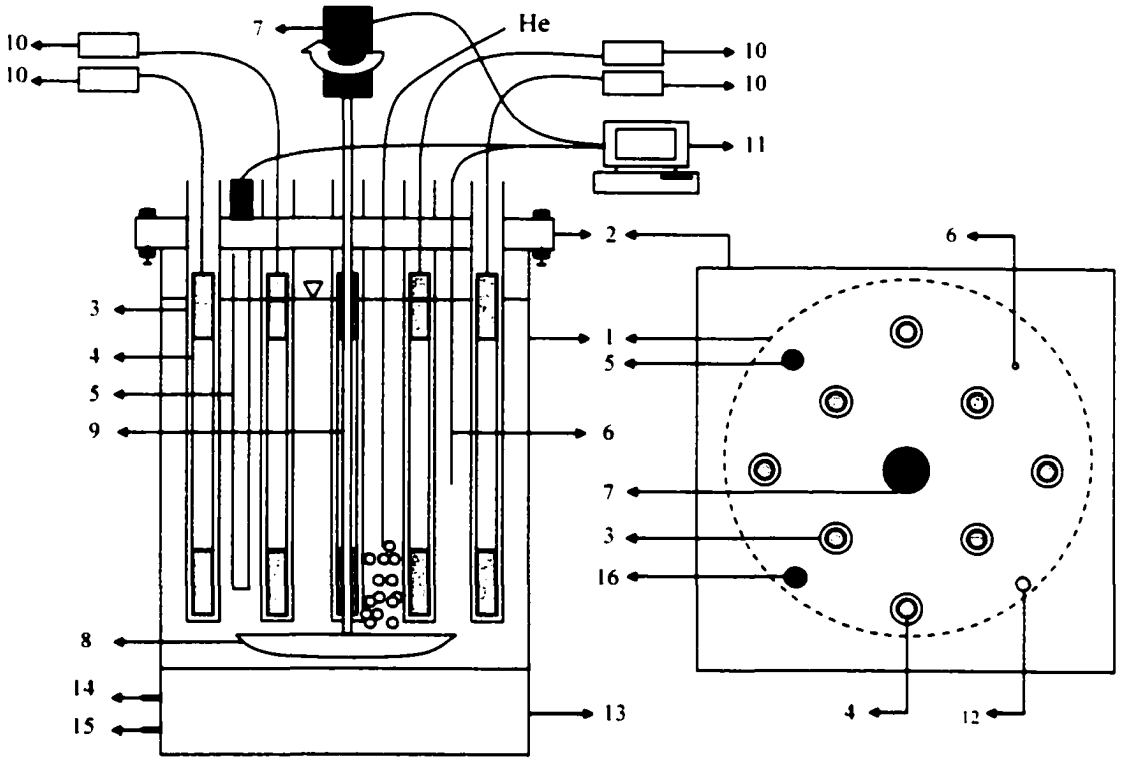

Figure 3.1.1. Schematic of Experimental-Setup. The reactor is connected to the bioreactor control panel, which is not shown here. (1) Reactor vessel; (2) Teflon cover; (3) Quartz tube; (4) UV lamp; (5) pH probe; (6) Thermocouple; (7) Mixing Motor; (8) Mixer Blade; (9) Mixing rod; (10) UV lamp power supply; (11) Computer for monitoring pH and temperature; (12) Sampling port; (13) Thermostat; (14) Thermostat water inlet; (15) Thermostat water outlet; (16) DO probe.

All experiments were run in batch mode. Prior to each experiment a selected number of lamps were turned on and allowed to warm-up for 15 minutes. At the end of the warm-up period the lamps were turned off and the reactor was filled with 5 L of ultra pure water with a specific resistance of 18.2 mega-ohm and TOC ≤ 5 ppb (MilliQ, Millipore S.A., Molsheim-France). The temperature and mixing were set to the desired levels and a predetermined volume of stock acid solution was spiked into the reactor to achieve the desired initial concentration. The solution was then vigorously mixed and a 25 ml sample was withdrawn from the middle of the reactor to analytically determine the initial conditions in the reactor medium. Turning the lamps back on commenced the experiment. Kinetic sampling involved withdrawal (by gravity and in less than 10 seconds) of 25 ml samples into pre-cleaned vials at the desired time intervals, of which 5 ml were used for determination of anion concentration(s) and 20 ml for NPOC (non-purgeable organic carbon) analysis. NPOC analyses were done less frequently than anion analysis. Whenever NPOC analyses were not deemed necessary, only 5 ml sample was withdrawn from the reactor for anion determination. The solution pH was adjusted to various initial levels using 1 N NaOH solution. Determination of anions concentration and NPOC were mostly done the same day as the experiment. When necessary, samples were refrigerated in amber vials for up to 3 days. Sampling vials were soap washed with tap water, rinsed with MilliQ water and then dried in oven at 105°C.

3.2. Analytical Methods

The chemicals used in the experiments are given in Table 3.2.1. MilliQ water was used in the preparation of all solutions.

Table 3.2.1. Chemicals Used in the Experiments.

Chemicals	Company	Purity (%)	Grade
Sodium Formate	Aldrich	99.998	-
Sodium Oxalate	Aldrich	99.99	-
Sodium Pyruvate	Fisher Biotech	99	Enzyme Grade
Glycolic Acid	Aldrich	99*	-
Glyoxylic Acid Monohydrate	Aldrich	98*	-
Potassium Iodide	Fisher	-	Certified ACS
Potassium Hydrogen Phthalate	Nacalai Tesque	-	Reagent Grade
Potassium Ferric Oxalate	ICN Biomedicals	-	-
1 N NaOH	Fisher	-	Certified
10 N NaOH	Fisher	-	Certified
10 N H_2SO_4	HACH	-	Std. Solution

*Highest available purity.

3.2.1. Determination of Anionic Species by Ion Chromatograph

A DX500 (Dionex Corporation, Sunnyvale, CA) ion chromatography (IC) system equipped with an autosampler (Dionex, AS40) was used to determine the formate (HCO_2^-), oxalate ($C_2O_4^{2-}$), glyoxalate ($HC_2O_3^-$), glycolate ($H_3C_2O_3^-$) and pyruvate ($H_3C_3O_3^-$) concentrations. The system consisted of GP40 gradient pump, CD20 conductivity detector, a 100-μL sample loop, IONPAC® AS11-4 mm analytical column,

AG11-4 mm guard column and ASRS-I (self-regenerating) anion suppressor operated in external water mode. Gradient elution with 100 mM NaOH eluent at a flow rate of 2 mL/min was used for the analysis with the gradient elution program shown in Table 3.2.1.1. NaOH solution was prepared by diluting 10 ml of 10 N NaOH solution in MilliQ water to a final volume of 1000 ml.

Stock solutions (1000 mg/L as C) were prepared for each compound while calibration standards were prepared by diluting the stock solutions to a final volume of 100 ml. Combined HCO_2^-, $C_2O_4^{2-}$, $HC_2O_3^-$, $H_3C_2O_3^-$ and $H_3C_3O_3^-$standards were prepared from 10 mg/L (as C) standard solution and used in the analysis of the first three acids, while individual standards were used in the cases of HCO_2^- and $C_2O_4^{2-}$. Retention time and minimum detection limit for each anion in the IC system are listed in Table 3.2.1.2. Figure 3.2.1.1 shows a sample chromatogram of a solution containing all of the aforementioned anions.

3.2.2. Measurement of NPOC and TC by TOC Analyzer

A TOC analyzer (5000A, Shimadzu Corporation) was used to determine NPOC and TC. During NPOC measurements the samples were first acidified with 2 N HCl to a pH ≤ 3 and then bubbled with high purity bottled breathing air (TW Smith, zero grade) to remove inorganic and purgeable organic carbon. The following overall reaction occurs and all CO_2 is separated from carbonate when samples are acidified:

$$Na_2CO_3 + 2HCl \rightarrow CO_2 + 2\,NaCl + H_2O \qquad (3.2.2.1)$$

$$NaHCO_3 + HCl \rightarrow CO_2 + NaCl + H_2O \qquad (3.2.2.2)$$

Separated CO_2 and dissolved CO_2 are removed from samples when the samples were bubbled with CO_2 free air.

Stock organic carbon solution (1000 mg/L as C) was prepared by dissolving 0.2126 g of potassium hydrogen phthalate (Nacalai Tesque, reagent grade) in MilliQ water and diluting to a final volume of 100 ml. Standard solution of 10 mg/L (as C) was prepared diluting 1 ml of stock solution to 100 ml of volume with MilliQ water. Calibration standards were prepared from 10-mg/L (as C) standard solution.

Table 3.2.1.1. Gradient Elution Program for IC Analysis

Time (min)	Percent of 100 mM NaOH	Percent of DIW
0	3	97
1.50	3	97
1.51	5	95
2.50	5	95
6.50	38	62
6.51	3	97
10	3	97

Table 3.2.1.2. Retention Times and Minimum Detection Limits for Anions

Ion	Retention Time (min)	Minimum Detection Limit (μg/L)
HCO_2^-	1.28	1.0
$C_2O_4^{2-}$	3.98	1.0
$HC_2O_3^-$	1.71	1.0
$H_3C_2O_3^-$	1.15	1.0
$H_3C_3O_3^-$	1.39	1.0

Data File	: CA\GONCA\STANDA~1\STD02005.DXD	Report Date	: 7/1/103 7:26:28 PM
Sample Name	: AUTOCAL5R	Collected	: 4/17/101 12:07:42 PM
Inject #	: 5	Vial #	:
Method File	: c:\peaknet\method\as11.met	Calibrated	: 4/17/101 12:17:46 PM
System Name	: CCNY SYS#1	Detector	: CD20
Column Type	:	Operator	: Gonca
Data Points	: 2550	Rate	: 5.00 Hz
Module Name	: ID:34 C6 a6	Moduleware	: 2.10

Calibration	Volume	Dilution	Start	Stop	Area Reject	Pk. Width	Threshold
External	1	1	0.00	8.50	200	2.00	1.92

********** Peak Report: All Peaks **********

Pk. Num	Ret Time	Component Name	Concentration	Height	Area	Bl. Code	%Delta
1	1.15	Glycolate	0.500	65301	160142	1	0.00
2	1.28	Formate	0.500	118808	321322	1	0.00
3	1.39	Pyruvate	0.500	49916	112410	1	0.00
4	1.71	Glyoxylate	0.500	61428	159054	1	0.00
5	1.82		0.000	627	1182	1	
6	3.98	Oxalate	0.500	118351	334766	1	0.00
7	5.00		0.000	127	4270	1	
		Totals	2.500	414558	1093147		

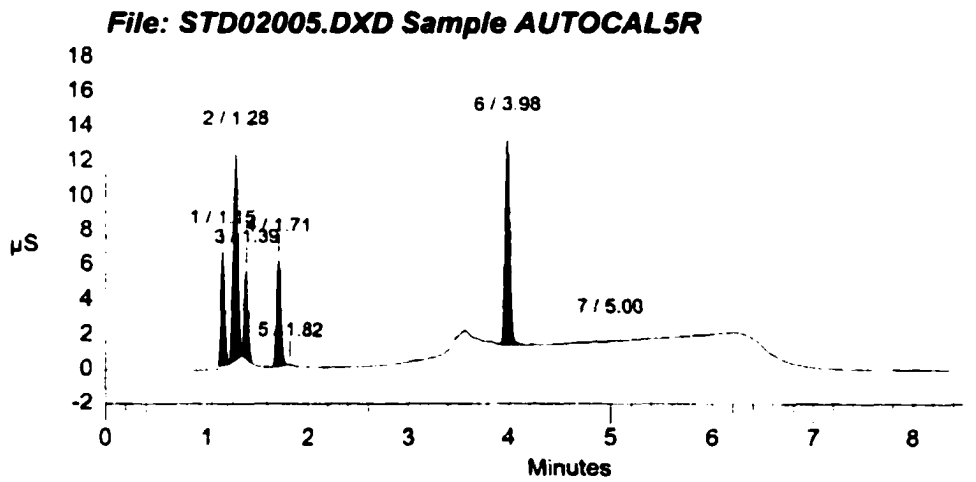

Schedule: c:\peaknet\schedule\cal.sch
Release 4.30 Page 1 of 1 7/1/103 7:26:28 PM

Figure 3.2.1.1. Sample Ion Chromatogram of a Mixture Containing HCO_2^-, $C_2O_4^{2-}$, $HC_2O_3^-$, $H_3C_2O_3^-$ and $H_3C_3O_3^-$ (0.5 mg/L as C for each compound).

3.2.3. Determination of Absorbed Light Intensity

Absorbed light intensity, which is defined as the moles of photons absorbed by the reactor per unit volume×time, was determined by potassium ferrioxalate chemical actinometric technique as described by Hatchard and Parker (1956). A five-liter 0.006 M potassium ferrioxalate ($K_3Fe(C_2O_4)_3 \cdot 3H_2O$) (ICN Biomedicals Inc., Aurora, Ohio) solution was prepared in MilliQ water containing 0.1 N H_2SO_4 in dark room. $K_3Fe(C_2O_4)_3 \cdot 3H_2O$ was desiccated for an hour before preparing the solution. After warming the selected number of lamps for 15 minutes, the reactor was filled with the potassium ferrioxalate solution. The temperature and mixing intensity were set to the desired level, the solution was mixed and 25 ml sample was withdrawn from the middle of the reactor to precleaned amber vial for determination of the initial Fe^{2+} concentration. The solution was irradiated for a period sufficient to produce Fe^{2+} concentration between 0.005×10^{-6} and 3×10^{-6} moles/ml as described by Hatchard and Parker (1956). After irradiation, the lamps were turned off and approximately 25 ml of sample was withdrawn from the reactor. One mL of the sample was diluted 200 times in MilliQ water in order to be in the range of the spectrophotometer. Fe^{2+} concentration in diluted sample was determined with Hach DR/4000 Spectrophotometer (Hach Company, Loveland, CO) using the 1,10 Phenanthroline Method (Method 8146, Hach Company, Loveland, CO). The procedure involved filling a Ferrous Iron AccuVac® ampule (containing 1,10 phenanthroline and sodium bicarbonate buffer) with the sample to be analyzed, inverting and mixing the ampule several times and allowing a 3-minute reaction time to elapse prior to reading the absorbance at 510 nm. The instrument was zeroed with MilliQ water

subjected to the aforementioned procedure. Then, dilutions of samples representing the initial and final Fe^{+2} concentrations in the irradiation experiment were analyzed. The absorbed light intensity was determined using equation 3.2.3.1.

$$I_a = \frac{1}{\phi_\lambda}\frac{d[P]}{dt} \qquad (3.2.3.1)$$

where I_a is the absorbed light intensity in Einstein/Ls, d[P]/dt is the change in Fe^{2+} concentration (mol/L s) with time and ϕ_λ is quantum yield. Hatchard and Parker (1956) recommended the value of quantum yield at 253.7 nm, as 1.25. The absorbed light intensity was determined for 1, 2, 3 and 4 UV lamp configurations, and was repeated several times, during the course of study.

3.2.4. Determination of Molar Absorption Coefficients

Molar absorption coefficients of the MilliQ water solutions of sodium formate ($NaHCO_2$), sodium oxalate ($Na_2C_2O_4$), glyoxylic acid monohydrate ($H_2C_2O_3 \cdot H_2O$), glycolic acid ($H_4C_2O_3$) and sodium pyruvate ($NaH_3C_3O_3$) at 253.7 nm ($\varepsilon_{253.7}$) were determined using a UV-visible diode-array spectrophotometer (Hewlett Packard, Model HP 8453) at path length (d) of 1 cm. $\varepsilon_{253.7}$ (HCO_2^-), $\varepsilon_{253.7}$ ($C_2O_4^{2-}$), $\varepsilon_{253.7}$ ($H_2C_2O_3 \cdot H_2O$), $\varepsilon_{253.7}$ ($H_4C_2O_3$) and $\varepsilon_{253.7}$ ($H_3C_3O_3^-$) were determined as 0.2 $M^{-1}cm^{-1}$ (Figure 3.2.4.1a), 25.1 $M^{-1}cm^{-1}$ (Figure 3.2.4.1b), 2.7 $M^{-1}cm^{-1}$ (Figure 3.2.4.2a), 0.3 $M^{-1}cm^{-1}$ (Figure 3.2.4.2b) and 80.7 $M^{-1}cm^{-1}$ (Figure 3.2.4.3), respectively. The pH ranges were 6.09 - 6.92, 5.95 - 6.58, 2.36 – 3.60, 2.60 - 3.76 and 5.80 – 6.31 for HCO_2^-, $C_2O_4^{2-}$, $H_2C_2O_3 \cdot H_2O$, $H_4C_2O_3$ and $H_3C_3O_3^-$, respectively.

Complete absorption spectra (190 – 900 nm) of kinetic samples during some of the photodecomposition experiments were also determined.

3.2.5. Measurement of pH and DO

Solution pH and DO were measured using pH electrode (Type 465-25-90-K9, Mettler Toledo Process Analytical, Inc., Wilmington, MA) and oxygen sensor (Ingold, Mettler Toledo Process Analytical, Inc., Wilmington, MA) connected to the system microprocessor and recorded at one-minute intervals.

3.2.6. Quality Assurance and Quality Control in Laboratory Analyses

Detailed discussion of the procedures used for measurement of anionic species, NPOC, TC, and absorbed light intensity has been presented in Appendix H.

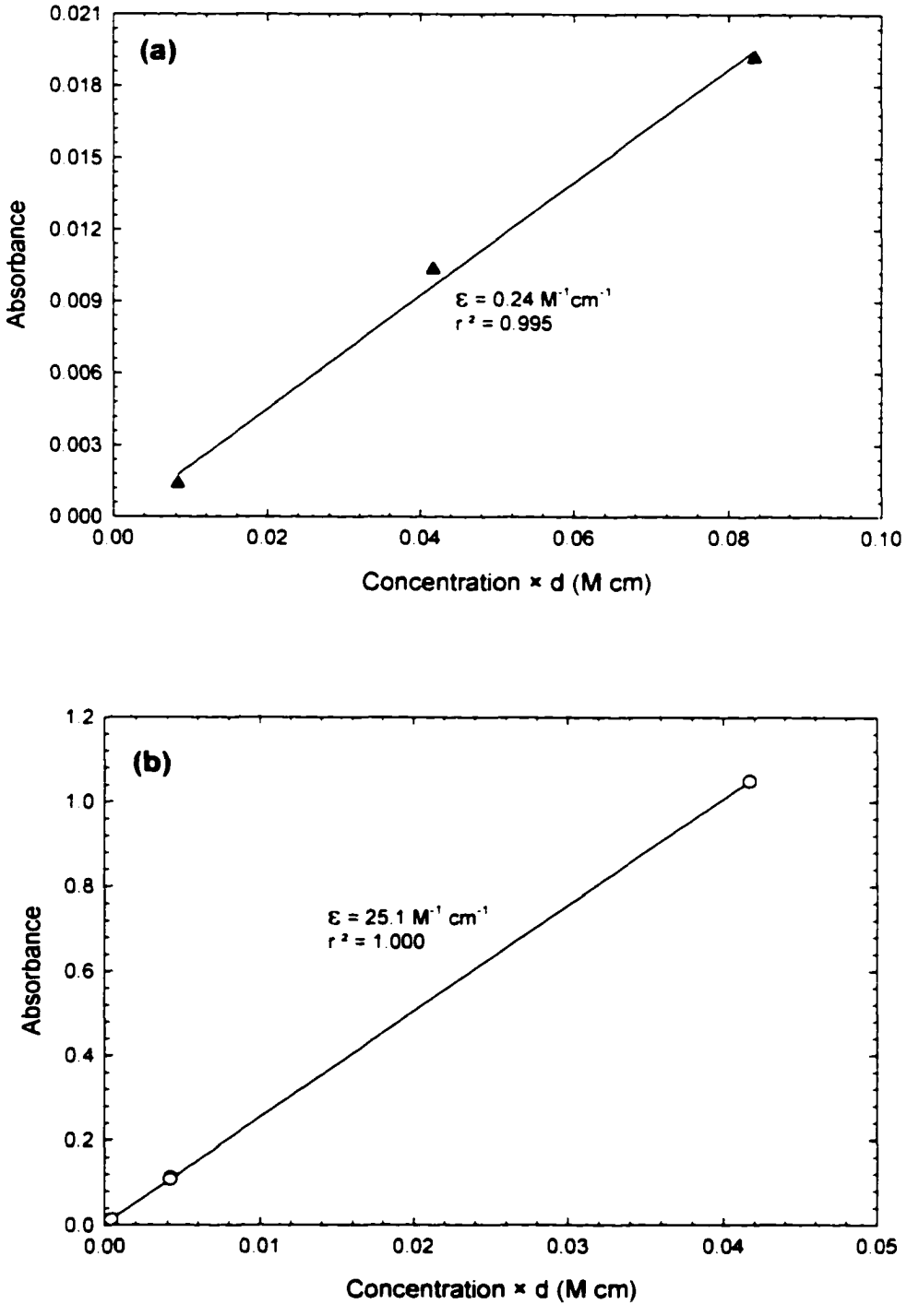

Figure 3.2.4.1. Absorbance Values of DIW solutions of **(a)** $NaHCO_2$, **(b)** $Na_2C_2O_4$ at 253.7 nm.

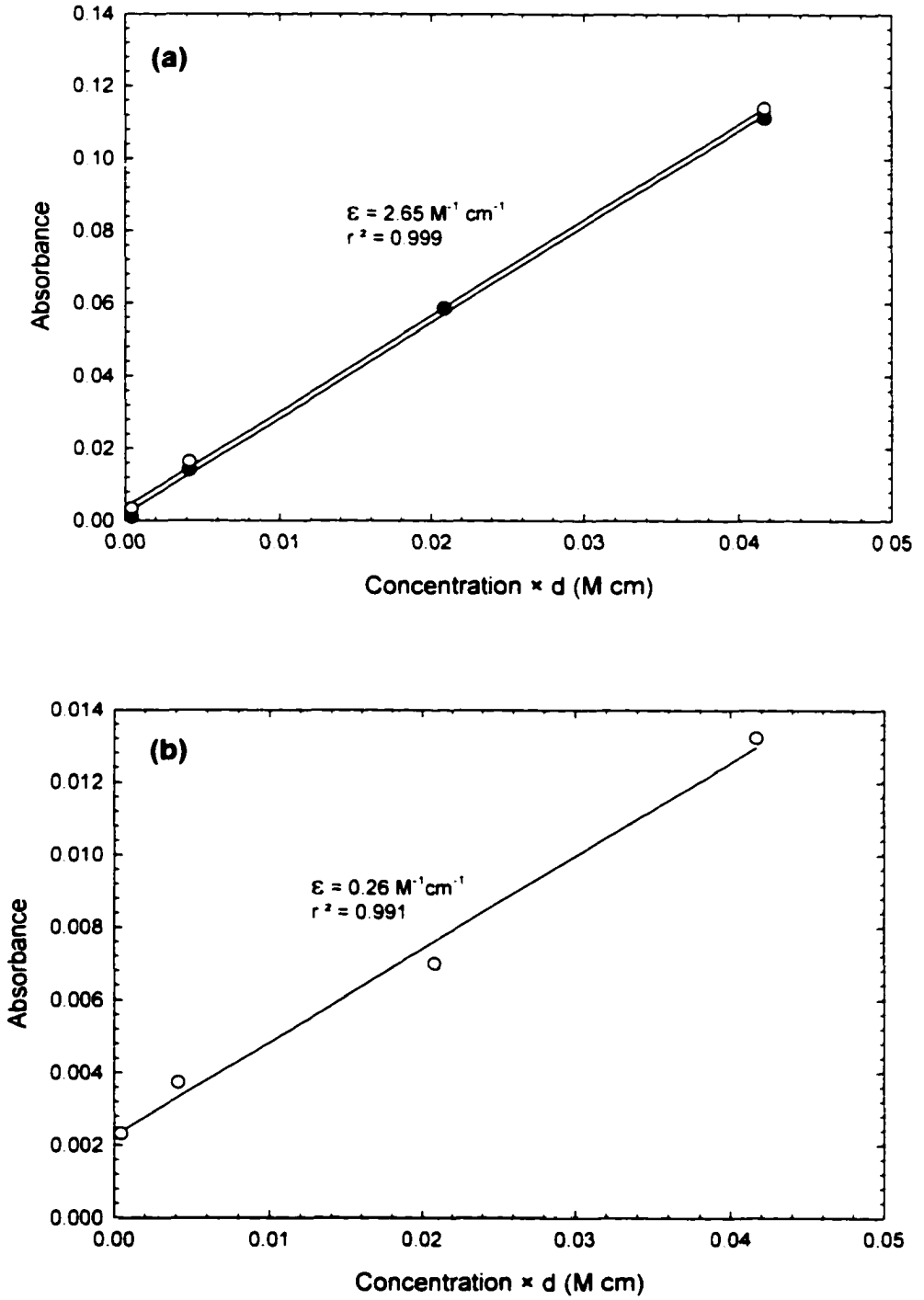

Figure 3.2.4.2. Absorbance Values of DIW solutions of **(a)** $H_2C_2O_3 \cdot H_2O$. **(b)** $H_4C_2O_3$ at 253.7 nm.

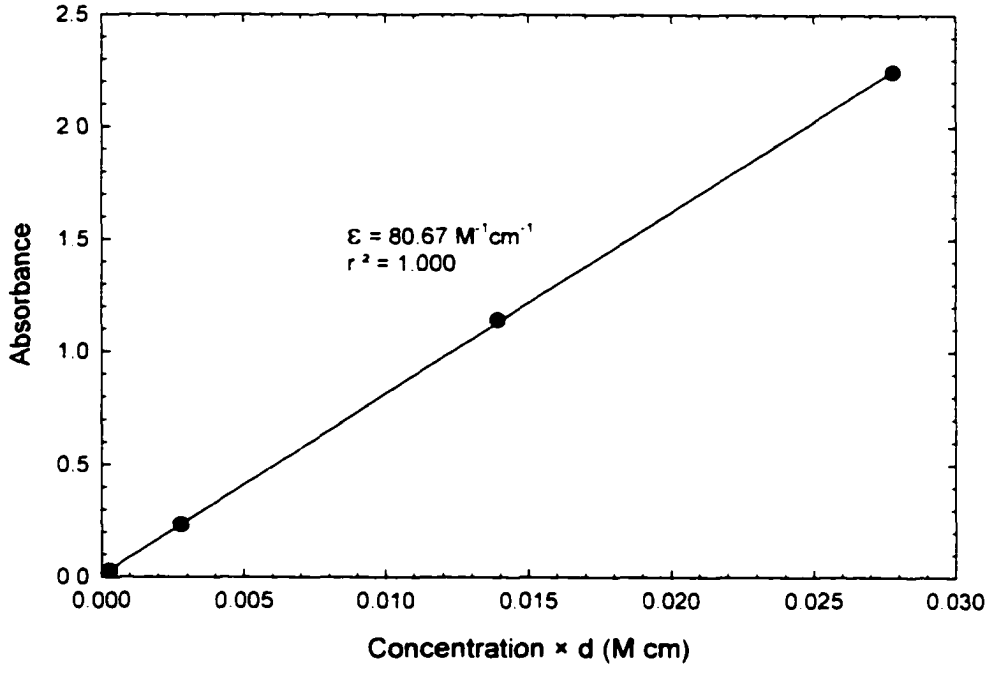

Figure 3.2.4.3. Absorbance Values of DIW solutions of $NaH_3C_3O_3$ at 253.7 nm.

CHAPTER 4

RESULTS AND DISCUSSION

4.1. General

Stability of the MilliQ water solutions of $NaHCO_2$, $Na_2C_2O_4$, $H_2C_2O_3 \cdot H_2O$, $H_4C_2O_3$ and $NaH_3C_3O_3$ were tested in dark at 20 °C with the results shown in Table 4.1.1 where concentrations reported as $[HC_2O_3^-]$ and $[H_3C_2O_3^-]$ represent the total concentration of $\{H_2C_2O_3 + HC_2O_3^-\}$ and $\{H_4C_2O_3 + H_3C_2O_3^-\}$, respectively since in the range of experimental pH both acidic and ionic forms exist in the solution. All acid solutions were stable over a period of 120 min.

Table 4.1.1. Stability of $NaHCO_2$, $Na_2C_2O_4$, $H_2C_2O_3 \cdot H_2O$, $H_4C_2O_3$ and $NaH_3C_3O_3$ Solutions in the Absence of UV Light.

Time (min)	$[HCO_2^-] \times 10^5$ (M)	$[C_2O_4^{2-}] \times 10^5$ (M)	$[HC_2O_3^-] \times 10^5$ (M)	$[H_3C_2O_3^-] \times 10^5$ (M)	$[H_3C_3O_3^-] \times 10^5$ (M)
0	4.39	2.09	2.11	2.07	1.44
15	4.37	2.12	2.10	2.15	1.43
30	4.39	2.13	2.11	2.15	1.45
60	4.33	2.10	2.10	2.10	1.47
120	4.48	2.17	1.97	2.14	1.33
Mean	4.39±0.06	2.12 ± 0.03	2.08 ± 0.06	2.12±0.04	1.42±0.06

The experiments were run at $I_\alpha = 2.60 \times 10^{-6}$ E L^{-1} s^{-1}, and 25°C, except those for temperature and UV intensity dependencies. pH_0 was adjusted to various levels for pH_0

dependency experiments. Table 4.1.2 shows experimental parameters and ranges during UV irradiation of individual compounds.

Table 4.1.2. Experimental Conditions During UV Irradiation of $NaHCO_2$, $Na_2C_2O_4$, $H_2C_2O_3 \cdot H_2O$, $H_4C_2O_3$ and $NaH_3C_3O_3$ solutions.

Parameter	Experimental Range				
	HCO_2^-	$C_2O_4^{2-}$	$HC_2O_3^-$	$H_3C_2O_3^-$	$H_3C_3O_3^{-\bullet}$
C_0 (M)	$(1.73–38.3)\times10^{-5}$	$(2.05–21.11)\times10^{-5}$	$(1.73–20.51)\times10^{-5}$	$(2.00–18.87)\times10^{-5}$	$(1.45–14.33)\cdot10^{-5}$
pH_0	5.41 - 8.97	5.45 - 8.94	4.00 - 9.10	4.06 - 9.12	5.43 - 5.60
I_a ($EL^{-1}s^{-1}$)	$(1.38–3.99)\times10^{-6}$	$(1.38–5.27)\times10^{-6}$	$(1.38–5.27)\times10^{-6}$	$(1.38–5.27)\times10^{-6}$	2.60×10^{-6}
T (°C)	18-35	15-35	15-35	15-35	25

*Two experiments

4.2. Kinetic Analysis of Experimental Observations

Kinetic analysis of each acid studied is presented in individual sections.

4.2.1. Formate

Typical HCO_2^-, NPOC and pH profiles during HCO_2^- decomposition in the presence and absence of $NaHCO_3$ are given in Figure 4.2.1.1. HCO_2^- readily decomposed while NPOC closely followed the $[HCO_2^-]$ profiles (Figures 4.2.1.1 a and b). A separate experiment showed that total carbon (TC), which includes CO_2, remained unchanged during HCO_2^- decay as depicted in insert "c" of Figure 4.2.1.1. Since $\Delta[HCO_2^-] \approx \Delta$NPOC through both time profiles in Figures 4.2.1.1a and 4.2.1.1b, it can be suggested that HCO_2^- is consistently converted to CO_2. Time profiles of $[HCO_2^-]$ followed split rate pseudo-zero

order kinetics, as shown in Figure 4.2.1.2, with the switch between observed rate constants k_1 and k_2 ($k_1 < k_2$ in the presence of dissolved oxygen (DO)) occurring at average percent HCO_2^- conversion of 20 ± 3.

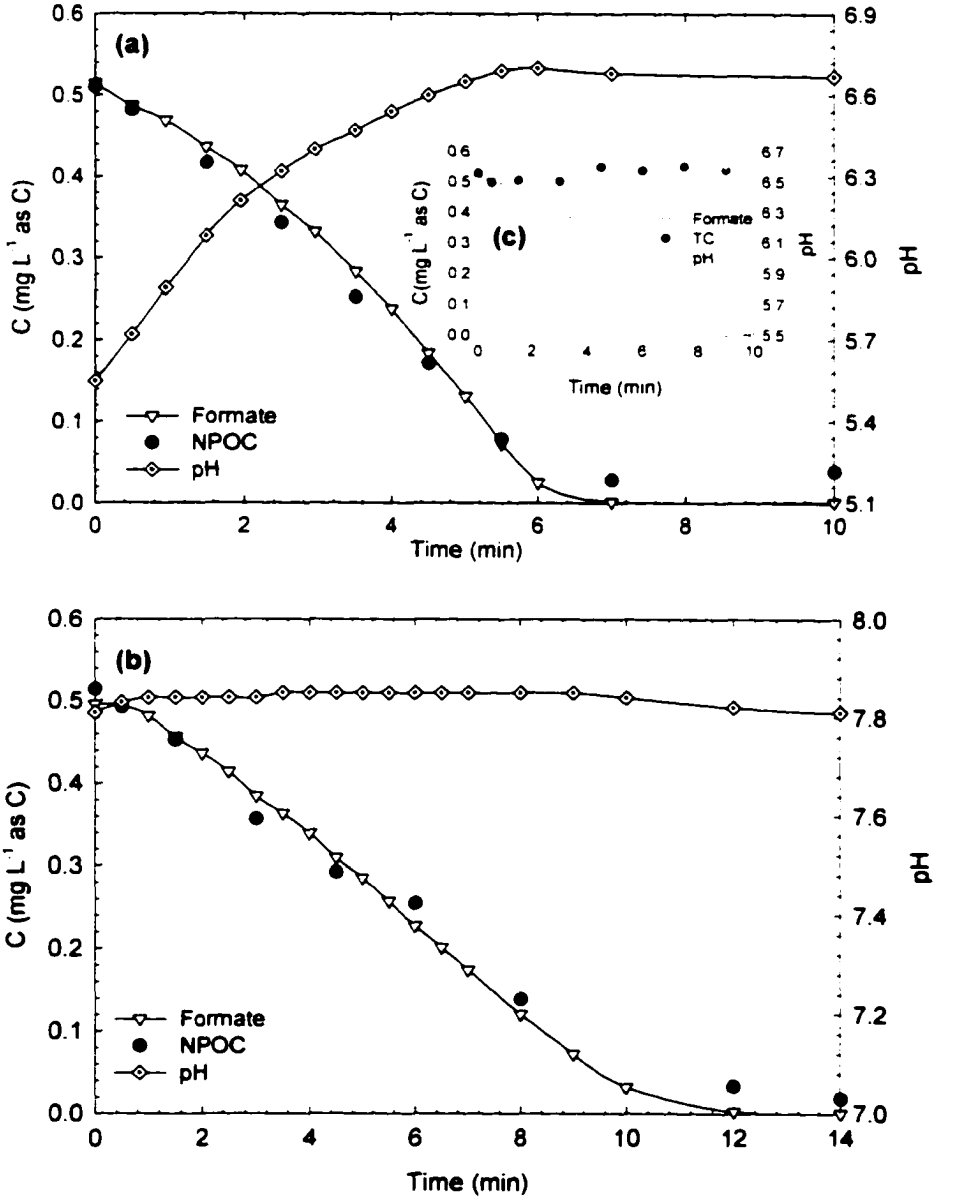

Figure 4.2.1.1. Concentration and pH Profiles during UV Irradiation of HCO_2^- in **(a)** DIW (I_a = 3.99 × 10^{-6} $EL^{-1}s^{-1}$, C_0 = 4.28 × 10^{-5} M, pH_0 = 5.55, T = 25°C), **(b)** DIW Containing $NaHCO_3$ = 25 mgL^{-1} as $CaCO_3$ (I_a = 2.60 ×10^{-6} $EL^{-1}s^{-1}$, C_0 = 4.13 × 10^{-5} M, pH_0 = 7.81, Temperature = 25°C), **(c)** DIW (I_a = 2.60 × 10^{-6} $EL^{-1}s^{-1}$, C_0 = 4.28 × 10^{-5} M, pH_0 = 5.52, T = 25°C).

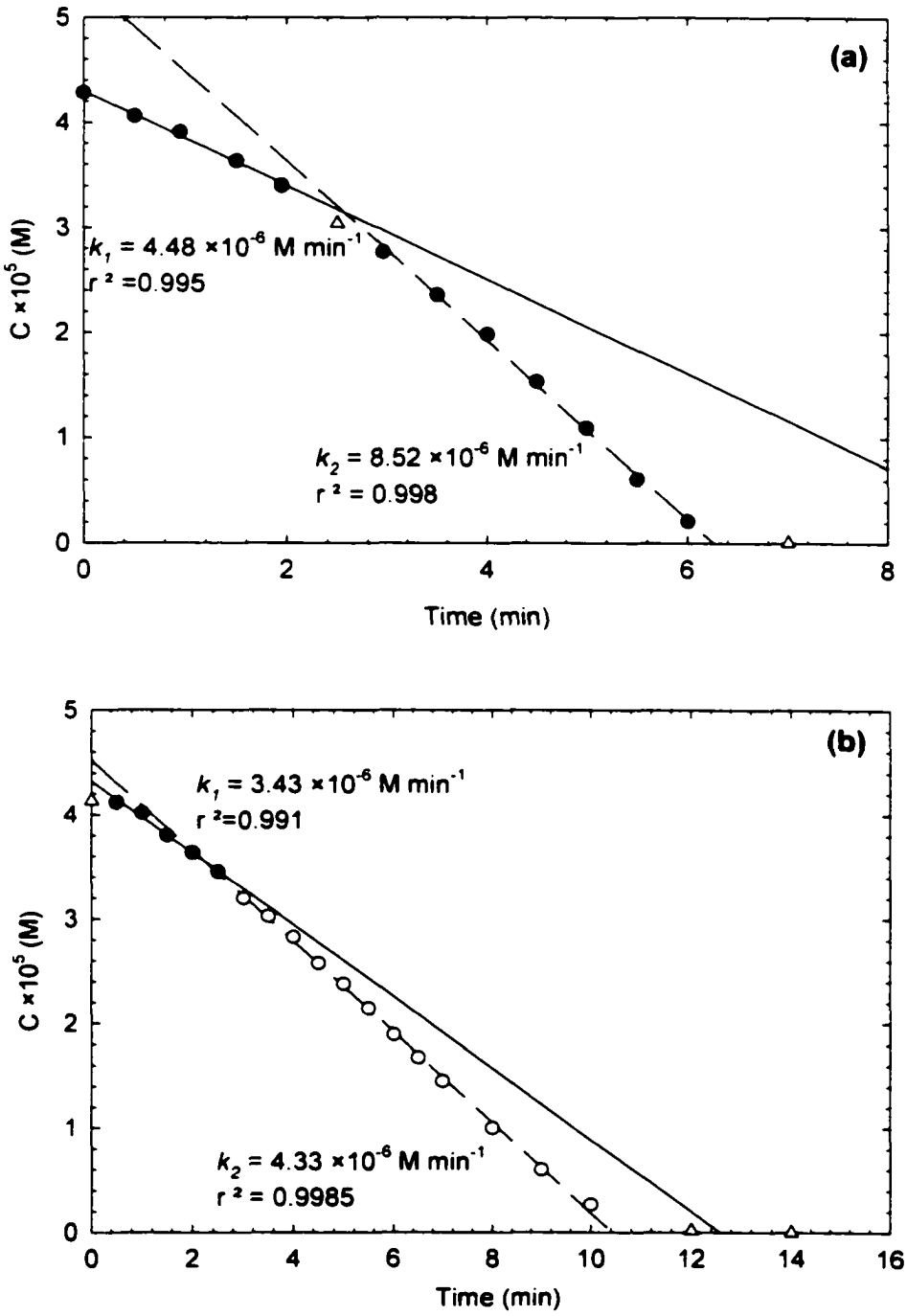

Figure 4.2.1.2. Kinetic Analysis of the HCO_2^- Decay Data **(a)** DIW (I_a = 3.99 × 10^{-6} $EL^{-1}s^{-1}$, C_0 = 4.28 × 10^{-5} M, pH_0 = 5.55, T = 25°C) **(b)** DIW $NaHCO_3$ = 25 mgL^{-1} as $CaCO_3$ (I_a = 2.60 ×10^{-6} $EL^{-1}s^{-1}$, C_0 = 4.13 × 10^{-5} M, pH_0 = 7.81, T = 25°C).

The values of k_1 and k_2 ranged between (1.7 - 7.3) $\times 10^{-6}$ M min^{-1}, and (2.6 - 12.4) $\times 10^{-6}$ M min^{-1}, respectively and the ratio of k_1/k_2 remained at 0.72 ± 0.08 for all experiments in the presence of DO. Karpel Vel Leitner and Doré (1994) also observed zero order kinetics for HCO_2^- decomposition under UV/ H_2O_2 in the presence of DO. The authors found the HCO_2^- decay rate to be highly insensitive to pH_0 in the range of 2.0 to 6.0 at $[H_2O_2]_0$ = 2.77 $\times 10^{-4}$ M, and linearly dependent on $[H_2O_2]_0$ as shown in Figure 4.2.1.3. The results of the study reported herein are also presented in Figure 4.2.1.3 at H_2O_2 = 0 M. Despite the differences in pH_0 and $[HCO_2^-]_0$ between the two studies, in the absence of H_2O_2, comparison of k_2 at I_a = 1.38 × 10^{-6} $EL^{-1}s^{-1}$ (this study) and 1.45 × 10^{-6} $EL^{-1}s^{-1}$ (Karpel Vel Leitner and Doré (1994)) suggests that k remains insensitive to $[H_2O_2]_0$ up to a critical concentration which by inspection of Figure 4.2.1.3 occurs between (90 – 95) × 10^{-6} M. The comparison also shows that the effect of $[H_2O_2]_0$ can be achieved by higher applied UV intensities.

The reaction pH increased rapidly during irradiation of $NaHCO_2$ solutions and reached a plateau at $[HCO_2^-]_t$ = BDL (below detection limit) (Figures 4.2.1.1a and 4.2.1.1c), while very weak pH dependency was observed during irradiation of {$NaHCO_2$ + $NaHCO_3$} solution (Figure 4.2.1.1b). The overall pH change, ΔpH (ΔpH = pH_f – pH_0, and pH_f occurs at $[HCO_2^-]_t$ = BDL), in $NaHCO_2$ solution at 25 °C and I_a = 2.60 $\times 10^{-6}$ $EL^{-1}s^{-1}$ increased with increasing $[HCO_2^-]_0$ at pH_0 = 5.39 – 5.75 as shown in Figure 4.2.1.4. This is due to the increase in $[HCO_3^-]$ in the reaction medium as a result of HCO_2^- decay.

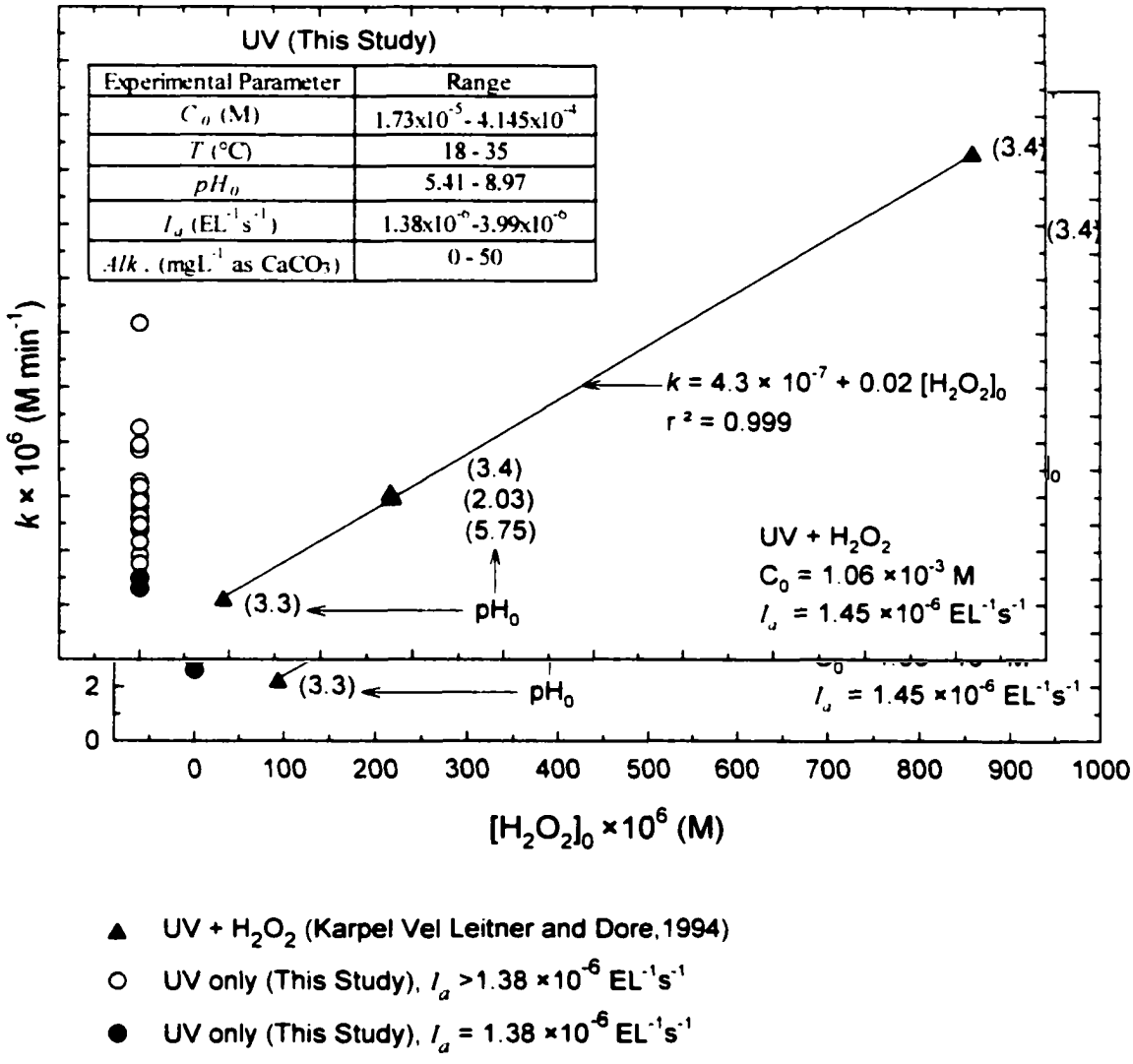

Figure 4.2.1.3. Comparison of $HCO_2^{\cdot}$ Decay Rate Constants Between UV Irradiation (This Study) and UV Irradiation in the Presence of H_2O_2 (Karpel Vel Leitner and Doré(1994)).

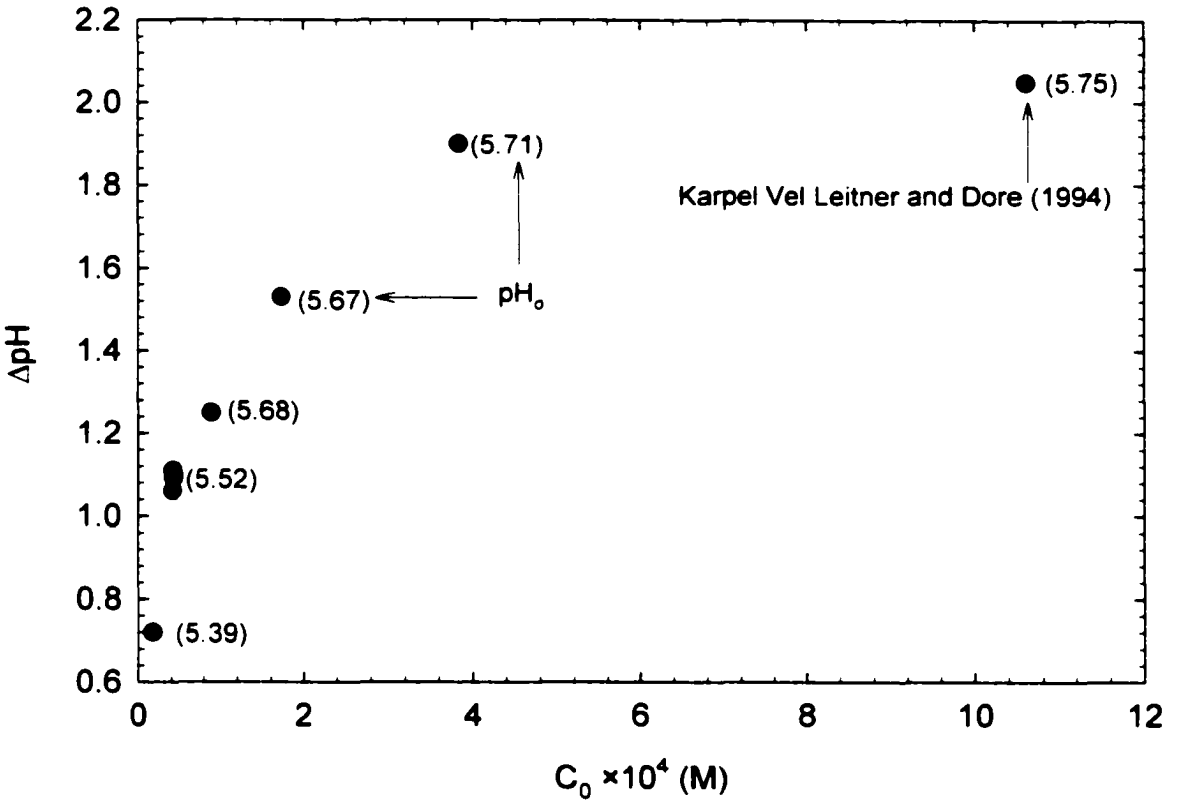

Figure 4.2.1.4. Dependency of ΔpH ($pH_f - pH_0$) on $[HCO_2^-]_0$.

The effect of pH_0 and $[HCO_2^-]_0$ on reaction pH was examined at I_a 2.60 × 10^{-6} $EL^{-1}s^{-1}$, with the results shown in Figure 4.2.1.5. The pH profiles of four experiments at $[HCO_2^-]_0$ = (4.15-4.26) × 10^{-5} M and pH_0 of 5.41 (no adjustment), 7.18, 8.06, and 8.97, adjusted using NaOH, are shown in Figure 4.2.1.5a, along with the HCO_2^- decay profile observed at pH_0 = 5.41. For pH_0< 8.5 ($CO_{3,T}$ = HCO_3^-) the profiles depicted a clear pH "breakpoint" at t ≈ t_b where $[HCO_2^-]$ = BDL as shown in Figure 4.2.1.5a. pH_{max}, observed at $t \leq t_b$, is a linear function of t_{pHmax}/t_b as shown in Figure 4.2.1.5a, and expressed with the correlations shown below:

$$pH_{max} = 8.5 - 2.0 \times (t_{pHmax}/t_b) \qquad (4.2.1.1)$$

The correlations are case specific as they underestimated pH_{max} by 0.7 units at $[HCO_2^-]_0 = 3.83 \times 10^{-4}$ M shown in Figure 4.2.1.5b. Extrapolation of the pH profiles in time depicts a pH_f of about 6.7 which was also observed in Figure 4.2.1.1a for $pH_0 = 5.55$. Figure 4.2.1.5 depicts $[HCO_2^-]$ and pH profiles for two experiments run at $[HCO_2^-]_0$ of 4.26×10^{-5} M (box 4.2.1.5a). and 3.83×10^{-4} M (box 4.2.1.5b) ($I_a = 2.60 \times 10^{-6}$ $EL^{-1}s^{-1}$ and 25 °C) where detailed DO profiles were monitored and shown in Figure 4.2.1.5c. The DO drop in DIW supersaturated in the MilliQ system is shown as "DIW". Lines A and B show that "breakpoint" pH (pH at t_b), DO_{min}, and $[HCO_2^-]$ = BDL occur at t_b. The DO profile remained virtually constant beyond t_b at $[HCO_2^-]_0 = 4.26 \times 10^{-5}$ M, as it reached saturation, whereas at $[HCO_2^-]_0 = 3.83 \times 10^{-4}$ M oxygen uptake began immediately, at 32.4% DO saturation, and continued until data collection was terminated (prior to reaching DO saturation). The pH drop at $t<t_b$ appears to be dependent on $[HCO_2^-]_0$ in Figures 4.2.1.5 (a) and (b). The ΔpH at $[HCO_2^-]_0 = 3.83 \times 10^{-4}$ M was computed as described earlier and plotted in Figure 4.2.1.5 at $pH_0 = 5.71$. Observed DO utilization, corrected for DO loss in "DIW", was 0.48 and 0.46 mol of O_2/ mol of HCO_2^-, for $[HCO_2^-]_0 = 4.26 \times 10^{-5}$ M and 3.83×10^{-4} M, respectively. In addition, at $I_a = 3.99 \times 10^{-6}$ $EL^{-1}s^{-1}$, $[HCO_2^-]_0 = 4.15 \times 10^{-4}$ M, and $pH_0 = 5.81$, DO utilization was found to be 0.53 mol of O_2/ mol of HCO_2^-. This observation in combination with NPOC profiles suggests that the overall reaction stoichiometry can be represented as:

$$HCO_2^- + \tfrac{1}{2} O_2 \rightarrow CO_2 + OH^- \qquad (4.2.1.2)$$

Karpel Vel Leitner and Doré (1994,1996) reported DO utilization of 0.5 moles of O_2/ mole of HCO_2^- during photodecomposition of formic acid in the presence of H_2O_2 (I_a =

1.45×10^{-6} $EL^{-1}s^{-1}$, $[HCO_2^-]_0 = 1.06 \times 10^{-3}$ M, $[H_2O_2]_0 = 9.19 \times 10^{-4}$ M, $pH_0 = 3.4$). Similarities between this study and Karpel Vel Leitner and Doré (1994) in terms of DO utilization and very close rate constants at low H_2O_2 concentration ($[H_2O_2]_0 = 9.34 \times 10^{-5}$ M) (Figure 4.2.1.3) might be due to limited formation of $OH^\bullet$ during the decomposition of HCO_2^- under UV irradiation. This can also explain the increase in HCO_2^- decay rate in the presence of DO. Karpel Vel Leitner and Doré (1994) proposed that in the presence of DO, $OH^\bullet$ produced from H_2O_2 by UV irradiation reacts with formic acid to form $\bullet COO^-$ /•COOH which combines with DO to form $HO_2^\bullet/O_2^\bullet$ and CO_2. H_2O_2 is then regenerated from $HO_2^\bullet$ radicals. The same authors also suggested that in the absence of DO, $\bullet COO^-$ /•COOH radicals react with H_2O_2, instead of oxygen, producing CO_2 and $OH^\bullet$. It could be surmised that in the presence of DO, UV photolysis of HCO_2^- could result in $CO_2^{\bullet-}$ formation via hydrogen abstraction followed by formation of $O_2^{\bullet-}$ from the reaction between $CO_2^{\bullet-}$ and DO. $O_2^{\bullet-}$ radicals then hydrolyze to $HO_2^\bullet$, which leads to H_2O_2 formation. Finally, $OH^\bullet$ is regenerated by photolysis of H_2O_2.

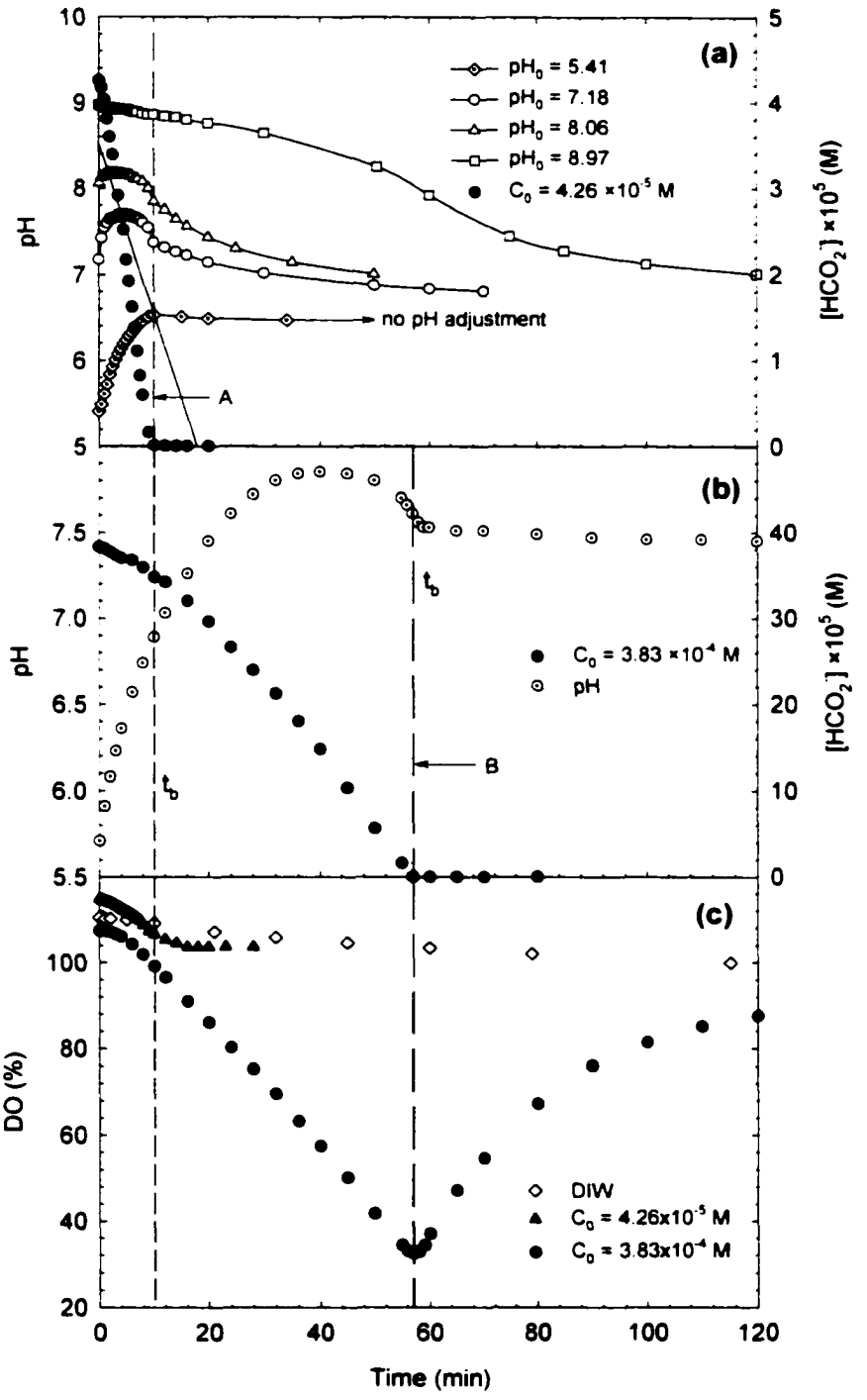

Figure 4.2.1.5. **(a)** Dependency of pH Profile on pH_0 (I_a = 2.60 × 10^{-6} $EL^{-1}s^{-1}$, C_0 = (4.15-4.26) × 10^{-4} M, T = 25 °C). **(b)** Concentration and pH Profiles During UV Irradiation of HCO_2^- (I_a = 2.60 × 10^{-6} $EL^{-1}s^{-1}$, C_0 = 3.83 × 10^{-4} M, pH_0 = 5.71, T = 25°C), and **(c)** DO Loss from DIW at 25 °C and DO Profiles for the Experiments Depicted in Boxes (a) and (b).

4.2.2. Oxalate

Figure 4.2.2.1 shows observed $C_2O_4^{2-}$, NPOC and pH profiles in the course of two experiments involving solutions of $Na_2C_2O_4$ (box a) and {$Na_2C_2O_4$ + $NaHCO_3$} (box b). NPOC, which is a measure of the non-volatile DOM, also decreased in the course of the reaction closely following the $C_2O_4^{2-}$ profile in the early stages of the reaction, to later reach steady but trace levels as $C_2O_4^{2-}$ reached BDL (Figure 4.2.2.1, box a), while TC, which includes CO_2, was stable during $C_2O_4^{2-}$ decay in another experiment (Figure 4.2.2.1, box c). The DO profile was monitored during the experiment at 2.60×10^{-6} $EL^{-1}s^{-1}$, 25 °C, $C_0 = 21.11 \times 10^{-5}$ M with the results shown in Figure 4.2.2.2 (box a) along with $[C_2O_4^{2-}]$ and pH profiles and the DO drop in supersaturated MilliQ water. The DO dropped up to 2/3 $C_2O_4^{2-}$ conversion and began to rise when the uptake rate exceeded the rate of DO consumption at lower $C_2O_4^{2-}$ concentrations. The DO utilization during $C_2O_4^{2-}$ decay ranged between 0.8 – 0.3 mol O_2 / mol $C_2O_4^{2-}$. The absorption spectra of the samples were also generated during UV irradiation of $Na_2C_2O_4$. As depicted in Figure 4.2.2.2 (b), absorbance of the kinetic samples at 190, 200, 220 and 253.7 nm decreased with $C_2O_4^{2-}$ decay. Comparison of NPOC and $C_2O_4^{2-}$, measured at the same contact times in all experiments is shown in Figure 4.2.2.3. The data between 8.3×10^{-5} and 1.7×10^{-4} M as C were obtained at $C_0 = 8.75 \times 10^{-5}$ M. At low concentrations, NPOC is slightly higher than $C_2O_4^{2-}$, albeit with very limited scatter. Since NPOC that is measured following stripping of CO_2 from water by bubbling CO_2-free air followed $C_2O_4^{2-}$ profile closely and TC remained constant in the reactor, the carbon not accounted for in NPOC is likely to have been converted to CO_2.

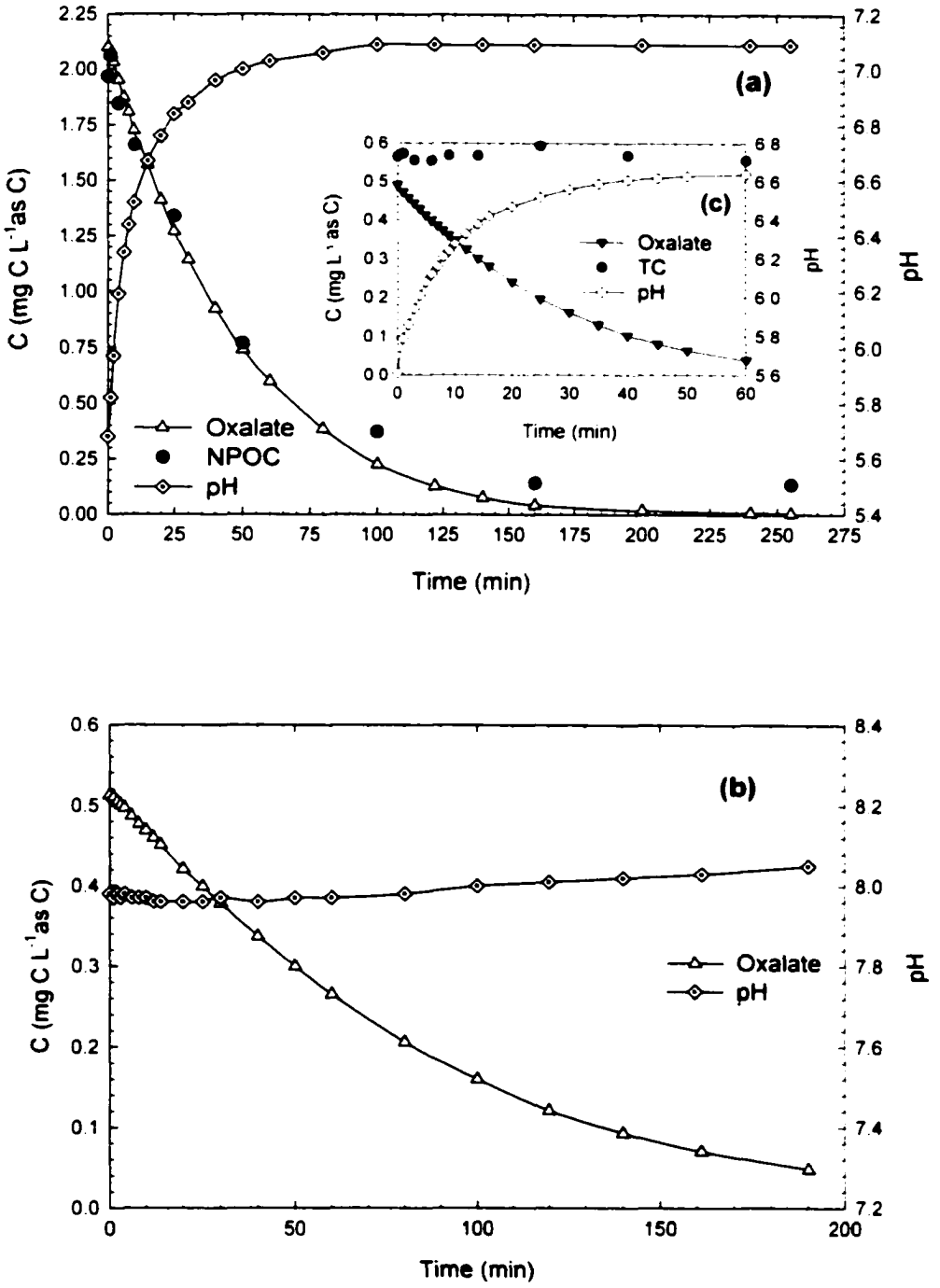

Figure 4.2.2.1.Concentration and pH Profiles During UV Irradiation (253.7 nm) of $C_2O_4^{2-}$ in **(a)** DIW (I_a = 2.60 × 10^{-6} $EL^{-1}s^{-1}$, C_0 = 8.75 × 10^{-5} M, pH_0 = 5.68, T = 25°C), and **(b)** DIW Containing $NaHCO_3$ = 50 mgL^{-1} as $CaCO_3$ (I_a = 2.60×10^{-6} $EL^{-1}s^{-1}$, C_0 = 2.14 × 10^{-5} M, pH_0 = 7.98, T = 25°C). **(c)** DIW (I_a = 2.60 × 10^{-6} $EL^{-1}s^{-1}$, C_0 = 2.05 × 10^{-5} M, pH_0 = 5.61, T = 25°C).

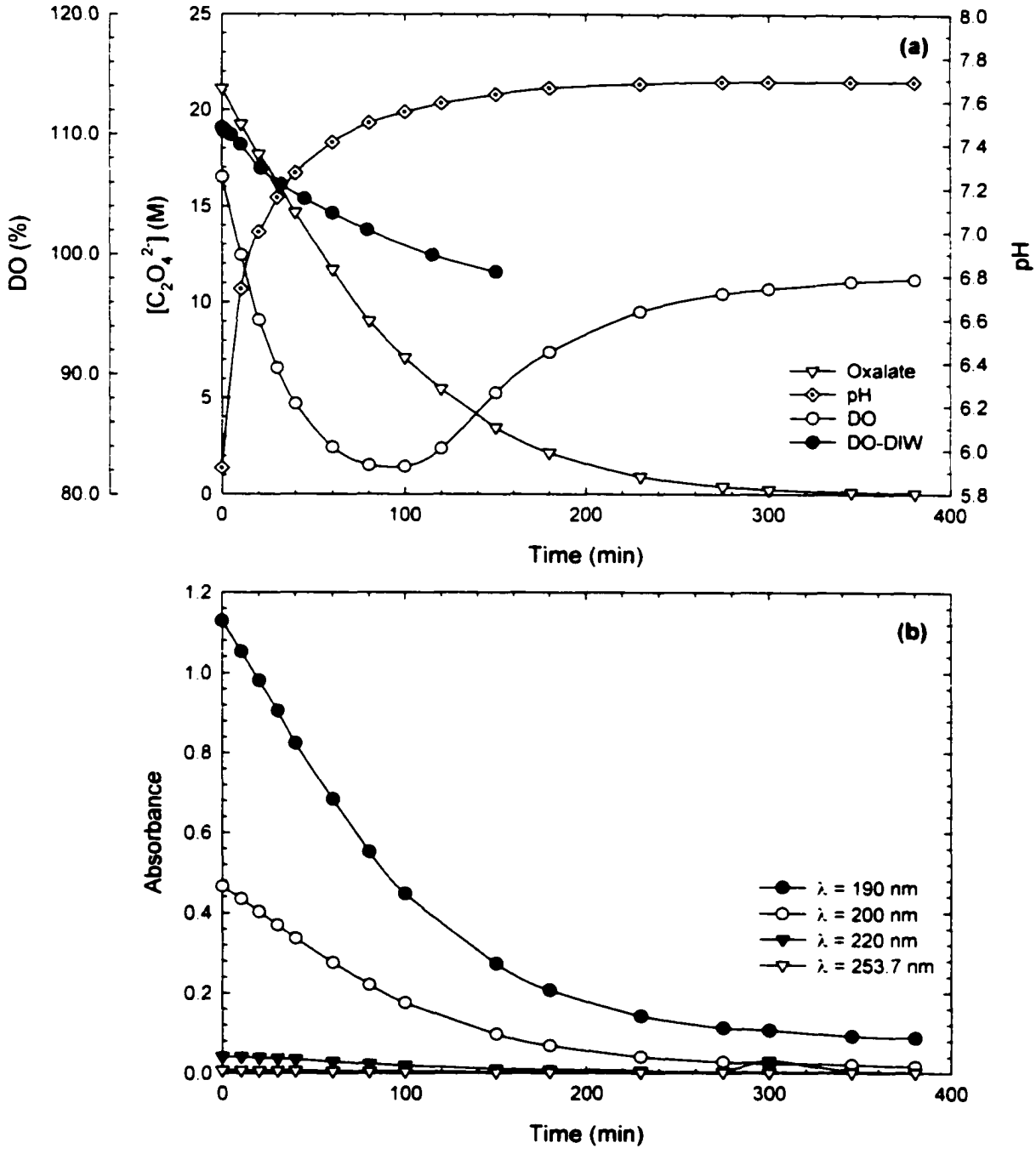

Figure 4.2.2.2. **(a)** $[C_2O_4^{2-}]$, pH and DO Profiles During UV Irradiation (253.7 nm) of $C_2O_4^{2-}$ in DIW (I_a = 2.60 × 10^{-6} $EL^{-1}s^{-1}$, C_0 = 2.11 × 10^{-3} M, pH_0 = 5.92, T = 25°C) and DO Loss from DIW at 25 °C, **(b)** Absorbance of Samples at Various Wavelengths During UV Irradiation of $C_2O_4^{2-}$.

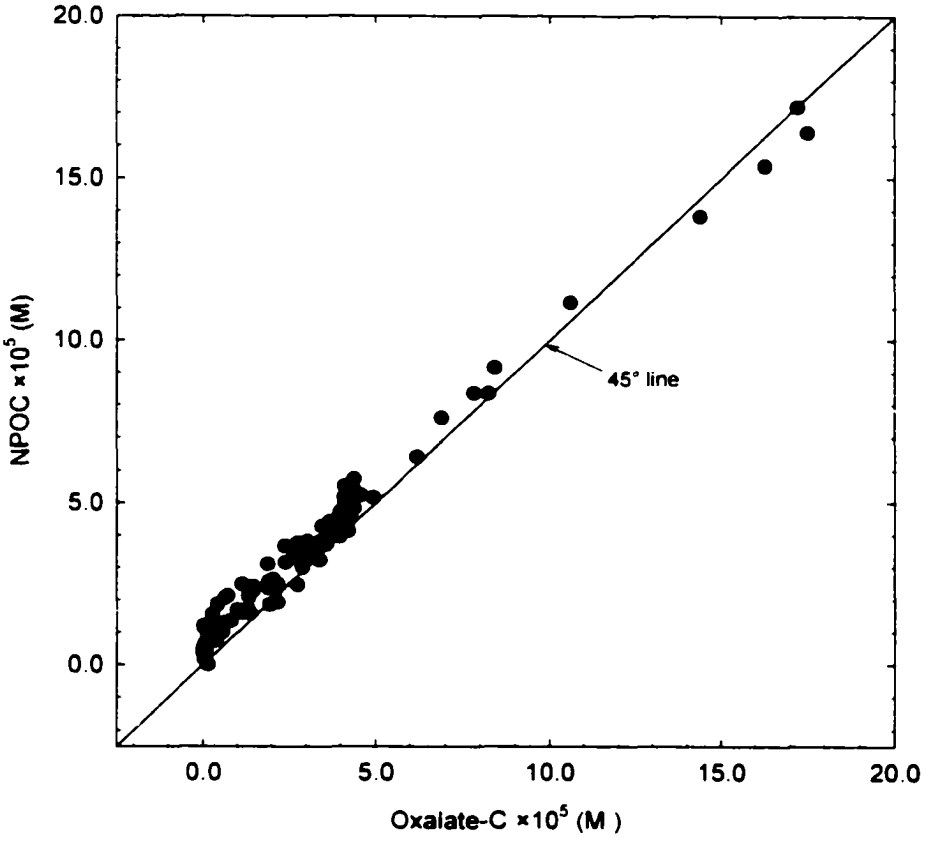

Figure 4.2.2.3. Comparison of Observed NPOC and $C_2O_4^{2-}$ Concentrations.

The reaction pH in $Na_2C_2O_4$ solution increased rapidly during irradiation, reaching a plateau at $C_2O_4^{2-}$ conversion >90 percent while, overall pH change ($\Delta pH = pH_f - pH_0$) increased with $[C_2O_4^{2-}]_0$ (Figure 4.2.2.4). $NaHCO_3$ addition (pH_0>7.0) virtually eliminated this pH change (Figure 4.2.2.1, box b).

During irradiation of solution with pH_0 adjustment the reaction pH decreased with oxalate decay and reached a plateau at $[C_2O_4^{2-}] \approx$ BDL as depicted in Figure 4.2.2.5 where pH_0 = 5.45 represents reaction pH profile without pH_0 adjustment.

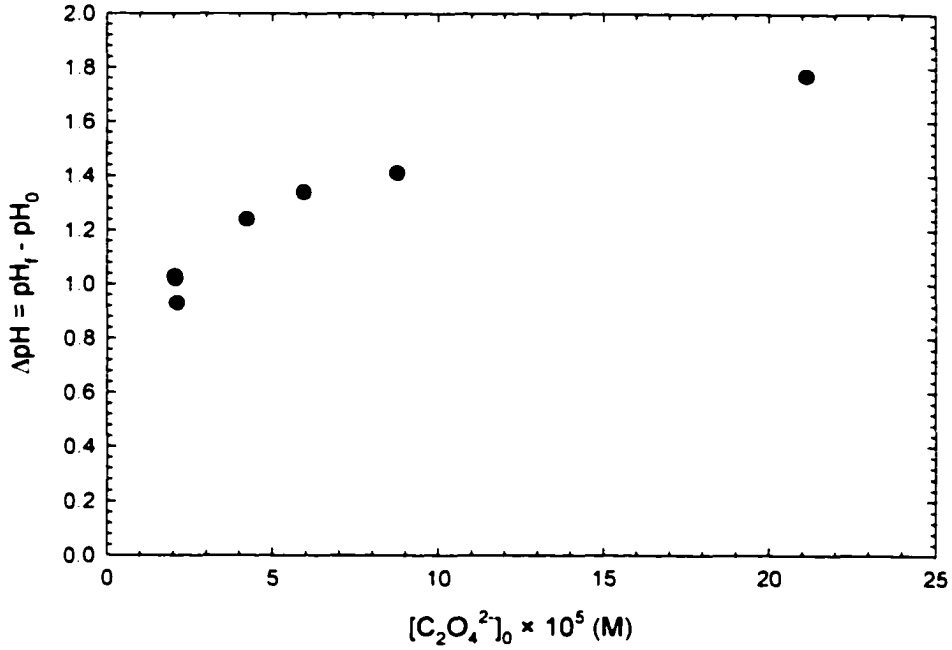

Figure 4.2.2.4. Dependency of ΔpH ($pH_f - pH_0$) on $[C_2O_4^{2-}]_0$ During $C_2O_4^{2-}$ Decay.

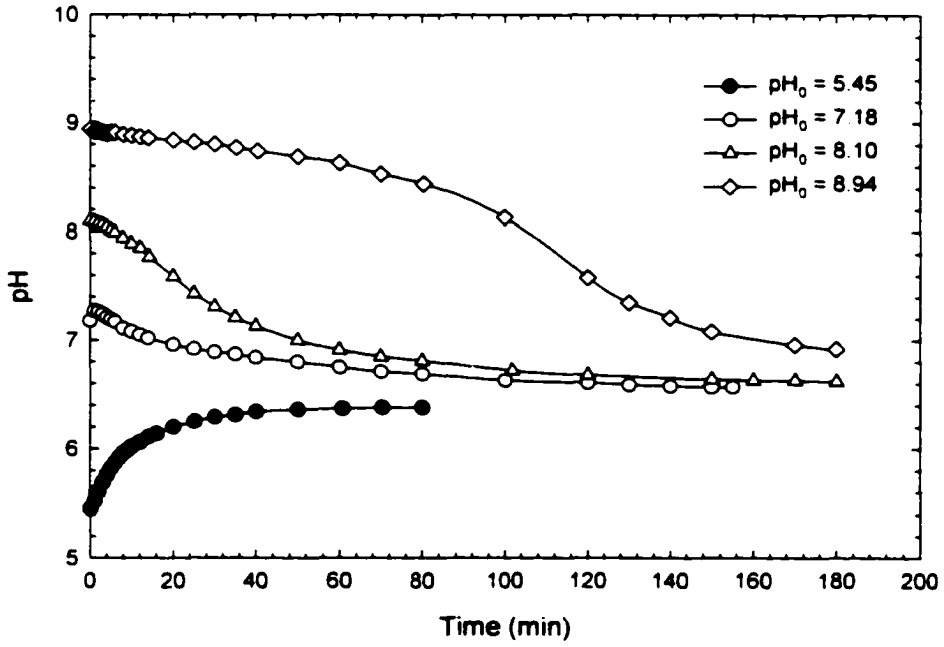

Figure 4.2.2.5. Dependency of pH Profile During $C_2O_4^{2-}$ Decay on pH_0 (I_a = 2.60 × 10^{-6} $EL^{-1}s^{-1}$. $[C_2O_4^{2-}]_0$ = (2.04 – 2.19) × 10^{-5} M. T = 25°C).

The kinetic analysis of the oxalate-time profile in Figure 4.2.2.1a is shown in Figure 4.2.2.6. Zero order kinetics described only the initial rate of oxalate decay as shown in Figure 4.2.2.6a, while pseudo-first order kinetics revealed split rate reaction as shown in Figure 4.2.2.6b, with k_1 and k_2 as corresponding observed rate constants. The later approach was adapted in the analysis. Excluding the experiments with {$Na_2C_2O_4$ + $NaHCO_3$} and {$Na_2C_2O_4$ + PPFE (pilot plant filter effluent)}, the average percent conversion of $C_2O_4^{2-}$ where the rate change from k_1 to k_2 occurred was 56 ± 5.1, and $k_1 < k_2$ at all times. The value of k_1 ranged between 0.01 and 0.07 min^{-1}, while k_2 ranged between 0.02 and 0.10 min^{-1} at 25°C and no pH_0 adjustment. The ratio of k_1/k_2 remained relatively constant throughout all the experiments at 25 °C (0.75 ± 0.08) while it increased with temperature as depicted in Figure 4.2.2.7. The same kinetic behavior in $C_2O_4H_2$ decay was observed in data manually extracted from Figure 4.4 of Karpel Vel Leitner and Doré (1997) involving UV irradiation of a mixture of $[C_2O_4H_2]_0 = 1.0 \times 10^{-3}$ M and $[H_2O_2]_0 = 9.4 \times 10^{-4}$ M in DIW at pH_0 of 2.9 in the presence and absence of oxygen, as shown in Figures 4.2.2.8a and 4.2.2.8b. The values of k_1 and k_2 were $8.08 \times 10^{-3} min^{-1}$ and 11.14×10^{-3} min^{-1} in the presence and 9.0×10^{-3} min^{-1} and 10.51×10^{-3} min^{-1} in the absence of oxygen, respectively, all much lower than the values observed in this study. At pH = 5.6 and same initial conditions, in absence of O_2, the initial decay rate of $C_2O_4^{2-}$ was 1.96×10^{-3} min^{-1} with no second reaction step.

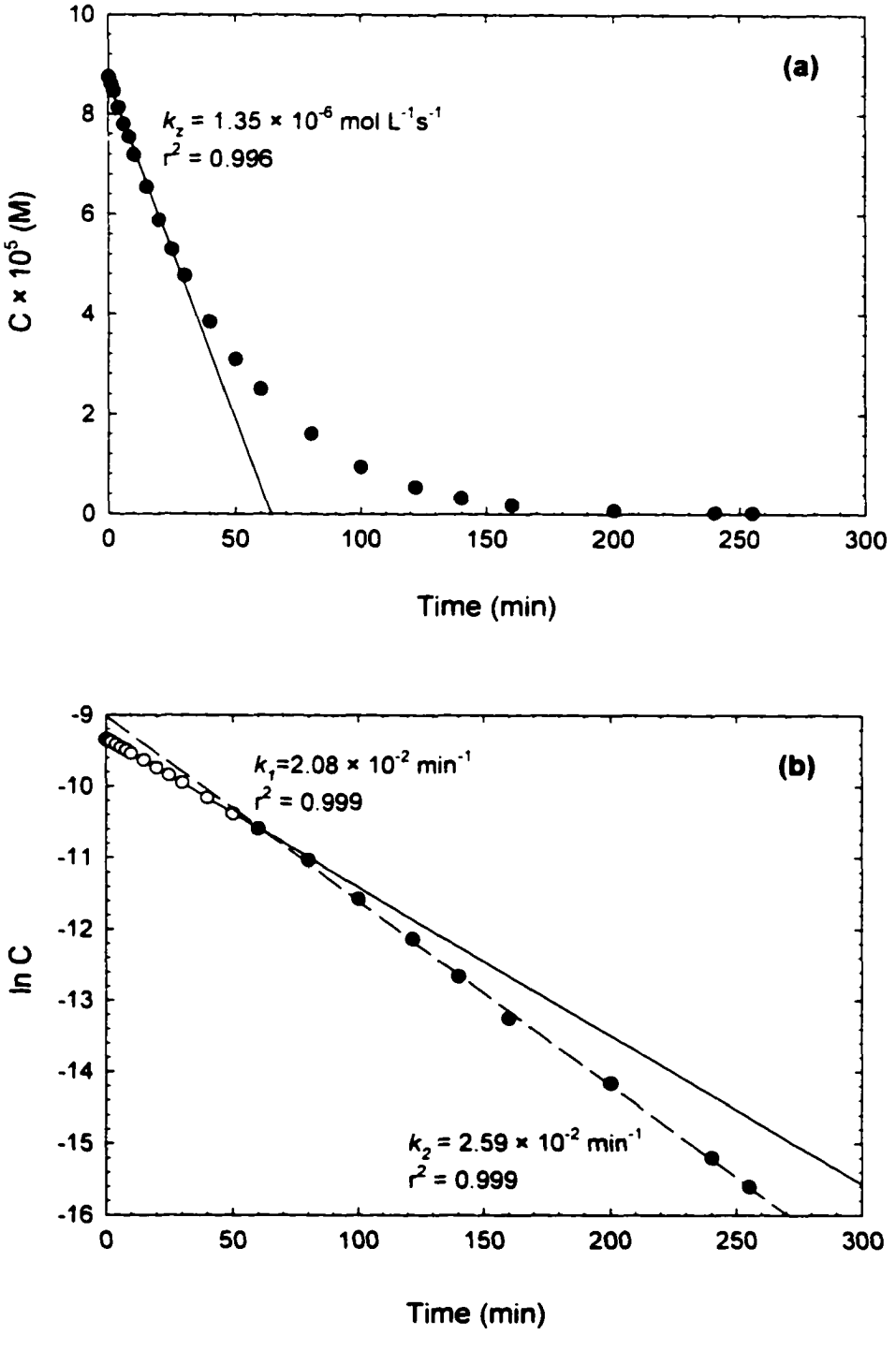

Figure 4.2.2.6. Kinetic Analysis of the $C_2O_4^{2-}$ Data **(a)** Zero-Order, and **(b)** Pseudo-First Order (I_a = 2.60 × 10^{-6} EL^{-1}s^{-1}, C_0 = 8.75 × 10^{-5} M, pH_0 = 5.68, T = 25°C).

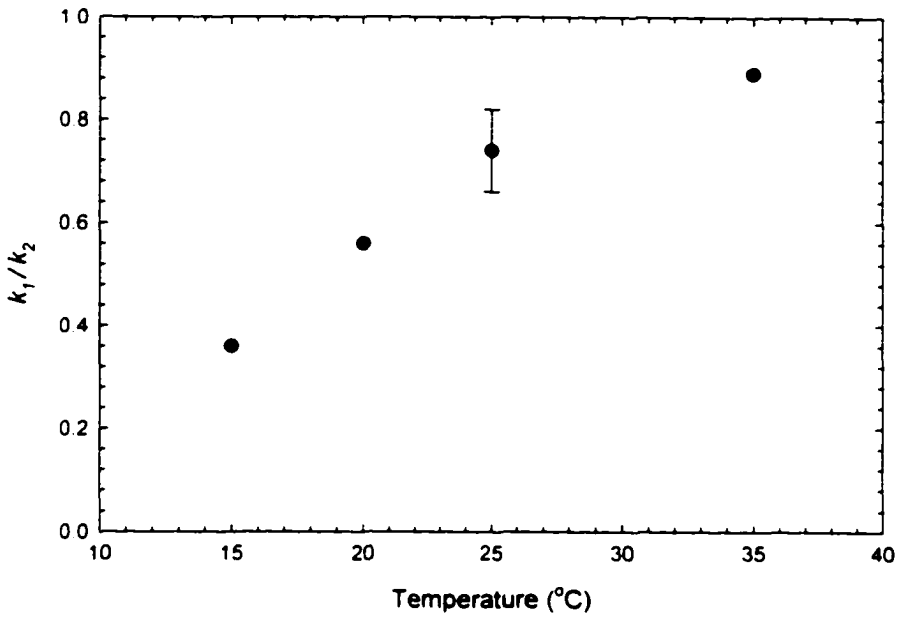

Figure 4.2.2.7. Temperature Dependency of k_1/k_2.

The observed decay rate of oxalate can be empirically formulated as:

$$dC_{OX}/dt = - k C_{OX} \quad (4.2.2.1)$$

where

$$k = f k_1 + (1\text{-}f) k_2 \quad (4.2.2.2)$$

C_{OX} is the molar oxalate concentration while k_1 and k_2 are the pseudo-first order rate constants described earlier. Coefficient "f" was estimated to be 0.8 based on data of one experiment without initial pH adjustment. The empirical formulation

$$C_{OX} = C_{OX,o}\, e^{-(0.8 k_1 + 0.2 k_2)} \quad (4.2.2.3)$$

was then used to predict observed oxalate profiles at various initial conditions and all four UV intensities studied with the results shown in Figure 4.2.2.9. Application of this formulation would necessitate estimation of "f" specific to the water matrix at hand.

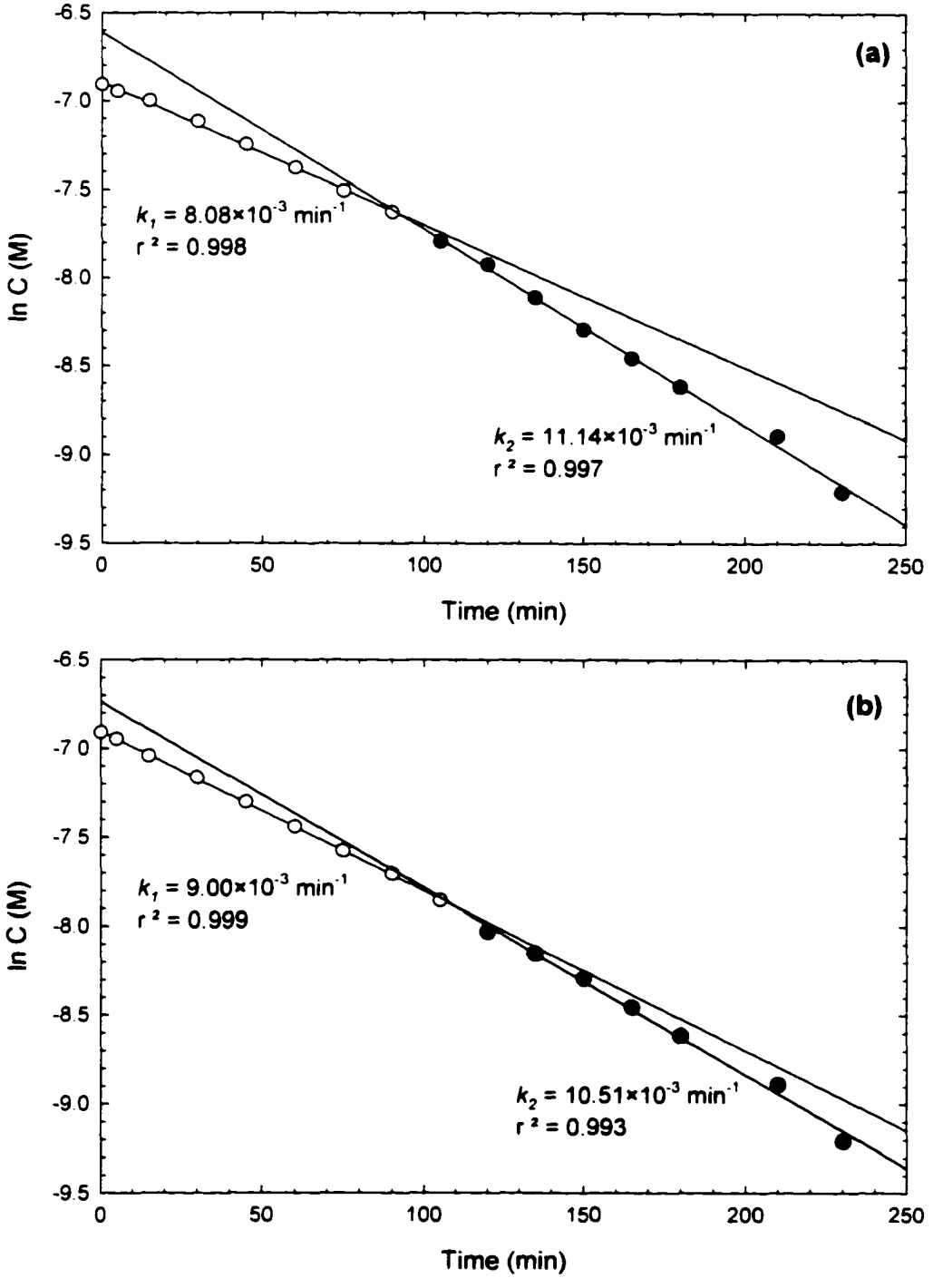

Figure 4.2.2.8. UV Irradiation of Oxalic Acid and Hydrogen Peroxide Mixture in DIW at pH_0=2.9, with Initial Concentrations $[C_2O_4H_2]_0 = 1.0\times10^{-3}$ M, $[H_2O_2]_0 = 9.4\times10^{-4}$ M in The **(a)** Presence of Oxygen, and **(b)** Absence of Oxygen (Karpel vel Leitner and Doré, 1997).

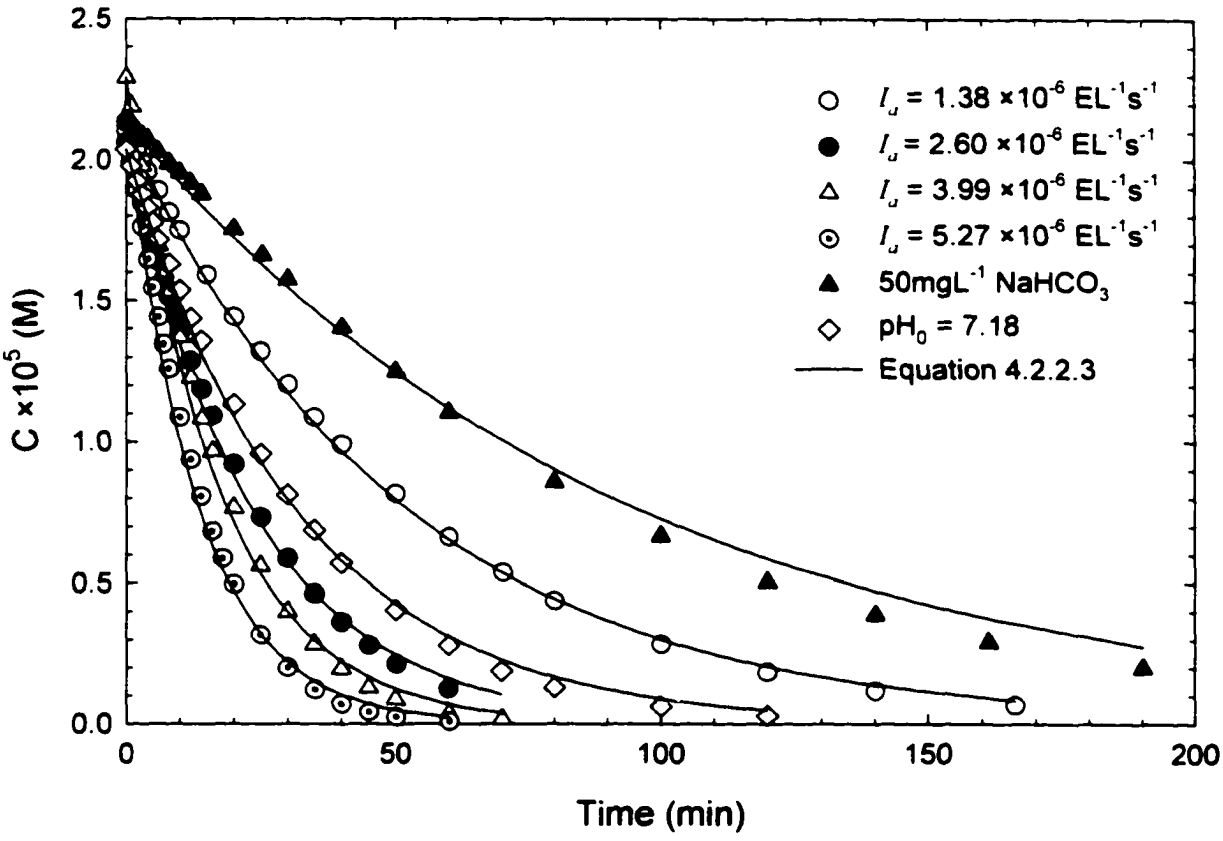

Figure 4.2.2.9. Comparison of Observed $C_2O_4^{2-}$ Concentration Profiles at Various Experimental Conditions with Prediction of Empirical Kinetic Formulation (Equation 4.2.2.3).

4.2.3. Glyoxalate

$HC_2O_3^-$ readily decomposed to formate (HCO_2^-) and oxalate ($C_2O_4^{2-}$). Figures 4.2.3.1, 4.2.3.2 and 4.2.3.3 show typical time profiles of $[HC_2O_3^-]$, NPOC, pH, $[C_2O_4^{2-}]$, $[HCO_2^-]$, and the kinetic analysis $HC_2O_3^-$ decomposition at I_a of 2.60×10^{-6} E $L^{-1}s^{-1}$ and 25°C. NaOH solution was used to adjust pH_0 to 9.10 in the experiments depicted in Figure 4.2.3.2. Figure 4.2.3.3 depicts the profiles of an experiment conducted in the presence of 25 mg L^{-1} $NaHCO_3$ as $CaCO_3$. Both HCO_2^- and $C_2O_4^{2-}$ gradually formed in all experiments, with clear maxima occurring at $[HC_2O_3^-] \approx [C_2O_4^{2-}]$ and $[HCO_2^-] \approx$ BDL, respectively, and decayed to form CO_2 and H_2O as reported in Chapters 4.2.1 and 4.2.2. $[C_2O_4^{2-}]_{max}$ and $[HCO_2^-] \approx$ BDL occurred virtually concurrently. $[C_2O_4^{2-}]_{max}$ and $[HCO_2^-]_{max}$ were found to be linear functions of $[HC_2O_3^-]_0$ as shown in Figure 4.2.3.4, and expressed with correlations 4.2.3.1 and 4.2.3.2 below:

$$[C_2O_4^{2-}]_{max} = 5.44 \times 10^{-6} + 0.59 \times [HC_2O_3^-]_0 \qquad (4.2.3.1)$$

$$[HCO_2^-]_{max} = -2.85 \times 10^{-6} + 0.31 \times [HC_2O_3^-]_0 \qquad (4.2.3.2)$$

The total measured organic carbon (TMOC = $[HC_2O_3^-$-C] + $[C_2O_4^{2-}$-C] + $[HCO_2^-$-C]) decreased during photodecomposition, while NPOC closely following TMOC. This indicates that $C_2O_4^{2-}$ and HCO_2^- are the non-purgeable major intermediates during $HC_2O_3^-$ decomposition. In a separate experiment run at $[HC_2O_3^-]_0 = 2.05 \times 10^{-4}$ M (I_a = 2.60×10^{-6} $EL^{-1}s^{-1}$, pH_0 = 6.01 and 25 °C) TC was also monitored along with NPOC during $HC_2O_3^-$ decay (Figure 4.2.3.5). As depicted in Figure 4.2.3.5a, NPOC profile

followed TMOC while TC gradually decayed during irradiation of $HC_2O_3^-$. At $[HC_2O_3^-] \approx$ BDL about 50 % of TC was unaccounted for. This suggests the possibility of formation of volatile products during $HC_2O_3^-$ decay. The DO profile was also monitored during the experiment with the results shown in Figure 4.2.3.5b. DO in the reactor decreased until $[HC_2O_3^-] \approx$ BDL and $[C_2O_4^{2-}] = [C_2O_4^{2-}]_{max}$ followed by DO increase. Observed DO utilization was 0.6 mol O_2 /mol $HC_2O_3^-$. Figure 4.2.3.5c shows absorbance of the kinetic samples at wavelengths of 190, 200, 220 and 253.7 nm. Absorbance at t = 0 represents $HC_2O_3^-$ solution. As $HC_2O_3^-$ decayed, absorbance at each wavelength increased and reached a maximum when $[HC_2O_3^-] \approx$ BDL and $[C_2O_4^{2-}] = [C_2O_4^{2-}]_{max}$ to later decreased with $C_2O_4^{2-}$ decay. The increase in absorbance values can be due to $C_2O_4^{2-}$ formation. Time profiles of $[HC_2O_3^-]$ followed split rate pseudo-zero order kinetics, as shown in Figures 4.2.3.1b, 4.2.3.2b and 4.2.3.3b, with the split between observed rate constants k_1 and k_2 ($k_1 > k_2$) occurring at average percent $HC_2O_3^-$ conversion of 55 ± 4. The values of k_1 and k_2 ranged between (1.9 – 6.5) $\times 10^{-6}$ M min^{-1}, and (0.7 – 3.7) $\times 10^{-6}$ M min^{-1}, respectively.

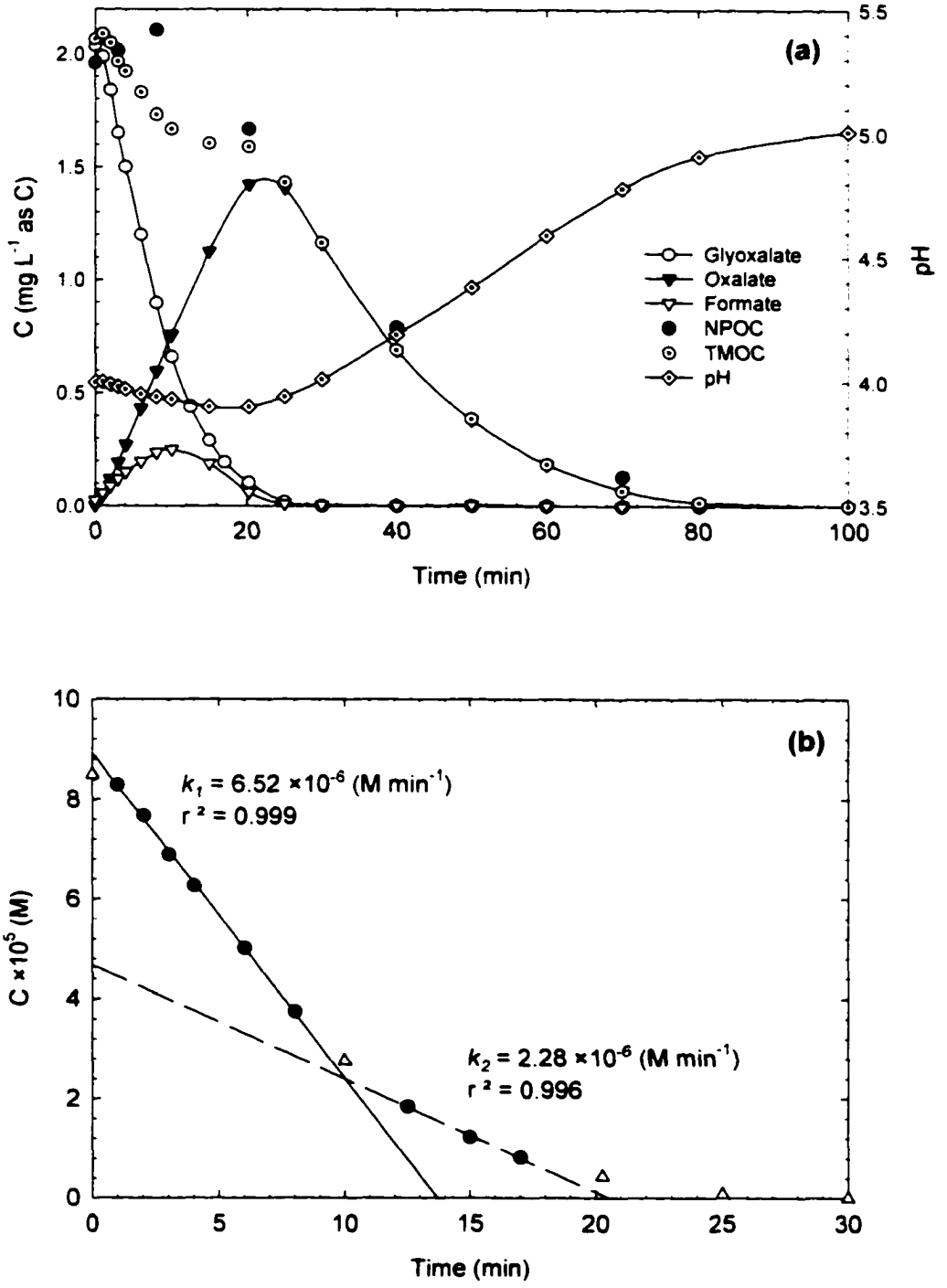

Figure 4.2.3.1. **(a)** Concentration and pH Profiles During UV Irradiation of $HC_2O_3^-$ in DIW; **(b)** Kinetic Analysis of the $HC_2O_3^-$ Data (I_a = 2.60 × 10^{-6} E L^{-1} s^{-1}, C_0= 8.49 × 10^{-5} M, pH_0 = 4.00, T = 25°C).

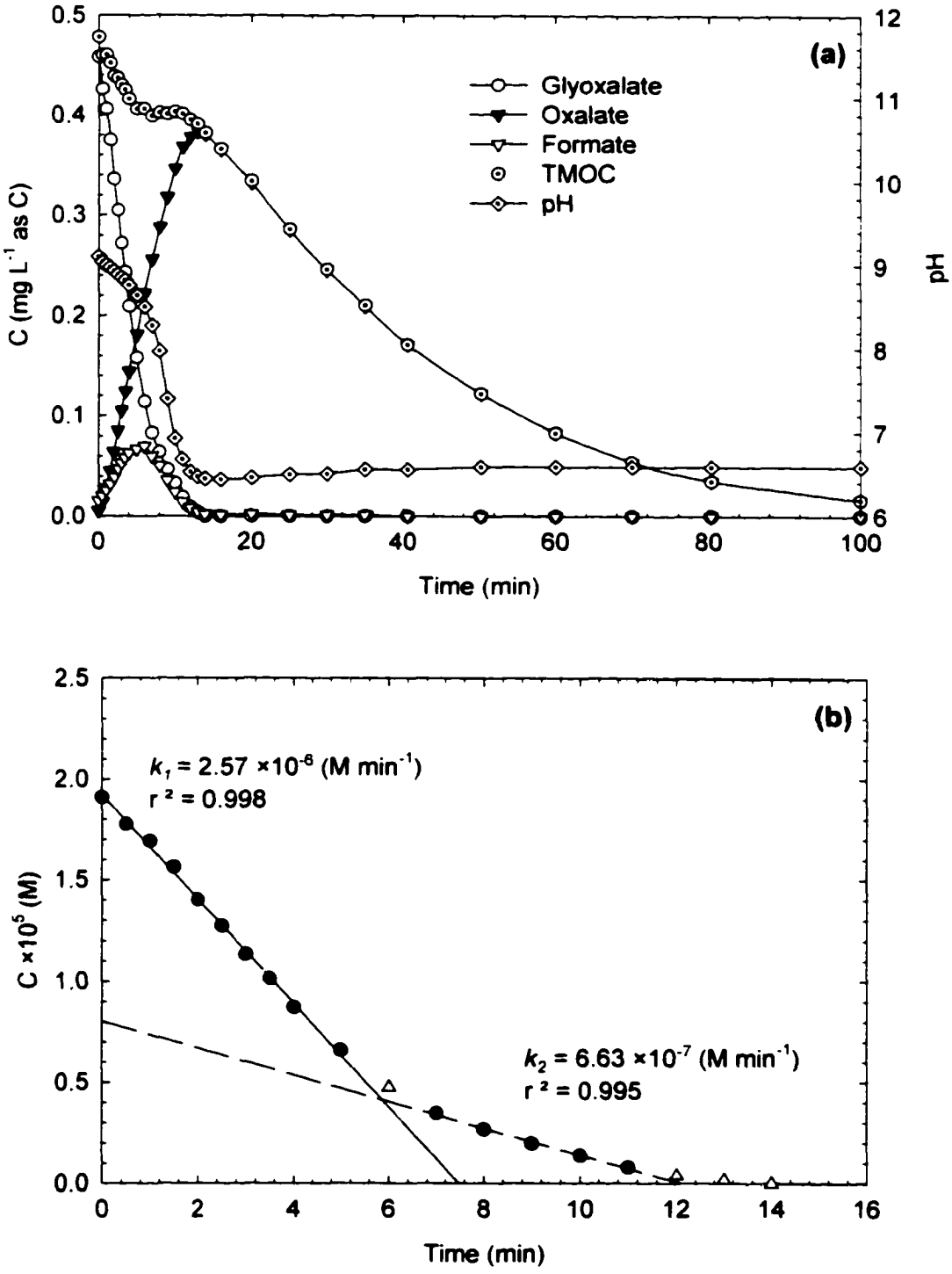

Figure 4.2.3.2. **(a)** Concentration and pH Profiles During UV Irradiation of $HC_2O_3^-$ in DIW at pH_0 Adjusted to 9.10 with Concentrated NaOH; **(b)** Kinetic Analysis of the $HC_2O_3^-$ Data ($I_a = 2.60 \times 10^{-6}$ E L^{-1} s^{-1}, $C_0 = 1.91 \times 10^{-5}$ M, $pH_0 = 9.10$, T = 25°C).

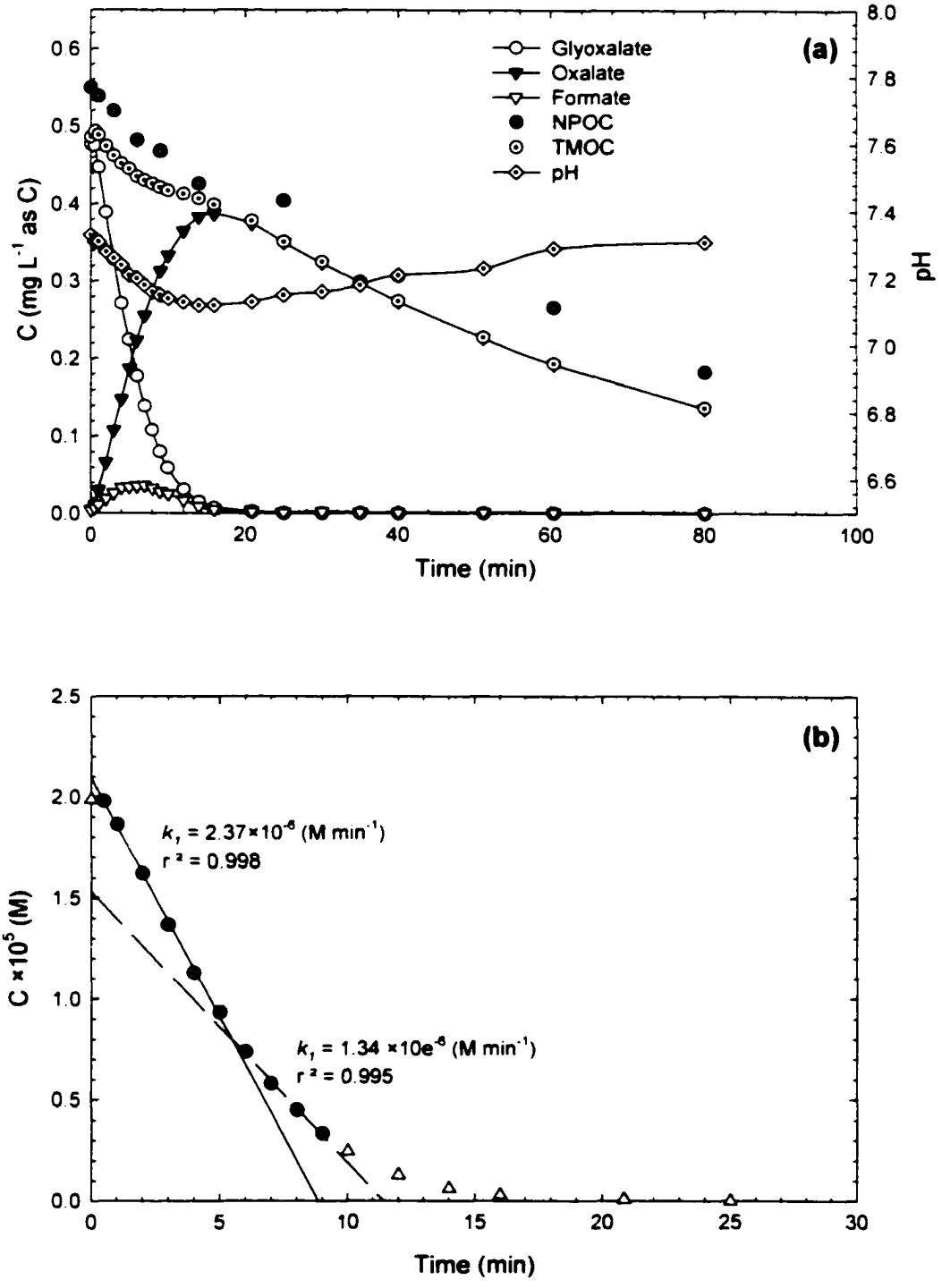

Figure 4.2.3.3. **(a)** Concentration and pH Profiles During UV Irradiation of $HC_2O_3^-$ in DIW Containing $NaHCO_3$ = 25 mgL^{-1} as $CaCO_3$; **(b)** Kinetic Analysis of the $HC_2O_3^-$ Data ($I_a = 2.60 \times 10^{-6}$ E L^{-1} s^{-1}, $C_0 = 1.99 \times 10^{-5}$ M, $pH_0 = 7.33$, T = 25°C).

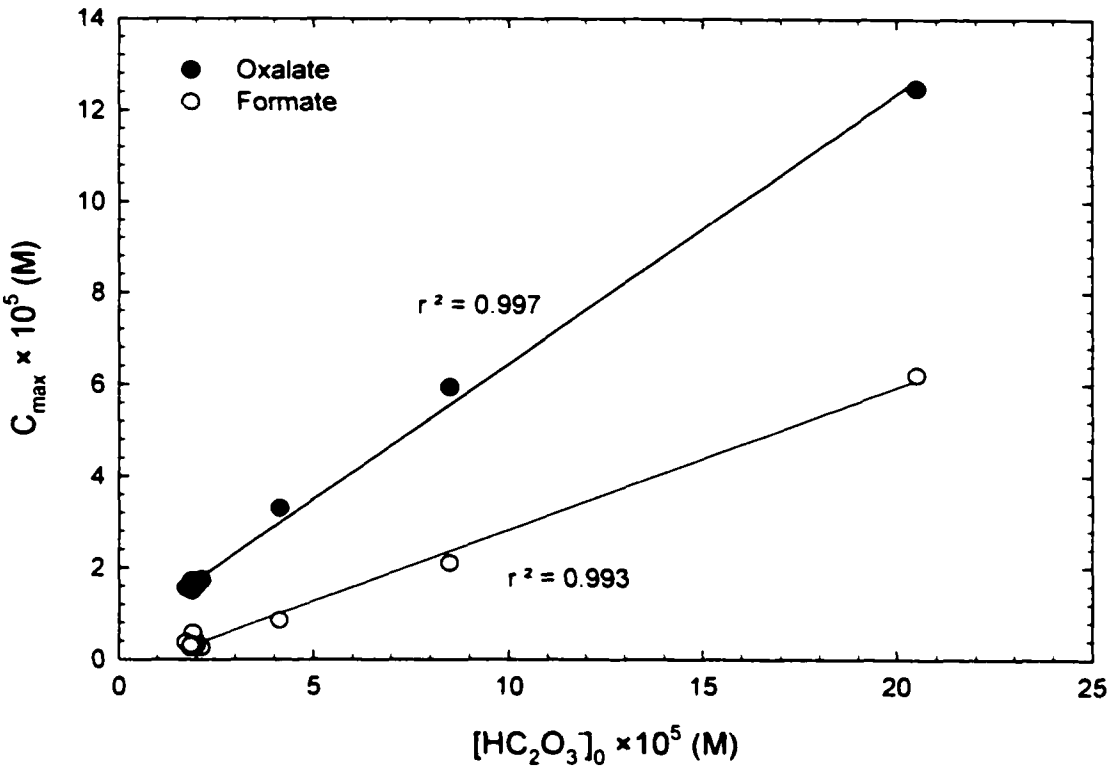

Figure 4.2.3.4. Dependency of $[C_2O_4^{2-}]_{max}$ and $[HCO_2^-]_{max}$ on $[HC_2O_3^-]_0$.

Figure 4.2.3.6 depicts $[HC_2O_3^-]$, $[C_2O_4^{2-}]$ and $[HCO_2^-]$ profiles (box a), the kinetic analysis of $[HC_2O_3^-]$ (box b) and comparison of $[HC_2O_3^-]$ with $\{[C_2O_4^{2-}] + [HCO_2^-]\}$ (box c) for an experiment conducted at 2.60×10^{-6} $EL^{-1}s^{-1}$ and 25 °C with $[HC_2O_3^-]_0 = 1.87 \times 10^{-5}$ M. At $t=t_c$, where the switch of observed decay rate constant from k_1 to k_2 begins, $[HC_2O_3^-] \approx [C_2O_4^{2-}] + [HCO_2^-]$. This is the characteristic of all experiments (except the ones with $[HC_2O_3^-]_0 = 4.13 \times 10^{-5}$ and 8.49×10^{-5} M) as depicted in Figure 4.2.3.7 where $[HC_2O_3^-]$ and $\{[C_2O_4^{2-}] + [HCO_2^-]\}$ are compared at $t<t_c$ (box a), $t=t_c$ (box b) and $t>t_c$ (box c). At $t<t_c$ $[HC_2O_3^-] > \{[C_2O_4^{2-}] + [HCO_2^-]\}$ while at $t > t_c$ $[HC_2O_3^-] < \{[C_2O_4^{2-}] + [HCO_2^-]\}$.

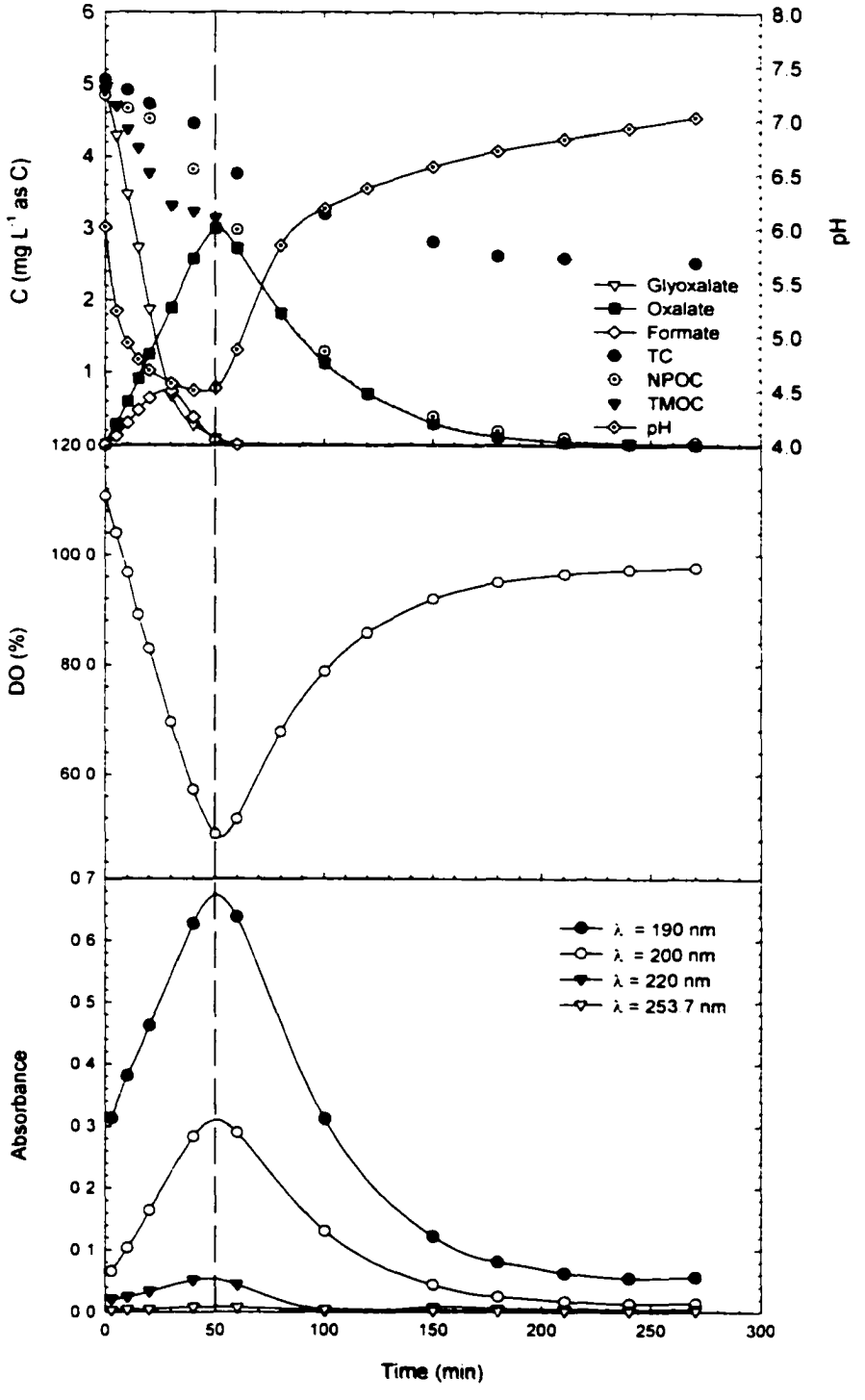

Figure 4.2.3.5. **(a)** Concentration and pH Profiles; **(b)** DO Profile; **(c)** Absorbance of The Samples at Various Wavelengths During UV Irradiation of $HC_2O_3^-$ in DIW [(I_a = 2.60 × 10^{-6} E L^{-1} s^{-1}, C_0= 2.05 × 10^{-4} M, pH_0 = 6.01, T = 25°C).

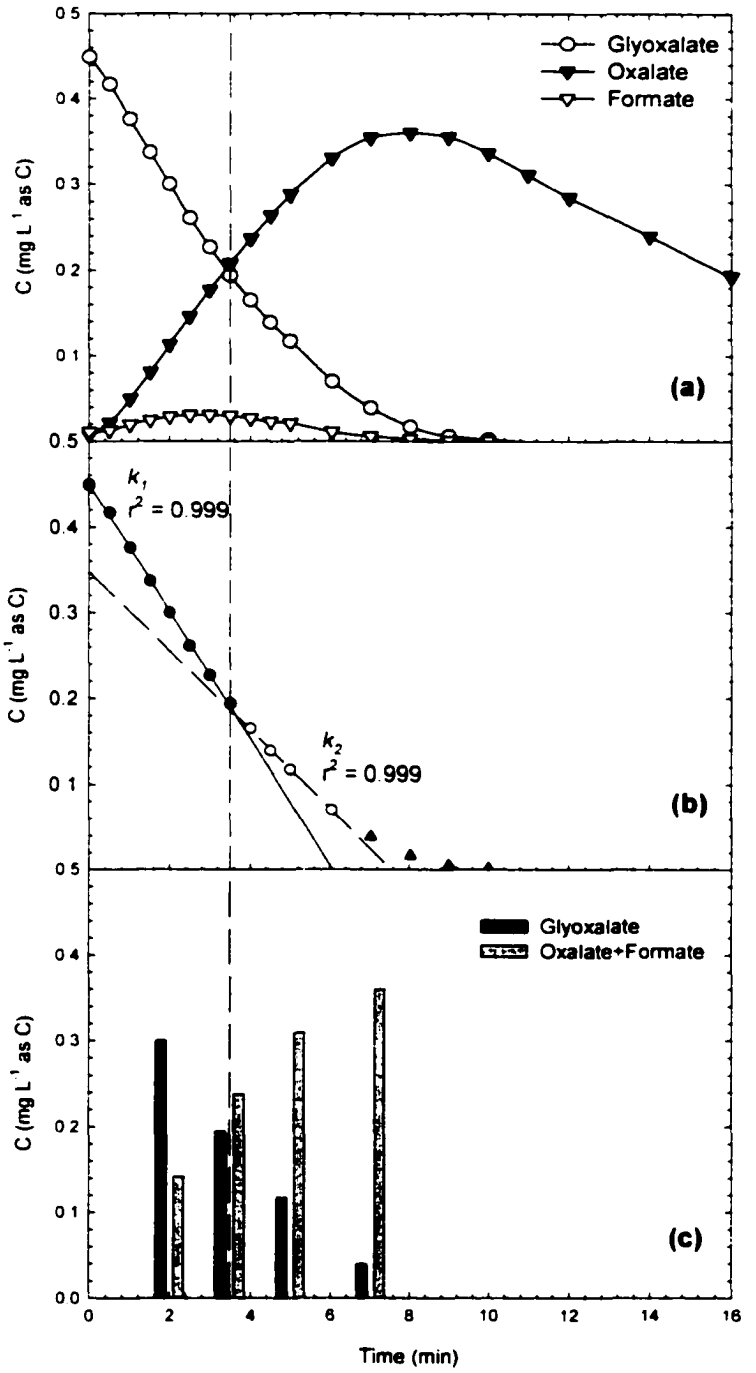

Figure 4.2.3.6. **(a)** Concentration and pH Profiles During UV Irradiation of $HC_2O_3^-$ in DIW; **(b)** Kinetic Analysis of the $HC_2O_3^-$ Data; **(c)** Comparison of $[HC_2O_3^-]$ and $\{[C_2O_4^{2-}] + [HCO_2^-]\}$ at Various Irradiation Times [(I_a = 2.60 × 10^{-6} E L^{-1} s^{-1}, C_0= 1.87 × 10^{-5} M, pH_0 = 4.53, T = 25°C).

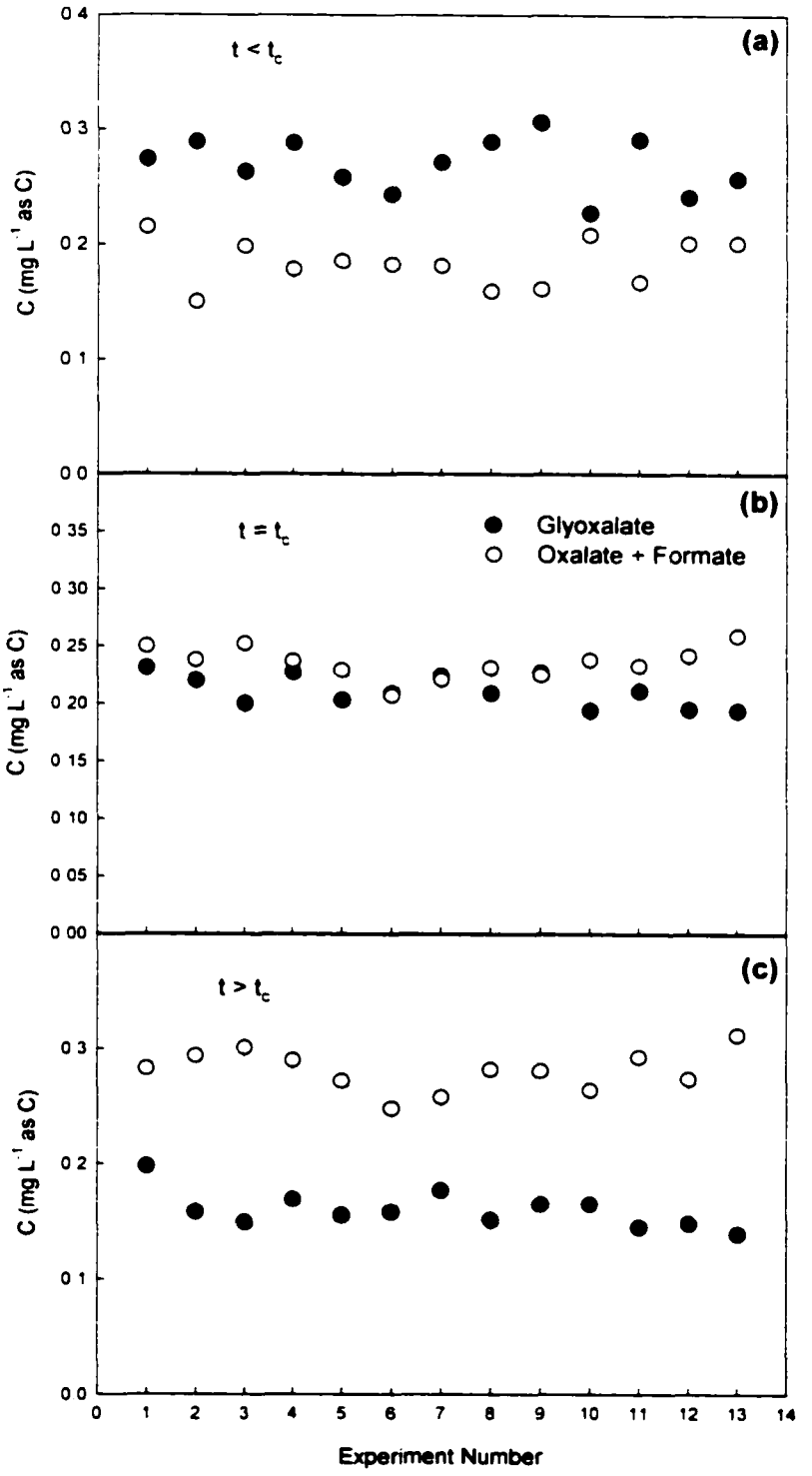

Figure 4.2.3.7. Comparison of $[HC_2O_3^-]$ and $\{[C_2O_4^{2-}] + [HCO_2^-]\}$ for The Experiments with $[HC_2O_3^-]_0 = (1.73 - 2.12) \times 10^{-5}$ M at **(a)** $t < t_c$; **(b)** $t = t_c$ and **(c)** $t > t_c$.

Since $\varepsilon_{253.7}(C_2O_4^{2-}) > \varepsilon_{253.7}(HC_2O_3^-)$, when $[HC_2O_3^-] > [C_2O_4^{2-}]$, $HC_2O_3^-$ absorbs the light energy and forms $C_2O_4^{2-}$ until $[HC_2O_3^-] \approx [C_2O_4^{2-}]$, while at $[C_2O_4^{2-}] > [HC_2O_3^-]$, $C_2O_4^{2-}$ could absorb most of the available light energy. Thus, the rate of $HC_2O_3^-$ photodecomposition decreases after $[C_2O_4^{2-}]$ becomes the dominant species in solution.

The ratio of k_1/k_2 increased with $[HC_2O_3^-]_0$ as depicted in Figure 4.2.3.8 while it remained stable (1.68 ± 0.13) during all experiments at $[HC_2O_3^-]_0 = (1.73\text{-}2.12) \times 10^{-5}$ M (except when pH_0 was adjusted to 9.10) .

During photodecomposition, pH_{min} occurred slightly before $[C_2O_4^{2-}] \approx [C_2O_4^{2-}]_{max}$ and as $[HC_2O_3^-] \approx [HCO_2^-] \approx$ BDL to later rise to a constant level of pH_f at $[C_2O_4^{2-}] \approx$ BDL for all experiments except when $pH_0 = 9.10$. In the experiment with $pH_0 = 9.10$, solution pH decreased with photodecomposition and reached a constant level at $[C_2O_4^{2-}] \approx [C_2O_4^{2-}]_{max}$ as depicted in Figure 4.2.3.2. The effect of pH_0 on the pH profile was investigated at I_a 2.60×10^{-6} $EL^{-1}s^{-1}$ and $[HC_2O_3^-]_0 = (1.88\text{-}2.12) \times 10^{-5}$ M. Figure 4.2.3.9 shows pH profiles of four experiments at pH_0 of 4.55 (no adjustment) and 6.86, 8.22, 9.10 (adjusted using NaOH). The observed pH change to pH_{min} ($\Delta pH_0 = pH_0 - pH_{min}$) increased with pH_0 as depicted in Figure 4.2.3.9. The pH change after pH_{min} ($\Delta pH_f = pH_f - pH_{min}$) increased with increasing $[C_2O_4^{2-}]_{max}$ (Figure 4.2.3.10) as it was observed during $C_2O_4^{2-}$ decay (Figure 4.2.2.4), where the overall pH change ($\Delta pH = pH_f - pH_0$) increased with $[C_2O_4^{2-}]_0$. This was expected since $C_2O_4^{2-}$ is the only compound in solution after $[C_2O_4^{2-}]_{max}$.

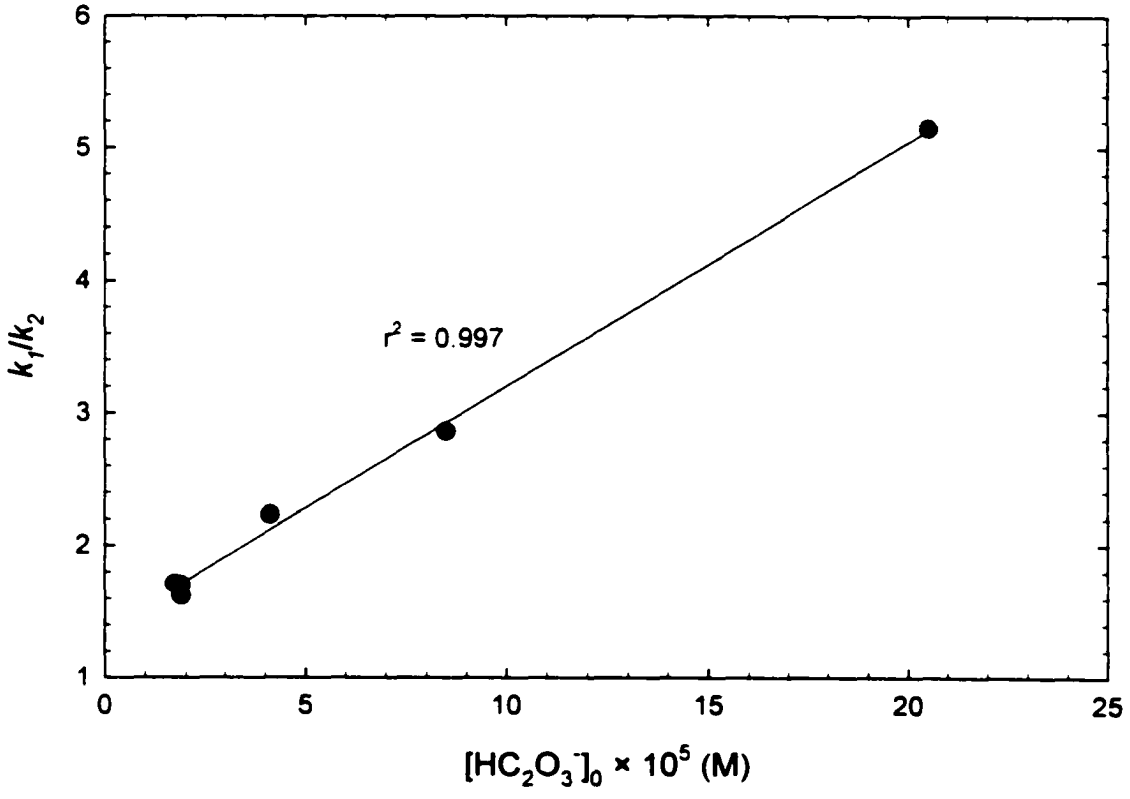

Figure 4.2.3.8. Dependency of the Ratio of k_1/k_2 on $[HC_2O_3^-]_0$ (I_a = 2.60 × 10^{-6} $EL^{-1}s^{-1}$, pH_0 = 4.00 - 4.66, T = 25 °C).

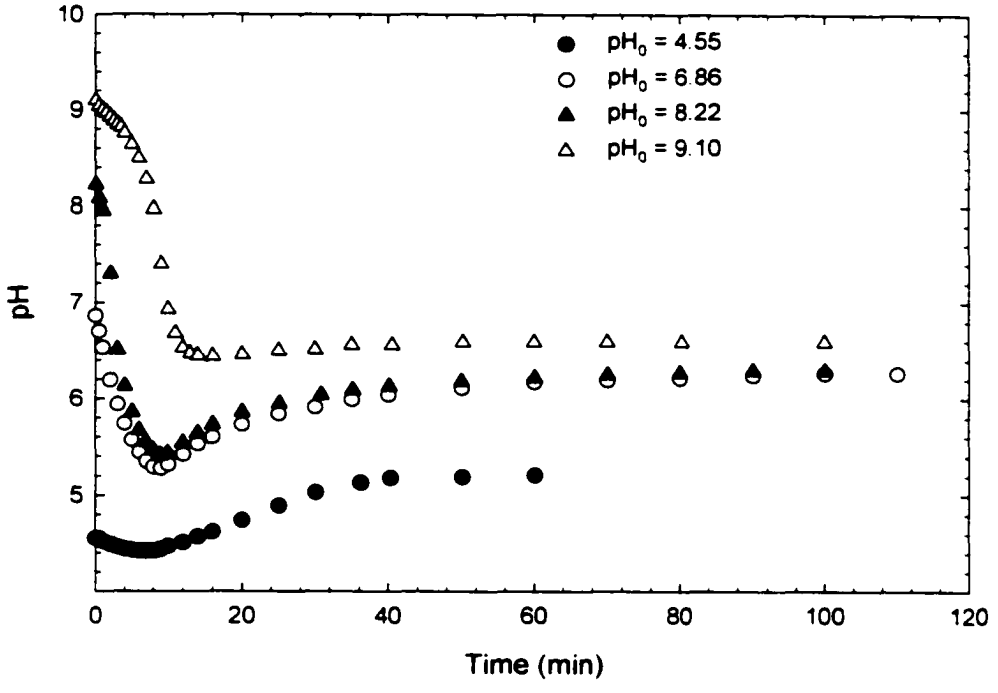

Figure 4.2.3.9. Dependency of pH Profile on pH_0 (I_a = 2.60 × 10^{-6} $EL^{-1}s^{-1}$, $[HC_2O_3^-]_0$ = (1.88 - 2.12) × 10^{-5} M, T = 25 °C).

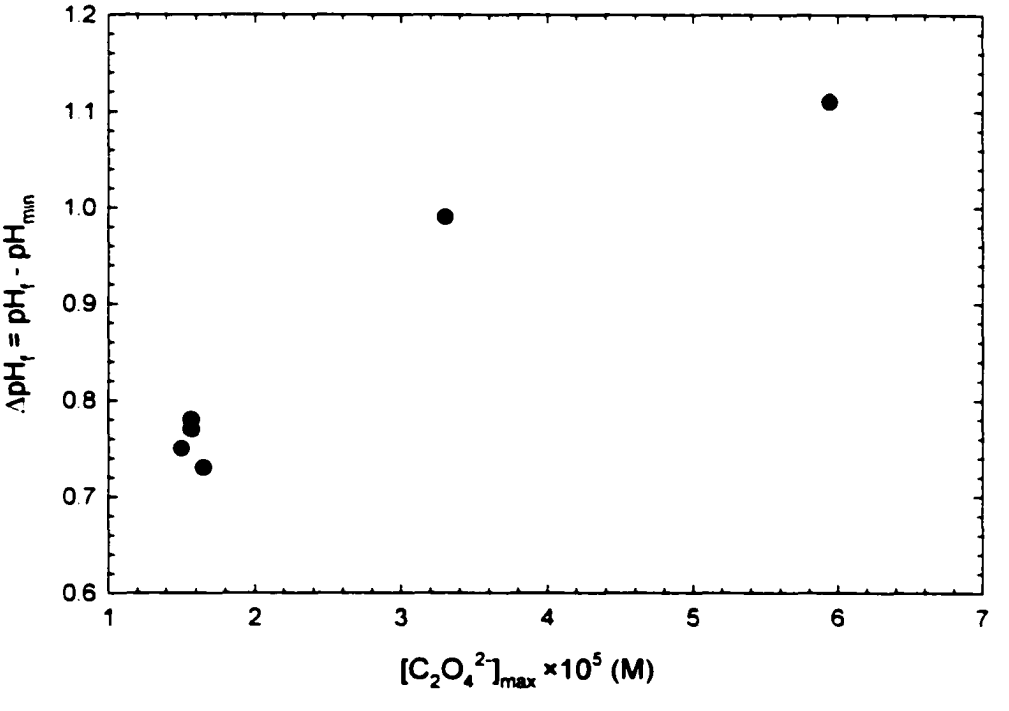

Figure 4.2.3.10. Dependency of ΔpH_f ($pH_f - pH_{min}$) on $[C_2O_4^{2-}]_{max}$ During $HC_2O_3^-$ Decay.

Karpel Vel Leitner and Doré (1997) observed $C_2O_4^{2-}$ formation during photodecomposition of $H_2C_2O_3$ in H_2O_2/UV system while they did not report any HCO_2^- formation. Detailed analysis of data extracted from figures in the manuscript revealed near split rate zero order kinetics for $H_2C_2O_3$ decay, with the split between k_1 and k_2 ($k_1 > k_2$) occurring at 55 percent $HC_2O_3^-$ conversion and $[H_2C_2O_3] \approx [H_2C_2O_4]$ during UV irradiation of the mixture of $[H_2C_2O_3]_0 \approx 5 \times 10^{-4}$ M and $[H_2O_2]_0 = 4.6 \times 10^{-4}$ M at pH_0 = 3.4 and in the presence and absence of DO. The values of k_1 and k_2 were 8.2×10^{-6} M min^{-1} and 3.8×10^{-6} M min^{-1} in the presence and 13.8×10^{-6} M min^{-1} and 4.7×10^{-6} M min^{-1} in the absence of DO. The observed rate constants in the presence of DO are higher than the values observed in this study.

4.2.4. Glycolate

Figures 4.2.4.1 shows $[H_3C_2O_3^-]$, NPOC, pH and observed intermediate profiles during two experiments at 1.38×10^{-6} (box a) and 2.60×10^{-6} $EL^{-1}s^{-1}$ (box b). $HC_2O_3^-$ that was observed as stable intermediate for all $H_3C_2O_3^-$ experiments, further decomposed to $C_2O_4^{2-}$ and HCO_2^- (as reported in Section 4.2.3). $C_2O_4^{2-}$ and HCO_2^- also decayed after reaching maximum concentrations at approximately $[H_3C_2O_3] \approx [HC_2O_3^-] \approx [HCO_2^-] \approx$ BDL and $[H_3C_2O_3] \approx [C_2O_4^{2-}]$, respectively. $[HC_2O_3^-]_{max}$, $[C_2O_4^{2-}]_{max}$ and $[HCO_2^-]_{max}$ were reached after 52 ± 6 %, 99 ± 1 % and 73 ± 6 % $H_3C_2O_3^-$ decay and are linear functions of $[H_3C_2O_3^-]_0$ as shown in Figure 4.2.4.2 with the correlations shown below:

$$[HC_2O_3^-]_{max} = 3.91 \times 10^{-6} + 0.07 \times [H_3C_2O_3^-]_0 \quad (4.2.4.1)$$

$$[C_2O_4^{2-}]_{max} = 1.05 \times 10^{-6} + 0.52 \times [H_3C_2O_3^-]_0 \quad (4.2.4.2)$$

$$[HCO_2^-]_{max} = -2.57 \times 10^{-6} + 0.27 \times [H_3C_2O_3^-]_0 \quad (4.2.4.3)$$

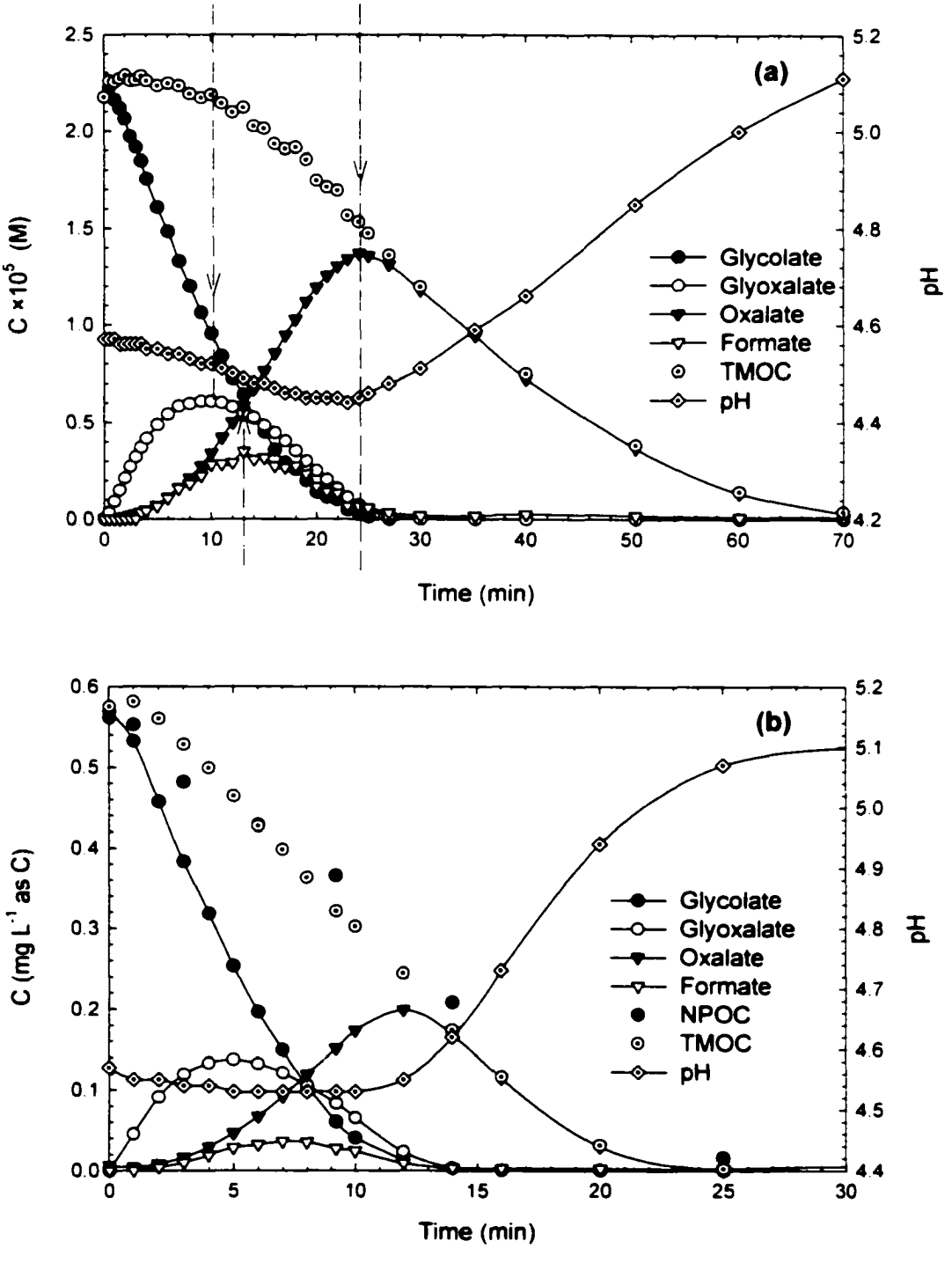

Figure 4.2.4.1. Concentration and pH Profiles During UV Irradiation of $H_3C_2O_3^-$ in DIW **(a)** $I_a = 1.38 \times 10^{-6}$ E L^{-1} s^{-1}, $C_0 = 2.18 \times 10^{-5}$ M, $pH_0 = 4.57$, T = 25°C; **(b)** $I_a = 2.60 \times 10^{-6}$ E L^{-1} s^{-1}, $C_0 = 2.37 \times 10^{-5}$ M, $pH_0 = 4.57$, T = 25°C.

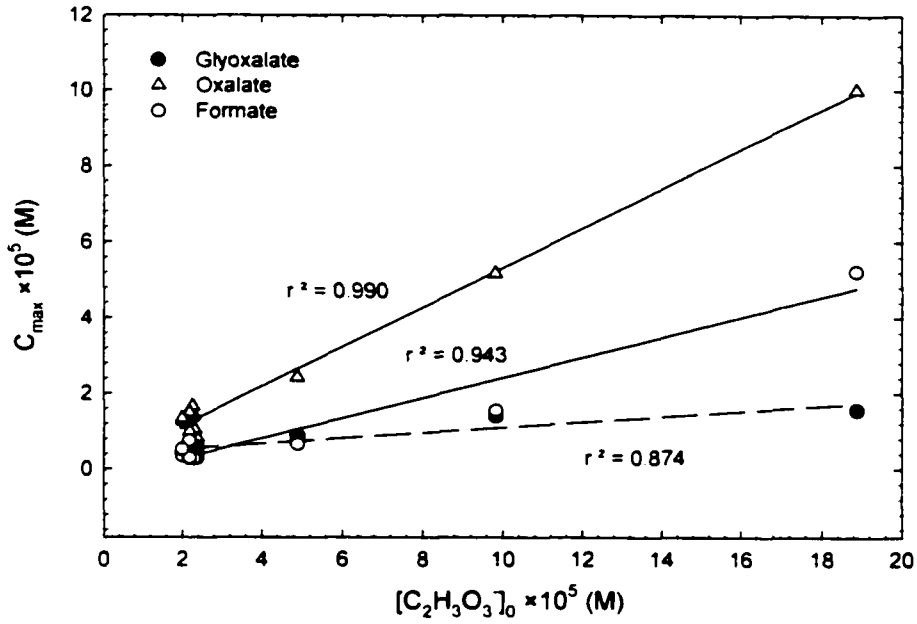

Figure 4.2.4.2. Dependency of $[HC_2O_3^-]_{max}$, $[C_2O_4^{2-}]_{max}$ and $[HCO_2^-]_{max}$ on $[H_3C_2O_3^-]_0$.

NPOC profile closely followed the TMOC ($[H_3C_2O_3^-$ -C] + $[HC_2O_3^-$ -C] + $[C_2O_4^{2-}$-C] + $[HCO_2^-$-C]) profile. This observation confirms that $HC_2O_3^-$, $C_2O_4^{2-}$ and HCO_2^- were the major non-purgeable $H_3C_2O_3^-$ photodecomposition intermediates. Figure 4.2.4.3 depicts photodecomposition of $H_3C_2O_3^-$ run at $[H_3C_2O_3^-]_0$ of 1.89 ×10^{-4} M (I_a = 2.60 ×10^{-6} EL^{-1}s^{-1}, pH_0 = 7.07 and 25 °C). This experiment was run in order to compare NPOC and TC profiles. As seen in box (a) of Figure 4.2.4.3, TC gradually decreased as $H_3C_2O_3^-$ decayed while NPOC followed TMOC. This could be attributed to formation of volatile products. At $H_3C_2O_3^-$ ≈ BDL, about 40 % of TC was unaccounted for. The DO profile during $H_3C_2O_3^-$ decay is given in box b. DO was consumed until $[H_3C_2O_3^-]$ ≈ $[HC_2O_3^-]$ ≈ $[HCO_2^-]$ ≈ BDL and $[C_2O_4^{2-}] = [C_2O_4^{2-}]_{max}$. Later DO uptake rate became dominant since DO in the reactor was only 25 percent of saturation and $C_2O_4^{2-}$ decayed at a slower rate.

The observed DO utilization was 1.1 mol O_2 / mol $H_3C_2O_3^{\cdot}$. The absorbance profiles at 199, 200, 220 and 253.7 nm were also monitored during the experiment (box c). Similar to $HC_2O_3^{\cdot}$ decay, absorbance values at all wavelengths increased as $H_3C_2O_3^{\cdot}$ decayed, to later decrease after $[C_2O_4^{2-}]_{max}$ was reached. $H_3C_2O_3^{\cdot}$ decay followed pseudo-zero order kinetics with split rate as shown in the kinetic analysis of $[H_3C_2O_3^{\cdot}]$ profiles (Figure 4.2.4.4) during the experiments shown in Figure 4.2.4.1. The switch between k_1 and k_2 ($k_1 > k_2$) occurred after 61 ± 6 percent $H_3C_2O_3^{\cdot}$ conversion when $[H_3C_2O_3^{\cdot}] \approx [HC_2O_3^{\cdot}] + [C_2O_4^{2-}] + [HCO_2^{-}]$ and $[HC_2O_3^{\cdot}] \approx [HC_2O_3^{\cdot}]_{max}$ ($t=t_c$). This observation is demonstrated in Figure 4.2.4.5 in an experiment run at 2.60×10^{-6} $EL^{-1}s^{-1}$ and 17 °C with $[H_3C_2O_3^{\cdot}]_0 = 2.24 \times 10^{-5}$ M. Kinetic analysis of the $[H_3C_2O_3^{\cdot}]$ profile is given in box b, while comparison of $[H_3C_2O_3^{\cdot}]$ and $\{[HC_2O_3^{\cdot}] + [C_2O_4^{2-}] + [HCO_2^{-}]\}$ at different irradiation times is given in (box c).

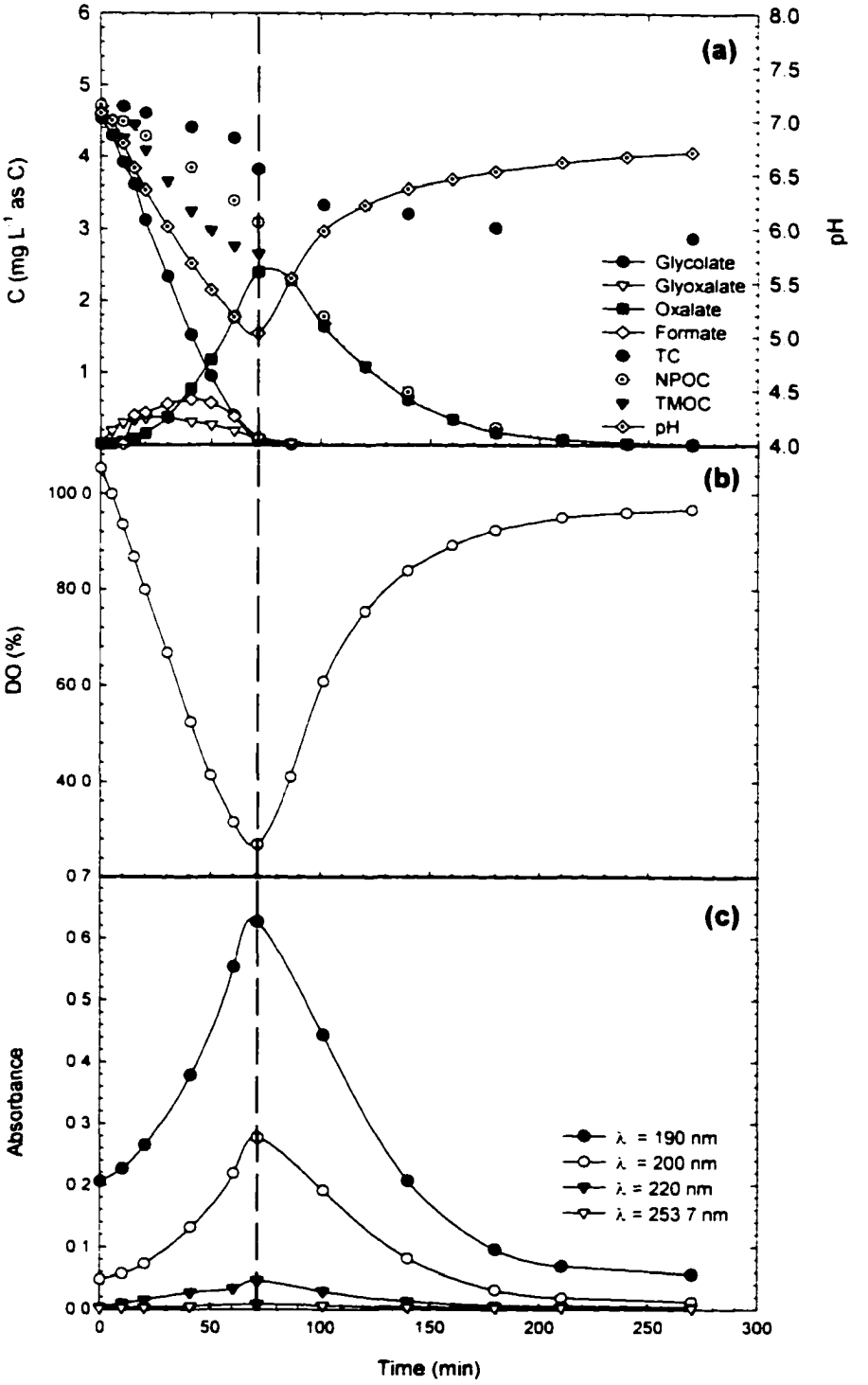

Figure 4.2.4.3. **(a)** Concentration and pH Profiles; **(b)** DO Profile; **(c)** Absorbance of The Samples at Various Wavelengths During UV Irradiation of $H_3C_2O_3^{\cdot}$ in DIW [(I_a = 2.60 × 10^{-6} E L^{-1} s^{-1}, C_0= 1.89 ×10^{-4} M, pH_0 = 7.07, T = 25°C).

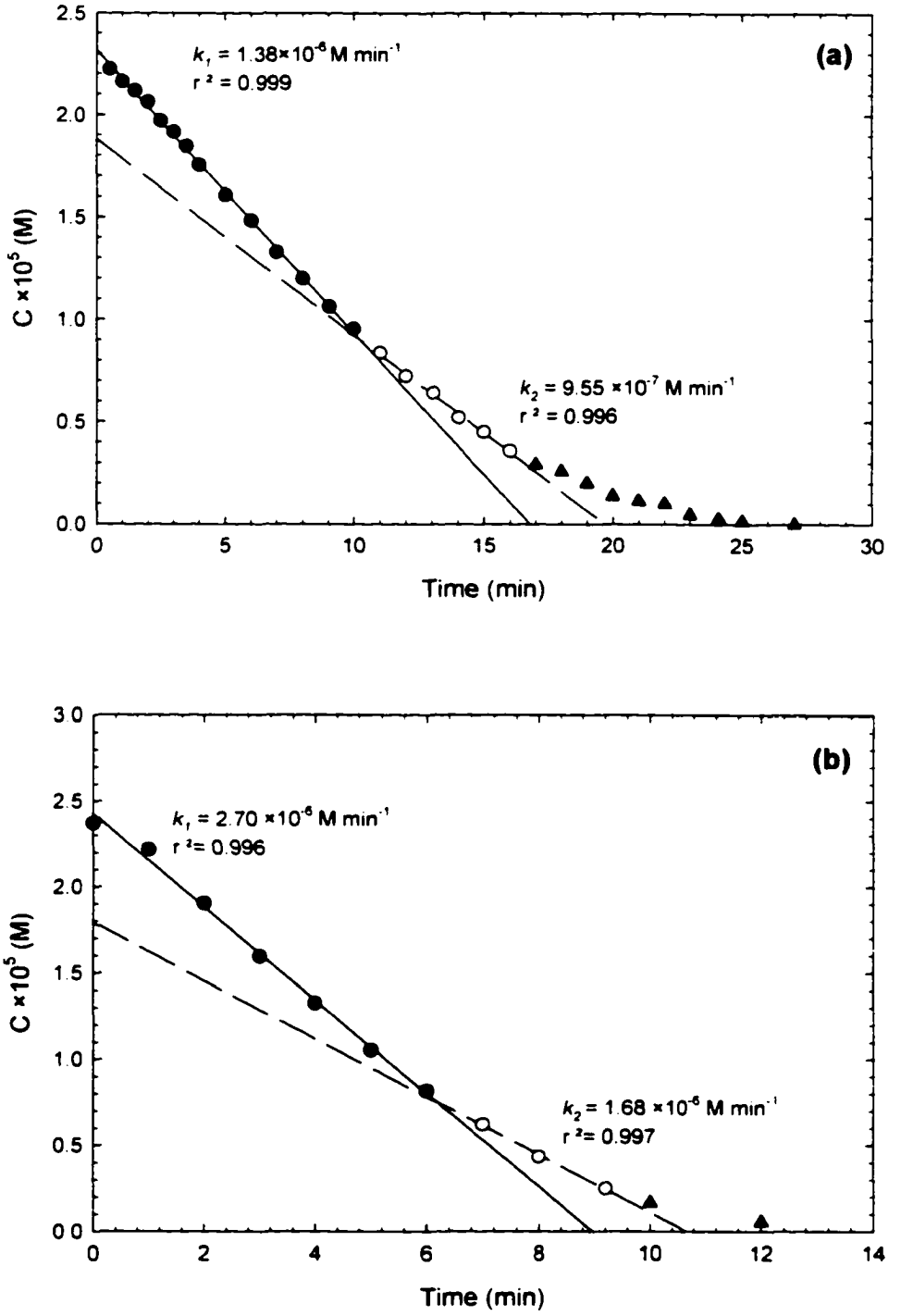

Figure 4.2.4.4. Kinetic Analysis of the $H_3C_2O_3^-$ Data **(a)** I_a = 1.38 × 10^{-6} E L^{-1} s^{-1}, C_0= 2.18 × 10^{-5} M, pH_0 = 4.57, T = 25°C **(b)** I_a = 2.60 × 10^{-6} E L^{-1} s^{-1}, C_0= 2.37 × 10^{-5} M, pH_0 = 4.57, T = 25°C.

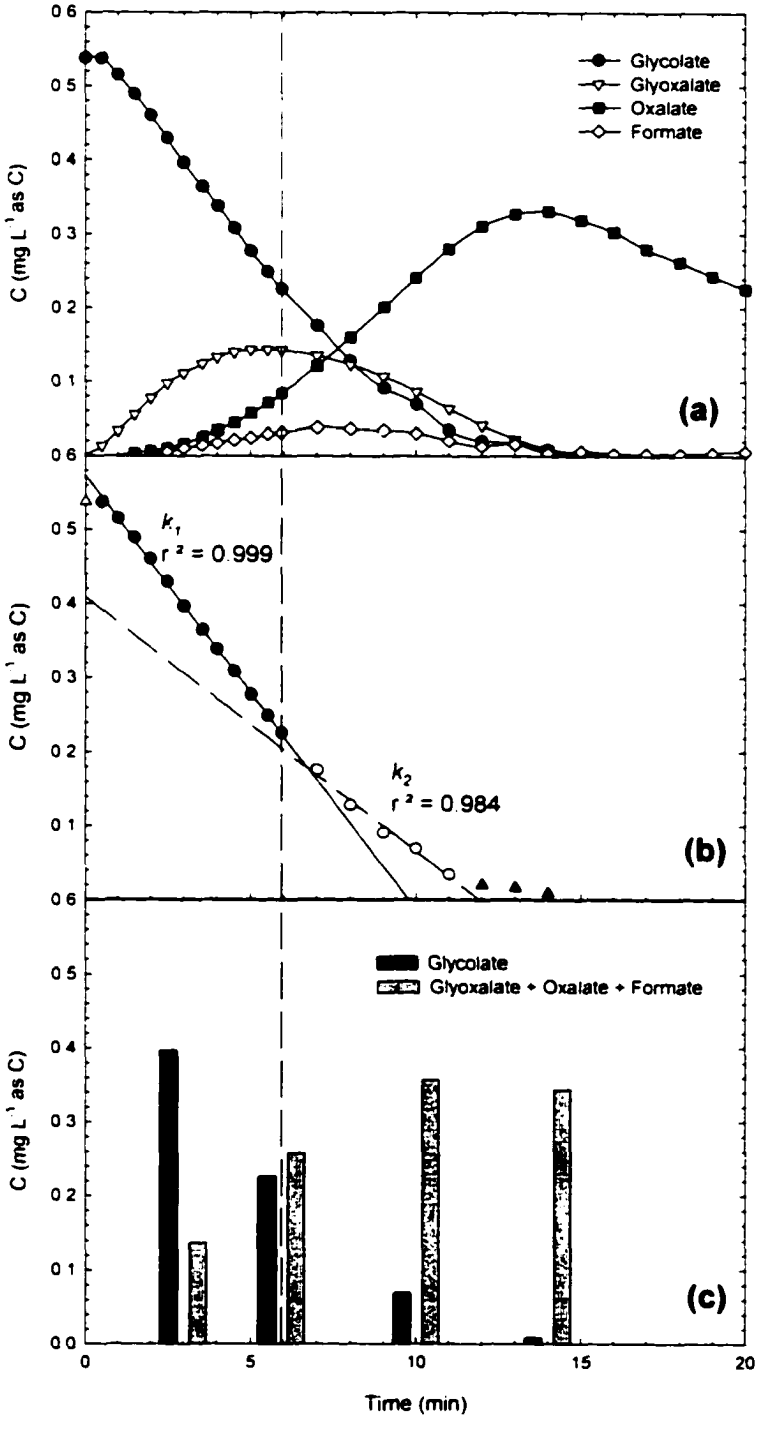

Figure 4.2.4.5. **(a)** Concentration and pH Profiles During UV Irradiation of $H_3C_2O_3^-$ in DIW; **(b)** Kinetic Analysis of the $H_3C_2O_3^-$ Data; **(c)** Comparison of $[H_3C_2O_3^-]$ and $[HC_2O_3^-] + [C_2O_4^{2-}] + [HCO_2^-]$ at Various Irradiation Times [($I_a = 2.60 \times 10^{-6}$ E L^{-1} s^{-1}, $C_0 = 2.24 \times 10^{-5}$ M, $pH_0 = 4.57$, T = 17°C).

The same kinetic behavior was observed for all experiments except the ones at $[H_3C_2O_3^-]_0 = 4.89 \times 10^{-5}$ and 9.83×10^{-5} M as shown in Figure 4.2.4.6. The light energy absorbed by $H_3C_2O_3^-$ could drop after $[H_3C_2O_3^-]$ reaches a concentration less than the total concentration of $HC_2O_3^-$, $C_2O_4^{2-}$ and HCO_2^-. Thus, the decomposition rate decreases after t_c. The values of k_1 and k_2 ranged between $(1.4 - 5.1) \times 10^{-6}$ M min^{-1}, and $(1.0 - 3.4) \times 10^{-6}$ M min^{-1}, respectively and the ratio of k_1/k_2 remained within a narrow range during all experiments (1.59 ± 0.14).

Figure 4.2.4.7 shows pH profiles of four experiments with different pH_0 (box a) and corresponding $[C_2O_4^{2-}]$ profiles (box b). Solution pH decreased until pH_{min} ($\Delta pH_0 = pH_0 - pH_{min}$), then started increasing at $[C_2O_4^{2-}]_{max}$ to approach a plateau at $[C_2O_4^{2-}] \approx$ BDL for all experiments except at $pH_0 = 9.12$. In the absence of pH_0 adjustment ($pH_0 = 4.57$ in Figure 4.2.4.7) ΔpH_0 was very little and it increased with increasing pH_0. In the experiment with $pH_0 = 9.12$, solution pH decreased rapidly until $[C_2O_4^{2-}] = [C_2O_4^{2-}]_{max}$, then decreased slightly and reached to a constant value when $[C_2O_4^{2-}]$ = BDL. ΔpH_f ($\Delta pH_f = pH_{min} - pH_f$) of the experiments without pH_0 adjustment increased with $[C_2O_4^{2-}]_{max}$ (Figure 4.2.4.8).

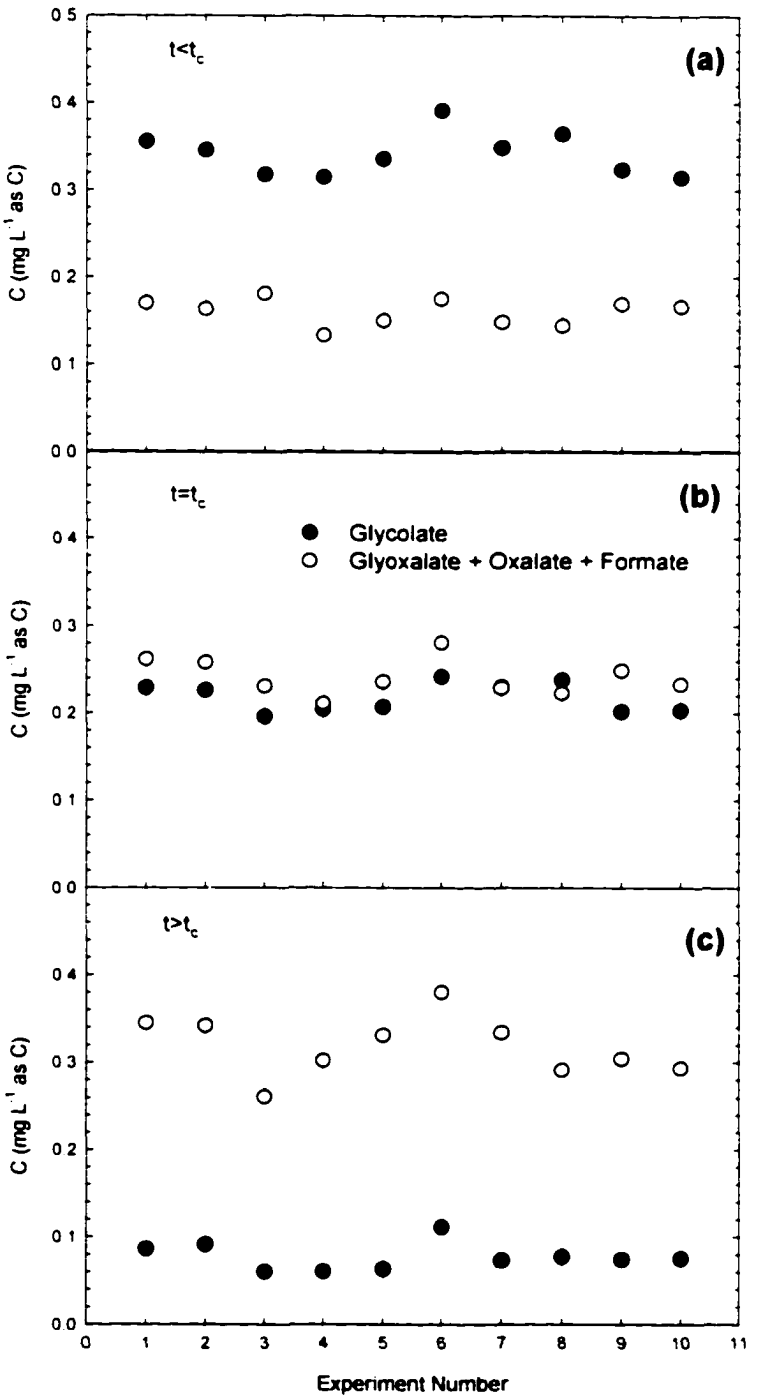

Figure 4.2.4.6. Comparison of $[H_3C_2O_3^-]$ and $[HC_2O_3^-] + [C_2O_4^{2-}] + [HCO_2^-]$ for The Experiments with $[H_3C_2O_3^-]_0 = (2.00 - 2.37) \times 10^{-5}$ M at **(a)** $t<t_c$; **(b)** $t=t_c$ and **(c)** $t>t_c$.

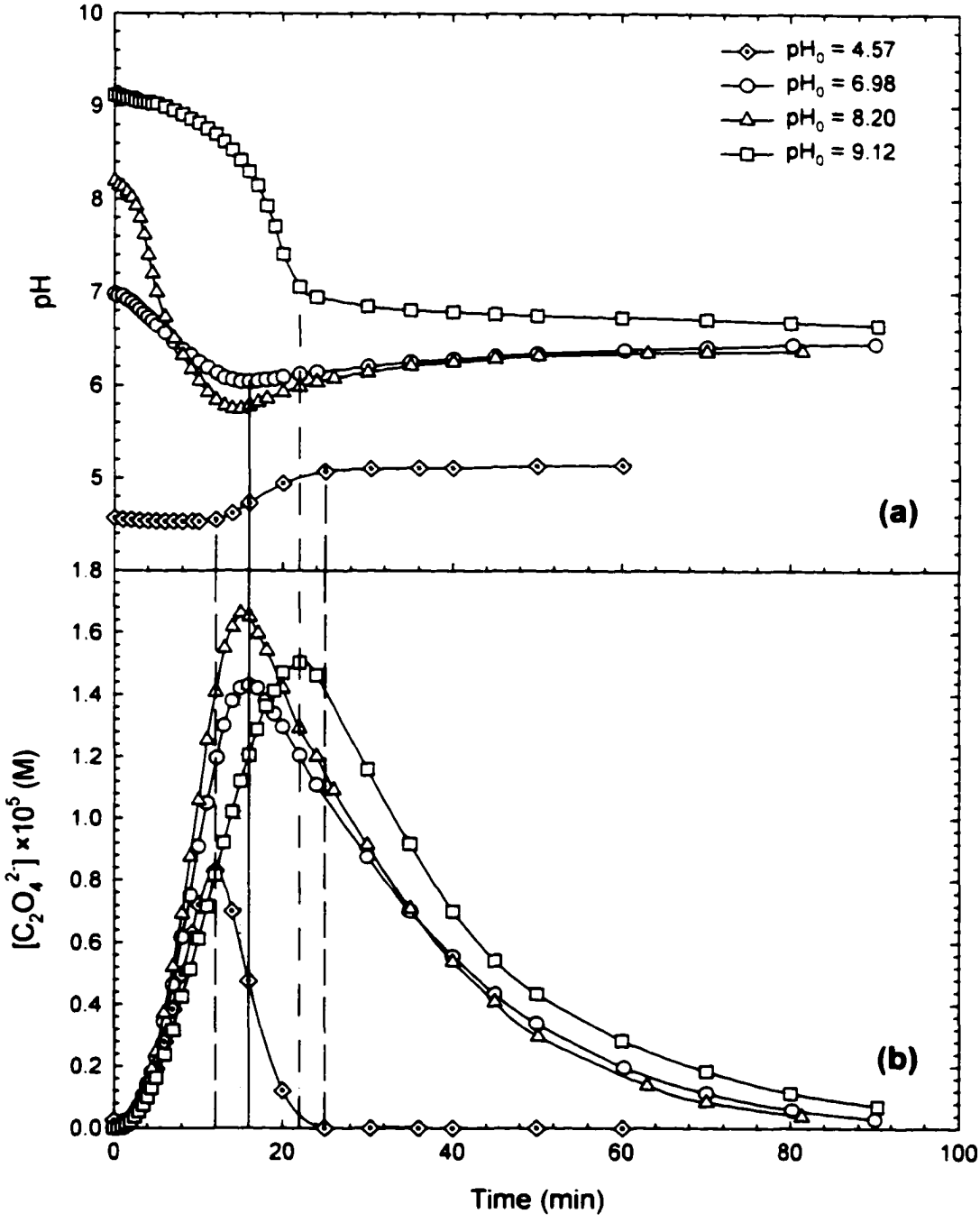

Figure 4.2.4.7. **(a)** Dependency of pH Profile on pH_0 During $H_3C_2O_3^-$ Decay; **(b)** Corresponding $[C_2O_4^{2-}]$ Profiles (I_a = 2.60 × 10^{-6} $EL^{-1}s^{-1}$, $[H_3C_2O_3^-]_0$ = (2.12-2.37) × 10^{-5} M, T = 25 °C).

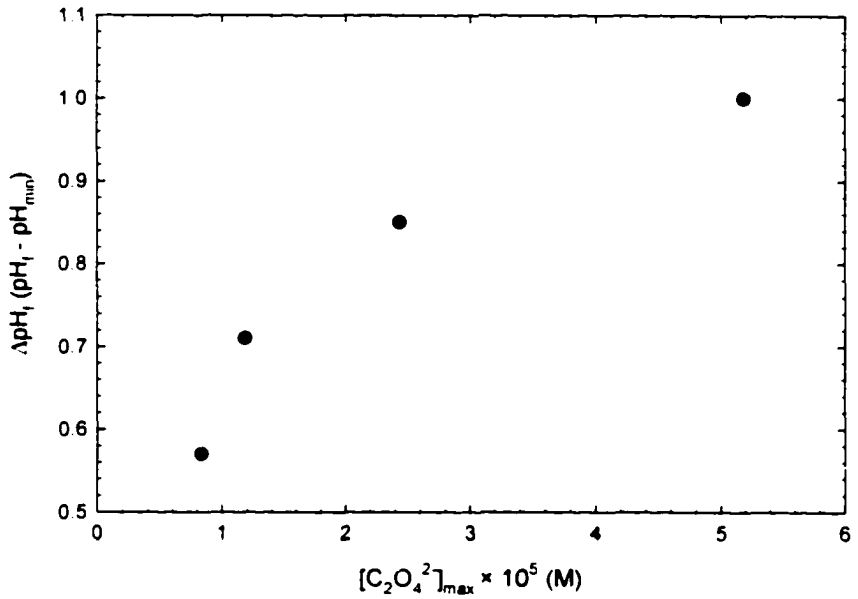

Figure 4.2.4.8. Dependency of $\Delta pH_f (pH_f - pH_{min})$ on $[C_2O_4^{2-}]_{max}$ During $H_3C_2O_3^-$ Decay.

Karpel Vel Leitner and Doré (1997) also observed $H_2C_2O_3$, $C_2O_4H_2$, and H_2CO_2 as decomposition intermediates of $H_4C_2O_3$ in the presence of DO at pH_0 = 6.8. However, they did not report H_2CO_2 as intermediate of $H_4C_2O_3$ photodecomposition at pH_0 of 3.3. The data manually extracted from Figure 1a in Karpel Vel Leitner and Doré (1997) involving UV irradiation of a mixture of $[H_4C_2O_3]_0 = 1.0 \times 10^{-3}$ M and $[H_2O_2]_0 = 9.4 \times 10^{-4}$ M in DIW at pH_0 of 3.3 in the presence of oxygen showed that the initial $H_4C_2O_3$ photodecomposition followed zero order kinetics and decay rate diverge from zero order when $[H_4C_2O_3] \approx \{[H_2C_2O_3] + [C_2O_4H_2] + [H_2CO_2]\}$ and $[H_2C_2O_3] \approx [H_2C_2O_3]_{max}$ as it was observed in this study. The observed initial rate constant was 10×10^{-6} M min^{-1}, which is higher than the values observed in this study.

Mazzarino et al. (1999), who studied photo-catalytic degradation of $H_4C_2O_3$ in aqueous solutions ($[H_4C_2O_3]_0$ = 200 mg L^{-1}), observed that $H_4C_2O_3$ decomposition in a continuous flow reactor followed "apparent first order kinetics" and TOC decay was much slower than the $H_4C_2O_3$ decomposition. They attributed the difference between acid and TOC decay to the formation of a significant amount of intermediates during the degradation process. The only intermediate they identified was H_2CO_2. They also reported that $H_4C_2O_3$ and its oxidative intermediates are stable in the UV light range of λ>240 nm, which is not in agreement with the results observed in this study.

4.2.5. Pyruvate

UV irradiation of sodium pyruvate ($NaH_3C_3O_3$) solution at 25 °C and 2.60 × 10^{-6} $EL^{-1}s^{-1}$ with $[H_3C_3O_3^-]_0$ = 1.45 × 10^{-5} M (Figure 4.2.5.1) showed that $H_3C_3O_3^-$ decomposed to form $H_3C_2O_3^-$, $C_2O_4^{2-}$, trace levels of $HC_2O_3^-$ and HCO_2^- (not shown in Figure 4.2.5.1) and two unidentified products with retention times of 3.79 min (UP1) and 4.30 min (UP2). $[UP2]_{max}$ and $[C_2O_4^{2-}]_{max}$ were reached at [UP1] ≈ BDL and $[H_3C_3O_3^-]$ ≈ BDL, respectively. $C_2O_4^{2-}$ reached BDL after $H_3C_3O_3^-$ and its observed intermediates completely decomposed. Kinetic analysis of $H_3C_3O_3^-$, which is given in Figure 4.2.5.1b, depicts split rate pseudo-first order kinetics with the split between k_1 and k_2 ($k_1 < k_2$) occurring at percent $H_3C_3O_3^-$ conversion of 53. Solution pH decreased to pH_{min} at $[UP2]_{max}$, to later increase following decay of $H_3C_3O_3^-$ and its intermediates. Figure 4.2.5.2 shows the photodecomposition of $NaH_3C_3O_3$ solution at a higher initial concentration of $H_3C_3O_3^-$ ($[H_3C_3O_3^-]_0$ = 1.43 × 10^{-4} M, I_a = 2.60 × 10^{-6} $EL^{-1}s^{-1}$ and 25

°C). Both NPOC and TC profiles were monitored during the experiment (box a). The difference between NPOC and TMOC depicts unidentified intermediate formation besides $H_3C_2O_3^-$, $HC_2O_3^-$, and $C_2O_4^{2-}$ during $H_3C_3O_3^-$ decay. Two unidentified products, referred to herein as UP1 and UP2, were also observed by IC during this experiment (box b). TC gradually decreased and reached a plateau where about 60% of TC was unaccounted for, indicating potential formation of volatile compounds from decomposition of $H_3C_3O_3^-$. The DO profile during UV irradiation of $H_3C_3O_3^-$ is given in box c. The DO decreased up to 88 % $H_3C_3O_3^-$ conversion and the observed DO utilization was 1.4 mol O_2 / mol $H_3C_3O_3^-$. Absorbance of the samples at 190, 200, 220 and 253.7 nm decreased during UV irradiation of $NaH_3C_3O_3$ solution and reached a plateau when all observed intermediates reached BDL.

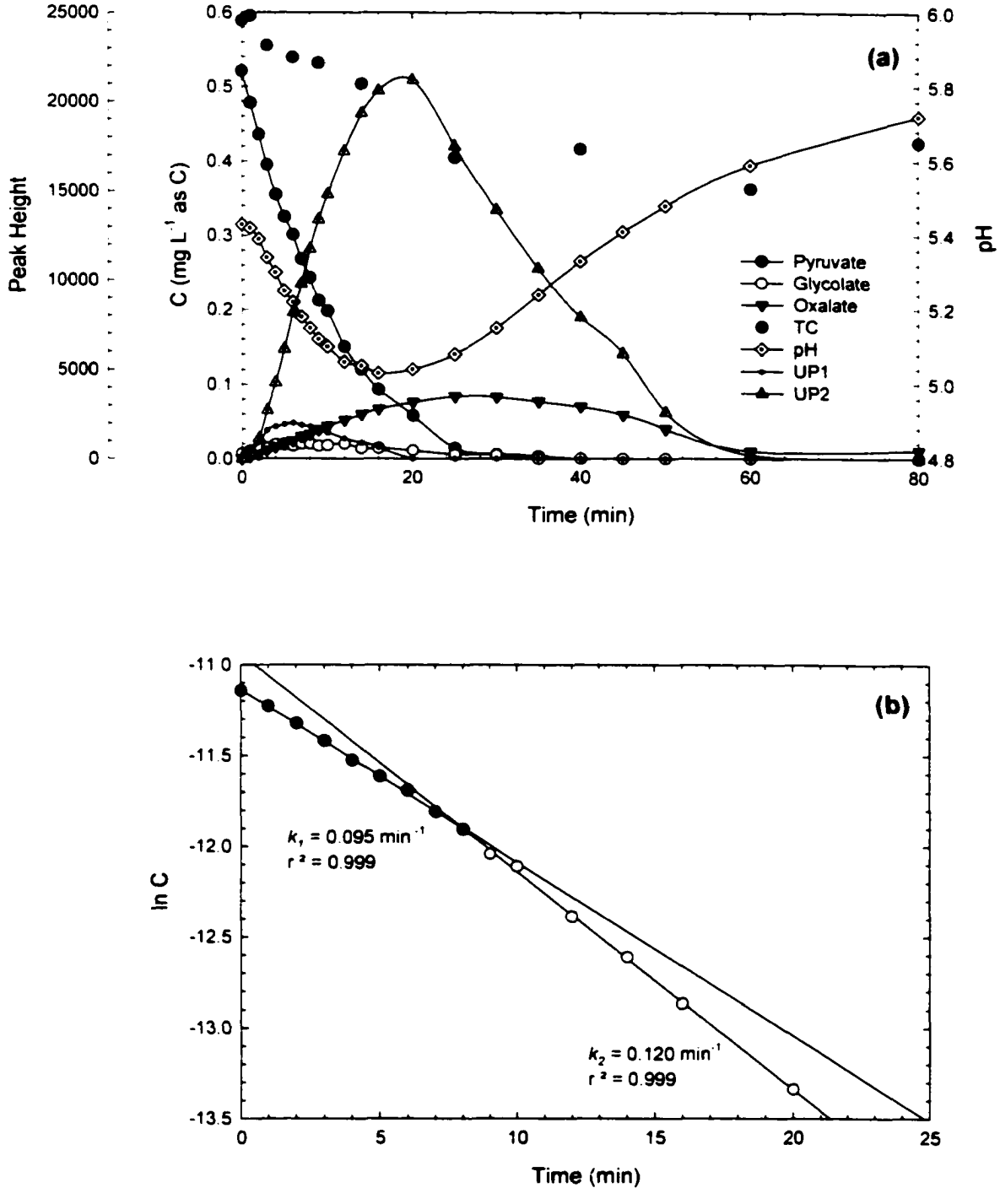

Figure 4.2.5.1. **(a)** Concentration and pH Profiles During UV Irradiation of $H_3C_3O_3^-$ in DIW; **(b)** Kinetic Analysis of the $H_3C_3O_3^-$ Data ($I_a = 2.60 \times 10^{-6}$ E L^{-1} s^{-1}, $C_0 = 1.45 \times 10^{-5}$ M, $pH_0 = 5.43$, T = 25°C).

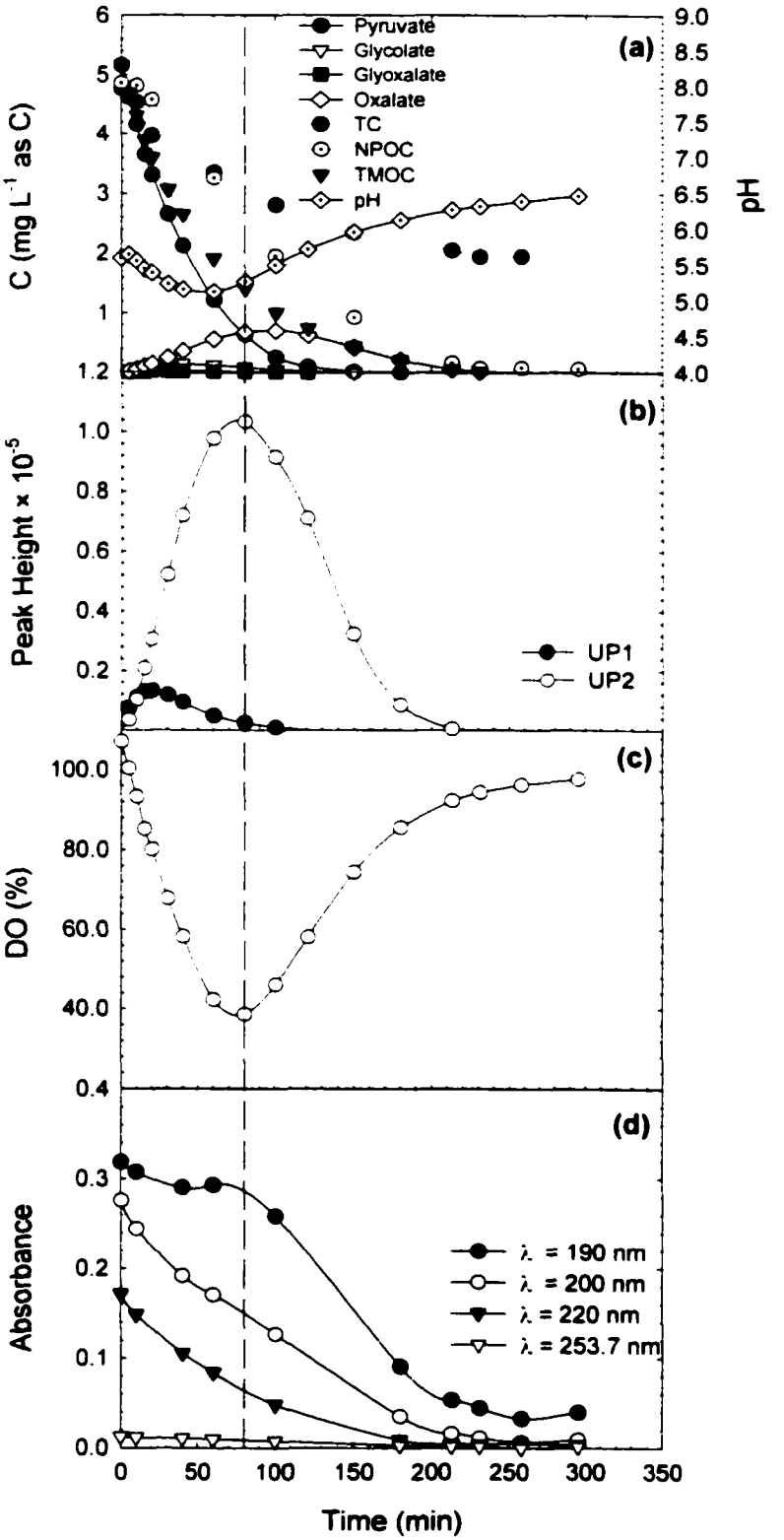

Figure 4.2.5.2. **(a)** Concentration and pH Profiles; **(b)** Unidentified Product Profiles; **(c)** DO Profile; **(d)** Absorbance Profiles at Various Wavelengths During UV Irradiation of $H_3C_3O_3^-$ in DIW [(I_a = 2.60 × 10^{-6} E L^{-1} s^{-1}, C_0= 1.43 ×10^{-4} M, pH_0 = 5.60, T = 25°C).

4.3. Effect of Experimental Conditions on Decay Kinetics

Initial concentration, I_a, pH_0 and temperature effects on k_1 and k_2 were investigated for HCO_2^-, $C_2O_4^{2-}$, $HC_2O_3^-$ and $H_3C_2O_3^-$ decomposition. Alkalinity effect was investigated only for HCO_2^- and $C_2O_4^{2-}$ decay. I_a and temperature were kept constant at 2.60×10^{-6} $EL^{-1}s^{-1}$ and 25 °C, respectively, except in experiments for evaluation of I_a and temperature dependencies.

4.3.1. Formate

$[HCO_2^-]_0$ effect was studied without pH_0 adjustment in the concentration range of (1.73-38.33) $\times 10^{-5}$ M with the results shown in Figure 4.3.1.1a. Both k_1 and k_2 increased curvilinearly with increasing $[HCO_2^-]_0$. The dependency of k_1 and k_2 on I_a was studied at 25 °C while $[HCO_2^-]_0$ and pH_0 were kept in the range of (4.04-4.28) $\times 10^{-5}$ M and (5.52-5.64), respectively. As depicted in Figure 4.3.1.1b, k_1 and k_2 are linear functions of I_a in the range of (1.38 – 3.99) $\times 10^{-6}$ $EL^{-1}s^{-1}$ and the difference between both rate constants increased with increasing I_a. The dependence of k_1 and k_2 on pH_0 was studied in the range of 5.4-9.0 by adjusting pH_0 with NaOH solution. $[HCO_2^-]_0$ ranged between (4.15-4.28) $\times 10^{-5}$ M during pH_0 dependency experiments. The effect of carbonate alkalinity was also studied at 25 and 50 mg/L as $CaCO_3$. Initial rate constant, k_1, slightly increased and k_2 slightly decreased (Figure 4.3.1.2a) with pH_0, while both rate constants decreased linearly with increasing carbonate alkalinity as depicted in Figure 4.3.1.2b. The effect of temperature was studied between 18-35 °C. $[HCO_2^-]_0$ was kept in a narrow range of

(4.15-4.37) × 10^{-5} M, while pH_0 was not adjusted and ranged between 5.27-5.62. As depicted in Figure 4.3.1.3, k_1 slightly increased with temperature while k_2 was not effected by it in the range of the experimental conditions. Regression equations for $[HCO_2^-]_0$, I_a, pH_0, alkalinity dependencies of k_1 and k_2 and Arrhenius' equation for temperature dependency of k_1 are given in Table 4.3.1.1.

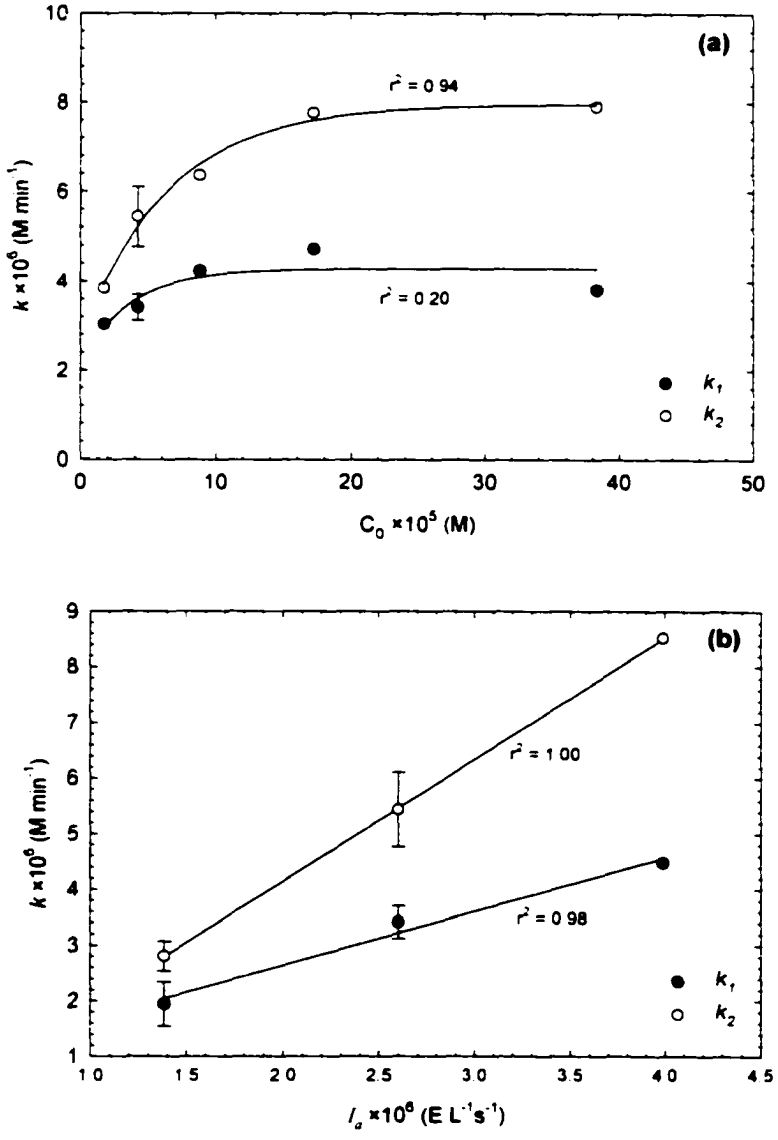

Figure 4.3.1.1. Dependency of HCO_2^- Photodecomposition Rate Constants k_1 and k_2 on (a) Initial HCO_2^- Concentration (I_a = 2.60 × 10^{-6} $EL^{-1}s^{-1}$, pH_0 = 5.39-5.68, T = 25°C). (b) UV Light Intensity (C_0 = 4.04 × 10^{-5} – 4.28 × 10^{-5} M, pH_0 = 5.52-5.64, T= 25°C).

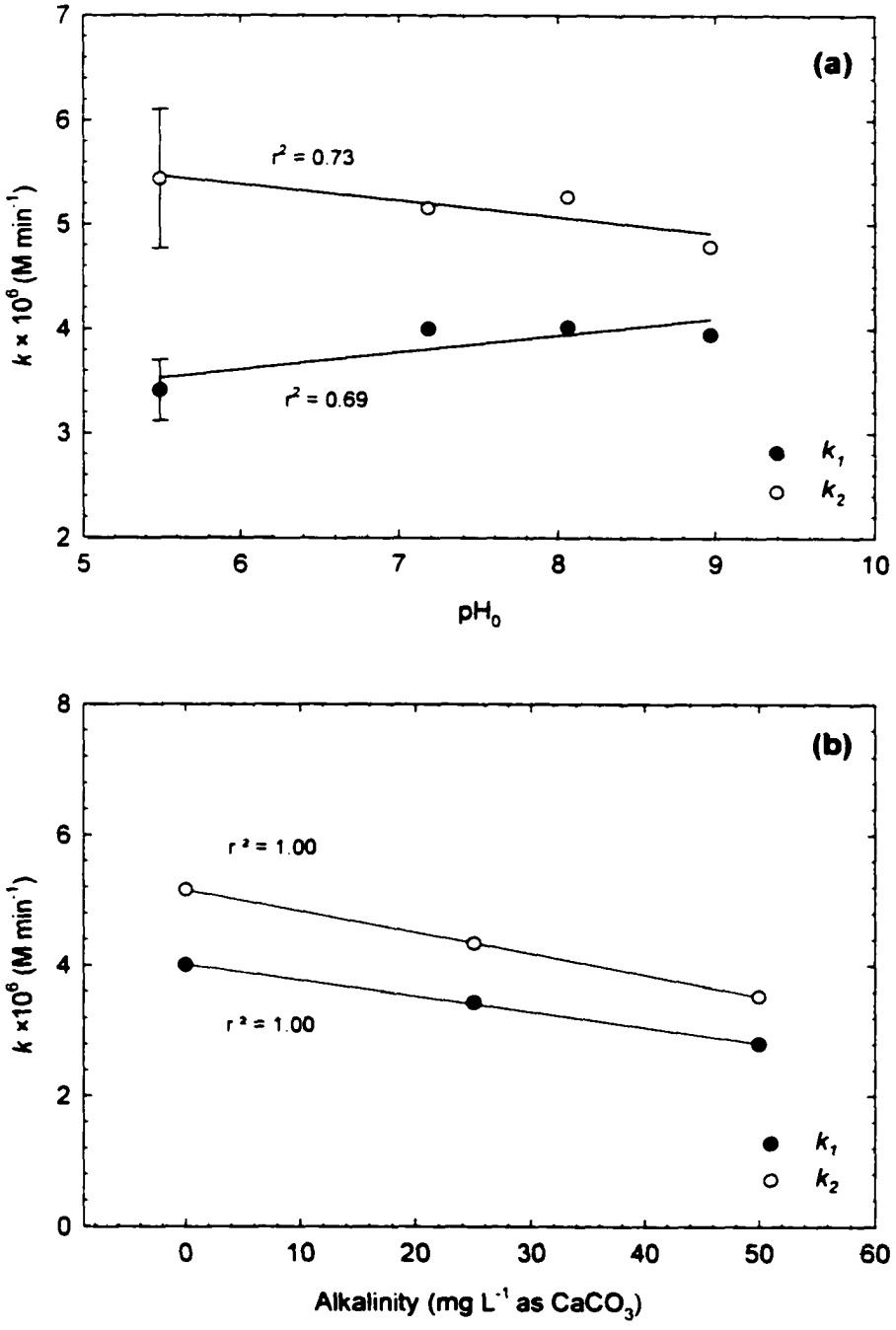

Figure 4.3.1.2. Dependency of HCO_2^- Photodecomposition Rate Constants k_1 and k_2 on **(a)** pH_0 (I_a = 2.60 × 10^{-6} $EL^{-1}s^{-1}$. C_0 = 4.15 × 10^{-5} – 4.28 × 10^{-5} M. T = 25°C). **(b)** Alkalinity (I_a = 2.60 × 10^{-6} $EL^{-1}s^{-1}$. C_0 = 4.13 × 10^{-5} – 4.30 × 10^{-5} M, pH_0 = 7.18-7.96 T = 25°C).

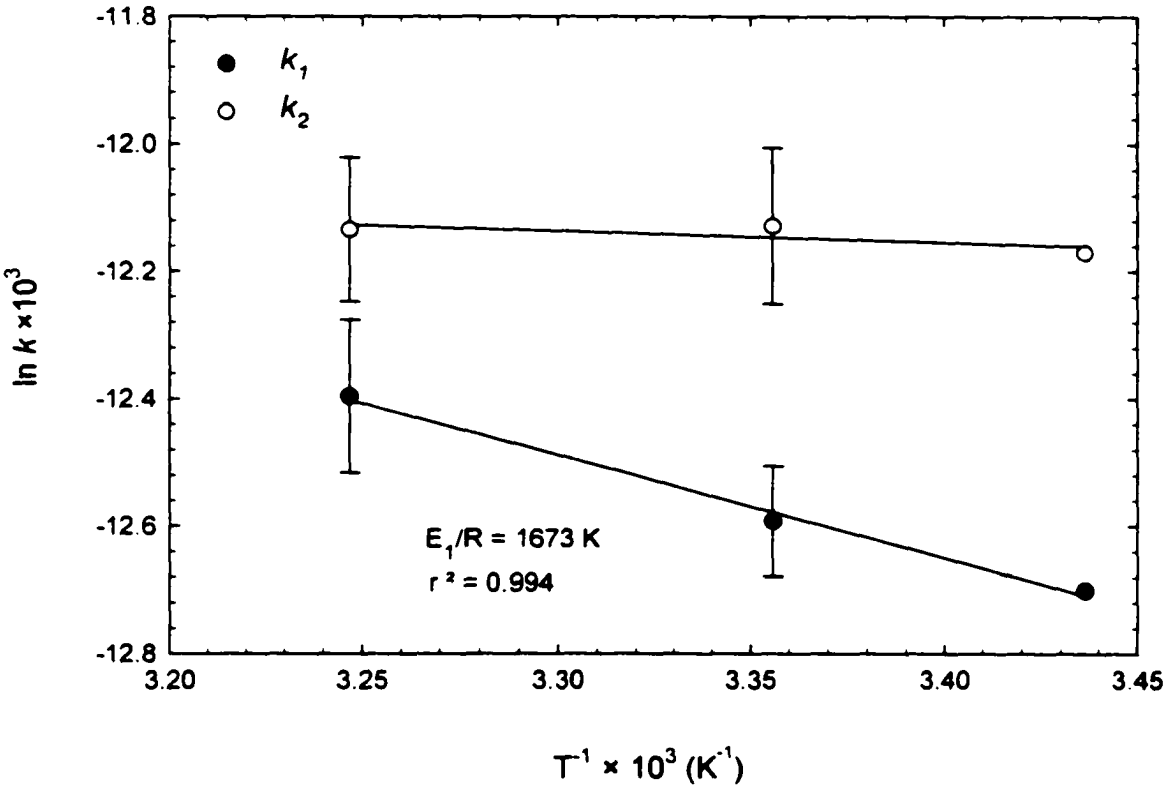

Figure 4.3.1.3. Dependency of HCO_2^- Photodecomposition Rate Constants k_1 and k_2 on Water Temperature ($I_a = 2.60 \times 10^{-6}$ $EL^{-1}s^{-1}$, $C_0 = 4.15 \times 10^{-5} - 4.37 \times 10^{-5}$ M, pH_0=5.27-5.62).

Table 4.3.1.1. Dependencies of k_1 and k_2 on Experimental Conditions During HCO_2^- Photodecomposition.

Parameter	Symbol	Experimental Range	k_1 (M min^{-1})	k_2 (M min^{-1})
Initial Formate Concentration (M)	C_0	1.73×10^{-5}-38.33×10^{-5}	$k_1 = 3.52 \times 10^{-6} + 1.51 \times 10^{-6}(1-e^{-19000 C_0})$	$k_2 = 1.28 \times 10^{-6} + 6.26 \times 10^{-6}(1-e^{-278000 C_0})$
Temperature (^oC)	T	18 - 35	$k_1 = 7.88 \times 10^{-4} e^{-1618/T}$	-*
Initial pH	pH_0	5.41 - 8.97	$k_1 = 2.63 \times 10^{-6} + 1.63 \times 10^{-7} pH_0$	$k_2 = 6.34 \times 10^{-6} - 1.59 \times 10^{-7} pH_0$
UV Light Intensity ($EL^{-1}s^{-1}$)	I_a	1.38×10^{-6}-3.99×10^{-6}	$k_1 = 7.10 \times 10^{-7} + 0.97 I_a$	$k_2 = -2.43 \times 10^{-7} + 2.19 I_a$
Alkalinity (mgL^{-1} as CaCO3)	A	0 - 50	$k_1 = 4.01 \times 10^{-6} - 2.40 \times 10^{-8} A$	$k_2 = 5.15 \times 10^{-6} - 3.25 \times 10^{-8} A$

*k_2 was independent of temperature

4.3.2. Oxalate

$[C_2O_4^{2-}]_0$ ((2.05 – 8.75) × 10^{-5} M) effect on k_1 and k_2 was investigated in DIW (no pH_0 adjustment) and 25°C. Dependency of k_1 and k_2 on $[C_2O_4^{2-}]_0$ are shown in Figure 4.3.2.1a. The mean k_1 and k_2 values at $[C_2O_4^{2-}]$ = (2.05 – 2.11) × 10^{-5} are 0.0372 ± 0.0027 and 0.0504 ± 0.0035 min^{-1}, respectively. The observed rate constants decreased with increasing $[C_2O_4^{2-}]_0$ with the exponential regression equations given in Table 4.3.2.1. According to Bolton and Cater (1994) the primary radicals formed during photochemical decomposition of any molecule in condense media such as aqueous solutions, are subject to "cage effect" which generally reduce the quantum yield of photolysis. When a pair of radicals is formed by homolysis, they are held in proximity by the surrounding solvent molecules (solvent cage). Until one or both of these radicals escape the solvent cage, a significant degree of radical recombination, called "cage effect", may occur. The decrease in observed rate constant with $[C_2O_4^{2-}]_0$ can be attributed to the "cage effect" described above. Karpel Vel Leitner and Doré (1997) proposed a $C_2O_4H_2$ decay mechanism involving recombination of $HOOCCOO^{\bullet}$ radicals within the "solvent cage". Two additional experiments were carried out in DIW as a system of {$Na_2C_2O_4$ + $NaHCO_3$} at $[C_2O_4^{2-}]_0$ of 2.14 and 4.46 × 10^{-5} M , 25°C, and alkalinity of 50 mg/L as $CaCO_3$. Although the data are very limited, the observed values for k_1 (0.0102 and 0.0112 min^{-1}) and k_2 (0.0131 and 0.0134 min^{-1}) depicted no significant $[C_2O_4^{2-}]_0$ dependency.

Four different I_a ranging between (1.4 – 5.3) × 10^{-6} $EL^{-1}s^{-1}$ were tested at $[C_2O_4^{2-}]_0$ = (2.05-2.29) × 10^{-5} M, pH_0 = 5.45-5.61 (no pH_0 adjustment), and 25°C. Both k_1 and k_2 were found to be linearly proportional to I_a as shown in Figure 4.3.2.1b, and $k_1 > k_2$ at all times with the difference increasing as I_a increased.

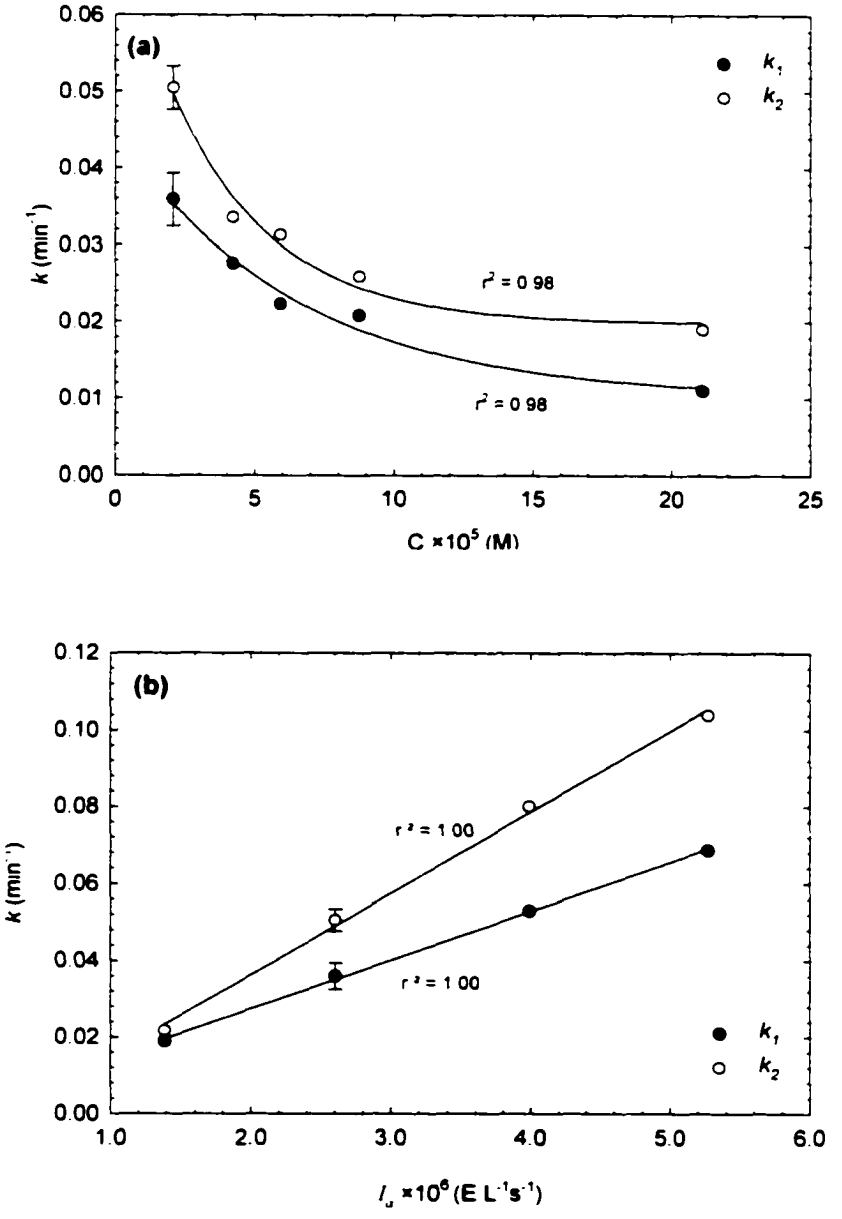

Figure 4.3.2.1. Dependency of $C_2O_4^{2-}$ Photodecomposition Rate Constants k_1 and k_2 on (a) Initial $C_2O_4^{2-}$ Concentration (I_a = 2.60 × 10^{-6} $EL^{-1}s^{-1}$, pH_0 = 5.45-5.68, T = 25°C), (b) UV Light Intensity (C_0 = 2.05 × 10^{-5} –2.29 × 10^{-5} M, pH_0 = 5.45-5.61, T= 25°C).

The effect of pH_0 on k_1 and k_2 was studied between 5.5 and 9.0, $[C_2O_4^{2-}]_0$ = (2.04-2.19) × 10^{-5} M, and 25°C. Carbonate species were not used in pH_0 adjustment. The values of both k_1 and k_2 decreased linearly with pH_0 as depicted in Figure 4.3.2.2a. Carbonate alkalinity effects were studied in the range of 10-50 mg/L as $CaCO_3$ with the results shown in Figure 4.3.2.2b.

The effect of temperature on k_1 and k_2 was tested at I_a = 2.60 × 10^{-6} E L^{-1} s^{-1}. pH_0 was not adjusted and ranged between 5.43-5.61, while $[C_2O_4^{-2}]_0$ = (2.05 – 2.18) × 10^{-5} M. The results indicated that k_1, which represents the early phase of the reaction with high pH change depicted in Figure 4.2.2.1a (Chapter 4.2.2), was independent of temperature, as shown in Figure 4.3.2.3. On the other hand, k_2 which represents the later half of the reaction with rather stable reaction pH, was highly affected by temperature at T<25°C. Regression equations for k_1 and k_2 as a function of $[C_2O_4^{-2}]_0$, pH_0, alkalinity, I_a and water temperature are given in Table 4.3.2.1.

The effect of naturally occurring DOC on $C_2O_4^{2-}$ decay was explored in filter effluent from a local water treatment pilot plant (PPFE, DOC = 2.31 mg C/L, alkalinity = 53.4 mg/L as $CaCO_3$, and pH_0 = 7.9) spiked with $C_2O_4^{2-}$ at 1.97 × 10^{-05} M, and irradiated at I_a = 2.60 × 10^{-6} E L^{-1} s^{-1} at 25°C. The decay kinetics shown in Figure 4.3.2.4 represents initial kinetics of $C_2O_4^{2-}$ photodecomposition with pseudo-first order decay rate constant of 4.58 × 10^{-3} min^{-1}, since the rate split occurs at average conversion of 56 ± 5.1. Furthermore, the decrease observed in pH at the early stages of the reaction is also markedly different than those observed in DIW.

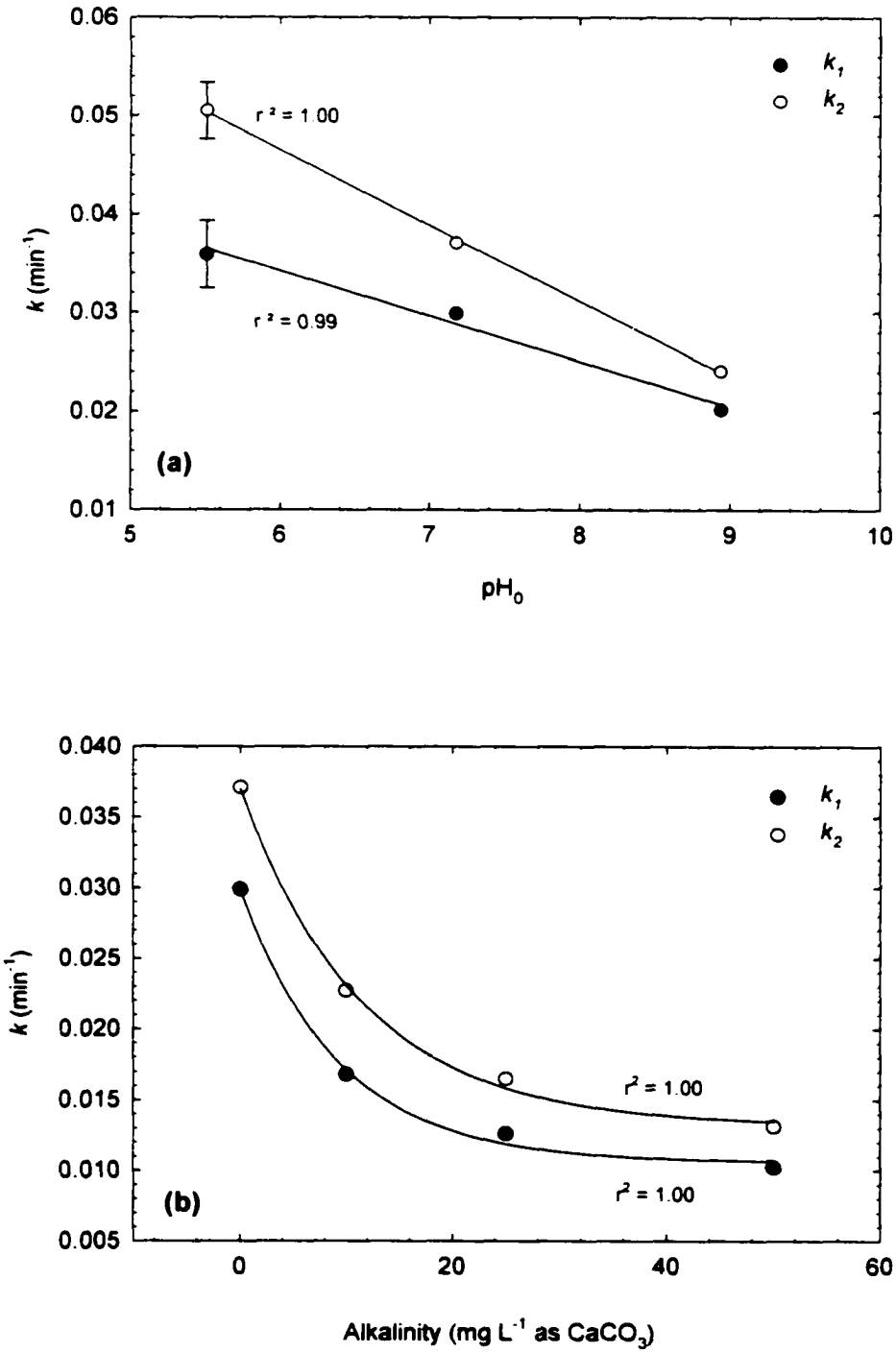

Figure 4.3.2.2. Dependency of $C_2O_4^{2-}$ Photodecomposition Rate Constants k_1 and k_2 on **(a)** pH_0 (I_a = 2.60 × 10^{-6} $EL^{-1}s^{-1}$, C_0 = 2.04 ×10^{-5} –2.19 ×10^{-5} M, T= 25°C), **(b)** Bicarbonate Alkalinity (I_a = 2.60 × 10^{-6} $EL^{-1}s^{-1}$, C_0 = 2.07 × 10^{-5}–2.14 × 10^{-5} M, pH_0 = 7.15 - 7.98, T= 25°C).

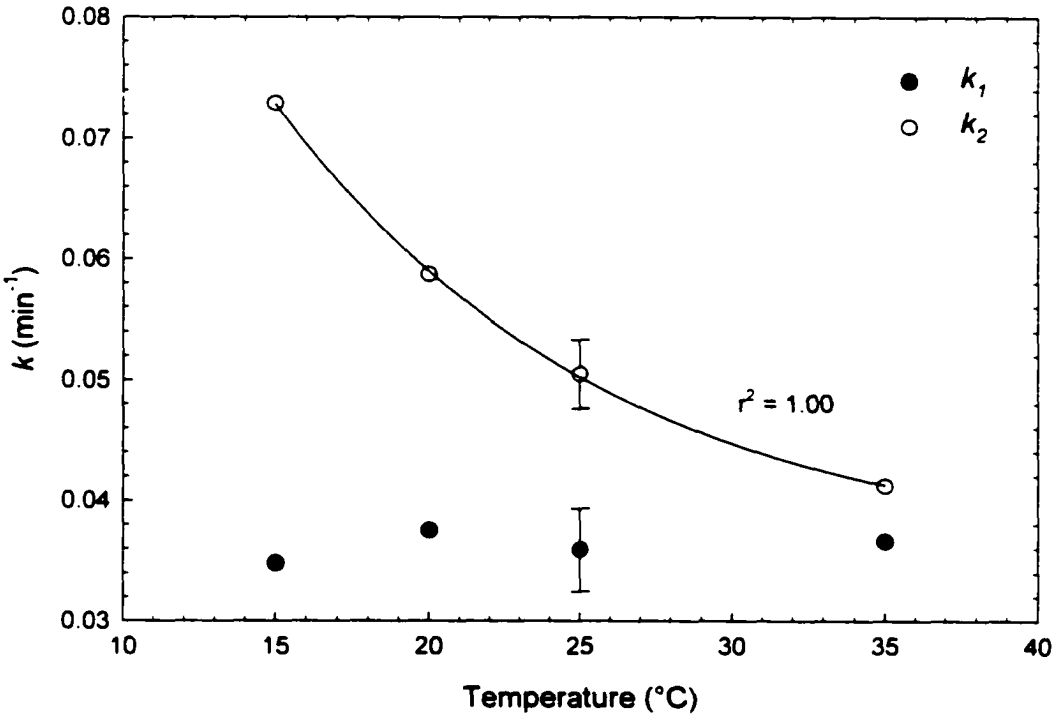

Figure 4.3.2.3. Dependency of $C_2O_4^{2-}$ Photodecomposition Rate Constants k_1 and k_2 on Water Temperature (I_a = 2.60 × 10^{-6} $EL^{-1}s^{-1}$. C_0 = 2.05 × 10^{-5} – 2.17 × 10^{-5} M. pH_0=5.43-5.61).

Table 4.3.2.1. Dependencies of k_1 and k_2 on Experimental Conditions During $C_2O_4^{2-}$ Photodecomposition.

Parameter	Symbol	Experimental Range	k_1 (min^{-1})	k_2 (min^{-1})
Initial Oxalate Concentration (M)	C_0	2.05×10^{-5}-21.11×10^{-5}	$k_1 = 0.010 + 0.035\ e^{-15840\,C_0}$	$k_2 = 0.020 + 0.053\ e^{-27830\,C_0}$
Temperature (^oC)	T	15 - 35	0.035*	$k_2 = 0.035 + 0.150\ e^{-0.093\,T}$
Initial pH	pH_0	5.45 - 8.94	$k_1 = 0.062 - 0.005\ pH_0$	$k_2 = 0.093 - 0.008\ pH_0$
UV Light Intensity ($EL^{-1}s^{-1}$)	I_a	1.38×10^{-6}-5.27×10^{-6}	$k_1 = 0.002 + 12720\ I_a$	$k_2 = -0.006 + 21140\ I_a$
Alkalinity (mgL^{-1} as $CaCO_3$)	A	10 - 50	$k_1 = 0.011 + 0.019\ e^{-0.11\,A}$	$k_2 = 0.013 + 0.024\ e^{-0.09\,A}$

*k_1 was independent of temperature

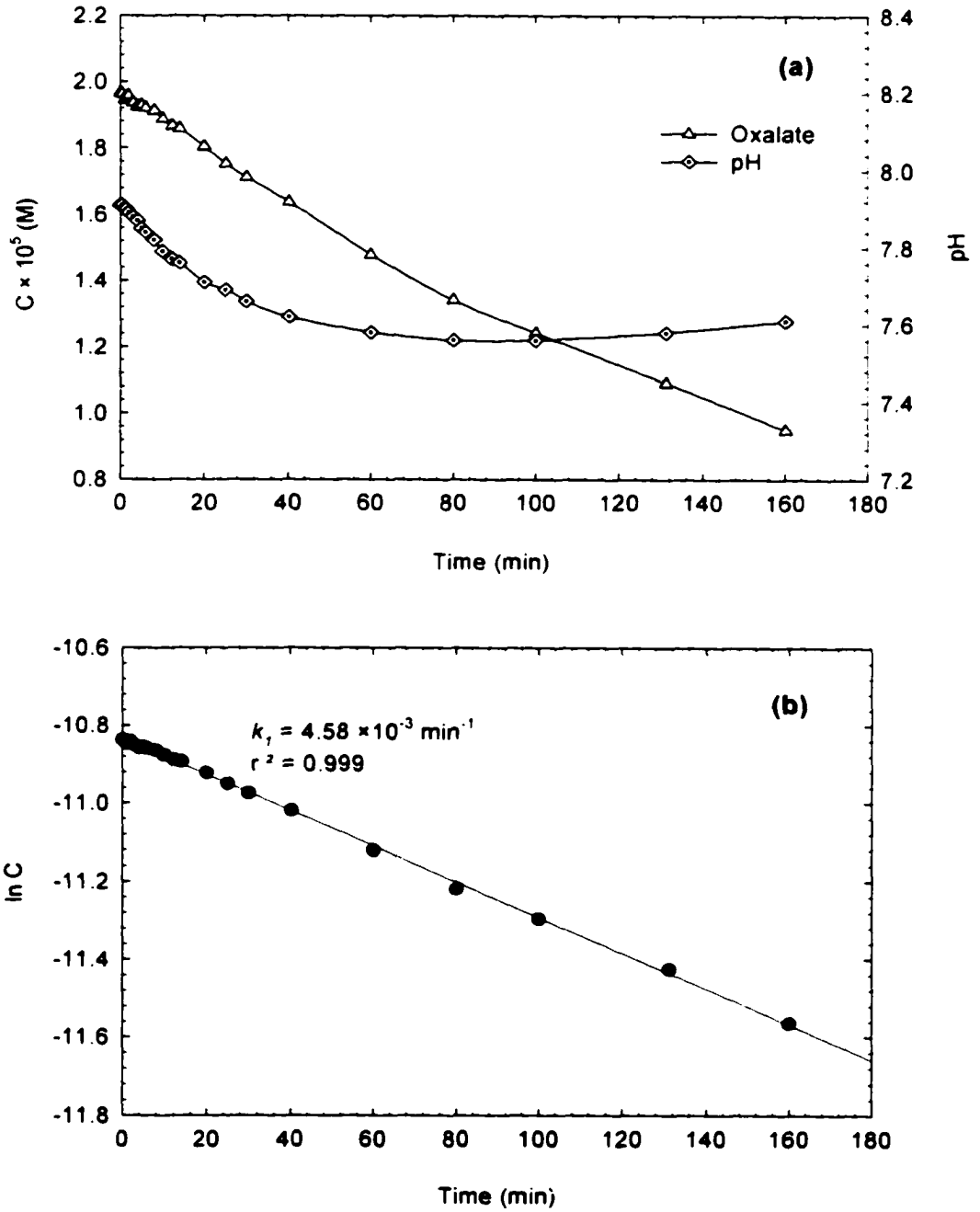

Figure 4.3.2.4. **(a)** Concentration and pH Profiles during UV Irradiation of $C_2O_4^{2-}$ in Pilot Plant Filter Effluent (DOC = 2.31 mg C/L, alkalinity = 53.4 mg/L as $CaCO_3$), and **(b)** Kinetic Analysis of $C_2O_4^{2-}$ Data ($I_a = 2.60 \times 10^{-6}$ $EL^{-1}s^{-1}$, $C_0 = 1.97 \times 10^{-5}$ M, $pH_0 = 7.91$, T = 25°C).

4.3.3. Glyoxalate

$[HC_2O_3^-]_0$ effects on k_1 and k_2 were studied without pH_0 adjustment at 25 °C and I_a of 2.60×10^{-6} E L^{-1} s^{-1}, in the concentration range of (1.73-8.49) × 10^{-5} M (Figure 4.3.3.1a). k_1 increased linearly with increasing $[HC_2O_3^-]_0$ while, k_2 only slightly increased with it. The mean k_1 and k_2 values at $[HC_2O_3^-]_0$= (1.73 – 1.88) × 10^{-5} are (3.4 ± 0.3) ×10^{-6} and (2.0 ± 0.1) ×10^{-6} min^{-1}, respectively.

The influence of I_a on k_1 and k_2 were investigated at 25 °C while $[HC_2O_3^-]_0$ was kept in the range of (1.73 – 1.94) × 10^{-5} M. Figure 4.3.3.1b depicts linear relationship between I_a and k_1 and k_2 in the range of (1.38 – 5.27) × 10^{-6} E L^{-1} s^{-1}.

The effect of temperature was studied between 15-35 °C at I_a of 2.60 x 10^{-6} E L^{-1} s^{-1}. $[HC_2O_3^-]_0$ was kept in the range of (1.73 – 1.88) ×10^{-5} M. pH_0 was not adjusted and ranged 4.50 – 4.66. k_1 increased with temperature while k_2 was not affected significantly by it in the range of experimental conditions (Figure 4.3.3.2a).

The effect of pH_0 on k_1 and k_2 was studied in the range of 4.53-9.10 by adjusting pH_0 with NaOH solution. All experiments were performed at same I_a (2.60×10^{-6} E $L^{-1}s^{-1}$) and temperature (25 °C), and $[HC_2O_3^-]_0$ was kept in the range of (1.73-2.12) × 10^{-5} M. Both k_1 and k_2 have negative linear dependency on pH_0. Figure 4.3.3.2b shows the relationship between pH_0 and k_1 and k_2. Addition of 25 mg/L $NaHCO_3$ (as $CaCO_3$) to the solution resulted 27 % decrease in k_1 and 33 % decrease in k_2. Regression equations for

$[HCO_2^-]_0$. I_a and pH_0 dependencies of k_1 and k_2 and Arrhenius' equation for temperature dependency of k_1 and k_2 are given in Table 4.3.3.1.

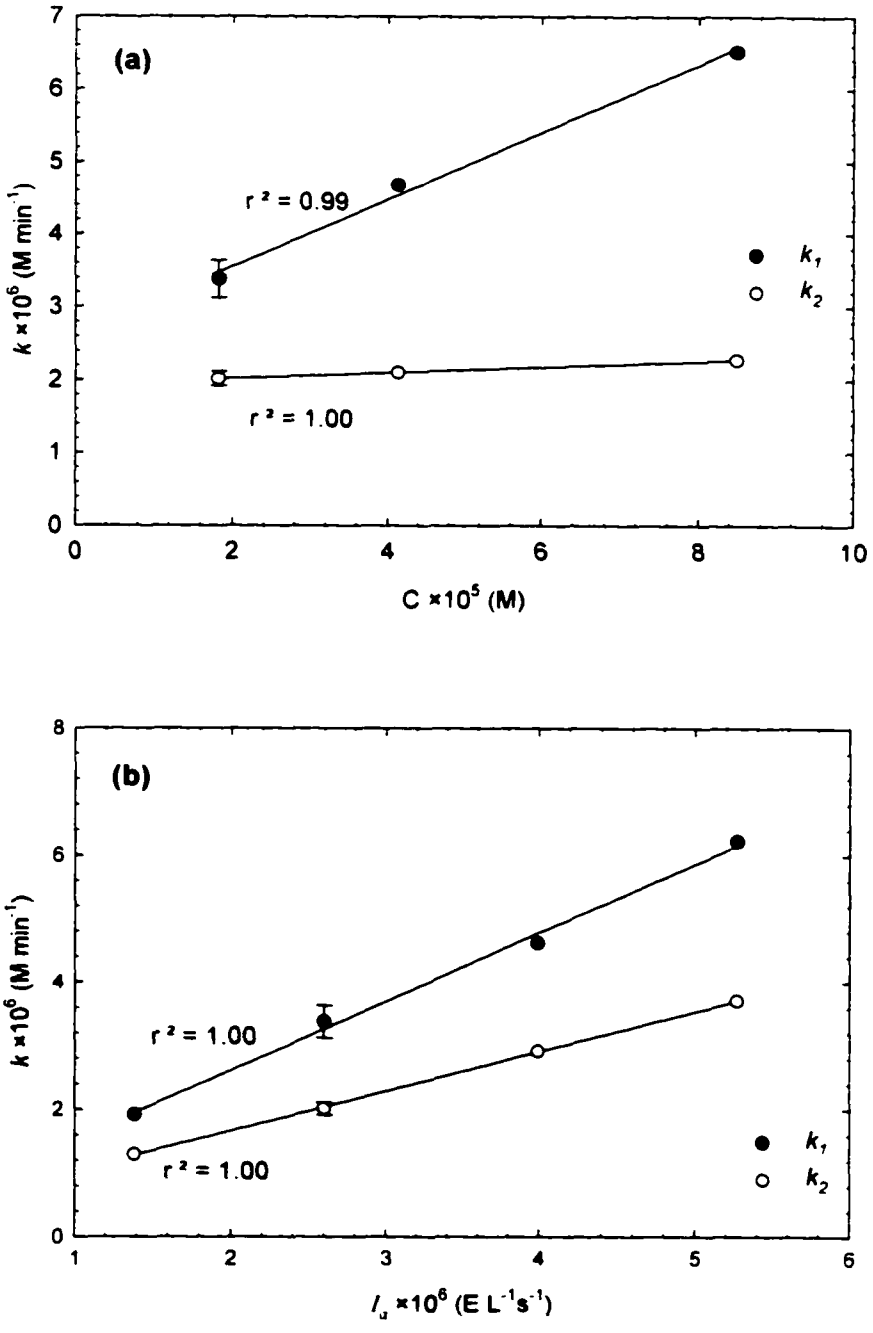

Figure 4.3.3.1. Dependency of $HC_2O_3^-$ Photodecomposition Rate Constants k_1 and k_2 on **(a)** Initial $HC_2O_3^-$ Concentration (I_a = 2.60 × 10^{-6} E L^{-1} s^{-1}, pH_0 = 4.00-4.66, T = 25°C), **(b)** UV Light Intensity (C_0 = 1.72 ×10^{-5} –1.94 ×10^{-5} M, pH_0 = 4.48-4.66, T= 25°C).

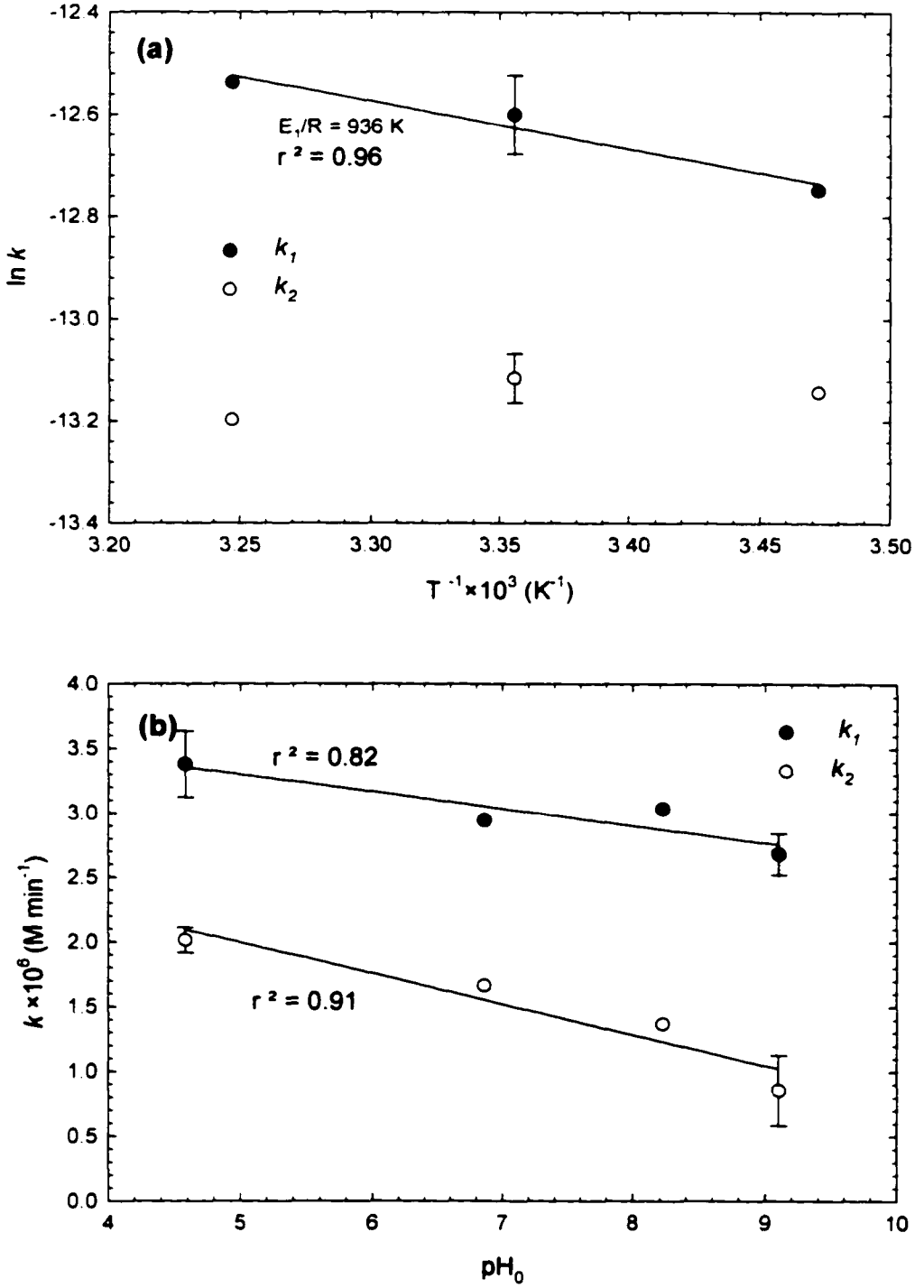

Figure 4.3.3.2. Dependency of $HC_2O_3^-$ Photodecomposition Rate Constants k_1 and k_2 on **(a)** Water Temperature ($I_a = 2.60 \times 10^{-6}$ E L^{-1} s^{-1}, $C_0 = 1.73 \times 10^{-5} - 1.88 \times 10^{-5}$ M, pH_0 = 4.50-4.66). **(b)** pH_0 ($I_a = 2.60 \times 10^{-6}$ E L^{-1} s^{-1}, $C_0 = 1.73 \times 10^{-5} - 2.12 \times 10^{-5}$ M, T = 25 °C).

Table 4.3.3.1. Dependencies of k_1 and k_2 on Experimental Conditions During $HC_2O_3^-$ Photodecomposition.

Parameter	Symbol	Experimental Range	k_1 (M min^{-1})	k_2 (M min^{-1})
Initial Glyoxalate Concentration (M)	C_0	$(1.73\text{-}8.49) \times 10^{-5}$	$k_1 = 2.62 \times 10^{-6} + 4.64 \times 10^{-2} C_0$	$k_2 = 1.94 \times 10^{-6} + 3.96 \times 10^{-3} C_0$
Temperature (^{0}C)	T	15 - 35	$k_1 = 7.59 \times 10^{-5}\, e^{-936/T}$	$k_2 = 1.97$*
Initial pH	pH_0	4.53-9.10	$k_1 = 3.96 \times 10^{-6} - 1.32 \times 10^{-7}\, pH_0$	$k_2 = 3.18 \times 10^{-6} - 2.38 \times 10^{-7}\, pH_0$
UV Light Intensity ($EL^{-1}s^{-1}$)	I_a	$(1.38 - 5.27) \times 10^{-6}$	$k_1 = 4.48 \times 10^{-7} + 1.08\, I_a$	$k_2 = 4.19 \times 10^{-7} + 0.62\, I_a$

*k_2 was independent of temperature

4.3.4. Glycolate

Both k_1 and k_2 increased linearly with $[H_3C_2O_3^-]_0$ and I_a in the range of experimental conditions as depicted in Figure 4.3.4.1a and Figure 4.3.4.1b, respectively. $[H_3C_2O_3^-]_0$ and I_a dependency experiments were conducted at 25 °C and without pH_0 adjustment.

The effect of pH_0 on k_1 and k_2 investigated in the range of 4.57-9.12 by adjusting with NaOH solution. Figure 4.3.4.2a shows negative linear relationship between observed rate constants and pH_0. Both k_1 and k_2 increased linearly with temperature (Figure 4.3.4.2b).

Influence of alkalinity addition was observed with addition of 25 mg L^{-1} $NaHCO_3$ (as $CaCO_3$) at 2.60×10^{-6} E L^{-1} s^{-1}, 25 °C and $[H_3C_2O_3^-]_0 = 2.00 \times 10^{-5}$ M and results were presented in Table 4.3.4.1. Both k_1 and k_2 were much lower in the presence of alkalinity. Regression equations for $[H_3C_2O_3^-]_0$, I_a and pH_0 dependencies of k_1 and k_2 and Arrhenius' equation for temperature dependency of k_1 and k_2 are given in Table 4.3.4.2.

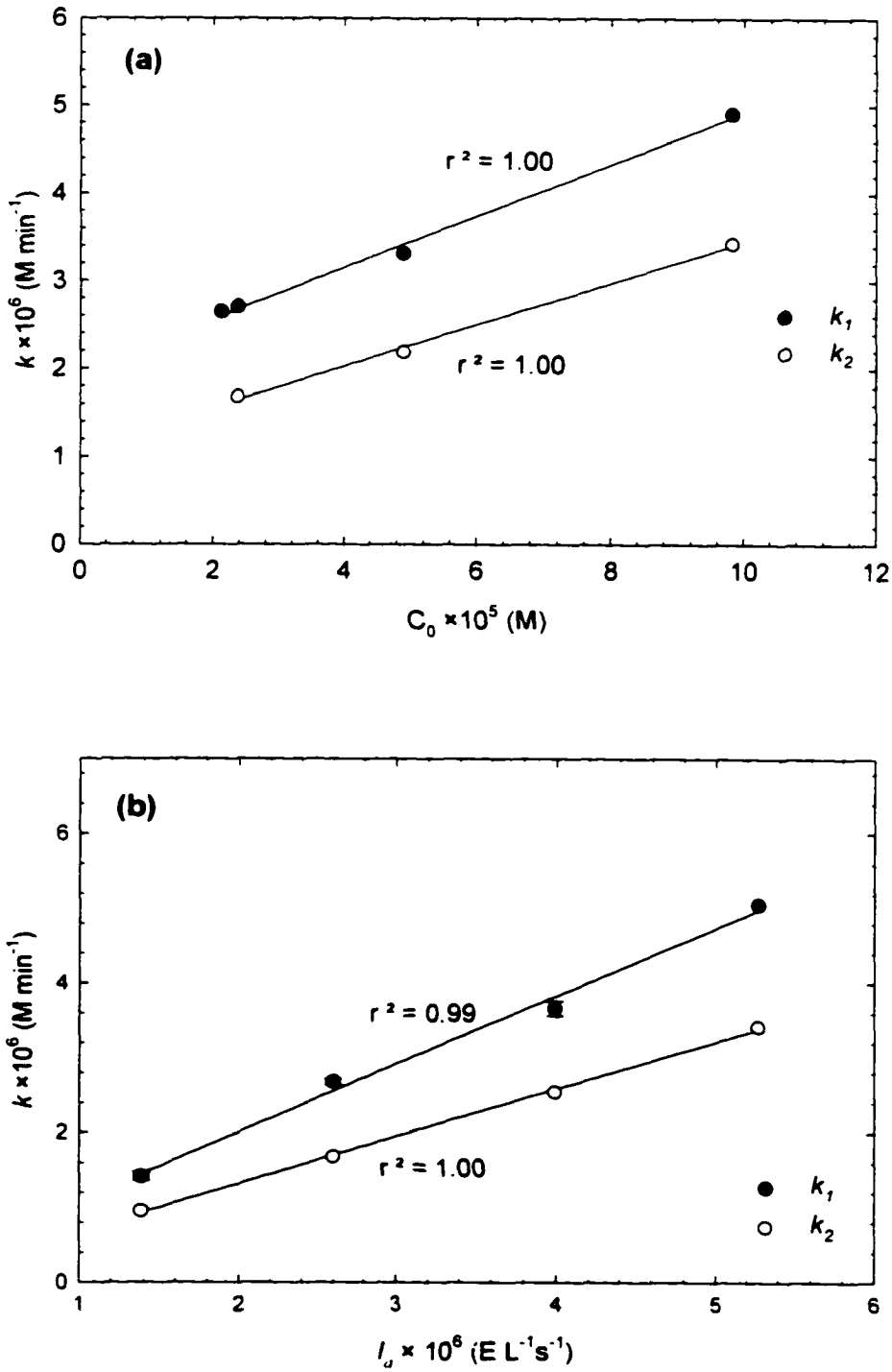

Figure 4.3.4.1. Dependency of $H_3C_2O_3^{\cdot}$ Photodecomposition Rate Constants k_1 and k_2 on **(a)** Initial $H_3C_2O_3^{\cdot}$ Concentration ($I_a = 2.60 \times 10^{-6}$ E L^{-1} s^{-1}, pH_0 = 4.06-4.63, T = 25°C). **(b)** UV Light Intensity ($C_0 = 2.00 \times 10^{-5} - 1.37 \times 10^{-5}$ M, pH_0 = 4.57-4.63, T= 25°C).

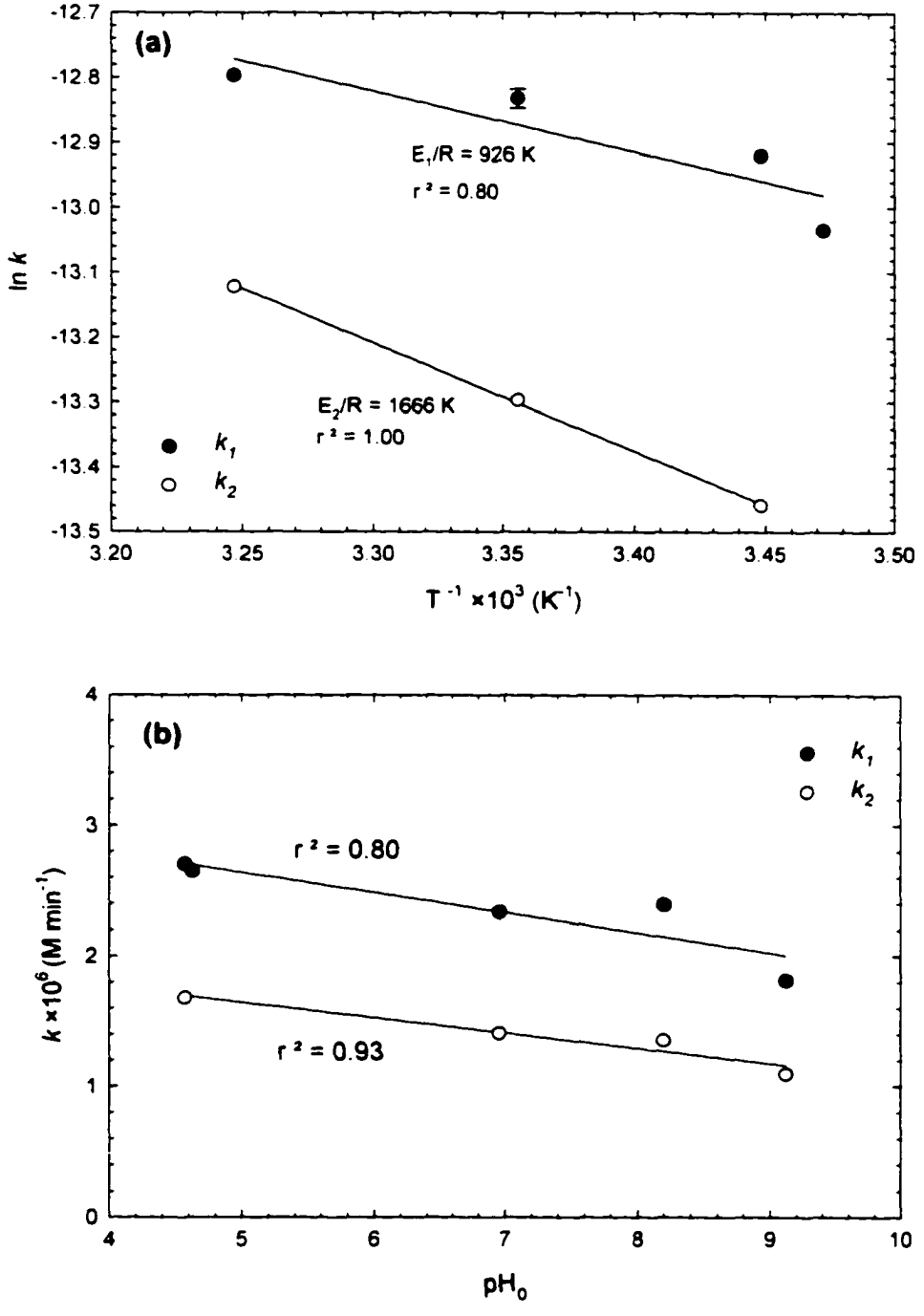

Figure 4.3.4.2. Dependency of $H_3C_2O_3^{\cdot}$ Photodecomposition Rate Constants k_1 and k_2 on **(a)** Water Temperature (I_a = 2.60 × 10^{-6} E L^{-1} s^{-1}, C_0 = (2.12 -2.37) ×10^{-5} M, pH_0 = 4.50-4.67). **(b)** pH_0 (I_a = 2.60 × 10^{-6} E L^{-1} s^{-1}, C_0 = (2.12 -2.37) ×10^{-5} M, T = 25°C).

Table 4.3.4.1. $H_3C_2O_3^-$ Decay Rate Constants in the Presence and Absence of $NaHCO_3$ ($I_a = 2.60 \times 10^{-6}$ $EL^{-1}s^{-1}$ and T = 25°C).

Alkalinity	$C_0 \times 10^5$ M	pH_0	$k_1 \times 10^6$ (M min^{-1})	$k_2 \times 10^6$ (M min^{-1})
25 mgL^{-1} as $CaCO_3$	2.00	7.36	1.704	0.992
-	2.12-2.37	4.57-4.63	2.68 ± 0.04*	1.680

*Average of two experiments.

Table 4.3.4.2. Dependencies of k_1 and k_2 on Experimental Conditions During $H_3C_2O_3^{\cdot}$ Photodecomposition.

Parameter	Symbol	Experimental Range	k_1 (M min^{-1})	k_2 (M min^{-1})
Initial Glycolate Concentration (M)	C_0	$(2.12\text{-}9.83) \times 10^{-5}$	$k_1 = 1.98 \times 10^{-6} + 2.94 \times 10^{-2}\, C_0$	$k_2 = 1.08 \times 10^{-6} + 2.37 \times 10^{-2}\, C_0$
Temperature ($^{\circ}$C)	T	15 - 35	$k_1 = 5.74 \times 10^{-5}\, e^{-926/T}$	$k_2 = 4.48 \times 10^{-4}\, e^{-1666/T}$
Initial pH	pH_0	4.57-9.12	$k_1 = 3.40 \times 10^{-6} - 1.53 \times 10^{-7}\, pH_0$	$k_2 = 2.23 \times 10^{-6} - 1.17 \times 10^{-7}\, pH_0$
UV Light Intensity ($EL^{-1}s^{-1}$)	I_a	$(1.38 - 5.27) \times 10^{-6}$	$k_1 = 1.87 \times 10^{-7} + 0.91\, I_a$	$k_2 = 5.61 \times 10^{-8} + 0.63\, I_a$

4.4. Dissolved Oxygen Effects on the Decay Kinetics

The dissolved oxygen (DO) was near saturation at the beginning of all experiments. The DO effects were studied in DIW solutions of HCO_2^- and $C_2O_4^{2-}$.

4.4.1. Formate

DO effects on HCO_2^- decay are given in Table 4.4.1.1, where k_1 and k_2 are compared in the presence and absence of DO. In the absence of DO the comparison shows that $k_1 > k_2$, while cross comparison shows that $k_{1,DO\ FREE} > k_{1,DO}$ and $k_{2,DO\ FREE} \leq k_{2,DO}$

The absorption spectra of samples were also generated during UV irradiation of $NaHCO_2$ solutions in the presence and absence of DO. Boxes (a) and (b) in Figure 4.4.1.1 show absorbance of the kinetic samples at 190, 200, 220 and 253.7 nm in the presence and absence of DO, respectively. Vertical lines represent $t = t_b$. In the presence of DO, the absorbance at 190 nm decreased with HCO_2^- decay and remained stable after HCO_2^- = BDL. However, in the absence of DO, absorbance at all wavelengths increased until $t = t_b$, then decreased with time. The observed change in absorbance profiles could be attributed to HCO_2^- decay since it clearly occurs at $t = t_b$. The difference in absorbance profiles observed in the presence and absence of DO depicts that HCO_2^- decomposition mechanism and decomposition intermediates in the presence of DO are different than those in the absence of DO.

Table 4.4.1.1. HCO_2^- Photodecomposition Rate Constants in the Presence and Absence of Dissolved Oxygen (T = 25°C).

Dissolved O_2	$I_a \times 10^6$ $EL^{-1}s^{-1}$	$C_0 \times 10^5$ M	pH_0	$k_1 \times 10^6$ ($M\ min^{-1}$)	$k_2 \times 10^6$ ($M\ min^{-1}$)
Present	2.60	4.24 ± 0.06	5.50 ± 0.06	3.409 ± 0.292*	5.436 ± 0.669*
	2.60	38.33	5.71	3.803	7.914
	3.99	4.28	5.55	4.476	8.524
	3.99	41.45	5.81	7.300	12.356
Absent	2.60	4.17	6.49	6.625	5.912
	2.60	42.82	6.47	5.383	4.462
	3.99	40.51	7.50	7.772	5.673

* Average of five experiments.

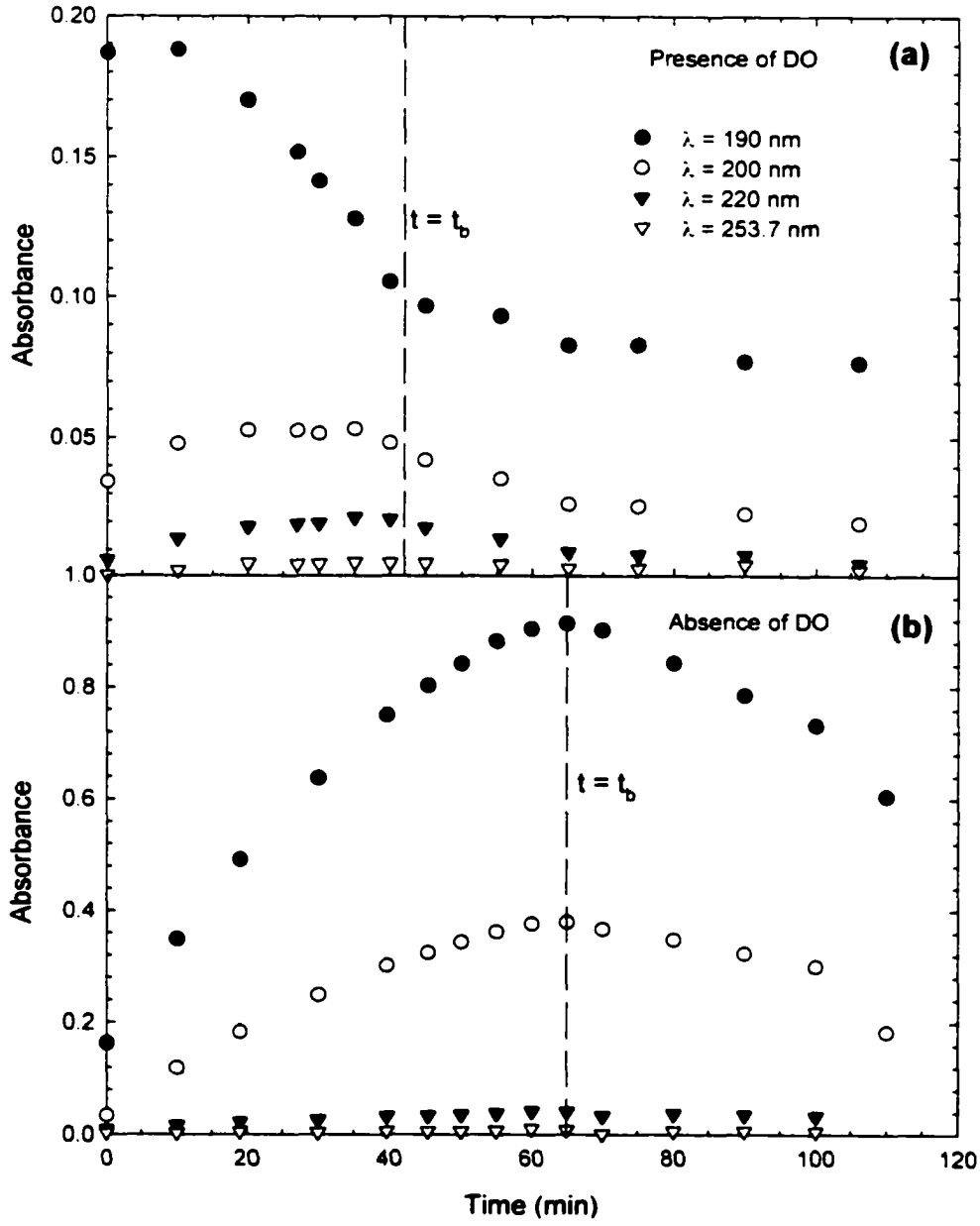

Figure 4.4.1.1. Absorbance of Samples at Various Wavelengths During UV Irradiation of HCO_2^- **(a)** In the Presence of DO ($I_a = 3.99 \times 10^{-6}$ $EL^{-1}s^{-1}$, $C_0 = 4.15 \times 10^{-4}$ M, $pH_0 = 5.81$, T = 25°C). **(b)** In the Absence of DO ($I_a = 3.99 \times 10^{-6}$ $EL^{-1}s^{-1}$, $C_0 = 4.05 \times 10^{-4}$ M, $pH_0 = 7.50$, T = 25°C).

4.4.2. Oxalate

The DO effect on $C_2O_4^{2-}$ decay at 25 °C and 2.60 × 10^{-6} $EL^{-1}s^{-1}$ is presented in Table 4.4.2.1. Four experiments were run in the presence and one in the absence of DO. Both k_1 and k_2 were lower in the absence of DO. Karpel Vel Leitner and Doré (1997) carried out a similar comparison in their UV/H_2O_2 system and found that k_1 increased while k_2 decreased in the absence of DO, as shown in Figure 4.2.2.7, with the change remaining within 10 percent.

Table 4.4.2.1. $C_2O_4^{2-}$ Decay Rate Constants in the Presence and Absence of Dissolved Oxygen (I_a = 2.60 × 10^{-6} $EL^{-1}s^{-1}$and T = 25°C).

Dissolved Oxygen	C_0 ×10^5 M	pH_0	k_1 (min^{-1})	k_2 (min^{-1})
Present	2.07 ± 0.03	5.51 ± 0.08	0.036 ± 0.003*	0.051 ± 0.003*
Absent	2.07	6.32	0.027	0.040

*Average of four experiments.

4.5. pH Profile Estimation During Decay of Acid Solutions

The reaction pH profile for HCO_2^- and $C_2O_4^{2-}$ solutions without prior pH_0 adjustment can be computed using closed system equilibrium analysis. The carbonate equilibria and mass balance equations are common to both HCO_2^- and $C_2O_4^{2-}$ solutions and are shown below:

Equilibria:

$$H_2O \leftrightarrows OH^- + H^+ \qquad pK_w = 14 \qquad (4.5.1)$$

$$H_2CO_3^* \leftrightarrows HCO_3^- + H^+ \qquad pK_{a1} = 6.35 \qquad (4.5.2)$$

$$HCO_3^- \leftrightarrows CO_3^{2-} + H^+ \qquad pK_{a2} = 10.33 \qquad (4.5.3)$$

Mass Balance:

$$[CO_3]_T = [H_2CO_3^*] + [HCO_3^-] + [CO_3^{2-}] \qquad (4.5.4)$$

The equilibria and mass balance equations for HCO_2^- and $C_2O_4^{2-}$ are given in Table 4.5.1.

Table 4.5.1. Equilibria and Mass Balance Equations for HCO_2^- and $C_2O_4^{2-}$.

Compound	Equilibrium Equations	Mass Balance Equations
HCO_2^-	$HCO_2H \leftrightarrows HCO_2^- + H^+$ (4.5.5)	$[HCO_2^-]_T = [HCO_2H] + [HCO_2^-]$ (4.5.8) $[Na^+] = [HCO_2^-]_{T,0}$ (4.5.9)
$C_2O_4^{2-}$	$H_2C_2O_4 \leftrightarrows HC_2O_4^- + H^+$ (4.5.6) $HC_2O_4^- \leftrightarrows C_2O_4^{2-} + H^+$ (4.5.7)	$[C_2O_4^{-2}]_T = [H_2C_2O_4] + [HC_2O_4^-] + [C_2O_4^{2-}]$ (4.5.10) $[Na^+] = 2 \times [C_2O_4^{2-}]_{T,0}$ (4.5.11)

The formate species ($[HCO_2H]$ and $[HCO_2^-]$) were determined based on a selected pH and equations (4.5.1), (4.5.5) and (4.5.8). The carbonate species ($[H_2CO_3^*]$, $[HCO_3^-]$ and $[CO_3^{2-}]$) were computed based on estimated $[CO_3]_{T,t}$, the selected pH and equations (4.5.1), (4.5.2), (4.5.3) and (4.5.4) where:

$$[CO_3]_{T,t} = [CO_3]_{T,t-1} + \Delta[HCO_2^-]_t \qquad (4.5.12)$$

$$\Delta[HCO_2^-]_t = [HCO_2^-]_{t-1} - [HCO_2^-]_t \qquad (4.5.13)$$

assuming all $\Delta[HCO_2^-]_t$ is converted CO_2 in water ($[CO_3]_{T,0}$ represents DIW). The charge balance for HCO_2^- shown in equation (4.5.14) below was used to check for equilibrium.

$$[Na^+] + [H^+] = [OH^-] + [HCO_2^-] + [HCO_3^-] + 2\,[CO_3^{2-}] \qquad (4.5.14)$$

The computation was repeated at each reaction time with $[HCO_2^-]$ observation, by modifying the selected pH by trial and error until the charge balance was satisfied. The "MINEQL+" Chemical Equilibrium Modeling System (Environmental Research Software, Hallowell, ME) was used for the aforementioned equilibrium pH calculations. Observed and predicted pH profiles for an experiment at 35 °C and 2.60×10^{-6} E/L s are given in Figure 4.5.1. $[HCO_2^-]_0$ was 4.23×10^{-5} M for the experiment and pH_0 was the equilibrium pH. Equilibrium pH calculations were performed for three different $[CO_3]_{T,0}$ levels of 4.0, 4.5 and 5.0×10^{-4} M (alkalinity = 4-5 mg/L as $CaCO_3$) which represent likely alkalinity levels in DIW. The results indicated that the equilibrium analysis could satisfactorily predict the pH-time profiles during photodecomposition of HCO_2^-.

Similarly, the oxalate species ($[H_2C_2O_4]$, $[HC_2O_4^-]$ and $[C_2O_4^{2-}]$) were determined based on selected pH and equations (4.5.1), (4.5.6), (4.5.7) and (4.5.10), while

$$[CO_3]_{T,t} = [CO_3]_{T,t-1} + 2 \times \Delta[C_2O_4^{2-}]_t \qquad (4.5.15)$$

$$\Delta[C_2O_4^{2-}]_t = [C_2O_4^{2-}]_{t-1} - [C_2O_4^{2-}]_t \qquad (4.5.16)$$

assuming all $\Delta[C_2O_4^{2-}]_t$ is converted CO_2 in water.

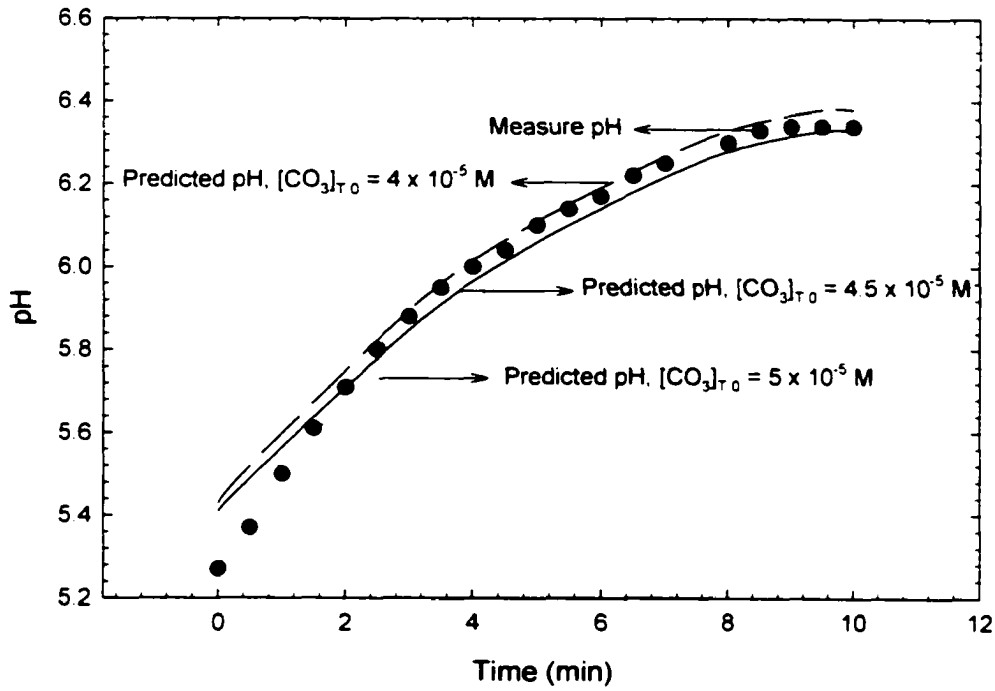

Figure 4.5.1. Observed and Predicted pH Versus Time Profiles During HCO_2^- Photodecomposition (I_a = 2.60 × 10^{-6} $EL^{-1}s^{-1}$, C_0 = 4.23 × 10^{-5} M, pH_0=5.27, T = 35 °C).

The carbonate species ($[H_2CO_3^*]$, $[HCO_3^-]$ and $[CO_3^{2-}]$) were computed based on the estimated $[CO_3]_{T,t}$, the selected pH and equations (4.5.1), (4.5.2), (4.5.3) and (4.5.4). The results were used in the charge balance shown in equation (4.5.17) below.

$$[Na^+] + [H^+] = [OH^-] + [HC_2O_4^-] + 2\,[C_2O_4^{2-}] + [HCO_3^-] + 2\,[CO_3^{2-}] \qquad (4.5.17)$$

The computation was repeated by modifying the selected pH until charge balance was satisfied. Figure 4.5.2 shows observed and predicted pH profiles for two experiments: (a) $[C_2O_4^{2-}]_{T,0}$ = 2.07 × 10^{-5} M, with added alkalinity (as $NaHCO_3$) of 10 mg/L as $CaCO_3$ and (b) $[C_2O_4^{2-}]_{T,0}$ = 8.75 × 10^{-5} M, at $[CO_3]_{T,0}$ levels of 2.5, 3.0 and 3.5 × 10^{-4} M (alkalinity

= 2.5-3.5 mg/L as $CaCO_3$. In addition, insert "c" of Figure 4.5.2 depicts the system in the absence of carbonate alkalinity and with $[CO_3^{2-}]_T$ produced from $C_2O_4^{2-}$ decay only ($[CO_3^{2-}]_{T,0} = 0$). The results show that higher initial alkalinity lowers the time dependent variability of pH in the reaction medium and that the equilibrium analysis can satisfactorily predict the pH-time profiles in decomposition of $C_2O_4^{2-}$ under UV irradiation.

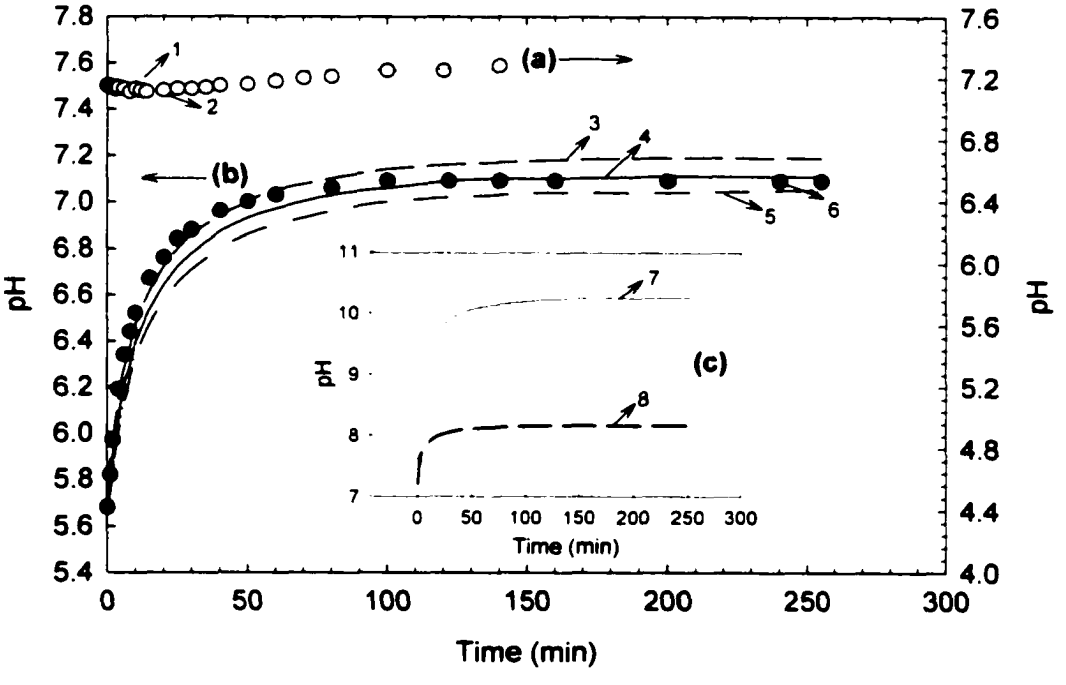

1. Predicted pH, $[CO_3]_{T,0} = 2.65 \times 10^{-4}$ M
2. Observed pH in (a)
3. Predicted pH, $[CO_3]_{T,0} = 2.5 \times 10^{-5}$ M
4. Predicted pH, $[CO_3]_{T,0} = 3.0 \times 10^{-5}$ M
5. Predicted pH, $[CO_3]_{T,0} = 3.5 \times 10^{-5}$ M
6. Observed pH in (b)
7. Equilibrium pH for Oxalate System ($[CO_3]_T = 0$)
8. Predicted pH, $[CO_3]_{T,0} = 0$

Figure 4.5.2. Observed and Predicted pH Versus Time Profiles during $C_2O_4^{2-}$ Photodecomposition **(a)** In DIW Containing $NaHCO_3$ = 10 mg/L as $CaCO_3$ ($I_a = 2.60 \times 10^{-6}$ $EL^{-1}s^{-1}$, $C_0 = 2.07 \times 10^{-5}$ M, $pH_0 = 7.15$, T = 25°C), **(b)** DIW ($I_a = 2.60 \times 10^{-6}$ $EL^{-1}s^{-1}$, $C_0 = 8.75 \times 10^{-5}$ M, $pH_0 = 5.68$, T = 25°C), and **(c)** Equilibrium pH of $C_2O_4^{2-}$ System: (7) in the absence of CO_3^{2-} and (8) for $[CO_3^{2-}]_{T,0} = 0$ and $[CO_3^{2-}]_{T,t} = [CO_3^{2-}]_{T,t-1} + 2 \times ([C_2O_4^{2-}]_{t-1} - [C_2O_4^{2-}]_t)$.

4.6. Photodecomposition of Acid Mixtures

The photodecomposition of acid mixtures was explored in Formate/Oxalate and Glycolate /Oxalate systems.

4.6.1. Formate / Oxalate Mixture

The photodecomposition of $HCO_2^-/C_2O_4^{2-}$ mixture was explored at 2.60×10^{-6} $EL^{-1}s^{-1}$ and 25°C in a solution containing $NaHCO_2$ and $Na_2C_2O_4$ at equal concentrations as C. Figure 4.6.1.1 shows HCO_2^-, $C_2O_4^{2-}$, NPOC and pH profiles observed during the experiment. HCO_2^- decomposed readily while $C_2O_4^{2-}$ remained virtually unchanged until HCO_2^- = BDL. Meanwhile, the solution pH increased rapidly until HCO_2^- = BDL to later increase slowly and reach a plateau when $C_2O_4^{2-}$ = BDL. HCO_2^- followed pseudo-zero order decay kinetics with split rate reaction with k_1 and k_2 of 3.07×10^{-6} M min^{-1} and 4.47×10^{-6} M min^{-1}, respectively. $C_2O_4^{2-}$ followed pseudo-first order kinetics with split rate reaction as well after HCO_2^- = BDL with k_1 and k_2 of 0.024 and 0.033 min^{-1}, respectively. The decay rate constants for HCO_2^- and $C_2O_4^{2-}$ during irradiation of the mixture were lower than those observed with solutions of individual species as shown in Table 4.6.1.1. Although, $\varepsilon_{253.7}$ ($C_2O_4^{2-}$) is about 100 times that of $\varepsilon_{253.7}$ (HCO_2^-), $C_2O_4^{2-}$ remained virtually unchanged until $t = t_c$ and HCO_2^- decayed much faster than $C_2O_4^{2-}$. Finally, the time dependent NPOC data closely followed TMOC ([HCO_2^--C] + [$C_2O_4^{2-}$-C]), suggesting that the unaccounted for carbon is converted to CO_2.

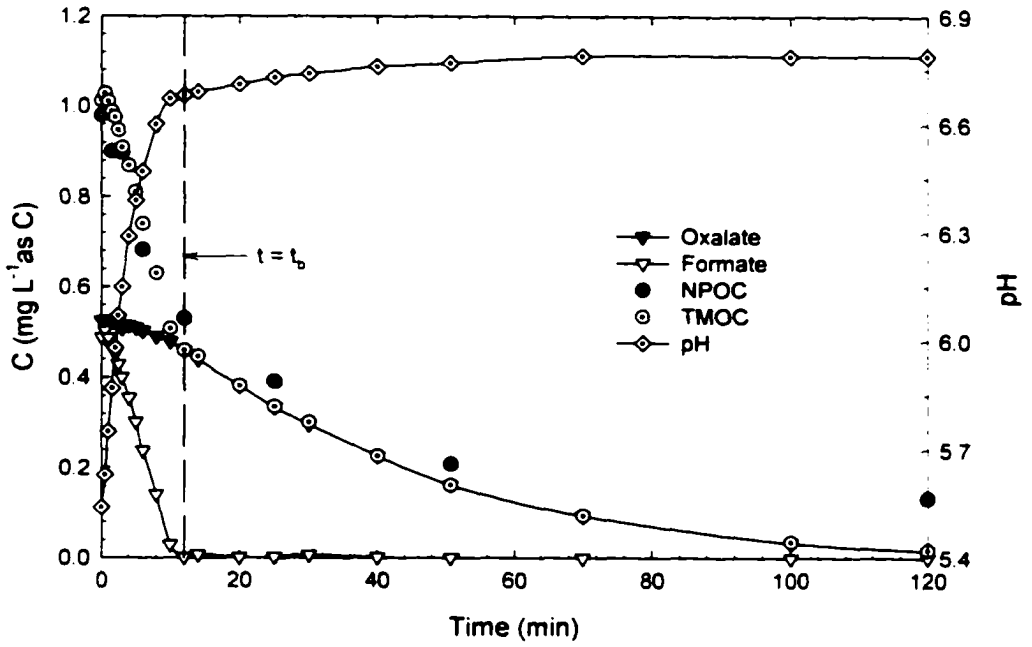

Figure 4.6.1.1. Concentration and pH Profiles during UV Irradiation of $\{HCO_2^- + C_2O_4^{2-}\}$ in DIW (I_a = 2.60 × 10^{-6} $EL^{-1}s^{-1}$, $[HCO_2^-]_0$ = 4.07 × 10^{-5} M, $[C_2O_4^{2-}]_0$ = 2.19 × 10^{-5} M, pH_0 = 5.54, T = 25°C).

Table 4.6.1.1. HCO_2^- and $C_2O_4^{2-}$ Photodecomposition Rate Constants in Individual Solutions and Mixture (I_a = 2.60 × 10^{-6} $EL^{-1}s^{-1}$ and T = 25°C).

Rate Constant	Oxalate	Formate	Mixture***	
			Oxalate	Formate
k_1	0.036 ± 0.003* min^{-1}	(3.409 ± 0.292) × 10^{-6}** $M \cdot min^{-1}$	0.024 min^{-1}	3.07 × 10^{-6} $M \cdot min^{-1}$
k_2	0.051 ± 0.003* min^{-1}	(5.436 ± 0.669) × 10^{-6}** $M \cdot min^{-1}$	0.033 min^{-1}	4.47 × 10^{-6} $M \cdot min^{-1}$

* Average of four experiments.
** Average of five experiments.
*** $[HCO_2^-]_0$ = 4.07 × 10^{-5} M, $[C_2O_4^{2-}]_0$ = 2.19 × 10^{-5} M.

4.6.2. Glycolate / Oxalate Mixture

Figure 4.6.2.1 shows observed $H_3C_2O_3^-$, $HC_2O_3^-$, $C_2O_4^{2-}$, HCO_2^-, NPOC and pH profiles during photodecomposition of the solution containing equal concentrations of $H_4C_2O_3$ and $Na_2C_2O_4$ at 5.27×10^{-6} $EL^{-1}s^{-1}$ and T = 25°C. $H_3C_2O_3^-$ decayed following pseudo-zero order kinetics (Figure 4.6.2.2a) with a rate constant of 4.12×10^{-6} M min^{-1}. $C_2O_4^{2-}$ remained stable initially until $[HC_2O_3^-] \approx [HC_2O_3^-]_{max}$, later increased and reached $[C_2O_4^{2-}]_{max}$ at $[H_3C_2O_3^-] \approx [HC_2O_3^-] \approx [HCO_2^-] \approx$ BDL (Figure 4.6.2.2.b), to subsequently decay following split-rate pseudo-first order kinetics with rate constants k_1 and k_2 of 0.086 and 0.202 min^{-1}, respectively. Solution pH was virtually constant until $[C_2O_4^{2-}]_{max}$, to later increase and reach a plateau after $[C_2O_4^{2-}]$ = BDL as it was observed during individual $C_2O_4^{2-}$ decay, reported in section 4.2.2.

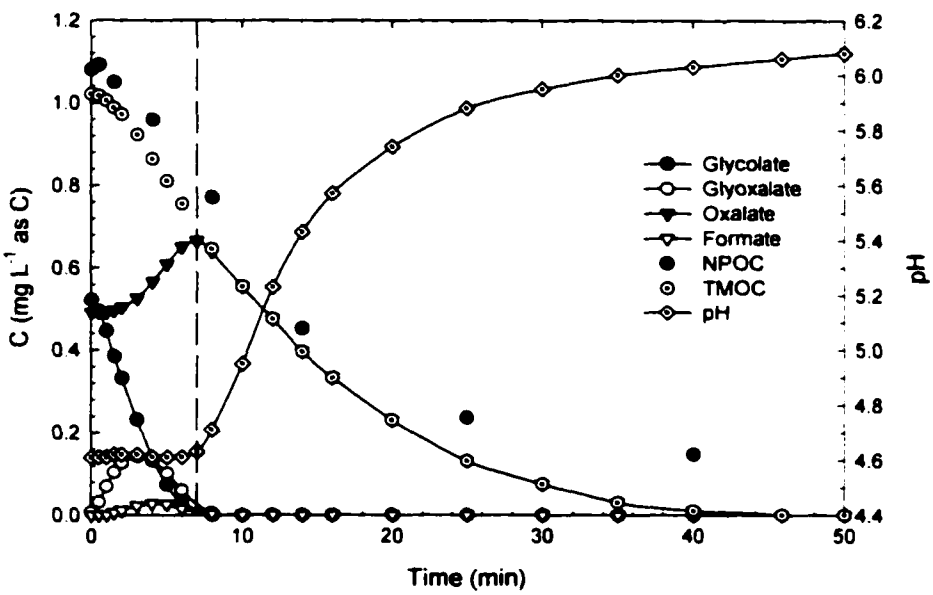

Figure 4.6.2.1. Concentration and pH Profiles during UV Irradiation of $\{H_3C_2O_3^- + C_2O_4^{2-}\}$ in DIW ($I_a = 5.27 \times 10^{-6}$ $EL^{-1}s^{-1}$, $[H_3C_2O_3^-]_0 = 2.18 \times 10^{-5}$ M, $[C_2O_4^{2-}]_0 = 2.05 \times 10^{-5}$ M, $pH_0 = 4.61$, T = 25°C).

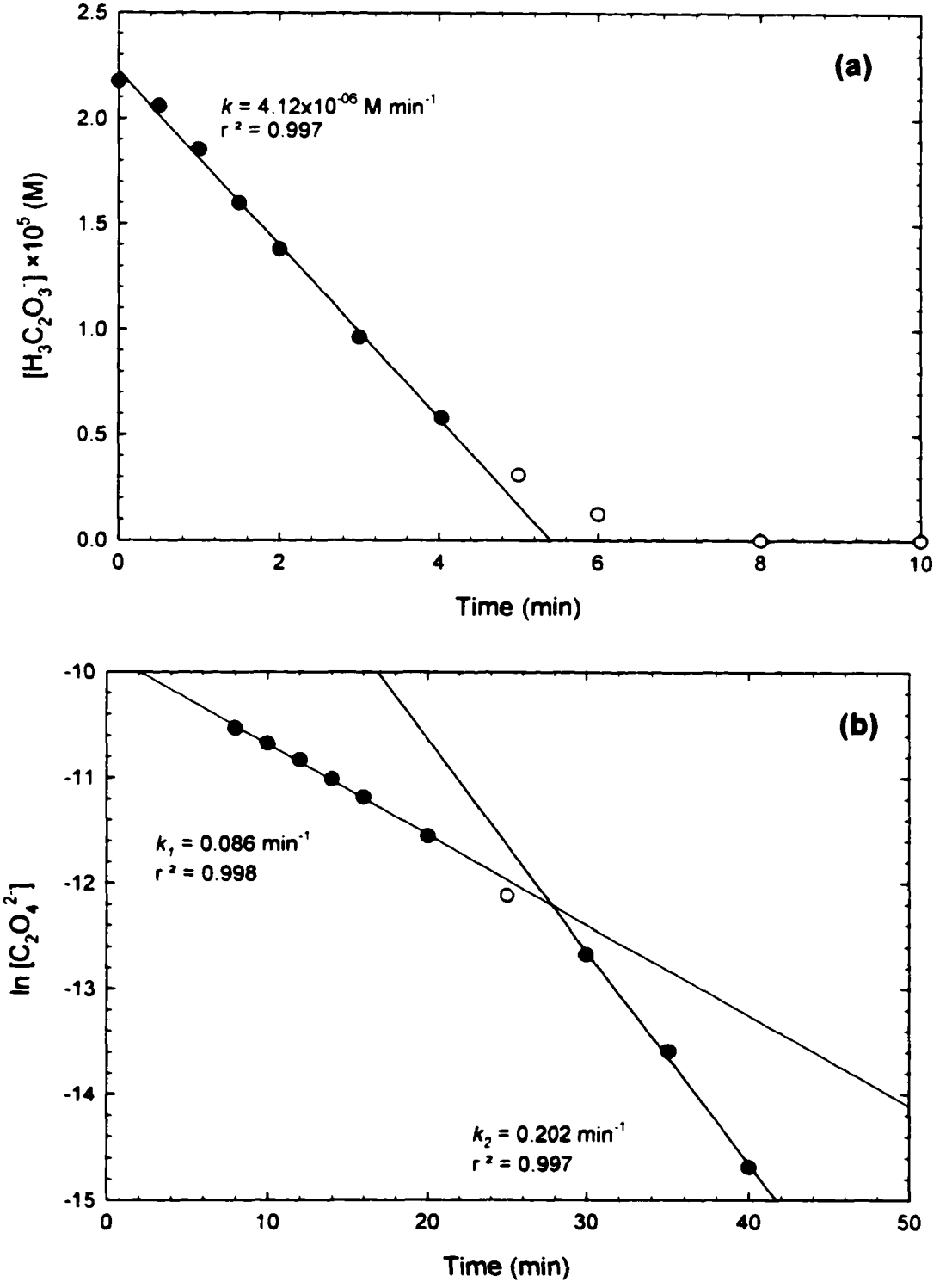

Figure 4.6.2.2. Kinetic Analysis of **(a)** $H_3C_2O_3^-$ Decay Data, **(b)** $C_2O_4^{2-}$ Decay Data.

Table 4.6.2.1 shows comparison of decay rate constants for $H_3C_2O_3^{\cdot}$ and $C_2O_4^{2-}$ alone and in a mixture. Both rate constants for oxalate are higher in the mixture, while initial $H_3C_2O_3^{\cdot}$ rate constant is lower during decay of the mixture.

Table 4.6.2.1. $H_3C_2O_3^{\cdot}$ and $C_2O_4^{2-}$ Photodecomposition Rate Constants During the Photodecomposition of Individual Solutions and Mixture ($I_a = 5.27 \times 10^{-6}$ $EL^{-1}s^{-1}$ and T = 25°C).

Rate Constant	Oxalate	Glycolate	Mixture*	
			Oxalate	Glycolate
k_1	0.069 min^{-1}	5.055×10^{-6} $M \cdot min^{-1}$	0.086 min^{-1}	4.12×10^{-6} $M \cdot min^{-1}$
k_2	0.104 min^{-1}	3.417×10^{-6} $M \cdot min^{-1}$	0.202 min^{-1}	-

* $[H_3C_2O_3^{\cdot}]_0 = 2.18 \times 10^{-5}$ M, $[C_2O_4^{2-}]_0 = 2.05 \times 10^{-5}$ M.

4.7. Decay of Formate, Oxalate and Glyoxalate as Products of Photodecomposition

$HCO_2^{\cdot}$ was observed as intermediate during $HC_2O_3^{\cdot}$ and $H_3C_2O_3^{\cdot}$ decay as reported in sections 4.2.3 and 4.2.4, respectively, and decayed following near zero order kinetics. A clear split in decay rate was not observed during intermediate $[HCO_2^{\cdot}]$ decay since $[HCO_2^{\cdot}]_0$ was very low (0.25 - 2.10 $\times 10^{-5}$ M) and limited kinetic data were available. Figure 4.7.1 shows the effects of experimental conditions on rate constants as well comparison of k_1 with k_{1go} (observed $HCO_2^{\cdot}$ decay rate constant during $HC_2O_3^{\cdot}$ decomposition) and k_{1g} (observed $HCO_2^{\cdot}$ decay rate constant during $H_3C_2O_3^{\cdot}$ decay).

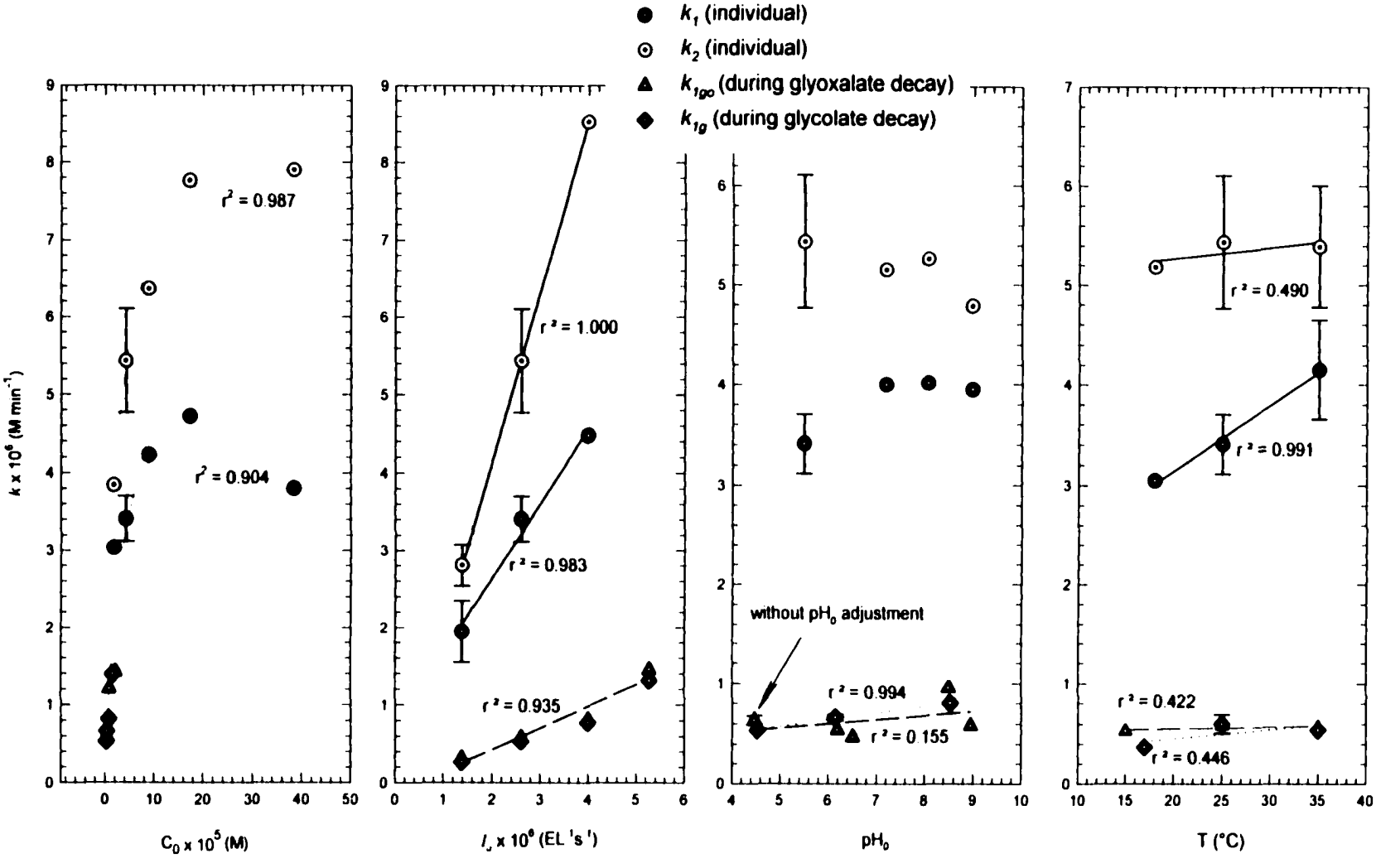

Figure 4.7.1. Dependency of HCO_2^- Decay Rate Constants k_1 and k_2 on **(a)** C_0, **(b)** I_a, **(c)** pH$_0$ and **(d)** T During Photodecomposition of HCO_2^-, $HC_2O_3^-$ and $H_3C_2O_3^-$.

As seen in Figure 4.7.1, k_{1go} and k_{1g} are much lower than k_1. This could be attributed to low $[HCO_2^-]_0$ ($[HCO_2^-]_{max}$ reached during $HC_2O_3^-$ and $H_3C_2O_3^-$ decay) since k_1 and k_2 decreased at low $[HCO_2^-]_0$ as depicted in Figure 4.7.1a. The regression line for k_1 in box (a) includes k_{1go} and k_{1g}. Similar to k_1, k_{1go} and k_{1g} increased with I_a, while they were not affected by pH_0 and temperature.

$C_2O_4^{2-}$, which was also observed as intermediate in $HC_2O_3^-$ and $H_3C_2O_3^-$ decay, followed split decay rate similar to individual decay. The values of k_1 and k_2 of $C_2O_4^{2-}$ decay were lower than the values of k_{1go}, k_{2go} and k_{1g}, k_{2g} as depicted in Figure 4.7.2. Inverse correlation between k_1, k_2 and $[C_2O_4^{2-}]_0$ could be the reason for low values observed during intermediate decay since $[C_2O_4^{2-}]_0$ range was lower ($1\text{-}1.7 \times 10^{-5}$ M). On the other hand, even at the same $[C_2O_4^{2-}]_0$, k_1 and k_2 were lower than k_{1go}, k_{2go}, k_{1g} and k_{2g}. This implies the existence of some other factors affecting $C_2O_4^{2-}$ decay rate during $HC_2O_3^-$ and $H_3C_2O_3^-$ photodecomposition. Rate constants k_{1go}, k_{2go}, k_{1g} and k_{2g} increased with I_a and decreased with pH_0 as it was observed in individual $C_2O_4^{2-}$ decay. Both k_{1go} and k_{2go} were not affected by temperature while k_{1g} and k_{2g} increased with it.

The comparison between k_1 and k_2 as well as k_{1g} and k_{2g} for $HC_2O_3^-$ decay is given in Figure 4.7.3. Both k_{1g} and k_{2g} were lower than k_1 and k_2, respectively since $[HC_2O_3^-]_0$ ranged between 0.5×10^{-5} and 1.4×10^{-5} M during $H_3C_2O_3^-$ photodecomposition, which are lower than $[HC_2O_3^-]_0$ of individual decay. Rate constants k_{1g} and k_{2g} increased with I_a and decreased with pH_0 while they were not affected by temperature.

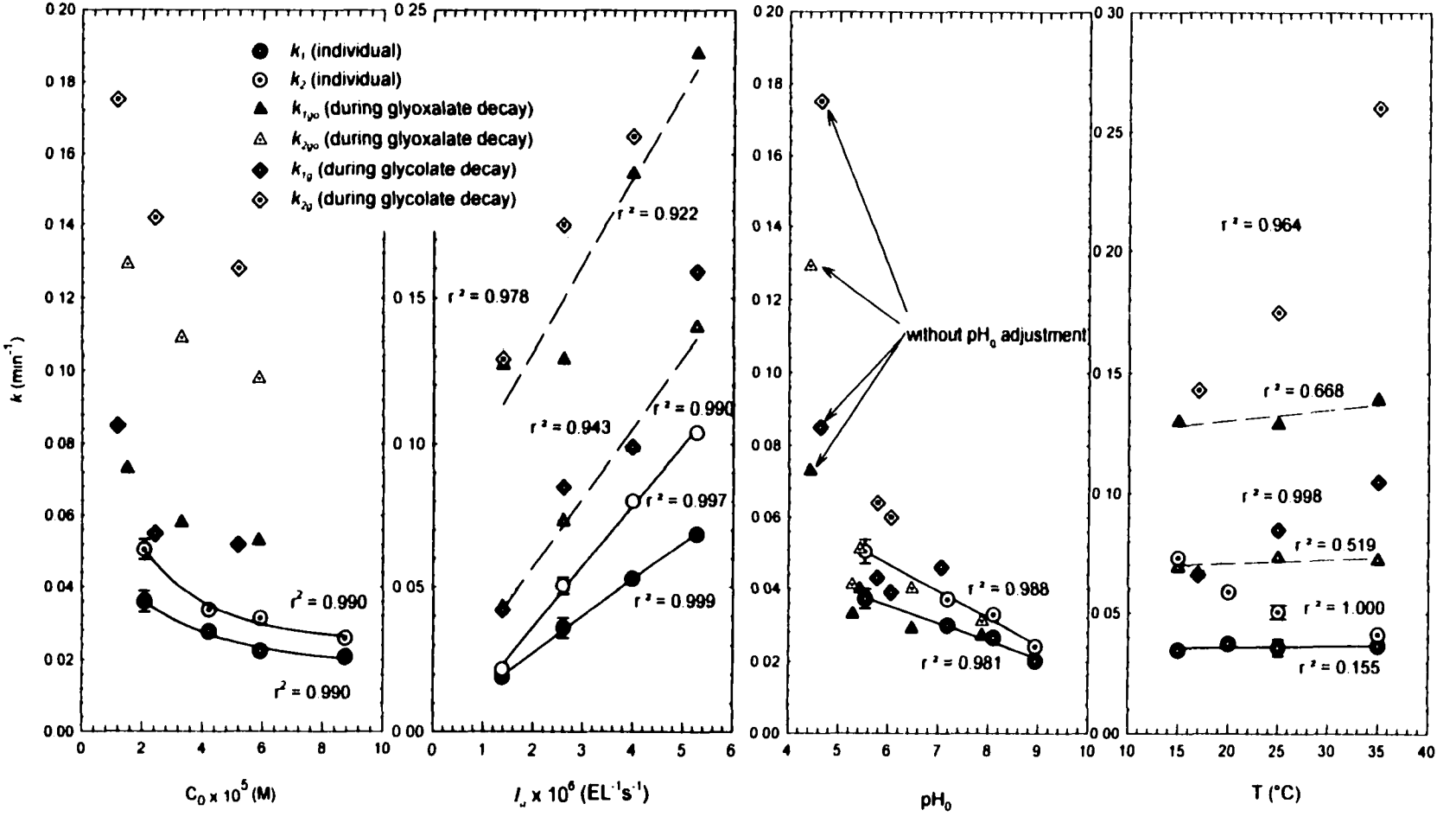

Figure 4.7.2. Dependency of $C_2O_4^{2-}$ Decay Rate Constants k_1 and k_2 on **(a)** C_0, **(b)** I_a, **(c)** pH_0 and **(d)** T During Photodecomposition of $C_2O_4^{2-}$, $HC_2O_3^-$ and $H_3C_2O_3^-$.

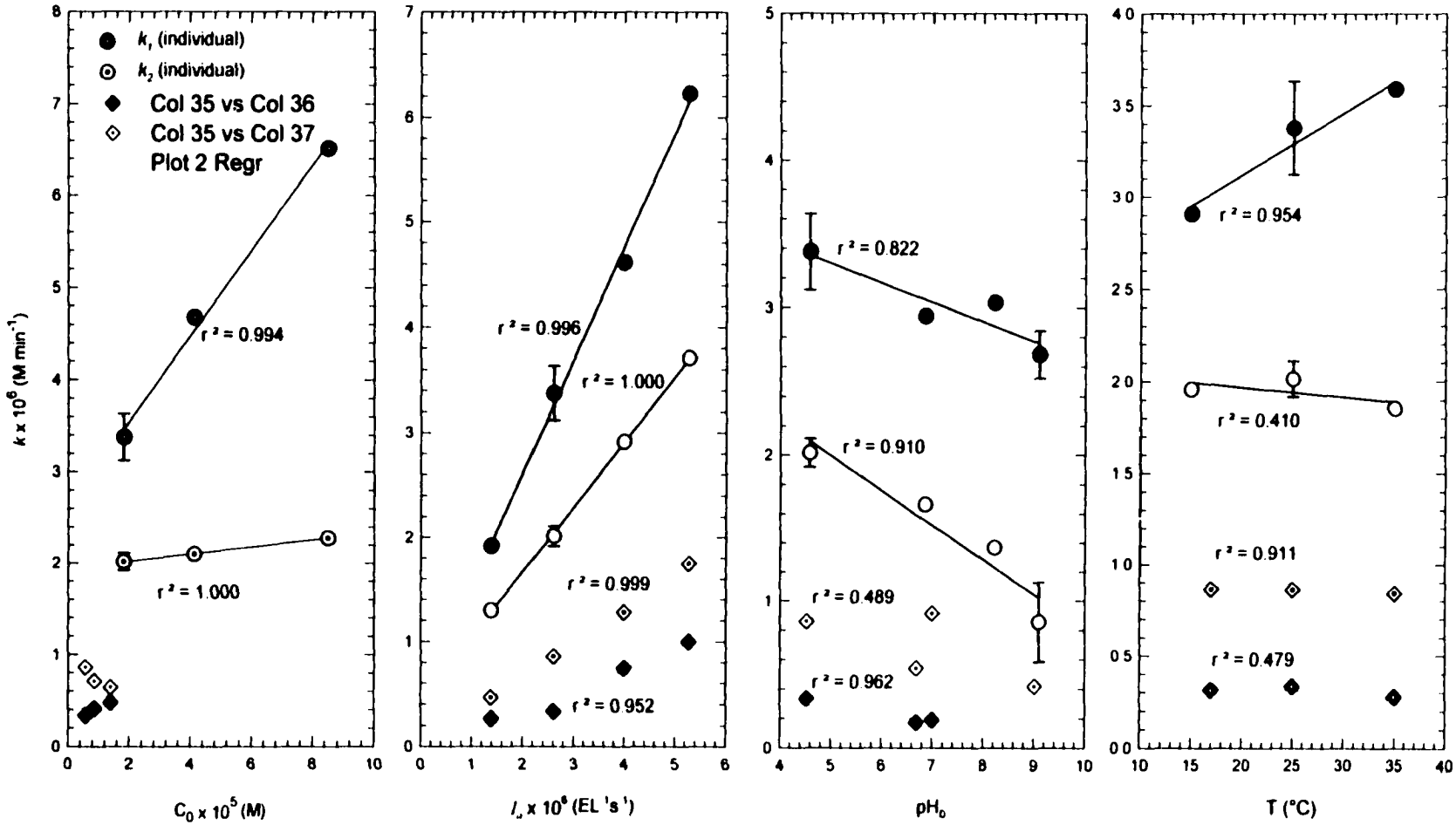

Figure 4.7.3. Dependency of $HC_2O_3^-$ Decay Rate Constants k_1 and k_2 on **(a)** C_0, **(b)** I_a, **(c)** pH_0 and **(d)** T During Photodecomposition of $HC_2O_3^-$ and $H_3C_2O_3^-$.

CHAPTER 5

CONCLUSIONS

1. UV irradiation at 253.7 nm used in disinfection of water and wastewater decomposes LMW organic acids.

2. All acids studied decayed under UV irradiation at 253.7 nm following split rate reaction. Formate (HCO_2^-), glyoxalate ($HC_2O_3^-$) and glycolate ($H_3C_2O_3^-$) decay followed pseudo-zero order kinetics while oxalate ($C_2O_4^{2-}$) and pyruvate ($H_3C_3O_3^-$) decay followed pseudo-first order kinetics.

3. The switch from k_1 to k_2 (rate constants before and after the rate split) occurred at average percent conversions of 20 ± 3, 55 ± 5, 56 ± 5, and 61 ± 6 for HCO_2^-, $C_2O_4^{2-}$, $HC_2O_3^-$ and $H_3C_2O_3^-$, respectively and at percent $H_3C_3O_3^-$ conversion of 58 (average of two experiments). The kinetic analysis revealed that $k_1 < k_2$ for HCO_2^-, $C_2O_4^{2-}$ and $H_3C_3O_3^-$ while $k_1 > k_2$ for $HC_2O_3^-$ and $H_3C_2O_3^-$.

4. The switch from k_1 to k_2 began at $t = t_c$, where the following concentration relationships were observed.

   During $HC_2O_3^-$ decay:

   $$[HC_2O_3^-] \approx [HCO_2^-] + [C_2O_4^{2-}]$$

   During $H_3C_2O_3^-$ decay:

   $$[H_3C_2O_3^-] \approx [HC_2O_3^-] + [C_2O_4^{2-}] + [HCO_2^-] \text{ and } [HC_2O_3^-] \approx [HC_2O_3^-]_{max}.$$

5. Both k_1 to k_2 increased with increasing absorbed UV light intensity (I_a) for all acids and initial concentration (C_0) except for $C_2O_4^{2-}$ in the experimental range tested. The values of both k_1 and k_2 for $C_2O_4^{2-}$ decreased with C_0. All rate constants decreased with pH_0 except k_1 for HCO_2^-, which slightly increased with pH_0. The temperature dependency of observed rate constants was not consistent for all anions. Both k_1 and k_2 for HCO_2^- and $C_2O_4^{2-}$ decreased with alkalinity.

6. DO utilizations were 0.5 mol of O_2/mol of HCO_2^-, (0.8 - 0.3) mol of O_2/mol of $C_2O_4^{2-}$, 0.6 mol O_2/mol $HC_2O_3^-$, 1.1 mol O_2/mol $H_3C_2O_3^-$ and 1.4 mol O_2/mol $H_3C_3O_3^-$ during HCO_2^-, $C_2O_4^{2-}$, $HC_2O_3^-$, $H_3C_2O_3^-$ and $H_3C_3O_3^-$ decay, respectively.

7. Overall reaction stoichiometry of HCO_2^- decay was observed to be:

$$HCO_2^- + \tfrac{1}{2} O_2 \rightarrow CO_2 + OH^-$$

8. $HC_2O_3^-$ decomposed to form HCO_2^-, $C_2O_4^{2-}$ and volatile compounds as shown in the flow diagram below (broken line represents unconfirmed transformation) which depicts the sequence of concentration maxima of the products occurring during $HC_2O_3^-$ decomposition.

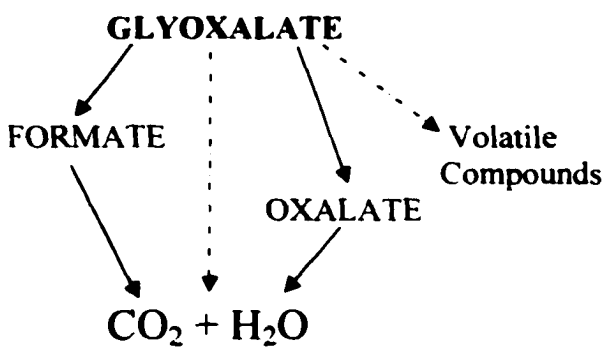

$[C_2O_4^{2-}]_{max}$ was reached when $[HC_2O_3^-] \approx [HCO_2^-] \approx$ BDL.

9. The sequence of transformation of $H_3C_2O_3^-$ and $H_3C_3O_3^-$ is given in the diagrams below:

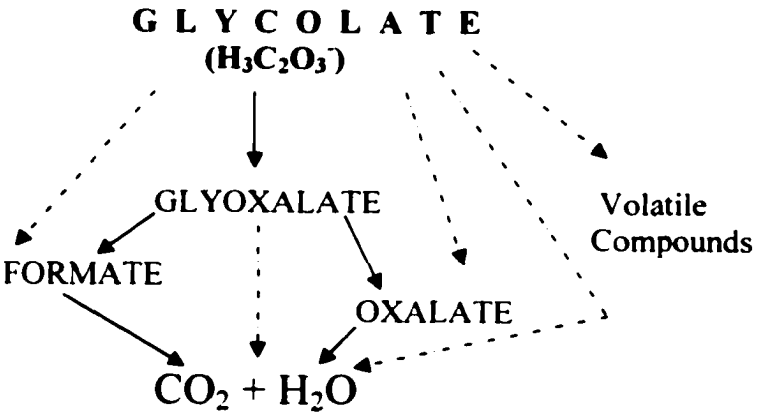

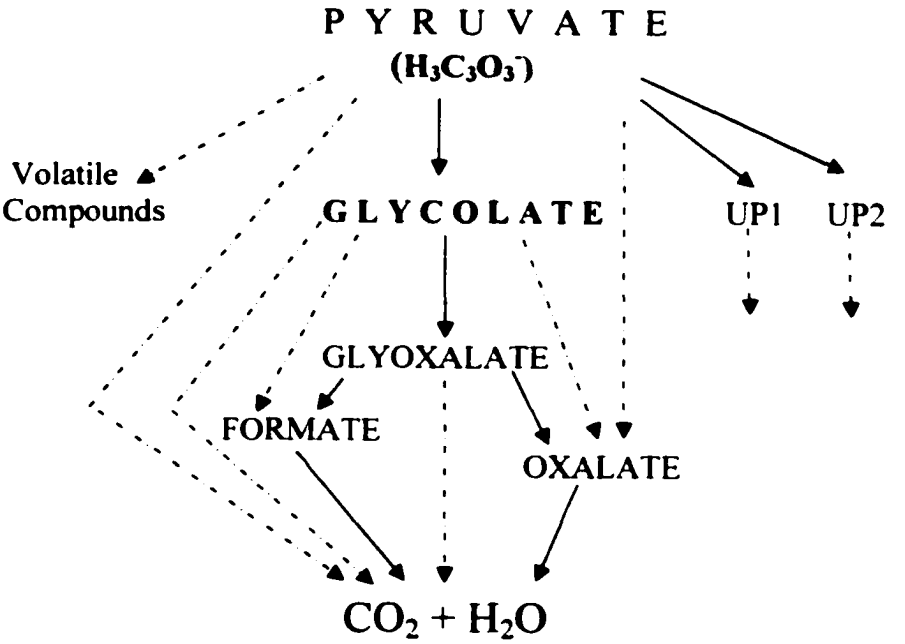

$H_3C_2O_3^{\cdot}$ was transformed to $HC_2O_3^{\cdot}$. UP1 and UP2 are unidentified anionic reaction products that formed and decayed in the course of the reaction. $[UP2]_{max}$ and $[C_2O_4^{2-}]_{max}$ were reached at [UP1] ≈ BDL and $[H_3C_3O_3^{\cdot}]$ ≈ BDL, respectively. $C_2O_4^{2-}$ reached BDL after $H_3C_3O_3^{\cdot}$ and its observed intermediates completely decomposed.

10. $C_2O_4^{2-}$ was the common intermediate product of the decay of low molecular weight carboxylic acids studied and decayed after the decay of all other intermediates.

11. The reaction pH during $HCO_2^{\cdot}$ and $C_2O_4^{2-}$ decay without prior pH_0 adjustment increased up to $[HCO_2^{\cdot}]$ ≈ $[C_2O_4^{2-}]$ ≈ BDL. The pH profile was predicted using closed system equilibrium analysis assuming that all $HCO_2^{\cdot}$ - C and $C_2O_4^{2-}$ - C is converted CO_2 in water. In the case of $HC_2O_3^{\cdot}$ and $H_3C_2O_3^{\cdot}$, pH_{min} occurred at $[C_2O_4^{2-}]_{max}$, while it occurred at ~$[UP2]_{max}$ for $H_3C_3O_3^{\cdot}$.

12. The decay of acid mixtures was evaluated in two cases.

    a) $HCO_2^{\cdot}/C_2O_4^{2-}$: Both k_1 and k_2 for $HCO_2^{\cdot}$ and $C_2O_4^{2-}$ during irradiation of the mixture were lower than those observed with solutions of individual species.

    b) $C_2O_4^{2-}/ H_3C_2O_3^{\cdot}$: Both k_1 and k_2 for $C_2O_4^{2-}$ during irradiation of mixture were higher than the observed values for individual $C_2O_4^{2-}$ decay, while k_1 for $H_3C_2O_3^{\cdot}$ was lower during decay of $C_2O_4^{2-}/ H_3C_2O_3^{\cdot}$ mixture.

13. Total Carbon (TC) remained constant during HCO_2^- and $C_2O_4^{2-}$ decay, while it gradually decayed during irradiation of $HC_2O_3^-$, $H_3C_2O_3^-$ and $H_3C_3O_3^-$. This suggests the possibility of formation of volatile products during the decomposition of the later group, while IC is the only product in the case of HCO_2^- and $C_2O_4^{2-}$.

14. Water containing LMW carboxylic acids will have different dissolved organic matter composition depending on the extent and intensity of UV irradiation. This variation could be diurnal and is likely to impact the DBPFP for the water.

APPENDIX A

TABLES OF EXPERIMENTAL DATA FOR OXALATE PHOTODECOMPOSITION

Table A1. Experimental Results of $C_2O_4^{2-}$ Photodecomposition in DIW ($C_0 = 2.104\times10^{-5}$ M. $I_a = 1.38 \cdot 10^{-6}$ E L^{-1} s^{-1}. T = 25°C).

Time (min)	$C_2O_4^{2-}$		NPOC (mg/L as C)	pH
	mg/L as C	M		
0.0	0.505	2.104×10^{-5}	0.497	5.47
1.0	0.497	2.071×10^{-5}	0.576	5.52
2.0	0.489	2.038×10^{-5}		5.57
3.0	0.478	1.992×10^{-5}	0.565	5.62
4.0	0.470	1.958×10^{-5}		5.67
6.0	0.454	1.892×10^{-5}		5.76
8.0	0.435	1.813×10^{-5}	0.467	5.83
10.0	0.420	1.750×10^{-5}		5.89
15.0	0.382	1.592×10^{-5}		6.01
20.0	0.346	1.442×10^{-5}	0.359	6.09
25.0	0.317	1.321×10^{-5}		6.16
30.0	0.289	1.204×10^{-5}		6.21
35.0	0.261	1.088×10^{-5}	0.231	6.25
40.0	0.238	9.917×10^{-6}		6.29
50.0	0.196	8.167×10^{-6}		6.35
60.1	0.159	6.625×10^{-6}	0.250	6.38
70.3	0.129	5.375×10^{-6}		6.41
80.0	0.105	4.375×10^{-6}		6.44
100.0	0.068	2.833×10^{-6}	0.120	6.46
120.0	0.044	1.833×10^{-6}		6.48
140.2	0.028	1.167×10^{-6}		6.50
166.2	0.016	6.667×10^{-7}	0.102	6.50

Table A2. Experimental Results of $C_2O_4^{2-}$ Photodecomposition in DIW ($C_0 = 2.167 \times 10^{-5}$ M, $I_a = 2.60 \times 10^{-6}$ E L^{-1} s^{-1}, T = 15°C).

Time (min)	$C_2O_4^{2-}$		O_2 (M)	pH
	mg/L as C	M		
0.0	0.520	2.167×10^{-5}	2.946×10^{-4}	5.47
1.0	0.503	2.096×10^{-5}	2.940×10^{-4}	5.53
2.0	0.486	2.025×10^{-5}	2.934×10^{-4}	5.63
3.0	0.474	1.975×10^{-5}	2.928×10^{-4}	5.71
4.0	0.458	1.908×10^{-5}	2.918×10^{-4}	5.78
5.0	0.446	1.858×10^{-5}	2.912×10^{-4}	5.84
8.0	0.403	1.679×10^{-5}	2.893×10^{-4}	5.98
10.0	0.379	1.579×10^{-5}	2.883×10^{-4}	6.05
12.0	0.354	1.475×10^{-5}	2.874×10^{-4}	6.10
14.0	0.329	1.371×10^{-5}	2.868×10^{-4}	6.15
16.0	0.308	1.283×10^{-5}	2.861×10^{-4}	6.19
20.0	0.269	1.121×10^{-5}	2.852×10^{-4}	6.26
25.0	0.220	9.167×10^{-6}	2.846×10^{-4}	6.32
30.0	0.180	7.500×10^{-6}	2.842×10^{-4}	6.36
35.0	0.145	6.042×10^{-6}	2.839×10^{-4}	6.39
40.0	0.114	4.750×10^{-6}	2.839×10^{-4}	6.42
50.0	0.070	2.917×10^{-6}	2.846×10^{-4}	6.45
60.0	0.042	1.750×10^{-6}	2.855×10^{-4}	6.48
70.0	0.022	9.167×10^{-7}	2.871×10^{-4}	6.49
80.0	0.011	4.583×10^{-7}	2.883×10^{-4}	6.50
90.0	0.005	2.083×10^{-7}	2.896×10^{-4}	6.50
102.0	0.002	8.333×10^{-8}	2.909×10^{-4}	6.50

Table A3. Experimental Results of $C_2O_4^{2-}$ Photodecomposition in DIW ($C_0 = 2.046 \times 10^{-5}$ M. $I_a = 2.60 \times 10^{-6}$ E L^{-1} s^{-1}. T = 20°C).

Time (min)	$C_2O_4^{2-}$		pH
	mg/L as C	M	
0.0	0.491	2.046×10^{-5}	5.45
1.0	0.476	1.983×10^{-5}	5.51
2.0	0.462	1.925×10^{-5}	5.60
3.0	0.445	1.854×10^{-5}	5.68
4.0	0.429	1.788×10^{-5}	5.75
5.0	0.415	1.729×10^{-5}	5.81
6.0	0.400	1.667×10^{-5}	5.87
7.0	0.385	1.604×10^{-5}	5.91
8.0	0.373	1.554×10^{-5}	5.95
9.0	0.359	1.496×10^{-5}	5.98
10.0	0.345	1.437×10^{-5}	6.01
12.0	0.320	1.333×10^{-5}	6.06
14.0	0.296	1.233×10^{-5}	6.11
16.0	0.274	1.142×10^{-5}	6.14
20.0	0.231	9.625×10^{-6}	6.20
25.0	0.185	7.708×10^{-6}	6.25
30.0	0.150	6.250×10^{-6}	6.29
35.0	0.117	4.875×10^{-6}	6.31
40.0	0.089	3.708×10^{-6}	6.34
50.0	0.052	2.167×10^{-6}	6.36
60.0	0.029	1.208×10^{-6}	6.38
70.9	0.014	5.833×10^{-7}	6.39
80.0	7.000e-3	2.917×10^{-7}	6.39

Table A4. Experimental Results of $C_2O_4^{2-}$ Photodecomposition in DIW Containing $NaHCO_3$ = 10 mg/L as $CaCO_3$ ($C_0 = 2.067\times10^{-5}$ M, $I_a = 2.60\times10^{-6}$ E L^{-1} s^{-1}, T = 25°C).

Time (min)	$C_2O_4^{2-}$		Bicarbonate Alkalinity (mg/L as $CaCO_3$)	pH
	mg/L as C	M		
0.0	0.496	2.067×10^{-5}	11.6	7.15
1.0	0.490	2.042×10^{-5}		7.15
2.0	0.485	2.021×10^{-5}		7.14
3.0	0.476	1.983×10^{-5}	14.0	7.13
4.0	0.472	1.967×10^{-5}		7.14
6.0	0.456	1.900×10^{-5}		7.13
8.0	0.444	1.850×10^{-5}	12.8	7.11
10.2	0.426	1.775×10^{-5}		7.13
12.0	0.414	1.725×10^{-5}		7.12
14.0	0.399	1.663×10^{-5}		7.11
20.0	0.360	1.500×10^{-5}	12.8	7.12
25.0	0.325	1.354×10^{-5}		7.13
30.0	0.294	1.225×10^{-5}	12.0	7.13
35.0	0.268	1.117×10^{-5}		7.14
40.0	0.241	1.004×10^{-5}		7.15
50.0	0.199	8.292×10^{-6}	13.2	7.16
60.0	0.157	6.542×10^{-6}		7.18
70.0	0.125	5.208×10^{-6}		7.20
80.0	0.097	4.042×10^{-6}	11.6	7.21
100.0	0.062	2.583×10^{-6}		7.25
120.1	0.039	1.625×10^{-6}		7.25
140.0	0.025	1.042×10^{-6}	13.2	7.28

Table A5. Experimental Results of $C_2O_4^{2-}$ Photodecomposition in DIW Containing $NaHCO_3$ = 25 mg/L as $CaCO_3$ ($C_0 = 2.117 \times 10^{-5}$ M, $I_a = 2.60 \times 10^{-6}$ E L^{-1} s^{-1}, T = 25°C).

Time (min)	$C_2O_4^{2-}$		NPOC (mg/L as C)	pH
	mg/L as C	M		
0.0	0.508	2.117×10^{-5}	0.649	7.78
1.0	0.505	2.104×10^{-5}		7.78
2.0	0.499	2.079×10^{-5}		7.78
3.0	0.492	2.050×10^{-5}	0.622	7.78
4.0	0.487	2.029×10^{-5}		7.78
5.0	0.482	2.008×10^{-5}		7.78
6.0	0.477	1.988×10^{-5}	0.525	7.77
8.0	0.465	1.938×10^{-5}		7.77
10.0	0.452	1.883×10^{-5}		7.77
12.1	0.441	1.838×10^{-5}	0.521	7.77
14.0	0.429	1.788×10^{-5}		7.76
20.0	0.395	1.646×10^{-5}		7.76
25.0	0.365	1.521×10^{-5}	0.458	7.75
30.0	0.339	1.413×10^{-5}		7.75
35.0	0.314	1.308×10^{-5}		7.74
40.0	0.288	1.200×10^{-5}	0.379	7.74
50.0	0.248	1.033×10^{-5}		7.73
60.1	0.207	8.625×10^{-6}		7.72
70.0	0.177	7.375×10^{-6}	0.289	7.71
80.0	0.150	6.250×10^{-6}		7.70
100.4	0.107	4.458×10^{-6}		7.69
120.0	0.076	3.167×10^{-6}	0.247	7.69

Table A6. Experimental Results of $C_2O_4^{2-}$ Photodecomposition in DIW Containing $NaHCO_3$ = 50 mg/L as $CaCO_3$ ($C_0 = 2.138\times10^{-5}$ M. $I_a = 2.60\times10^{-6}$ E L^{-1} s^{-1}. T = 25°C).

Time (min)	$C_2O_4^{2-}$		pH
	mg/L as C	M	
0.0	0.513	2.138×10^{-5}	7.98
1.0	0.510	2.125×10^{-5}	7.97
2.0	0.505	2.104×10^{-5}	7.98
3.0	0.501	2.088×10^{-5}	7.97
4.0	0.497	2.071×10^{-5}	7.98
6.0	0.487	2.029×10^{-5}	7.97
8.1	0.477	1.988×10^{-5}	7.97
10.0	0.469	1.954×10^{-5}	7.97
12.0	0.460	1.917×10^{-5}	7.96
14.0	0.451	1.879×10^{-5}	7.96
20.0	0.421	1.754×10^{-5}	7.96
25.3	0.399	1.663×10^{-5}	7.96
30.0	0.378	1.575×10^{-5}	7.97
40.1	0.337	1.404×10^{-5}	7.96
50.0	0.300	1.250×10^{-5}	7.97
60.1	0.265	1.104×10^{-5}	7.97
80.0	0.206	8.583×10^{-6}	7.98
100.0	0.160	6.667×10^{-6}	8.00
120.0	0.121	5.042×10^{-6}	8.01
140.2	0.093	3.875×10^{-6}	8.02
161.2	0.070	2.917×10^{-6}	8.03
190.1	0.048	2.000×10^{-6}	8.05

Table A7. Experimental Results of $C_2O_4^{2-}$ Photodecomposition in DIW at pH_0 Adjusted to 7.18 with Concentrated NaOH ($C_0 = 2.038\times10^{-5}$ M, $I_a = 2.60\times10^{-6}$ E L^{-1} s^{-1}, T = 25°C).

Time (min)	$C_2O_4^{2-}$		NPOC (mg/L as C)	pH
	mg/L as C	M		
0.0	0.489	2.038×10^{-5}	0.533	7.18
1.0	0.475	1.979×10^{-5}	0.492	7.27
2.0	0.462	1.925×10^{-5}		7.26
3.0	0.450	1.875×10^{-5}	0.486	7.24
4.0	0.439	1.829×10^{-5}		7.21
5.0	0.427	1.779×10^{-5}		7.19
6.0	0.412	1.717×10^{-5}	0.458	7.17
8.0	0.391	1.629×10^{-5}		7.11
10.0	0.369	1.538×10^{-5}		7.08
12.0	0.345	1.437×10^{-5}	0.367	7.05
14.0	0.326	1.358×10^{-5}		7.02
20.0	0.272	1.133×10^{-5}		6.96
25.0	0.230	9.583×10^{-6}	0.282	6.92
30.0	0.195	8.125×10^{-6}		6.89
35.0	0.165	6.875×10^{-6}		6.87
40.0	0.137	5.708×10^{-6}	0.192	6.84
50.0	0.097	4.042×10^{-6}		6.80
60.0	0.067	2.792×10^{-6}		6.75
70.0	0.045	1.875×10^{-6}	0.088	6.71
80.0	0.031	1.292×10^{-6}		6.69
100.0	0.015	6.250×10^{-7}		6.63
120.0	0.007	2.917×10^{-7}	0.079	6.61

Table A8. Experimental Results of $C_2O_4^{2-}$ Photodecomposition in DIW at pH_0 Adjusted to 8.10 with Concentrated NaOH ($C_0 = 2.088\times10^{-5}$ M, $I_a = 2.60\times10^{-6}$ E L^{-1} s^{-1}, T = 25°C).

Time (min)	$C_2O_4^{2-}$		NPOC (mg/L as C)	pH
	mg/L as C	M		
0.0	0.501	2.088×10^{-5}	0.543	8.10
1.0	0.490	2.042×10^{-5}	0.508	8.09
2.0	0.478	1.992×10^{-5}		8.07
3.0	0.465	1.938×10^{-5}	0.497	8.06
4.0	0.455	1.896×10^{-5}		8.04
5.0	0.444	1.850×10^{-5}		8.01
6.0	0.432	1.800×10^{-5}	0.447	7.99
8.0	0.411	1.713×10^{-5}		7.94
10.0	0.389	1.621×10^{-5}		7.89
12.1	0.368	1.533×10^{-5}	0.402	7.85
14.2	0.344	1.433×10^{-5}		7.77
20.0	0.296	1.233×10^{-5}		7.59
25.0	0.252	1.050×10^{-5}	0.275	7.43
30.0	0.218	9.083×10^{-6}		7.31
35.0	0.186	7.750×10^{-6}		7.21
40.0	0.155	6.458×10^{-6}	0.207	7.13
50.0	0.112	4.667×10^{-6}		7.00
60.0	0.077	3.208×10^{-6}		6.91
70.1	0.052	2.167×10^{-6}	0.119	6.85
80.1	0.035	1.458×10^{-6}		6.81
101.8	0.015	6.250×10^{-7}		6.72
120.0	0.007	2.917×10^{-7}	0.051	6.68

Table A9. Experimental Results of $C_2O_4^{2-}$ Photodecomposition in DIW at pH_0 Adjusted to 8.94 with Concentrated NaOH ($C_0 = 2.188 \times 10^{-5}$ M, $I_a = 2.60 \times 10^{-6}$ E L^{-1} s^{-1}, T = 25°C).

Time (min)	$C_2O_4^{2-}$		NPOC (mg/L as C)	pH
	mg/L as C	M		
0.0	0.525	2.188×10^{-5}	0.689	8.94
1.0	0.514	2.142×10^{-5}	0.559	8.92
2.0	0.504	2.100×10^{-5}		8.92
3.0	0.494	2.058×10^{-5}	0.594	8.91
4.0	0.486	2.025×10^{-5}		8.90
5.0	0.476	1.983×10^{-5}		8.91
6.0	0.465	1.938×10^{-5}	0.514	8.91
8.0	0.449	1.871×10^{-5}		8.89
10.0	0.431	1.796×10^{-5}		8.88
12.0	0.415	1.729×10^{-5}	0.514	8.87
14.0	0.399	1.663×10^{-5}		8.86
20.0	0.354	1.475×10^{-5}		8.84
25.0	0.318	1.325×10^{-5}	0.401	8.82
30.0	0.289	1.204×10^{-5}		8.80
35.2	0.258	1.075×10^{-5}		8.77
40.4	0.230	9.583×10^{-6}	0.308	8.74
50.0	0.191	7.958×10^{-6}		8.69
60.0	0.152	6.333×10^{-6}		8.63
70.0	0.119	4.958×10^{-6}	0.201	8.53
80.4	0.096	4.000×10^{-6}		8.44
100.0	0.059	2.458×10^{-6}		8.13
120.0	0.035	1.458×10^{-6}	0.094	7.58

Table A10. Experimental Results of $C_2O_4^{2-}$ Photodecomposition in DIW ($C_0 = 2.046\times10^{-5}$ M, $I_a = 2.60\times10^{-6}$ E L^{-1} s^{-1}, T = 25°C).

Time (min)	$C_2O_4^{2-}$		NPOC (mg/L as C)	pH
	mg/L as C	M		
0.0	0.491	2.046×10^{-5}	0.565	5.61
1.0	0.473	1.971×10^{-5}	0.573	5.79
2.0	0.458	1.908×10^{-5}		5.86
3.0	0.444	1.850×10^{-5}	0.555	5.94
4.0	0.430	1.792×10^{-5}		6.01
5.0	0.414	1.725×10^{-5}		6.08
6.0	0.400	1.667×10^{-5}	0.554	6.12
7.0	0.386	1.608×10^{-5}		6.16
8.0	0.373	1.554×10^{-5}		6.21
9.0	0.361	1.504×10^{-5}	0.568	6.24
10.0	0.348	1.450×10^{-5}		6.28
12.0	0.325	1.354×10^{-5}		6.33
14.0	0.300	1.250×10^{-5}	0.568	6.38
16.0	0.280	1.167×10^{-5}		6.42
20.0	0.240	1.000×10^{-5}		6.47
25.0	0.196	8.167×10^{-6}	0.593	6.52
30.0	0.161	6.708×10^{-6}		6.56
35.0	0.130	5.417×10^{-6}		6.59
40.0	0.103	4.292×10^{-6}	0.568	6.61
45.0	0.081	3.375×10^{-6}		6.62
50.0	0.064	2.667×10^{-6}		6.63
60.0	0.039	1.625×10^{-6}	0.555	6.64

Table A11. Experimental Results of $C_2O_4^{2-}$ Photodecomposition in DIW ($C_0 = 2.063 \times 10^{-5}$ M. $I_a = 2.60 \times 10^{-6}$ E L^{-1} s^{-1}. T = 25°C).

Time (min)	$C_2O_4^{2-}$		NPOC (mg/L as C)	pH
	mg/L as C	M		
0.0	0.495	2.063×10^{-5}	0.534	5.53
0.9	0.478	1.992×10^{-5}	0.519	5.60
2.1	0.459	1.913×10^{-5}		5.70
3.0	0.443	1.846×10^{-5}	0.532	5.79
4.0	0.427	1.779×10^{-5}		5.87
5.0	0.410	1.708×10^{-5}		5.94
6.0	0.393	1.638×10^{-5}	0.434	5.99
7.0	0.378	1.575×10^{-5}		6.04
8.0	0.363	1.513×10^{-5}		6.08
9.1	0.348	1.450×10^{-5}	0.421	6.13
10.0	0.333	1.388×10^{-5}		6.16
12.0	0.309	1.288×10^{-5}		6.22
14.0	0.285	1.187×10^{-5}	0.439	6.26
16.0	0.262	1.092×10^{-5}		6.30
20.0	0.221	9.208×10^{-6}		6.36
25.0	0.176	7.333×10^{-6}	0.275	6.42
30.0	0.141	5.875×10^{-6}		6.45
35.0	0.111	4.625×10^{-6}		6.49
40.0	0.087	3.625×10^{-6}	0.255	6.51
45.0	0.067	2.792×10^{-6}		6.53
50.1	0.051	2.125×10^{-6}		6.54
60.0	0.030	1.250×10^{-6}	0.123	6.55

Table A12. Experimental Results of $C_2O_4^{2-}$ Photodecomposition in DIW ($C_0 = 2.113 \times 10^{-5}$ M, $I_a = 2.60 \times 10^{-6}$ E L^{-1} s^{-1}, T = 25°C).

Time (min)	$C_2O_4^{2-}$		pH
	mg/L as C	M	
0.0	0.507	2.113×10^{-5}	5.45
1.0	0.488	2.033×10^{-5}	5.52
2.0	0.476	1.983×10^{-5}	5.61
3.1	0.461	1.921×10^{-5}	5.69
4.1	0.444	1.850×10^{-5}	5.76
5.0	0.431	1.796×10^{-5}	5.82
6.0	0.417	1.738×10^{-5}	5.87
7.0	0.404	1.683×10^{-5}	5.92
8.0	0.390	1.625×10^{-5}	5.96
9.1	0.371	1.546×10^{-5}	5.99
10.0	0.361	1.504×10^{-5}	6.02
12.0	0.339	1.413×10^{-5}	6.06
14.1	0.311	1.296×10^{-5}	6.11
16.0	0.289	1.204×10^{-5}	6.14
20.0	0.247	1.029×10^{-5}	6.20
25.1	0.196	8.167×10^{-6}	6.25
30.0	0.157	6.542×10^{-6}	6.29
35.0	0.123	5.125×10^{-6}	6.31
40.0	0.096	4.000×10^{-6}	6.34
50.0	0.057	2.375×10^{-6}	6.36
60.7	0.033	1.375×10^{-6}	6.37
70.3	0.018	7.500×10^{-7}	6.38
80.0	0.011	4.583×10^{-7}	6.38

Table A13. Experimental Results of $C_2O_4^{2-}$ Photodecomposition in DIW ($C_0 = 2.063\times10^{-5}$ M, $I_a = 2.60\times10^{-6}$ E L^{-1} s^{-1}, T = 25°C).

Time (min)	$C_2O_4^{2-}$		O_2 (M)	pH
	mg/L as C	M		
0.0	0.495	2.063×10^{-5}	2.755×10^{-4}	5.45
1.0	0.481	2.004×10^{-5}	2.753×10^{-4}	5.55
2.0	0.467	1.946×10^{-5}	2.750×10^{-4}	5.65
3.0	0.456	1.900×10^{-5}	2.742×10^{-4}	5.73
4.0	0.442	1.842×10^{-5}	2.735×10^{-4}	5.81
5.0	0.430	1.792×10^{-5}	2.724×10^{-4}	5.86
6.0	0.417	1.738×10^{-5}	2.716×10^{-4}	5.92
8.0	0.391	1.629×10^{-5}	2.698×10^{-4}	6.01
10.0	0.366	1.525×10^{-5}	2.685×10^{-4}	6.08
12.0	0.342	1.425×10^{-5}	2.673×10^{-4}	6.13
14.0	0.318	1.325×10^{-5}	2.660×10^{-4}	6.17
16.0	0.297	1.238×10^{-5}	2.649×10^{-4}	6.21
20.0	0.253	1.054×10^{-5}	2.631×10^{-4}	6.28
25.0	0.210	8.750×10^{-6}	2.608×10^{-4}	6.33
30.0	0.169	7.042×10^{-6}	2.590×10^{-4}	6.37
35.0	0.136	5.667×10^{-6}	2.574×10^{-4}	6.40
40.0	0.109	4.542×10^{-6}	2.562×10^{-4}	6.42
50.0	0.069	2.875×10^{-6}	2.543×10^{-4}	6.45
60.0	0.042	1.750×10^{-6}	2.528×10^{-4}	6.47
70.0	0.024	1.000×10^{-6}	2.515×10^{-4}	6.47
80.0	0.014	5.833×10^{-7}	2.505×10^{-4}	6.48
90.0	0.008	3.333×10^{-7}	2.494×10^{-4}	6.48
100.0	0.005	2.083×10^{-7}	2.484×10^{-4}	6.48
110.0	0.003	1.250×10^{-7}	2.479×10^{-4}	6.48

Table A14. Experimental Results of $C_2O_4^{2-}$ Photodecomposition in DIW Containing $NaHCO_3$ = 50 mg/L as $CaCO_3$ ($C_0 = 4.458\times10^{-5}$ M, $I_a = 2.60\times10^{-6}$ E L^{-1} s^{-1}, T = 25°C).

Time (min)	$C_2O_4^{2-}$		pH
	mg/L as C	M	
0.0	1.070	4.458×10^{-5}	7.80
1.0	1.069	4.454×10^{-5}	7.81
2.0	1.061	4.421×10^{-5}	7.80
3.0	1.061	4.421×10^{-5}	7.81
4.0	NA*	NA	7.80
6.0	NA	NA	7.80
8.0	NA	NA	7.80
10.0	NA	NA	7.80
12.0	0.974	4.058×10^{-5}	7.80
14.0	0.956	3.983×10^{-5}	7.81
20.0	0.897	3.738×10^{-5}	7.81
25.0	0.850	3.542×10^{-5}	7.82
30.0	0.799	3.329×10^{-5}	7.82
40.0	0.714	2.975×10^{-5}	7.83
50.0	0.629	2.621×10^{-5}	7.84
61.1	0.550	2.292×10^{-5}	7.84
81.8	0.427	1.779×10^{-5}	7.88
100.2	0.337	1.404×10^{-5}	7.90
120.0	0.255	1.063×10^{-5}	7.92
141.8	0.190	7.917×10^{-6}	7.95
161.5	0.144	6.000×10^{-6}	7.97
180.0	0.111	4.625×10^{-6}	7.98

*NA: The data is not available because of a problem during analysis

Table A15. Experimental Results of $C_2O_4^{2-}$ Photodecomposition in DIW ($C_0 = 4.208\times10^{-5}$ M, $I_a = 2.60\times10^{-6}$ E L^{-1} s^{-1}, T = 25°C).

Time (min)	$C_2O_4^{2-}$		NPOC (mg/L as C)	pH
	mg/L as C	M		
0.0	1.010	4.208×10^{-5}	1.098	5.60
1.0	0.989	4.121×10^{-5}	1.002	5.75
2.0	0.967	4.029×10^{-5}		5.87
3.0	0.939	3.912×10^{-5}	1.004	5.99
4.0	0.918	3.825×10^{-5}		6.08
6.0	0.875	3.646×10^{-5}		6.23
8.0	0.828	3.450×10^{-5}	0.912	6.32
10.0	0.786	3.275×10^{-5}		6.40
15.0	0.687	2.863×10^{-5}		6.53
20.1	0.591	2.463×10^{-5}	0.619	6.62
25.0	0.512	2.133×10^{-5}		6.69
30.0	0.442	1.842×10^{-5}		6.72
35.1	0.374	1.558×10^{-5}	0.418	6.75
40.0	0.318	1.325×10^{-5}		6.78
50.1	0.228	9.500×10^{-6}		6.82
60.0	0.159	6.625×10^{-6}	0.260	6.83
80.5	0.074	3.083×10^{-6}		6.84
100.0	0.036	1.500×10^{-6}		6.84
120.9	0.020	8.333×10^{-7}	0.000	6.84
140.3	0.010	4.167×10^{-7}		6.83
170.0	0.004	1.667×10^{-7}		6.84
180.0	0.003	1.250×10^{-7}	0.043	6.82

Table A16. Experimental Results of $C_2O_4^{2-}$ Photodecomposition in DIW ($C_0 = 5.917\times10^{-5}$ M. $I_a = 2.60\times10^{-6}$ E L^{-1} s^{-1}, T = 25°C).

Time (min)	$C_2O_4^{2-}$		NPOC (mg/L as C)	pH
	mg/L as C	M		
0.0	1.420	5.917×10^{-5}	1.438	5.59
1.0	1.390	5.792×10^{-5}	1.459	5.70
2.0	1.365	5.688×10^{-5}		5.81
3.0	1.343	5.596×10^{-5}	1.411	5.92
4.0	1.314	5.475×10^{-5}		6.01
6.0	1.266	5.275×10^{-5}		6.15
8.0	1.213	5.054×10^{-5}	1.309	6.25
10.0	1.166	4.858×10^{-5}		6.33
15.0	1.052	4.383×10^{-5}		6.46
20.0	0.938	3.908×10^{-5}	1.046	6.55
25.0	0.838	3.492×10^{-5}		6.62
30.0	0.741	3.088×10^{-5}		6.67
35.9	0.642	2.675×10^{-5}	0.824	6.72
40.0	0.578	2.408×10^{-5}		6.75
50.0	0.445	1.854×10^{-5}		6.80
60.0	0.334	1.392×10^{-5}	0.447	6.84
80.0	0.193	8.042×10^{-6}		6.88
100.0	0.098	4.083×10^{-6}		6.91
120.0	0.054	2.250×10^{-6}	0.187	6.92
140.0	0.026	1.083×10^{-6}		6.92
160.0	0.015	6.250×10^{-7}	0.076	6.93

Table A17. Experimental Results of $C_2O_4^{2-}$ Photodecomposition in DIW ($C_0 = 8.750\times10^{-5}$ M, $I_a = 2.60\times10^{-6}$ E L^{-1} s^{-1}, T = 25°C).

Time (min)	$C_2O_4^{2-}$		NPOC (mg/L as C)	pH
	mg/L as C	M		
0.0	2.100	8.750×10^{-5}	1.967	5.68
1.0	2.066	8.608×10^{-5}	2.062	5.82
2.0	2.033	8.471×10^{-5}		5.97
4.0	1.952	8.133×10^{-5}	1.845	6.19
6.0	1.872	7.800×10^{-5}		6.34
8.0	1.810	7.542×10^{-5}		6.44
10.0	1.726	7.192×10^{-5}	1.658	6.52
15.0	1.571	6.546×10^{-5}		6.67
20.0	1.411	5.879×10^{-5}		6.76
25.0	1.271	5.296×10^{-5}	1.339	6.84
30.0	1.144	4.767×10^{-5}		6.88
40.0	0.923	3.846×10^{-5}		6.96
50.0	0.742	3.092×10^{-5}	0.770	7.00
60.0	0.599	2.496×10^{-5}		7.03
80.0	0.386	1.608×10^{-5}		7.06
100.0	0.225	9.375×10^{-6}	0.373	7.09
121.9	0.128	5.333×10^{-6}		7.09
140.0	0.076	3.167×10^{-6}		7.09
160.0	0.042	1.750×10^{-6}	0.142	7.09
200.0	0.017	7.083×10^{-7}		7.09
240.1	0.006	2.500×10^{-7}		7.09
255.0	0.004	1.667×10^{-7}	0.135	7.09

Table A18. Experimental Results of $C_2O_4^{2-}$ Photodecomposition in DIW ($C_0 = 2.117\times10^{-5}$ M, $I_a = 2.60\times10^{-6}$ E L^{-1} s^{-1}, T = 35°C).

Time (min)	$C_2O_4^{2-}$		NPOC (mg/L as C)	pH
	mg/L as C	M		
0.0	0.508	2.117×10^{-5}	0.591	5.43
1.0	0.493	2.054×10^{-5}	0.662	5.54
2.0	0.477	1.988×10^{-5}		5.64
3.0	0.459	1.913×10^{-5}	0.498	5.72
4.0	0.442	1.842×10^{-5}		5.80
5.0	0.428	1.783×10^{-5}		5.87
6.0	0.411	1.713×10^{-5}	0.454	5.92
8.0	0.383	1.596×10^{-5}		6.01
10.0	0.358	1.492×10^{-5}		6.08
12.0	0.330	1.375×10^{-5}	0.451	6.14
14.0	0.306	1.275×10^{-5}		6.17
16.00	0.286	1.192×10^{-5}		6.23
20.0	0.245	1.021×10^{-5}	0.316	6.28
25.0	0.202	8.417×10^{-6}		6.34
30.0	0.167	6.958×10^{-6}		6.37
35.0	0.136	5.667×10^{-6}	0.298	6.40
40.0	0.111	4.625×10^{-6}		6.42
50.0	0.075	3.125×10^{-6}		6.46
60.5	0.048	2.000×10^{-6}	0.223	6.47
70.0	0.032	1.333×10^{-6}		6.49
80.2	0.021	8.750×10^{-7}		6.50
90.0	0.014	5.833×10^{-7}	0.077	6.49

Table A19. Experimental Results of $C_2O_4^{2-}$ Photodecomposition in DIW ($C_0 = 2.292 \times 10^{-5}$ M. $I_a = 3.99 \times 10^{-6}$ E L^{-1} s^{-1}. T = 25°C).

Time (min)	$C_2O_4^{2-}$		NPOC (mg/L as C)	pH
	mg/L as C	M		
0.0	0.550	2.292×10^{-5}	0.628	5.47
1.0	0.526	2.192×10^{-5}	0.581	5.59
2.0	0.502	2.092×10^{-5}		5.72
3.0	0.475	1.979×10^{-5}	0.475	5.82
4.0	0.453	1.888×10^{-5}		5.92
5.0	0.429	1.788×10^{-5}		5.98
6.0	0.407	1.696×10^{-5}	0.388	6.03
7.1	0.384	1.600×10^{-5}		6.09
8.0	0.367	1.529×10^{-5}		6.12
10.0	0.329	1.371×10^{-5}	0.295	6.19
12.0	0.295	1.229×10^{-5}		6.24
14.2	0.260	1.083×10^{-5}		6.29
16.1	0.232	9.667×10^{-6}	0.222	6.32
20.0	0.184	7.667×10^{-6}		6.37
25.0	0.135	5.625×10^{-6}		6.42
30.0	0.096	4.000×10^{-6}	0.161	6.44
35.0	0.068	2.833×10^{-6}		6.46
40.0	0.047	1.958×10^{-6}		6.47
45.0	0.031	1.292×10^{-6}	0.186	6.48
50.0	0.021	8.750×10^{-7}		6.48
60.1	0.009	3.750×10^{-7}		6.48
70.1	0.004	1.667×10^{-7}	0.020	6.48

Table A20. Experimental Results of $C_2O_4^{2-}$ Photodecomposition in DIW ($C_0 = 2.138 \times 10^{-5}$ M. $I_a = 5.27 \times 10^{-6}$ E L^{-1} s^{-1}. T = 25°C).

Time (min)	$C_2O_4^{2-}$		NPOC (mg/L as C)	pH
	mg/L as C	M		
0.0	0.513	2.138×10^{-5}	0.568	5.48
1.0	0.483	2.012×10^{-5}	0.550	5.63
2.0	0.454	1.892×10^{-5}		5.79
3.0	0.423	1.762×10^{-5}	0.451	5.92
4.1	0.395	1.646×10^{-5}		6.02
5.0	0.371	1.546×10^{-5}		6.08
6.0	0.346	1.442×10^{-5}	0.375	6.15
7.0	0.323	1.346×10^{-5}		6.19
8.0	0.302	1.258×10^{-5}		6.22
10.0	0.261	1.088×10^{-5}	0.298	6.29
12.0	0.225	9.375×10^{-6}		6.34
14.0	0.194	8.083×10^{-6}		6.38
16.0	0.164	6.833×10^{-6}	0.189	6.40
18.0	0.141	5.875×10^{-6}		6.43
20.0	0.119	4.958×10^{-6}		6.44
25.0	0.076	3.167×10^{-6}	0.154	6.47
30.0	0.048	2.000×10^{-6}		6.49
35.2	0.029	1.208×10^{-6}		6.49
40.0	0.017	7.083×10^{-7}	0.098	6.49
45.0	0.010	4.167×10^{-7}		6.49
50.0	0.006	2.500×10^{-7}		6.48
60.2	0.002	8.333×10^{-8}	0.063	6.47

Table A21. Experimental Results of $C_2O_4^{2-}$ Photodecomposition in DIW with air Bubbling ($C_0 = 2.104 \cdot 10^{-5}$ M, $I_a = 2.60 \times 10^{-6}$ E L^{-1} s^{-1}, T = 25°C).

Time (min)	$C_2O_4^{2-}$		pH
	mg/L as C	M	
0.0	0.505	2.104×10^{-5}	6.52
1.0	0.493	2.054×10^{-5}	7.03
2.0	0.483	2.012×10^{-5}	7.15
3.0	0.472	1.967×10^{-5}	7.22
4.0	0.460	1.917×10^{-5}	7.31
5.0	0.448	1.867×10^{-5}	7.39
6.0	0.438	1.825×10^{-5}	7.48
8.0	0.417	1.738×10^{-5}	7.61
10.0	0.396	1.650×10^{-5}	7.72
12.0	0.377	1.571×10^{-5}	7.82
14.0	0.356	1.483×10^{-5}	7.89
16.0	0.339	1.413×10^{-5}	7.95
20.0	0.303	1.263×10^{-5}	8.06
25.0	0.265	1.104×10^{-5}	8.16
30.0	0.227	9.458×10^{-6}	8.24
35.0	0.199	8.292×10^{-6}	8.28
40.0	0.170	7.083×10^{-6}	8.32
50.0	0.126	5.250×10^{-6}	8.38
60.0	0.094	3.917×10^{-6}	8.41
70.0	0.070	2.917×10^{-6}	8.45
80.0	0.053	2.208×10^{-6}	8.47
90.0	0.040	1.667×10^{-6}	8.50
100.0	0.030	1.250×10^{-6}	8.52
110.0	0.023	9.583×10^{-7}	8.54
120.0	0.018	7.500×10^{-7}	8.54

Table A22. Experimental Results of $C_2O_4^{2-}$ Photodecomposition in DIW in the Absence of DO ($C_0 = 2.167 \times 10^{-5}$ M, $I_a = 2.067 \times 10^{-6}$ E L^{-1} s^{-1}, T = 25°C).

Time (min)	$C_2O_4^{2-}$		pH
	mg/L as C	M	
0.0	0.496	2.067×10^{-5}	6.32
1.0	0.482	2.008×10^{-5}	6.85
2.0	0.469	1.954×10^{-5}	7.13
3.0	0.459	1.913×10^{-5}	7.30
4.0	0.447	1.863×10^{-5}	7.41
5.0	0.433	1.804×10^{-5}	7.49
6.0	0.424	1.767×10^{-5}	7.54
8.0	0.404	1.683×10^{-5}	7.63
10.0	0.384	1.600×10^{-5}	7.69
12.0	0.361	1.504×10^{-5}	7.74
14.0	0.344	1.433×10^{-5}	7.78
16.3	0.323	1.346×10^{-5}	7.82
20.0	0.291	1.213×10^{-5}	7.87
25.0	0.253	1.054×10^{-5}	7.93
30.0	0.219	9.125×10^{-6}	7.97
35.0	0.187	7.792×10^{-6}	8.02
40.2	0.158	6.583×10^{-6}	8.05
50.2	0.112	4.667×10^{-6}	8.12
60.0	0.076	3.167×10^{-6}	8.19
70.3	0.050	2.083×10^{-6}	8.26
80.0	0.033	1.375×10^{-6}	8.31
90.0	0.021	8.750×10^{-7}	8.36
100.0	0.014	5.833×10^{-7}	8.42
110.3	0.009	3.750×10^{-7}	8.46
120.0	0.007	2.917×10^{-7}	8.50

Table A23. Experimental Results of $C_2O_4^{2-}$ Photodecomposition in DIW ($C_0 = 2.111 \times 10^{-4}$ M, $I_a = 2.60 \times 10^{-6}$ E $L^{-1}s^{-1}$, T = 25°C).

Time (min)	$C_2O_4^{2-}$		O_2 (M)	pH
	mg/L as C	M		
0.0	5.067	2.111×10^{-4}	2.337×10^{-4}	5.92
10.3	4.620	1.925×10^{-4}	2.259×10^{-4}	6.74
20.0	4.245	1.769×10^{-4}	2.166×10^{-4}	7.00
30.1	3.898	1.624×10^{-4}	2.128×10^{-4}	7.16
40.0	3.521	1.467×10^{-4}	2.125×10^{-4}	7.27
60.0	2.804	1.168×10^{-4}	2.164×10^{-4}	7.41
80.0	2.166	9.025×10^{-5}	2.283×10^{-4}	7.50
100.0	1.704	7.100×10^{-5}	2.370×10^{-4}	7.55
120.0	1.311	5.463×10^{-5}	2.458×10^{-4}	7.59
150.0	0.833	3.471×10^{-5}	2.4970×10^{-4}	7.63
180.0	0.516	2.150×10^{-5}	2.507×10^{-4}	7.66
230.0	0.219	9.125×10^{-6}	2.523×10^{-4}	7.68
275.0	0.097	4.042×10^{-6}	2.528×10^{-4}	7.69
300.0	0.058	2.417×10^{-6}	2.337×10^{-4}	7.69
345.1	0.023	9.583×10^{-7}	2.259×10^{-4}	7.69
380.2	0.011	4.583×10^{-7}	2.166×10^{-4}	7.69

Table A24. Experimental Results of $C_2O_4^{2-}$ Photodecomposition in Poughkeepsie's Pilot Plant Filter Effluent (C_0 = 1.967×10^{-5} M, I_a = 2.60 x 10^{-6} E L^{-1} s^{-1}, T = 25°C).

Time (min)	$C_2O_4^{2-}$		pH
	mg/L as C	M	
0.0	0.472	1.967×10^{-5}	7.91
0.5	0.471	1.963×10^{-5}	7.91
1.0	0.467	1.946×10^{-5}	7.90
1.5	0.468	1.950×10^{-5}	7.90
2.0	0.470	1.958×10^{-5}	7.89
3.0	0.465	1.938×10^{-5}	7.88
4.0	0.462	1.925×10^{-5}	7.87
5.0	0.463	1.929×10^{-5}	7.85
6.0	0.461	1.921×10^{-5}	7.84
8.0	0.459	1.913×10^{-5}	7.82
10.0	0.453	1.888×10^{-5}	7.79
12.3	0.448	1.867×10^{-5}	7.77
14.0	0.446	1.858×10^{-5}	7.76
20.0	0.433	1.804×10^{-5}	7.71
25.0	0.421	1.754×10^{-5}	7.69
30.0	0.411	1.713×10^{-5}	7.66
40.3	0.393	1.638×10^{-5}	7.62
60.0	0.355	1.479×10^{-5}	7.58
80.0	0.322	1.342×10^{-5}	7.56
100.0	0.298	1.242×10^{-5}	7.56
131.2	0.262	1.092×10^{-5}	7.58
160.0	0.228	9.500×10^{-6}	7.61

Table A25. Observed Rate Constants for $C_2O_4^{2-}$ Photodecomposition

$C_0 \times 10^5$ (M)	NaHCO3 Alkalinity (mg L^{-1} as $CaCO_3$)	T (°C)	$I_a \times 10^6$ (E $L^{-1}s^{-1}$)	pH_0	Observed Rate Constants (min^{-1})			
					k_1	k_2	k_1/k_2	Conversion (%) at the rate switch
2.046	-	25	2.60	5.61	0.036	0.046	0.77	51
2.063	-	25	2.60	5.53	0.040	0.052	0.78	55
2.113	-	25	2.60	5.45	0.036	0.053	0.68	51
2.063	-	25	2.60	5.45	0.032	0.051	0.62	50
4.208	-	25	2.60	5.60	0.028	0.034	0.82	56
5.917	-	25	2.60	5.59	0.022	0.031	0.71	59
8.750	-	25	2.60	5.68	0.020	0.026	0.80	65
21.11	-	25	2.60	5.92	0.011	0.019	0.58	66
2.167	-	15	2.60	5.47	0.035	0.073	0.48	65
2.046	-	20	2.60	5.45	0.038	0.059	0.64	53
2.117	-	35	2.60	5.43	0.037	0.041	0.89	52
2.038	-	25	2.60	7.18	0.030	0.037	0.81	53
2.088	-	25	2.60	8.10	0.028	0.038	0.74	56
2.188	-	25	2.60	8.94	0.020	0.024	0.84	56
2.104	-	25	1.38	5.47	0.019	0.022	0.87	53
2.292	-	25	3.99	5.47	0.0539	0.080	0.66	53
2.138	-	25	5.27	5.48	0.069	0.104	0.66	56
2.067	10	25	2.60	7.15	0.017	0.023	0.74	35
2.117	25	25	2.60	7.78	0.013	0.017	0.76	22
2.138	50	25	2.60	7.98	0.010	0.013	0.77	26
4.458	50	25	2.60	7.80	0.011	0.013	0.84	33
1.967	(in PPFE)	25	2.60	7.91	0.005	0.0046	1	-
2.104 (air bubbling)	-	25	2.60	6.52	0.026	0.029	0.91	48
2.067(He bubbling)	-	25	2.60	6.32	0.0276	0.040	0.67	56

APPENDIX B

TABLES OF EXPERIMENTAL DATA FOR FORMATE

Table B1. Experimental Results of HCO_2^- Photodecomposition in DIW ($C_0 = 4.108\times10^{-5}$ M, $I_a = 1.38 \times 10^{-6}$ E L^{-1} s^{-1}, T = 25°C).

Time (min)	HCO_2^-		NPOC (mg/L as C)	pH
	mg/L as C	M		
0.0	0.493	4.108×10^{-5}	0.557	5.64
0.5	0.486	4.050×10^{-5}	0.546	
1.0	0.485	4.042×10^{-5}		
1.5	0.473	3.942×10^{-5}	0.505	
2.0	0.466	3.883×10^{-5}		6.00
3.0	0.437	3.642×10^{-5}		6.16
4.0	0.408	3.400×10^{-5}	0.435	6.25
5.0	0.379	3.158×10^{-5}		6.38
6.0	0.346	2.883×10^{-5}		6.44
7.0	0.317	2.642×10^{-5}	0.332	6.52
8.0	0.277	2.308×10^{-5}		6.58
9.0	0.244	2.033×10^{-5}		6.64
10.0	0.202	1.683×10^{-5}	0.229	6.67
12.0	0.130	1.083×10^{-5}		6.75
14.0	0.064	5.333×10^{-6}		6.78
16.0	0.016	1.333×10^{-6}	0.081	6.81
18.0	0.007	5.833×10^{-7}		6.82
20.0	0.007	5.833×10^{-7}		6.82
22.0	0.007	5.833×10^{-7}	0.085	6.80
24.0	0.007	5.833×10^{-7}	0.065	6.80

Table B2. Experimental Results of HCO_2^- Photodecomposition in DIW ($C_0 = 4.043 \times 10^{-5}$ M, $I_a = 1.38 \times 10^{-6}$ E L^{-1} s^{-1}, T = 25°C).

Time (min)	HCO_2^-		NPOC (mg/L as C)	pH
	mg/L as C	M		
0.0	0.485	4.043×10^{-5}	0.502	5.54
0.5	0.483	4.028×10^{-5}	0.499	5.58
1.0	0.475	3.961×10^{-5}		5.65
1.5	0.467	3.891×10^{-5}	0.470	5.72
2.0	0.456	3.798×10^{-5}		5.79
3.0	0.438	3.649×10^{-5}		5.93
4.0	0.416	3.465×10^{-5}	0.421	6.03
5.0	0.393	3.274×10^{-5}		6.13
6.0	0.369	3.076×10^{-5}		6.20
7.0	0.339	2.825×10^{-5}	0.315	6.27
8.0	0.313	2.611×10^{-5}		6.33
9.0	0.284	2.366×10^{-5}		6.37
10.0	0.253	2.105×10^{-5}	0.237	6.42
12.0	0.190	1.586×10^{-5}		6.50
14.0	0.116	9.666×10^{-6}		6.57
16.0			0.078	6.61
18.0				6.63
20.0				6.62
22.0			0.022	6.62
25.0			0.030	6.61
30.0			0.020	6.61
35.1			0.018	6.59
40.2			0.032	6.58
46.2			0.027	6.59

Table B3. Experimental Results of HCO_2^- Photodecomposition in DIW ($C_0 = 4.367\times10^{-5}$ M, $I_a = 2.60 \times 10^{-6}$ E L^{-1} s^{-1}, T = 18°C).

Time (min)	HCO_2^-		NPOC (mg/L as C)	pH
	mg/L as C	M		
0.0	0.524	4.367×10^{-5}	0.490	5.62
0.6	0.508	4.233×10^{-5}	0.474	5.72
1.0	0.495	4.125×10^{-5}		5.79
1.5	0.476	3.967×10^{-5}	0.472	5.91
2.0	0.455	3.792×10^{-5}		6.03
2.5	0.433	3.608×10^{-5}		6.14
3.0	0.406	3.383×10^{-5}	0.368	6.23
3.5	0.376	3.133×10^{-5}		6.30
4.0	0.346	2.883×10^{-5}		6.37
5.0	0.284	2.367×10^{-5}	0.245	6.49
6.0	0.225	1.875×10^{-5}		6.58
7.0	0.161	1.342×10^{-5}		6.65
8.0	0.093	7.750×10^{-6}	0.099	6.70
10.0	0.004	3.333×10^{-7}		6.73
12.0	0.001	8.333×10^{-8}		6.72
14.0	0.001	8.333×10^{-8}	0.089	6.71
16.0	0.001	8.333×10^{-8}		6.71
20.0	0.001	8.333×10^{-8}		6.70
25.0	0.000	0.000	0.010	6.70

Table B4. Experimental Results of HCO_2^- Photodecomposition in DIW ($C_0 = 1.733 \times 10^{-5}$ M, $I_a = 2.60 \times 10^{-6}$ E L^{-1} s^{-1}, T = 25°C).

Time (min)	HCO_2^-		pH
	mg/L as C	M	
0.0	0.208	1.733×10^{-5}	5.39
0.5	0.194	1.617×10^{-5}	5.47
1.0	0.174	1.450×10^{-5}	5.59
1.5	0.154	1.283×10^{-5}	5.71
2.0	0.132	1.100×10^{-5}	5.82
2.5	0.109	9.083×10^{-6}	5.89
3.0	0.084	7.000×10^{-6}	5.95
3.5	0.060	5.000×10^{-6}	6.02
4.0	0.038	3.167×10^{-6}	6.07
4.5	0.018	1.500×10^{-6}	6.10
5.0	0.005	4.167×10^{-7}	6.12
5.5	0.001	8.333×10^{-8}	6.12
6.0	0.000	0.000	6.11
6.5	0.000	0.000	6.11

Table B5. Experimental Results of HCO_2^- Photodecomposition in DIW Containing $NaHCO_3$ = 25 mg/L as $CaCO_3$ ($C_0 = 4.133 \times 10^{-5}$ M, $I_a = 2.60 \times 10^{-6}$ E L^{-1} s^{-1}, T = 25°C).

Time (min)	HCO_2^-		NPOC (mg/L as C)	pH
	mg/L as C	M		
0.0	0.496	4.133×10^{-5}	0.514	7.81
0.5	0.494	4.117×10^{-5}	0.492	7.83
1.0	0.482	4.017×10^{-5}		7.84
1.5	0.456	3.800×10^{-5}	0.452	7.84
2.0	0.436	3.633×10^{-5}		7.84
2.5	0.414	3.450×10^{-5}		7.84
3.0	0.384	3.200×10^{-5}	0.356	7.84
3.5	0.363	3.025×10^{-5}		7.85
4.0	0.339	2.825×10^{-5}		7.85
4.5	0.309	2.575×10^{-5}	0.292	7.85
5.0	0.285	2.375×10^{-5}		7.85
5.5	0.257	2.142×10^{-5}		7.85
6.0	0.227	1.892×10^{-5}	0.254	7.85
6.5	0.201	1.675×10^{-5}		7.85
7.0	0.174	1.450×10^{-5}		7.85
8.0	0.120	1.000×10^{-5}	0.138	7.85
9.0	0.072	6.000×10^{-6}		7.85
10.0	0.032	2.667×10^{-6}		7.84
12.0	0.002	1.667×10^{-7}	0.033	7.82
14.0	0.000	0.000	0.018	7.81
16.0	0.000	0.000		7.81

Table B6. Experimental Results of HCO_2^- Photodecomposition in DIW Containing $NaHCO_3$ = 50 mg/L as $CaCO_3$ ($C_0 = 4.300 \times 10^{-5}$ M, $I_a = 2.60 \times 10^{-6}$ E L^{-1} s^{-1}, T = 25°C).

Time (min)	HCO_2^-		pH
	mg/L as C	M	
0.0	0.516	4.300×10^{-5}	7.96
0.5	0.506	4.217×10^{-5}	7.96
1.0	0.491	4.092×10^{-5}	7.96
1.5	0.475	3.958×10^{-5}	7.97
2.0	0.457	3.808×10^{-5}	7.97
2.5	0.439	3.658×10^{-5}	7.96
3.0	0.419	3.492×10^{-5}	7.96
3.5	0.400	3.333×10^{-5}	7.96
4.0	0.380	3.167×10^{-5}	7.96
4.5	0.360	3.000×10^{-5}	7.96
5.0	0.338	2.817×10^{-5}	7.96
5.5	0.315	2.625×10^{-5}	7.96
6.0	0.293	2.442×10^{-5}	7.96
6.5	0.272	2.267×10^{-5}	7.96
7.0	0.251	2.092×10^{-5}	7.96
7.5	0.229	1.908×10^{-5}	7.96
8.0	0.205	1.708×10^{-5}	7.96
9.0	0.163	1.358×10^{-5}	7.96
10.0	0.116	9.667×10^{-6}	7.95
12.0	0.049	4.083×10^{-6}	7.94
14.0	0.010	8.333×10^{-7}	7.93

Table B7. Experimental Results of HCO_2^- Photodecomposition in DIW ($C_0 = 4.150\times10^{-5}$ M, $I_a = 2.60 \times 10^{-6}$ E L^{-1} s^{-1}, T = 25°C).

Time (min)	HCO_2^-		TC (mg L^{-1} as C)	pH
	mg/L as C	M		
0.0	0.498	4.150×10^{-5}	0.577	5.52
1.0	0.478	3.983×10^{-5}	0.558	5.77
2.0	0.443	3.692×10^{-5}		5.97
3.0	0.395	3.292×10^{-5}	0.537	6.14
4.0	0.344	2.867×10^{-5}		6.27
5.0	0.288	2.400×10^{-5}		6.37
7.5	0.113	9.417×10^{-6}	0.511	6.56
10.0	0.005	4.167×10^{-7}		6.58
12.5	0.000	0.000		6.58
15.0	0.000	0.000	0.552	6.58
20.0	0.000	0.000	0.532	6.56
30.0	0.000	0.000	0.595	6.55

Table B8. Experimental Results of HCO_2^- Photodecomposition in DIW ($C_0 = 4.275\times10^{-5}$ M, $I_a = 2.6 \times 10^{-6}$ E L^{-1} s^{-1}, T = 25°C).

Time (min)	HCO_2^-		TC (mg L^{-1} as C)	pH
	mg/L as C	M		
0.0	0.513	4.275×10^{-5}	0.530	5.52
0.5	0.504	4.200×10^{-5}	0.497	
1.0	0.490	4.083×10^{-5}		5.57
1.5	0.470	3.917×10^{-5}	0.506	
2.0	0.449	3.742×10^{-5}		5.82
2.5	0.432	3.600×10^{-5}		
3.0	0.399	3.325×10^{-5}	0.503	6.05
3.5	0.378	3.150×10^{-5}		
4.0	0.351	2.925×10^{-5}		6.26
4.5	0.318	2.650×10^{-5}	0.550	
5.0	0.294	2.450×10^{-5}		6.33
5.5	0.262	2.183×10^{-5}		
6.0	0.225	1.875×10^{-5}	0.538	6.42
6.5	0.193	1.608×10^{-5}		
7.0	0.157	1.308×10^{-5}		6.56
7.5	0.115	9.583×10^{-6}	0.551	
8.0	0.079	6.583×10^{-6}		6.57
8.5	0.043	3.583×10^{-6}		
9.0	0.014	1.167×10^{-6}	0.541	6.61
10.0	0.001	8.300×10^{-8}		6.61

Table B9. Experimental Results of HCO_2^- Photodecomposition in DIW (C_0 = 4. 267×10^{-5} M, I_a = 2.60 × 10^{-6} E L^{-1} s^{-1}, T = 25°C).

Time (min)	HCO_2^-		NPOC (mg/L as C)	pH
	mg/L as C	M		
0.0	0.512	4.267×10^{-5}	0.531	5.53
0.5	0.503	4.192×10^{-5}	0.503	5.62
1.0	0.492	4.100×10^{-5}		5.76
1.5	0.474	3.950×10^{-5}	0.454	5.89
2.0	0.457	3.808×10^{-5}		6.01
2.5	0.439	3.658×10^{-5}		6.10
3.0	0.411	3.425×10^{-5}	0.368	6.18
3.5	0.382	3.183×10^{-5}		6.26
4.0	0.357	2.975×10^{-5}		6.32
4.5	0.325	2.708×10^{-5}	0.282	6.38
5.0	0.295	2.458×10^{-5}		6.42
5.5	0.258	2.150×10^{-5}		6.46
6.0	0.216	1.800×10^{-5}	0.197	6.51
6.5	0.180	1.500×10^{-5}		6.53
7.0	0.137	1.142×10^{-5}		6.57
8.0	0.052	4.333×10^{-6}	0.069	6.62
9.0	0.006	5.000×10^{-7}		6.64
10.0	0.002	1.667×10^{-7}		6.63
11.0	0.001	8.333×10^{-8}	0.054	6.62
15.0	0.001	8.333×10^{-8}	0.030	6.62
20.0	0.001	8.333×10^{-8}	0.033	6.61

Table B10. Experimental Results of HCO_2^- Photodecomposition in DIW ($C_0 = 4.258 \times 10^{-5}$ M, $I_a = 2.6 \times 10^{-6}$ E L^{-1} s^{-1}, T = 25°C).

Time (min)	HCO_2^-		pH
	mg/L as C	M	
0.0	0.511	4.258×10^{-5}	5.41
0.5	0.497	4.142×10^{-5}	5.49
1.0	0.481	4.008×10^{-5}	5.61
1.5	0.458	3.817×10^{-5}	5.72
2.0	0.436	3.633×10^{-5}	5.84
2.5	0.415	3.458×10^{-5}	5.93
3.0	0.388	3.233×10^{-5}	6.01
3.5	0.364	3.033×10^{-5}	6.08
4.0	0.336	2.800×10^{-5}	6.14
4.5	0.310	2.583×10^{-5}	6.20
5.0	0.282	2.350×10^{-5}	6.24
5.5	0.254	2.117×10^{-5}	6.29
6.0	0.224	1.867×10^{-5}	6.33
6.5	0.193	1.608×10^{-5}	6.37
7.0	0.164	1.367×10^{-5}	6.41
7.5	0.132	1.100×10^{-5}	6.44
8.0	0.105	8.750×10^{-6}	6.46
9.0	0.050	4.167×10^{-6}	6.51
10.0	0.009	7.500×10^{-7}	6.53
15.1	0.000	0.000	6.51
20.0	0.000	0.000	6.49
34.0	0.000	0.000	6.47

Table B11. Experimental Results of HCO_2^- Photodecomposition in DIW at Initial pH Adjusted to 7.18 with Concentrated NaOH ($C_0 = 4.258 \times 10^{-5}$ M, $I_a = 2.60 \times 10^{-6}$ $EL^{-1}s^{-1}$, T = 25°C).

Time (min)	HCO_2^-		NPOC (mg/L as C)	pH
	mg/L as C	M		
0.0	0.511	4.258×10^{-5}	0.640	7.18
0.5	0.501	4.175×10^{-5}	0.572	7.43
1.0	0.484	4.033×10^{-5}		7.55
1.5	0.457	3.808×10^{-5}	0.644	7.60
2.0	0.432	3.600×10^{-5}		7.65
2.5	0.407	3.392×10^{-5}		7.66
3.0	0.381	3.175×10^{-5}	0.473	7.67
3.5	0.350	2.917×10^{-5}		7.69
4.0	0.321	2.675×10^{-5}		7.69
4.5	0.303	2.525×10^{-5}	0.491	7.69
5.0	0.261	2.175×10^{-5}		7.69
5.5	0.231	1.925×10^{-5}		7.69
6.0	0.195	1.625×10^{-5}	0.233	7.68
6.5	0.166	1.383×10^{-5}		7.67
7.0	0.133	1.108×10^{-5}		7.66
7.5	0.099	8.250×10^{-6}	0.151	7.64
8.0	0.072	6.000×10^{-6}		7.61
9.0	0.020	1.667×10^{-6}	0.076	7.55
10.0	0.002	1.667×10^{-7}		7.38
12.0	0.001	8.333×10^{-8}	0.050	7.32
14.0	0.001	8.333×10^{-8}		7.27
16.0	0.001	8.333×10^{-8}	0.146	7.23
20.0	0.001	8.333×10^{-8}	0.011	7.15

Table B12. Experimental Results of HCO_2^- Photodecomposition in DIW at Initial pH Adjusted to 8.06 with Concentrated NaOH ($C_0 = 4.150 \times 10^{-5}$ M, $I_a = 2.60 \times 10^{-6}$ $EL^{-1}s^{-1}$, T = 25°C).

Time (min)	HCO_2^-		NPOC (mg/L as C)	pH
	mg/L as C	M		
0.0	0.498	4.150×10^{-5}	0.568	8.06
0.5	0.490	4.083×10^{-5}	0.518	8.13
1.0	0.471	3.925×10^{-5}		8.15
1.5	0.445	3.708×10^{-5}	0.449	8.18
2.0	0.420	3.500×10^{-5}		8.17
2.5	0.395	3.292×10^{-5}		8.17
3.0	0.366	3.050×10^{-5}	0.377	8.16
3.5	0.341	2.842×10^{-5}		8.17
4.0	0.306	2.550×10^{-5}		8.16
4.5	0.273	2.275×10^{-5}	0.262	8.16
5.0	0.242	2.017×10^{-5}		8.15
5.5	0.214	1.783×10^{-5}		8.15
6.0	0.179	1.492×10^{-5}	0.179	8.14
6.5	0.146	1.217×10^{-5}		8.11
7.0	0.117	9.750×10^{-6}		8.11
8.0	0.053	4.417×10^{-6}	0.075	8.08
9.0	0.010	8.333×10^{-7}		8.00
10.0	0.001	8.333×10^{-8}		7.85
12.0	0.000	0.000	0.009	7.75
14.0	0.000	0.000	0.000	7.65

Table B13. Experimental Results of HCO_2^- Photodecomposition in DIW at Initial pH Adjusted to 8.97 with Concentrated NaOH ($C_0 = 4.200 \times 10^{-5}$ M, $I_a = 2.60 \times 10^{-6}$ $EL^{-1}s^{-1}$, T = 25°C).

Time (min)	HCO_2^-		NPOC (mg/L as C)	pH
	mg/L as C	M		
0.0	0.504	4.200×10^{-5}	0.533	8.97
0.5	0.495	4.125×10^{-5}	0.501	8.96
1.0	0.476	3.967×10^{-5}		8.95
1.5	0.453	3.775×10^{-5}	0.513	8.94
2.0	0.431	3.592×10^{-5}		8.94
2.5	0.399	3.325×10^{-5}		8.94
3.0	0.373	3.108×10^{-5}	0.414	8.93
3.5	0.350	2.917×10^{-5}		8.92
4.0	0.324	2.700×10^{-5}		8.92
4.5	0.291	2.425×10^{-5}	0.307	8.92
5.0	0.264	2.200×10^{-5}		8.92
5.5	0.235	1.958×10^{-5}		8.91
6.0	0.202	1.683×10^{-5}	0.219	8.90
6.5	0.173	1.442×10^{-5}		8.89
7.0	0.145	1.208×10^{-5}		8.89
8.0	0.087	7.250×10^{-6}	0.141	8.87
9.0	0.037	3.083×10^{-6}	0.104	8.86
10.0	0.009	7.500×10^{-7}		8.86
12.0	0.001	8.333×10^{-8}		8.84
14.0	0.001	8.333×10^{-8}	0.033	8.83
16.0	0.000	0.000	0.027	8.80
20.0	0.000	0.000	0.063	8.76

Table B14. Experimental Results of HCO_2^- Photodecomposition in DIW (C_0 = 8.850 × 10^{-5} M, I_a = 2.60 × 10^{-6} E L^{-1} s^{-1}, T = 25°C).

Time (min)	HCO_2^-		NPOC (mg/L as C)	pH
	mg/L as C	M		
0.0	1.062	8.850×10^{-5}	0.986	5.68
0.5	1.040	8.667×10^{-5}	0.973	5.73
1.0	1.024	8.533×10^{-5}		5.85
1.5	0.992	8.267×10^{-5}	0.957	6.00
2.0	0.971	8.092×10^{-5}		6.12
2.5	0.943	7.858×10^{-5}		6.22
3.0	0.907	7.558×10^{-5}	0.821	6.29
3.5	0.873	7.275×10^{-5}		6.37
4.0	0.840	7.000×10^{-5}		6.43
4.5	0.813	6.775×10^{-5}	0.752	6.48
5.0	0.771	6.425×10^{-5}		6.54
5.5	0.738	6.150×10^{-5}		6.58
6.0	0.706	5.883×10^{-5}	0.658	6.61
6.5	0.668	5.567×10^{-5}		6.66
7.0	0.624	5.200×10^{-5}		6.70
8.0	0.545	4.542×10^{-5}	0.553	6.76
9.0	0.469	3.908×10^{-5}		6.81
10.0	0.382	3.183×10^{-5}		6.86
12.0	0.212	1.767×10^{-5}	0.260	6.94
15.0	0.021	1.750×10^{-6}		7.00
20.0	0.001	8.333×10^{-8}	0.085	6.95
25.0	0.000	0.000	0.097	6.93
30.0	0.000	0.000	0.109	6.91

Table B15. Experimental Results of HCO_2^- Photodecomposition in DIW (C_0 = 1.723 × 10^{-4} M, I_a = 2.60 × 10^{-6} E L^{-1} s^{-1}, T = 25°C).

Time (min)	HCO_2^-		NPOC (mg/L as C)	pH
	mg/L as C	M		
0.0	2.067	1.723 × 10^{-4}	2.039	5.67
0.5	2.027	1.689 × 10^{-4}	2.016	5.74
1.0	1.999	1.666 × 10^{-4}		5.86
1.5	1.998	1.665 × 10^{-4}	1.888	5.97
2.0	1.967	1.639 × 10^{-4}		6.09
2.5	1.970	1.642 × 10^{-4}		6.18
3.0	1.920	1.600 × 10^{-4}	1.905	6.26
3.5	1.899	1.583 × 10^{-4}		6.34
4.0	1.852	1.543 × 10^{-4}		6.40
4.5	1.810	1.508 × 10^{-4}	1.933	6.47
5.0	1.786	1.488 × 10^{-4}		6.52
6.0	1.735	1.446 × 10^{-4}		6.61
7.0	1.668	1.390 × 10^{-4}	1.677	6.69
8.0	1.619	1.349 × 10^{-4}		6.76
9.0	1.526	1.272 × 10^{-4}		6.83
10.0	1.439	1.199 × 10^{-4}	1.440	6.89
12.0	1.276	1.063 × 10^{-4}		7.00
14.0	1.109	9.242 × 10^{-5}		7.09
16.0	0.919	7.658 × 10^{-5}	0.880	7.16
18.0	0.734	6.117 × 10^{-5}		7.21
20.0	0.516	4.300 × 10^{-5}	0.628	7.26
22.0	0.307	2.558 × 10^{-5}	0.434	7.29
25.0	0.057	4.750 × 10^{-6}	0.213	7.29
30.0	0.001	8.333 × 10^{-8}	0.098	7.22
35.0	0.000	0.000	0.053	7.20

Table B16. Experimental Results of HCO_2^- Photodecomposition in DIW (C_0 = 4.308 × 10^{-5} M, I_a = 2.60 × 10^{-6} E L^{-1} s^{-1}, T = 35°C).

Time (min)	HCO_2^-		NPOC (mg/L as C)	pH
	mg/L as C	M		
0.0	0.517	4.308×10^{-5}	0.620	5.44
0.5	0.492	4.100×10^{-5}	0.474	5.48
1.0	0.472	3.933×10^{-5}		5.54
1.5	0.440	3.667×10^{-5}	0.429	5.70
2.0	0.408	3.400×10^{-5}		5.95
2.5	0.379	3.158×10^{-5}		6.02
3.0	0.350	2.917×10^{-5}	0.392	6.10
3.5	0.318	2.650×10^{-5}		6.16
4.0	0.286	2.383×10^{-5}		6.23
4.5	0.245	2.042×10^{-5}	0.262	6.28
5.0	0.212	1.767×10^{-5}		6.33
5.6	0.165	1.375×10^{-5}		6.40
6.1	0.128	1.067×10^{-5}	0.155	6.42
6.5	0.103	8.583×10^{-6}		6.46
7.0	0.071	5.917×10^{-6}		6.49
7.5	0.036	3.000×10^{-6}	0.146	6.51
8.0	0.015	1.250×10^{-6}		6.52
8.5	0.003	2.500×10^{-7}		6.54
9.0	0.001	8.333×10^{-8}	0.068	6.54
10.0	0.001	8.333×10^{-8}	0.044	6.54

Table B17. Experimental Results of HCO_2^- Photodecomposition in DIW (C_0 = 4.225 × 10^{-5} M, I_a = 2.60 × 10^{-6} E L^{-1} s^{-1}, T = 35°C).

Time (min)	HCO_2^-		pH
	mg/L as C	M	
0.0	0.507	4.225×10^{-5}	5.27
0.5	0.485	4.042×10^{-5}	5.37
1.0	0.462	3.850×10^{-5}	5.50
1.5	0.437	3.642×10^{-5}	5.61
2.0	0.417	3.475×10^{-5}	5.71
2.5	0.387	3.225×10^{-5}	5.80
3.0	0.364	3.033×10^{-5}	5.88
3.5	0.333	2.775×10^{-5}	5.95
4.0	0.306	2.550×10^{-5}	6.00
4.5	0.277	2.308×10^{-5}	6.04
5.0	0.249	2.075×10^{-5}	6.10
5.5	0.217	1.808×10^{-5}	6.14
6.0	0.187	1.558×10^{-5}	6.17
6.5	0.154	1.283×10^{-5}	6.22
7.0	0.122	1.017×10^{-5}	6.25
7.5	0.092	7.667×10^{-6}	-
8.0	0.060	5.000×10^{-6}	6.30
8.5	0.033	2.750×10^{-6}	6.33
9.0	0.014	1.167×10^{-6}	6.34
9.5	0.004	3.333×10^{-7}	6.34
10.0	0.001	8.333×10^{-8}	6.34

Table B18. Experimental Results of HCO_2^- Photodecomposition in DIW (C_0 = 4.283 × 10^{-5} M, I_a = 3.9 × 10^{-6} E L^{-1} s^{-1}, T = 25°C).

Time (min)	HCO_2^-		NPOC (mg/L as C)	pH
	mg/L as C	M		
0.0	0.514	4.283×10^{-5}	0.510	5.55
0.5	0.487	4.058×10^{-5}	0.482	5.72
1.0	0.469	3.908×10^{-5}		5.89
1.5	0.436	3.633×10^{-5}	0.417	6.08
2.0	0.408	3.400×10^{-5}		6.21
2.5	0.365	3.042×10^{-5}	0.343	6.32
3.0	0.332	2.767×10^{-5}		6.40
3.5	0.283	2.358×10^{-5}	0.252	6.47
4.0	0.238	1.983×10^{-5}		6.54
4.5	0.184	1.533×10^{-5}	0.171	6.60
5.0	0.131	1.092×10^{-5}		6.65
5.5	0.073	6.083×10^{-6}	0.078	6.69
6.0	0.025	2.083×10^{-6}		6.70
7.0	0.001	8.333×10^{-8}	0.028	6.68
10.0	0.001	8.333×10^{-8}	0.039	6.67
15.0	0.001	8.333×10^{-8}	0.030	6.66
20.0	0.001	8.333×10^{-8}	0.028	6.65
25.1	0.001	8.333×10^{-8}	0.018	6.64

Table B19. Experimental Results of HCO_2^- Photodecomposition in DIW (C_0 = 4.117 × 10^{-5} M, I_a = 3.9 × 10^{-6} E L^{-1} s^{-1}, T = 25°C, Mixing Intensity = 250 rpm).

Time (min)	HCO_2^-		pH
	mg/L as C	M	
0.0	0.494	4.117×10^{-5}	5.51
0.5	0.478	3.983×10^{-5}	5.66
1.0	0.451	3.758×10^{-5}	5.86
1.5	0.418	3.483×10^{-5}	6.03
2.0	0.383	3.192×10^{-5}	6.16
2.5	0.345	2.875×10^{-5}	6.26
3.0	0.310	2.583×10^{-5}	6.35
3.5	0.266	2.217×10^{-5}	6.42
4.0	0.224	1.867×10^{-5}	6.48
4.5	0.184	1.533×10^{-5}	6.55
5.0	0.138	1.150×10^{-5}	6.58
5.5	0.091	7.583×10^{-6}	6.62
6.0	0.050	4.167×10^{-6}	6.64
7.0	0.002	1.667×10^{-7}	6.60
10.0	0.000	0.000	6.57

Table B20. Experimental Results of HCO_2^- Photodecomposition in DIW (C_0 = 3.983 × 10^{-5} M, I_a = 3.99 × 10^{-6} E L^{-1} s^{-1}, T = 25°C, Mixing Intensity = 50 rpm).

Time (min)	HCO_2^-		pH
	mg/L as C	M	
0.0	0.478	3.983×10^{-5}	5.60
0.5	0.464	3.867×10^{-5}	5.72
1.0	0.440	3.667×10^{-5}	5.89
1.5	0.410	3.417×10^{-5}	6.02
2.0	0.382	3.183×10^{-5}	6.15
2.6	0.344	2.867×10^{-5}	6.26
3.1	0.315	2.625×10^{-5}	6.35
3.5	0.285	2.375×10^{-5}	6.40
4.0	0.250	2.083×10^{-5}	6.47
4.5	0.214	1.783×10^{-5}	6.52
5.0	0.177	1.475×10^{-5}	6.56
5.5	0.139	1.158×10^{-5}	6.60
6.0	0.105	8.750×10^{-6}	6.65
7.0	0.040	3.333×10^{-6}	6.69
10.0	0.001	8.333×10^{-8}	6.69

Table B21. Experimental Results of HCO_2^- Photodecomposition in DIW ($C_0 = 4.175 \times 10^{-5}$ M, $I_a = 2.6 \times 10^{-6}$ E L^{-1} s^{-1}, T = 25°C).

Time (min)	HCO_2^-		O_2 (M)	pH
	mg/L as C	M		
0.0	0.501	4.175×10^{-5}	2.964×10^{-4}	5.48
0.5	0.474	3.950×10^{-5}	2.954×10^{-4}	5.61
1.0	0.454	3.783×10^{-5}	2.949×10^{-4}	5.77
1.5	0.433	3.608×10^{-5}	2.946×10^{-4}	5.88
2.0	0.411	3.425×10^{-5}	2.939×10^{-4}	5.99
2.5	0.385	3.208×10^{-5}	2.933×10^{-4}	6.07
3.0	0.360	3.000×10^{-5}	2.923×10^{-4}	6.16
3.5	0.332	2.767×10^{-5}	2.915×10^{-4}	6.22
4.0	0.309	2.575×10^{-5}	2.905×10^{-4}	6.27
4.5	0.281	2.342×10^{-5}	2.895×10^{-4}	6.32
5.0	0.253	2.108×10^{-5}	2.884×10^{-4}	6.36
5.5	0.223	1.858×10^{-5}	2.877×10^{-4}	6.41
6.0	0.191	1.592×10^{-5}	2.866×10^{-4}	6.44
6.5	0.163	1.358×10^{-5}	2.856×10^{-4}	6.49
7.0	0.134	1.117×10^{-5}	2.846×10^{-4}	6.52
7.5	0.104	8.667×10^{-6}	2.833×10^{-4}	6.54
8.0	0.073	6.083×10^{-6}	2.809×10^{-4}	6.56
9.0	0.023	1.917×10^{-6}	2.771×10^{-4}	6.60
10.0	0.001	8.333×10^{-8}	2.753×10^{-4}	6.60
12.0	0.000	0.000	2.719×10^{-4}	6.59
14.0	0.000	0.000	2.698×10^{-4}	6.59
16.0	0.000	0.000	2.675×10^{-4}	
18.0	0.000	0.000	2.675×10^{-4}	
20.0	0.000	0.000	2.675×10^{-4}	
23.0	0.000	0.000	2.678×10^{-4}	
28.0	0.000	0.000	2.675×10^{-4}	

Table B22. Experimental Results of HCO_2^- Photodecomposition in DIW with air Bubbling ($C_0 = 4.308 \times 10^{-5}$ M, $I_a = 2.60 \times 10^{-6}$ E L^{-1} s^{-1}, T = 25°C).

Time (min)	HCO_2^-		pH
	mg/L as C	M	
0.0	0.517	4.308×10^{-5}	6.48
0.5	0.493	4.108×10^{-5}	7.53
1.0	0.474	3.950×10^{-5}	7.80
1.5	0.452	3.767×10^{-5}	7.92
2.0	0.433	3.608×10^{-5}	8.00
2.5	0.407	3.392×10^{-5}	8.07
3.0	0.382	3.183×10^{-5}	8.10
3.6	0.356	2.967×10^{-5}	8.15
4.0	0.333	2.775×10^{-5}	8.19
4.5	0.308	2.567×10^{-5}	8.22
5.0	0.280	2.333×10^{-5}	8.25
5.5	0.251	2.092×10^{-5}	8.27
6.0	0.226	1.883×10^{-5}	8.30
6.5	0.196	1.633×10^{-5}	8.32
7.0	0.169	1.408×10^{-5}	8.34
7.5	0.139	1.158×10^{-5}	8.35
8.0	0.114	9.500×10^{-6}	8.36
9.0	0.061	5.083×10^{-6}	8.39
10.0	0.018	1.500×10^{-6}	8.39
12.0	0.001	8.333×10^{-8}	8.35
14.0	0.000	0	8.35

Table B23. Experimental Results of HCO_2^- Photodecomposition in DIW in the Absence of DO ($C_0 = 4.167 \times 10^{-5}$ M, $I_a = 2.60 \times 10^{-6}$ E L^{-1} s^{-1}, T = 25°C).

Time (min)	HCO_2^-		pH
	mg/L as C	M	
0.0	0.500	4.167×10^{-5}	6.49
0.6	0.475	3.958×10^{-5}	6.93
1.0	0.434	3.617×10^{-5}	7.11
1.6	0.390	3.250×10^{-5}	7.30
2.0	0.355	2.958×10^{-5}	7.42
2.5	0.312	2.600×10^{-5}	7.54
3.0	0.267	2.225×10^{-5}	7.62
3.5	0.232	1.933×10^{-5}	7.70
4.0	0.190	1.583×10^{-5}	7.77
4.5	0.152	1.267×10^{-5}	7.83
5.1	0.114	9.500×10^{-6}	7.90
5.5	0.079	6.583×10^{-6}	7.94
6.0	0.048	4.000×10^{-6}	7.99
6.5	0.023	1.917×10^{-6}	8.05
7.0	0.009	7.500×10^{-7}	8.09
7.5	0.002	1.667×10^{-7}	8.12
8.0	0.001	8.333×10^{-8}	8.12
9.0	0.001	8.333×10^{-8}	8.14
10.0	0.000	0.000	8.14
12.0	0.000	0.000	8.15
14.0	0.000	0.000	8.15

Table B24. Experimental Results of HCO_2^- Photodecomposition in DIW (C_0 = 3.830 × 10^{-4} M, I_a = 2.60 × 10^{-6} E L^{-1} s^{-1}, T = 25°C).

Time (min)	HCO_2^-		O_2 (M)	pH
	mg/L as C	M		
0.0	4.596	3.830×10^{-4}	2.773×10^{-4}	5.71
1.0	4.573	3.811×10^{-4}	2.771×10^{-4}	5.91
2.0	4.524	3.770×10^{-4}	2.766×10^{-4}	6.08
3.0	4.478	3.732×10^{-4}	2.753×10^{-4}	6.23
4.0	4.436	3.697×10^{-4}	2.737×10^{-4}	6.36
6.0	4.409	3.674×10^{-4}	2.691×10^{-4}	6.57
8.0	4.307	3.589×10^{-4}	2.629×10^{-4}	6.74
10.0	4.170	3.475×10^{-4}	2.559×10^{-4}	6.89
12.0	4.103	3.419×10^{-4}	2.492×10^{-4}	7.03
16.0	3.841	3.201×10^{-4}	2.347×10^{-4}	7.26
20.0	3.555	2.963×10^{-4}	2.221×10^{-4}	7.47
24.0	3.194	2.662×10^{-4}	2.071×10^{-4}	7.61
28.0	2.874	2.395×10^{-4}	1.942×10^{-4}	7.72
32.0	2.546	2.122×10^{-4}	1.795×10^{-4}	7.80
36.0	2.165	1.804×10^{-4}	1.632×10^{-4}	7.84
40.0	1.775	1.479×10^{-4}	1.482×10^{-4}	7.85
45.0	1.240	1.033×10^{-4}	1.294×10^{-4}	7.84
50.0	0.674	5.617×10^{-5}	1.077×10^{-4}	7.80
55.0	0.192	1.600×10^{-5}	8.857×10^{-5}	7.70
57.0	0.000	0.000	8.366×10^{-5}	7.61
58.0			8.470×10^{-5}	7.56
59.0			8.857×10^{-5}	7.53
60.0			9.554×10^{-5}	7.53
65.0			1.216×10^{-4}	7.51
70.0			1.410×10^{-4}	7.51
80.0			1.735×10^{-4}	7.49
90.0			1.962×10^{-4}	7.47
100.0			2.102×10^{-4}	7.46
110.0			2.197×10^{-4}	7.46
120.0			2.259×10^{-4}	7.45
125.0			2.280×10^{-4}	7.45
130.0			2.298×10^{-4}	7.45

Table B25. Experimental Results of HCO_2^- Photodecomposition in DIW in the Absence of DO ($C_0 = 4.282 \times 10^{-4}$ M, $I_a = 2.60 \times 10^{-6}$ E L^{-1} s^{-1}, T = 25°C).

Time (min)	HCO_2^-		pH
	mg/L as C	M	
0.0	5.138	4.282×10^{-4}	6.47
5.0	4.806	4.005×10^{-4}	8.24
10.0	4.497	3.748×10^{-4}	8.57
15.0	4.156	3.463×10^{-4}	8.75
20.0	3.848	3.207×10^{-4}	8.87
30.0	3.267	2.722×10^{-4}	9.01
40.0	2.685	2.238×10^{-4}	9.11
50.0	2.141	1.784×10^{-4}	9.17
60.0	1.617	1.348×10^{-4}	9.29
80.0	0.578	4.817×10^{-4}	9.36
100.0	0.025	2.083×10^{-4}	9.40
120.0	0.009	7.500×10^{-4}	9.40

Table B26. Experimental Results of HCO_2^- Photodecomposition in DIW (C_0 = 4.145 × 10^{-4} M. I_a = 3.99 × 10^{-6} E L^{-1} s^{-1}, T = 25°C).

Time (min)	HCO_2^-		O_2 (M)	pH
	mg/L as C	M		
0.0	4.974	4.145×10^{-4}	2.634×10^{-4}	5.81
5.0	4.597	3.831×10^{-4}	2.512×10^{-4}	6.91
10.0	4.159	3.466×10^{-4}	2.285×10^{-4}	7.55
15.0	3.660	3.050×10^{-4}		7.93
20.0	3.082	2.568×10^{-4}	1.725×10^{-4}	8.11
27.0	2.094	1.745×10^{-4}	1.255×10^{-4}	8.18
30.0	1.643	1.369×10^{-4}	1.030×10^{-4}	8.16
35.0	0.898	7.483×10^{-5}	6.378×10^{-5}	8.08
40.0	0.117	9.750×10^{-6}	2.453×10^{-5}	7.84
41.0			1.911×10^{-5}	7.72
42.0			1.704×10^{-5}	7.66
43.0			1.911×10^{-5}	7.65
44.0			2.298×10^{-5}	7.64
45.0	0.004	3.333×10^{-7}	2.789×10^{-5}	7.64
55.5	0.000	0.000	7.049×10^{-5}	7.62
65.2	0.000	0.000	9.141×10^{-5}	7.61
75.0	0.000	0.000	1.061×10^{-4}	7.61
90.0	0.000	0.000	1.136×10^{-4}	7.61
106.1	0.000	0.000	1.180×10^{-4}	7.61

Table B27. Experimental Results of HCO_2^- Photodecomposition in DIW in the Absence of DO ($C_0 = 4.051 \times 10^{-4}$ M, $I_a = 3.99 \times 10^{-6}$ E L^{-1} s^{-1}, T = 25°C).

Time (min)	HCO_2^-		pH
	mg/L as C	M	
0.0	4.861	4.051×10^{-4}	7.50
5.1	4.517	3.764×10^{-4}	8.59
10.0	3.928	3.273×10^{-4}	8.86
19.0	3.131	2.609×10^{-4}	9.10
30.0	2.254	1.878×10^{-4}	9.24
39.7	1.476	1.230×10^{-4}	9.31
45.5	1.088	9.067×10^{-5}	9.34
50.0	0.800	6.667×10^{-5}	9.36
55.0	0.474	3.950×10^{-5}	9.37
60.0	0.210	1.750×10^{-5}	9.39
65.0	0.041	3.417×10^{-6}	9.39
70.0	0.009	7.500×10^{-7}	9.39
80.0	0.000	0.000	9.38
90.0	0.000	0.000	9.36
100.0	0.000	0.000	9.35
110.0	0.000	0.000	

Table B28. Observed Rate Constants for HCO_2^- Photodecomposition

$C_0 \times 10^5$ (M)	$NaHCO_3$ Alkalinity (mg L^{-1} as $CaCO_3$)	T (°C)	$I_a \times 10^6$ (E $L^{-1}s^{-1}$)	pH_0	Observed Rate Constants			
					$k_1 \times 10^6$ mol $L^{-1}min^{-1}$	$k_2 \times 10^6$ mol $L^{-1}min^{-1}$	k_1/k_2	Conversion (%) at the rate switch
4.108	-	25	1.383	5.64	2.228	2.994	0.74	23
4.043	-	25	1.383	5.54	1.662	2.615	0.67	19
4.367	-	18	2.599	5.62	3.048	5.181	0.59	17
1.733	-	25	2.599	5.39	3.033	3.843	0.79	26
4.150	-	25	2.599	5.52	3.458	5.564	0.62	21
4.275	-	25	2.599	5.52	3.560	5.746	0.62	26
4.267	-	25	2.599	5.53	2.996	6.328	0.47	20
4.258	-	25	2.599	5.41	3.267	4.772	0.68	19
4.258	-	25	2.599	7.18	4.000	5.153	0.78	20
4.150	-	25	2.599	8.06	4.017	5.264	0.76	21
4.200	-	25	2.599	8.97	3.950	4.786	0.83	21
8.850	-	25	2.599	5.68	4.226	6.361	0.66	15
17.225	-	25	2.599	5.67	4.719	7.763	0.61	19
38.300	-	25	2.599	5.71	3.803	7.914	0.48	16
4.308	-	35	2.599	5.44	4.500	5.823	0.77	21
4.225	-	35	2.559	5.27	3.800	4.958	0.77	18
4.283	-	25	3.991	5.55	4.476	8.524	0.53	21
4.117 (250 rpm)	-	25	3.991	5.51	5.242	7.111	0.74	23
3.983 (50 rpm)	-	25	3.991	5.60	4.600	5.849	0.79	20
4.133	25	25	2.599	7.81	3.433	4.333	0.79	17
4.300	50	25	2.599	7.96	2.800	3.530	0.79	15
4.175	-	25	2.599	5.48	3.762	4.772	0.79	23
4.167 (no oxygen)	-	25	2.599	6.49	6.625	5.912	1.12	54
42.817 (no oxygen)	-	25	2.599	6.47	5.383	4.462	1.21	25
4.308 (aerated)	-	25	2.599	6.48	3.581	4.457	0.80	21
41.450		25	3.991	5.81	7.300	12.356	0.59	26
40.51 (no oxygen)	-	25	3.991	7.50	7.772	5.673	1.37	36

APPENDIX C

TABLES OF EXPERIMENTAL DATA FOR GLYOXALATE

Table C1. Experimental Results of $HC_2O_3^-$ Photodecomposition in DIW (C_0 = 1.942 × 10^{-5} M, I_a = 1.38 x 10^{-6} E L^{-1} s^{-1}, T = 25°C).

Time (min)	$HC_2O_3^-$ (mg/L as C)	$C_2O_4^{2-}$ (mg/L as C)	HCO_2^- (mg/L as C)	NPOC (mg/L as C)	pH
0.0	0.466	0.002	0.019	0.631	4.48
0.5	0.482	0.009	0.028		4.47
1.0	0.457	0.024	0.028	0.692	4.46
2.0	0.418	0.058	0.034		4.45
3.0	0.360	0.096	0.035	0.570	4.43
4.0	0.312	0.138	0.038		4.41
5.0	0.274	0.176	0.039		4.39
6.0	0.231	0.216	0.034	0.535	4.38
7.0	0.198	0.252	0.031		4.37
8.0	0.164	0.286	0.030		4.36
9.0	0.131	0.316	0.019	0.517	4.35
10.0	0.105	0.347	0.017		4.34
12.0	0.058	0.389	0.011		4.34
14.0	0.024	0.407	0.006	0.594	4.34
16.0	0.008	0.408	0.004		4.35
20.0	0.000	0.363	0.005		4.40
25.3	0.000	0.294	0.002	0.364	4.47
30.1	0.000	0.240	0.004		4.53
35.0	0.000	0.192	0.002		4.60
40.0	0.000	0.147	0.001	0.180	4.67
50.2	0.000	0.081	0.002		4.82
60.1	0.000	0.038	0.001		4.95
80.1	0.000	0.002	0.001	0.204	5.10
90.0	0.000	0.000	0.001	0.115	5.12

Table C2. Experimental Results of $HC_2O_3^-$ Photodecomposition in DIW (C_0 = 1.854 × 10^{-5} M, I_a = 2.60 x 10^{-6} E L^{-1} s^{-1}, T = 15°C).

Time (min)	$HC_2O_3^-$ (mg/L as C)	$C_2O_4^{2-}$ (mg/L as C)	HCO_2^- (mg/L as C)	NPOC (mg/L as C)	pH
0.0	0.445	0.002	0.014	0.578	4.54
0.5	0.460	0.009	0.020		4.53
1.0	0.435	0.003	0.023	0.586	4.52
2.0	0.359	0.080	0.030		4.49
3.0	0.289	0.147	0.030	0.545	4.46
4.0	0.220	0.210	0.028		4.43
5.0	0.158	0.273	0.021		4.41
6.0	0.104	0.328	0.014	0.542	4.39
7.0	0.064	0.368	0.009		4.39
8.0	0.031	0.394	0.005		4.38
9.0	0.011	0.399	0.002	0.463	4.39
10.0	0.003	0.391	0.002		4.40
12.0	0.000	0.353	0.002		4.43
14.0	0.000	0.310	0.001	0.387	4.47
16.5	0.000	0.266	0.001		4.52
20.4	0.000	0.210	0.001		4.59
25.0	0.000	0.151	0.001	0.215	4.68
30.1	0.000	0.104	0.002		4.78
35.7	0.000	0.067	0.002		4.88
43.5	0.000	0.029	0.001	0.104	5.00
50.0	0.000	0.014	0.002		5.07
60.0	0.000	0.003	0.001	0.070	5.14
70.0	0.000	0.001	0.002	0.109	5.16

Table C3. Experimental Results of $HC_2O_3^-$ Photodecomposition in DIW at Initial pH Adjusted to 6.86 with Concentrated NaOH ($C_0 = 1.883 \times 10^{-5}$ M, $I_a = 2.60 \times 10^{-6}$ E L^{-1} s^{-1}, T = 25°C).

Time (min)	$HC_2O_3^-$ (mg/L as C)	$C_2O_4^{2-}$ (mg/L as C)	HCO_2^- (mg/L as C)	NPOC (mg/L as C)	pH
0.0	0.452	0.003	0.018	0.559	6.86
0.5	0.446	0.017	0.027		6.70
1.0	0.408	0.041	0.030	0.541	6.53
2.0	0.334	0.097	0.035		6.19
3.0	0.263	0.164	0.034	0.520	5.94
4.0	0.200	0.223	0.029		5.74
5.0	0.149	0.279	0.022		5.57
6.0	0.098	0.334	0.014	0.515	5.44
7.0	0.059	0.373	0.009		5.35
8.0	0.029	0.400	0.005		5.29
9.0	0.011	0.411	0.002	0.495	5.28
10.0	0.003	0.409	0.002		5.32
12.0	0.000	0.387	0.001		5.42
14.0	0.000	0.361	0.001	0.418	5.53
16.0	0.000	0.339	0.001		5.60
20.0	0.000	0.295	0.001		5.73
25.0	0.000	0.245	0.001	0.277	5.84
30.0	0.000	0.204	0.002		5.91
35.0	0.000	0.167	0.002		5.99
40.0	0.000	0.135	0.000	0.172	6.04
50.1	0.000	0.091	0.002		6.11
60.0	0.000	0.058	0.001	0.156	6.17

Table C4. Experimental Results of $HC_2O_3^-$ Photodecomposition in DIW at Initial pH Adjusted to 8.22 with Concentrated NaOH ($C_0 = 2.121 \times 10^{-5}$ M, $I_a = 2.60 \times 10^{-6}$ E L^{-1} s^{-1}, T = 25°C).

Time (min)	$HC_2O_3^-$ (mg/L as C)	$C_2O_4^{2-}$ (mg/L as C)	HCO_2^- (mg/L as C)	NPOC (mg/L as C)	pH
0.0	0.509	0.003	0.005	0.521	8.22
0.5	0.482	0.015	0.010		8.08
1.0	0.447	0.036	0.016	0.542	7.95
2.0	0.372	0.086	0.025		7.30
3.0	0.288	0.147	0.031	0.524	6.51
4.0	0.227	0.207	0.030		6.13
5.0	0.169	0.264	0.026		5.86
6.0	0.120	0.319	0.017	0.447	5.67
7.0	0.079	0.362	0.012		5.55
8.0	0.048	0.393	0.007		5.46
9.0	0.022	0.410	0.003	0.433	5.41
10.0	0.009	0.417	0.002		5.43
12.0	0.000	0.397	0.002		5.54
14.0	0.000	0.369	0.000	0.357	5.64
16.0	0.000	0.343	0.001		5.73
20.0	0.000	0.293	0.001		5.86
25.1	0.000	0.234	0.001	0.263	5.95
30.8	0.000	0.188	0.001		6.04
35.1	0.000	0.150	0.001		6.09
40.1	0.000	0.118	0.001	0.164	6.13
50.0	0.000	0.073	0.002		6.18
60.1	0.000	0.042	0.000	0.085	6.22

Table C5. Experimental Results of $HC_2O_3^-$ Photodecomposition in DIW at Initial pH Adjusted to 9.10 with Concentrated NaOH ($C_0 = 1.942 \times 10^{-5}$ M, $I_a = 2.60 \times 10^{-6}$ E L^{-1} s^{-1}, T = 25°C).

Time (min)	$HC_2O_3^-$ (mg/L as C)	$C_2O_4^{2-}$ (mg/L as C)	HCO_2^- (mg/L as C)	NPOC (mg/L as C)	pH
0.0	0.466	0.002	0.028	0.529	9.10
0.5	0.436	0.014	0.032		9.07
1.0	0.397	0.035	0.038	0.506	9.05
2.0	0.325	0.081	0.047		9.00
3.0	0.258	0.132	0.053	0.490	8.95
4.0	0.203	0.179	0.050		8.87
5.0	0.155	0.226	0.046		8.79
6.0	0.104	0.273	0.045	0.467	8.71
7.0	0.082	0.313	0.031		8.60
8.0	0.056	0.346	0.022		8.48
9.0	0.029	0.376	0.017	0.447	8.34
10.0	0.020	0.394	0.009		8.18
12.0	0.005	0.407	0.003		7.87
14.0	0.000	0.396	0.001	0.383	7.69
16.0	0.000	0.381	0.001		7.57
20.0	0.000	0.345	0.001		7.40
25.0	0.000	0.300	0.000	0.336	7.27
30.0	0.000	0.261	0.001		7.18
35.0	0.000	0.228	0.000		7.11
40.0	0.000	0.193	0.000	0.215	7.05
50.1	0.000	0.143	0.001		6.96
60.0	0.000	0.103	0.000	0.144	6.88

Table C6. Experimental Results of $HC_2O_3^-$ Photodecomposition in DIW at Initial pH Adjusted to 9.10 with Concentrated NaOH ($C_0 = 1.908 \times 10^{-5}$ M, $I_a = 2.60 \times 10^{-6}$ E L^{-1} s^{-1}, T = 25°C).

Time (min)	$HC_2O_3^-$ (mg/L as C)	$C_2O_4^{2-}$ (mg/L as C)	HCO_2^- (mg/L as C)	pH
0.0	0.458	0.005	0.015	9.10
0.5	0.426	0.014	0.020	9.04
1.0	0.406	0.028	0.026	9.00
1.5	0.375	0.045	0.032	8.97
2.0	0.336	0.064	0.039	8.93
2.0	0.305	0.085	0.047	8.89
3.0	0.272	0.105	0.053	8.85
3.5	0.243	0.124	0.058	8.82
4.0	0.209	0.144	0.063	8.76
5.0	0.158	0.181	0.067	8.64
6.0	0.114	0.222	0.070	8.50
7.0	0.083	0.256	0.060	8.28
8.0	0.064	0.288	0.050	7.97
9.0	0.047	0.318	0.036	7.40
10.0	0.033	0.346	0.024	6.93
11.0	0.019	0.368	0.014	6.68
12.0	0.009	0.378	0.008	6.53
13.0	0.004	0.383	0.004	6.47
14.0	0.000	0.380	0.002	6.45
16.0	0.000	0.365	0.001	6.44
20.0	0.000	0.332	0.002	6.46
25.0	0.000	0.285	0.001	6.50
30.0	0.000	0.245	0.001	6.51
35.0	0.000	0.209	0.001	6.56
40.6	0.000	0.171	0.000	6.56
50.2	0.000	0.122	0.000	6.59
60.0	0.000	0.083	0.000	6.59
70.0	0.000	0.054	0.000	6.59
80.3	0.000	0.035	0.000	6.59
100.0	0.000	0.016	0.000	6.59

Table C7. Experimental Results of $HC_2O_3^-$ Photodecomposition in DIW Containing $NaHCO_3$ = 25 mg/L as $CaCO_3$ ($C_0 = 1.988 \times 10^{-5}$ M, $I_a = 2.60 \times 10^{-6}$ E L^{-1} s^{-1}, T = 25 °C).

Time (min)	$HC_2O_3^-$ (mg/L as C)	$C_2O_4^{2-}$ (mg/L as C)	HCO_2^- (mg/L as C)	NPOC (mg/L as C)	pH
0.0	0.477	0.005	0.004	0.550	7.33
0.5	0.475	0.011	0.007		7.31
1.0	0.447	0.030	0.011	0.538	7.31
2.0	0.389	0.066	0.019		7.28
3.0	0.328	0.108	0.026	0.519	7.26
4.0	0.271	0.148	0.033		7.24
5.0	0.224	0.187	0.034		7.21
6.0	0.177	0.223	0.035	0.482	7.20
7.0	0.139	0.255	0.036		7.18
8.0	0.108	0.286	0.032		7.16
9.0	0.080	0.313	0.028	0.468	7.15
10.0	0.059	0.333	0.025		7.14
12.0	0.031	0.365	0.017		7.13
14.0	0.015	0.383	0.009	0.426	7.12
16.0	0.007	0.387	0.005		7.12
20.9	0.002	0.374	0.002		7.13
25.0	0.000	0.350	0.001	0.404	7.15
30.0	0.000	0.323	0.002		7.16
35.0	0.000	0.298	0.001		7.18
40.0	0.000	0.273	0.001	0.307	7.21
51.2	0.000	0.226	0.001		7.23
60.4	0.000	0.192	0.001	0.266	7.29
80.0	0.000	0.136	0.001	0.183	7.31

Table C8. Experimental Results of $HC_2O_3^-$ Photodecomposition in DIW (C_0 = 1.725 × 10^{-5} M, I_a = 2.60 x 10^{-6} E L^{-1} s^{-1}, T = 25°C).

Time (min)	$HC_2O_3^-$ (mg/L as C)	$C_2O_4^{2-}$ (mg/L as C)	HCO_2^- (mg/L as C)	NPOC (mg/L as C)	pH
0.0	0.414	0.002	0.027	0.556	4.66
1.0	0.375	0.045		0.550	4.65
2.0	0.289	0.114	0.045		4.61
3.0	0.209	0.190	0.041	0.533	4.57
4.0	0.151	0.249	0.033		4.55
5.0	0.099	0.304	0.022		4.53
6.0	0.054	0.350	0.011	0.487	4.52
7.0	0.026	0.369	0.005		4.51
8.0	0.009	0.374	0.002		4.53
9.0	0.002	0.360	0.001	0.427	4.55
10.0	0.000	0.342	0.001		4.56
12.0	0.000	0.303	0.002		4.61
14.0	0.000	0.260	0.001	0.339	4.66
16.0	0.000	0.227	0.001		4.72
18.0	0.000	0.194	0.001		4.77
20.0	0.000	0.165	0.001	0.266	4.81
25.0	0.000	0.110	0.001		4.94
30.0	0.000	0.070	0.001		5.05
35.0	0.000	0.039	0.001	0.182	5.15
40.0	0.000	0.021	0.001		5.22
45.0	0.000	0.008	0.001	0.176	5.27
50.0	0.000	0.003	0.001		5.31
60.0	0.000	0.000	0.001	0.161	5.32
90.0	0.000	0.000	0.001	0.195	5.32

Table C9. Experimental Results of $HC_2O_3^-$ Photodecomposition in DIW (C_0 = 1.875 × 10^{-5} M, I_a = 2.60 x 10^{-6} E L^{-1} s^{-1}, T = 25°C).

Time (min)	$HC_2O_3^-$ (mg/L as C)	$C_2O_4^{2-}$ (mg/L as C)	HCO_2^- (mg/L as C)	NPOC (mg/L as C)	pH
0.0	0.450	0.004	0.019	0.620	4.55
0.5	0.446	0.022	0.029		4.55
1.0	0.395	0.053	0.031	0.570	4.52
2.0	0.306	0.122	0.039		4.49
3.0	0.227	0.192	0.033	0.602	4.46
4.0	0.165	0.255	0.026		4.44
5.0	0.113	0.307	0.017		4.43
6.0	0.063	0.353	0.008	0.473	4.42
7.0	0.030	0.374	0.005		4.42
8.0	0.018	0.377	0.005		4.42
9.0	0.003	0.364	0.004	0.533	4.44
10.0	0.000	0.340	0.005		4.47
12.0	0.000	0.295	0.002		4.51
14.0	0.000	0.252	0.000	0.295	4.57
16.0	0.000	0.212	0.003		4.62
20.0	0.000	0.146	0.003		4.74
25.0	0.000	0.078	0.002	0.156	4.89
30.1	0.000	0.040	0.003		5.03
36.2	0.000	0.010	0.005		5.13
40.3	0.000	0.001	0.001	0.148	5.18
50.1	0.000	0.000	0.002		5.19
60.1	0.000	0.000	0.000	0.135	5.21

Table C10. Experimental Results of $HC_2O_3^-$ Photodecomposition in DIW (C_0 = 1.996 × 10^{-5} M, I_a = 2.60 x 10^{-6} E L^{-1} s^{-1}, T = 25°C).

Time (min)	$HC_2O_3^-$ (mg/L as C)	$C_2O_4^{2-}$ (mg/L as C)	HCO_2^- (mg/L as C)	pH
0.0	0.479	0.002	0.007	4.53
0.5	0.417	0.022	0.013	4.50
1.0	0.376	0.050	0.020	4.48
1.5	0.337	0.081	0.025	4.47
2.0	0.300	0.113	0.029	4.45
2.5	0.261	0.146	0.031	4.43
3.0	0.227	0.177	0.031	4.42
3.5	0.194	0.208	0.030	4.41
4.0	0.165	0.237	0.027	4.40
4.5	0.139	0.264	0.023	4.39
5.0	0.117	0.288	0.021	4.38
6.1	0.070	0.330	0.011	4.37
7.0	0.039	0.354	0.006	4.36
8.0	0.017	0.360	0.003	4.37
9.0	0.006	0.355	0.001	4.39
10.0	0.002	0.336	0.001	4.41
11.0	0.000	0.311	0.000	4.44
12.0	0.000	0.285	0.000	4.47
14.0	0.000	0.240	0.000	4.53
16.0	0.000	0.193	0.000	4.61
20.0	0.000	0.115	0.000	4.75
25.0	0.000	0.038	0.000	4.96
30.7	0.000	0.006	0.000	5.07
35.0	0.000	0.000	0.000	5.11

Table C11. Experimental Results of $HC_2O_3^-$ Photodecomposition in DIW (C_0 = 4.129 × 10^{-5} M, I_a = 2.60 x 10^{-6} E L^{-1} s^{-1}, T = 25°C).

Time (min)	$HC_2O_3^-$ (mg/L as C)	$C_2O_4^{2-}$ (mg/L as C)	HCO_2^- (mg/L as C)	NPOC (mg/L as C)	pH
0.0	0.991	0.004	0.026	1.096	4.21
1.0	0.927	0.050	0.049		4.19
2.0	0.799	0.126	0.072		4.18
3.1	0.662	0.210	0.087	1.024	4.16
4.0	0.551	0.284	0.099		4.15
5.0	0.457	0.365	0.102		4.14
6.0	0.369	0.444	0.097	0.966	4.12
7.0	0.292	0.519	0.089		4.11
8.0	0.236	0.585	0.077		4.10
9.0	0.185	0.647	0.058	0.901	4.10
10.0	0.141	0.703	0.044		4.09
12.0	0.067	0.776	0.018		4.09
14.1	0.019	0.791	0.005	0.790	4.10
16.4	0.003	0.732	0.002		4.13
20.0	0.000	0.610	0.001		4.20
25.0	0.000	0.452	0.001	0.466	4.29
30.0	0.000	0.335	0.003		4.40
35.6	0.000	0.228	0.004		4.51
41.7	0.000	0.140	0.001	0.229	4.63
50.0	0.000	0.068	0.003		4.78
60.0	0.000	0.020	0.002		4.91
81.5	0.000	0.002	0.001	0.097	5.04
100.8	0.000	0.000	0.002	0.128	5.08

Table C12. Experimental Results of $HC_2O_3^-$ Photodecomposition in DIW (C_0 = 8.492 × 10^{-5} M, I_a = 2.60 x 10^{-6} E L^{-1} s^{-1}, T = 25°C).

Time (min)	$HC_2O_3^-$ (mg/L as C)	$C_2O_4^{2-}$ (mg/L as C)	HCO_2^- (mg/L as C)	NPOC (mg/L as C)	pH
0.0	2.038	0.003	0.027	1.962	4.00
1.0	1.989	0.045	0.056		4.00
2.0	1.841	0.119	0.090		3.99
3.0	1.653	0.194	0.120	2.016	3.98
4.0	1.502	0.271	0.151		3.97
6.0	1.201	0.432	0.198		3.95
8.0	0.897	0.598	0.238	2.108	3.94
10.0	0.661	0.757	0.252		3.93
15.0	0.291	1.126	0.189		3.90
20.3	0.104	1.425	0.062	1.670	3.90
25.0	0.017	1.407	0.009		3.94
30.0	0.000	1.161	0.004		4.01
40.0	0.000	0.690	0.001	0.788	4.19
50.0	0.000	0.382	0.004		4.38
60.0	0.000	0.184	0.001		4.59
70.0	0.000	0.069	0.000	0.130	4.78
80.2	0.000	0.016	0.000		4.91
100.0	0.000	0.000	0.001		5.01
120.3	0.000	0.000	0.001	0.080	5.05
140.2	0.000	0.000	0.001	0.082	5.10

Table C13. Experimental Results of $HC_2O_3^-$ Photodecomposition in DIW (C_0 = 1.858 × 10^{-5} M, I_a = 2.60 x 10^{-6} E L^{-1} s^{-1}, T = 35°C).

Time (min)	$HC_2O_3^-$ (mg/L as C)	$C_2O_4^{2-}$ (mg/L as C)	HCO_2^- (mg/L as C)	NPOC (mg/L as C)	pH
0.0	0.446	0.003	0.017	0.556	4.50
0.5	0.429	0.029	0.027		4.49
1.0	0.373	0.065	0.031	0.552	4.47
2.0	0.291	0.133	0.034		4.45
3.0	0.211	0.203	0.030	0.520	4.41
4.0	0.145	0.266	0.027		4.39
5.0	0.097	0.316	0.014		4.38
6.0	0.056	0.354	0.008	0.445	4.36
7.0	0.026	0.373	0.005		4.37
8.0	0.010	0.374	0.005		4.38
9.0	0.003	0.360	0.001	0.409	4.40
10.0	0.000	0.340	0.002		4.43
12.0	0.000	0.296	0.002		4.48
14.0	0.000	0.256	0.001	0.362	4.54
16.0	0.000	0.222	0.002		4.58
20.0	0.000	0.163	0.002		4.69
25.1	0.000	0.098	0.001	0.140	4.81
30.0	0.000	0.061	0.002		4.93
35.9	0.000	0.029	0.001		5.05
40.0	0.000	0.015	0.001	0.077	5.10
50.0	0.000	0.002	0.002		5.18
60.1	0.000	0.000	0.001	0.056	5.21

Table C14. Experimental Results of $HC_2O_3^-$ Photodecomposition in DIW (C_0 = 1.878 × 10^{-5} M, I_a = 3.99 x 10^{-6} E L^{-1} s^{-1}, T = 25°C).

Time (min)	$HC_2O_3^-$ (mg/L as C)	$C_2O_4^{2-}$ (mg/L as C)	HCO_2^- (mg/L as C)	NPOC (mg/L as C)	pH
0.0	0.450	0.002	0.021	0.566	4.51
0.5	0.413	0.025	0.027		4.51
1.0	0.359	0.067	0.033		4.48
1.5	0.294	0.119	0.034	0.570	4.46
2.0	0.241	0.167	0.034		4.43
2.5	0.195	0.213	0.029		4.42
3.0	0.148	0.252	0.022	0.551	4.40
4.0	0.078	0.334	0.013		4.38
5.0	0.027	0.377	0.005		4.38
6.0	0.005	0.372	0.001	0.443	4.39
7.0	0.000	0.347	0.003		4.42
8.0	0.000	0.315	0.003		4.46
9.0	0.000	0.279	0.001	0.426	4.49
10.0	0.000	0.257	0.001		4.53
12.0	0.000	0.207	0.004		4.60
14.0	0.000	0.154	0.001	0.258	4.68
16.0	0.000	0.123	0.003		4.75
20.3	0.000	0.067	0.002		4.90
25.0	0.000	0.028	0.001	0.091	5.03
30.2	0.000	0.008	0.002		5.12
35.3	0.000	0.000	0.003		5.16
40.0	0.000	0.000	0.001	0.152	5.17

Table C15. Experimental Results of $HC_2O_3^-$ Photodecomposition in DIW (C_0 = 1.858 × 10^{-5} M, I_a = 5.27 x 10^{-6} E L^{-1} s^{-1}, T = 25°C).

Time (min)	$HC_2O_3^-$ (mg/L as C)	$C_2O_4^{2-}$ (mg/L as C)	HCO_2^- (mg/L as C)	NPOC (mg/L as C)	pH
0.0	0.446	0.002	0.018	0.582	4.50
0.5	0.416	0.034	0.030		4.46
1.0	0.340	0.092	0.036		4.43
1.5	0.257	0.164	0.037	0.580	4.40
2.0	0.194	0.226	0.033		4.38
2.5	0.139	0.286	0.026		4.36
3.0	0.087	0.341	0.014	0.573	4.34
3.5	0.050	0.379	0.008		4.34
4.0	0.023	0.397	0.004		4.34
4.5	0.008	0.392	0.001	0.434	4.35
5.0	0.002	0.380	0.001		4.36
5.5	0.000	0.358	0.001		4.38
6.0	0.000	0.334	0.001	0.408	4.40
7.0	0.000	0.294	0.001		4.45
8.0	0.000	0.256	0.003		4.48
9.0	0.000	0.217	0.001	0.278	4.53
10.0	0.000	0.189	0.002		4.57
12.0	0.000	0.140	0.002		4.66
14.1	0.000	0.094	0.001	0.170	4.75
20.0	0.000	0.034	0.003		4.94
25.1	0.000	0.007	0.002		5.03
30.1	0.000	0.000	0.001	0.059	5.07
35.0	0.000	0.000	0.001	0.097	5.08

Table C16. Experimental Results of $HC_2O_3^-$ Photodecomposition in DIW (C_0=2.051×10^{-4} M, I_a = 2.60 × 10^{-6} E L^{-1}s^{-1}, T = 25°C).

Time (min)	$HC_2O_3^-$ (mg/L as C)	$C_2O_4^{2-}$ (mg/L as C)	HCO_2^- (mg/L as C)	NPOC (mg/L as C)	TC (mg/L as C)	O_2 (M)	pH
0.0	4.923	0.001	0.001	4.844	5.060	2.858 ×10^{-4}	6.01
5.0	4.287	0.290	0.122			2.685 ×10^{-4}	5.23
10.0	3.475	0.595	0.298	4.657	4.913	2.497 ×10^{-4}	4.93
15.0	2.729	0.906	0.478			2.298 ×10^{-4}	4.78
20.0	1.875	1.248	0.648	4.513	4.723	2.141 ×10^{-4}	4.68
30.0	0.684	1.889	0.745			1.795 ×10^{-4}	4.56
40.0	0.276	2.575	0.383	3.823	4.454	1.477 ×10^{-4}	4.50
50.1	0.087	2.994	0.064			1.268 ×10^{-4}	4.52
60.0	0.001	2.718	0.001	2.980	3.758	1.340 ×10^{-4}	4.87
80.0	0.000	1.816	0.000			1.751 ×10^{-4}	5.84
100.3	0.000	1.123	0.000	1.281	3.193	2.035 ×10^{-4}	6.18
120.0	0.000	0.704	0.000			2.216 ×10^{-4}	6.37
150.0	0.000	0.293	0.000	0.386	2.806	2.373 ×10^{-4}	6.57
180.0	0.000	0.109	0.000	0.189	2.615	2.453 ×10^{-4}	6.72
210.3	0.000	0.037	0.000	0.097	2.585	2.492 ×10^{-4}	6.83
240.0	0.000	0.013	0.000			2.512 ×10^{-4}	6.93
270.0	0.000	0.004	0.000	0.031	2.527	2.523 ×10^{-4}	7.03

Table C17. Observed Rate Constants for $HC_2O_3^-$ Photodecomposition

$C_0 \times 10^5$ (M)	NaHCO3 Alk. (mg L^{-1} as $CaCO_3$)	T (°C)	$I_a \times 10^6$ ($E\,L^{-1}s^{-1}$)	pH				$[C_2O_4^{2-}]_{max}$		$[HCO_2^-]_{max}$		Observed Rate Constants				
				pH_0	t_{pHmin} (min)	pH_{min}	pH_f	t (min)	$Cx10^5$ (M)	t (min)	$Cx10^6$ (M)	$k_1 * 10^6$ ($Mmin^{-1}$)	$k_2 * 10^6$ ($Mmin^{-1}$)	k_1/k_2	Rate switch	
															t(min)	% conv.
1.942	-	25	1.38	4.48	*12*	4.34	5.12	*16*	1.70	5	3.25	1.918	1.296	1.13	6	50
1.854	-	15	2.60	4.54	*8*	4.38	5.16	*9*	1.66	2-3	2.50	2.908	1.958	1.49	5	51
1.883	-	25	2.60	6.86	*9*	5.29	6.26	*9*	1.71	2	2.92	2.943	1.663	1.57	4	56
2.121	-	25	2.60	8.22	*9*	5.41	6.29	*10*	1.74	3	2.58	3.034	1.367	1.78	4	55
1.942	-	25	2.60	9.10	-	-	6.69	*12*	1.70	3	4.42	2.796	1.046	2.67	4	56
1.908	-	25	2.60	9.10	*16*	6.44	6.59	*13*	1.60	6	5.83	2.615	0.663	3.94	5	54
1.988	25	25	2.60	7.33	*16*	7.12	7.31	*16*	1.61	7	3.00	2.371	1.342	1.77	5	53
1.725	-	25	2.60	4.66	*7*	4.51	5.32	*8*	1.56	2	3.75	3.458	2.021	1.71	3	64
1.875	-	25	2.60	4.55	*7*	4.42	5.19	*8*	1.57	2	3.25	3.584	2.107	1.70	3	50
1.871	-	25	2.60	4.53	*7*	4.36	5.11	*8*	1.50	2.5	2.58	3.092	1.914	1.62	3.5	57
4.129	-	25	2.60	4.21	*12*	4.09	5.08	*14*	3.30	5	8.50	4.679	2.1	2.23	5	54
8.492	-	25	2.60	4.00	*20*	3.90	5.01	*20*	5.94	10	21.0	6.516	2.277	2.86	8	56
20.513	-	25	2.60	6.01	*40*	4.50	7.03	*50*	12.48	30	62.08	6.378	1.238	5.15	20	62
1.858	-	35	2.60	4.50	*6*	4.36	5.21	*8*	1.56	2	2.83	3.588	1.854	1.94	3	53
1.875	-	25	3.99	4.51	*5*	4.38	5.16	*5*	1.57	2	2.83	4.617	2.917	1.58	2.5	57
1.858	-	25	5.27	4.50	*3.5*	4.34	5.07	*4*	1.65	1.5	3.08	6.224	3.708	1.68	2	57
20.55 (absence of O_2)	-	25	2.60	7.97	*15*	5.16	-	*40*	6.32	20	0.33	7.55	2.72	2.78	15	55

APPENDIX D

TABLES OF EXPERIMENTAL DATA FOR GLYCOLATE

Table D1. Experimental Results of $H_3C_2O_3^-$ Photodecomposition in DIW (C_0 = 2.121 × 10^{-5} M, I_a = 1.38 × 10^{-6} E L^{-1} s^{-1}, T = 25°C).

Time (min)	$H_3C_2O_3^-$ (mg/L as C)	$HC_2O_3^-$ (mg/L as C)	$C_2O_4^{2-}$ (mg/L as C)	HCO_2^- (mg/L as C)
0.0	0.509	0.000	0.002	0.003
2.7	0.421	0.061	0.007	0.010
5.2	0.323	0.096	0.026	0.025
7.5	0.242	0.104	0.059	0.037
10.0	0.166	0.097	0.108	0.044
15.4	0.053	0.056	0.225	0.031
20.7	0.009	0.013	0.289	0.010
25.0	0.003	0.000	0.268	0.004
30.0	0.002	0.000	0.218	0.003
35.0	0.000	0.000	0.168	0.002
40.0	0.000	0.000	0.127	0.002
45.3	0.000	0.000	0.088	0.002
50.0	0.000	0.000	0.061	0.002
55.0	0.000	0.000	0.038	0.002
60.0	0.000	0.000	0.021	0.002
65.1	0.000	0.000	0.009	0.001
70.0	0.000	0.000	0.002	0.001
75.0	0.000	0.000	0.000	0.001

Table D2. Experimental Results of $H_3C_2O_3^-$ Photodecomposition in DIW (C_0 = 2.175 × 10^{-5} M, I_a = 1.38 × 10^{-6} E L^{-1} s^{-1}, T = 25°C).

Time (min)	$H_3C_2O_3^-$ (mg/L as C)	$HC_2O_3^-$ (mg/L as C)	$C_2O_4^{2-}$ (mg/L as C)	HCO_2^- (mg/L as C)	pH
0.0	0.522	0.000	0.000	0.000	4.57
0.5	0.534	0.008	0.000	0.000	4.57
1.0	0.519	0.022	0.000	0.000	4.57
1.5	0.508	0.036	0.001	0.000	4.56
2.0	0.495	0.051	0.003	0.000	4.56
2.5	0.473	0.065	0.004	0.000	4.56
3.0	0.460	0.077	0.006	0.000	4.56
3.5	0.443	0.089	0.008	0.004	4.56
4.0	0.421	0.100	0.011	0.005	4.55
5.0	0.386	0.117	0.017	0.008	4.55
6.0	0.356	0.130	0.027	0.013	4.54
7.0	0.319	0.140	0.039	0.019	4.54
8.0	0.288	0.143	0.051	0.022	4.53
9.1	0.255	0.146	0.066	0.027	4.52
10.0	0.229	0.146	0.082	0.034	4.52
11.0	0.201	0.144	0.101	0.034	4.51
12.0	0.174	0.139	0.120	0.035	4.50
13.1	0.154	0.131	0.140	0.042	4.49
14.0	0.125	0.126	0.161	0.037	4.48
15.0	0.108	0.116	0.183	0.038	4.48
16.0	0.086	0.107	0.205	0.033	4.47
17.0	0.070	0.097	0.227	0.032	4.46
18.0	0.062	0.085	0.247	0.033	4.46
19.0	0.048	0.072	0.269	0.028	4.45
20.0	0.033	0.060	0.286	0.020	4.45
21.0	0.027	0.049	0.301	0.017	4.45
22.0	0.024	0.038	0.313	0.016	4.45
23.0	0.011	0.027	0.322	0.008	4.44
24.1	0.006	0.017	0.329	0.008	4.45
25.0	0.003	0.011	0.326	0.007	4.46
27.0	0.000	0.004	0.315	0.004	4.48
30.0	0.000	0.000	0.283	0.002	4.51
35.2	0.000	0.000	0.227	0.002	4.59
40.0	0.000	0.000	0.174	0.002	4.66
50.4	0.000	0.000	0.088	0.002	4.85
60.1	0.000	0.000	0.032	0.001	5.00
70.0	0.000	0.000	0.007	0.001	5.11

Table D3. Experimental Results of $H_3C_2O_3^-$ Photodecomposition in DIW (C_0 = 2.129 × 10^{-5} M, I_a = 2.60 × 10^{-6} E L^{-1} s^{-1}, T = 15°C).

Time (min)	$H_3C_2O_3^-$ (mg/L as C)	$HC_2O_3^-$ (mg/L as C)	$C_2O_4^{2-}$ (mg/L as C)	HCO_2^- (mg/L as C)	NPOC (mg/L as C)	pH
0.0	0.511	0.000	0.002	0.000	0.523	4.67
2.5	0.412	0.085	0.010	0.010	0.527	4.66
4.9	0.280	0.125	0.050	0.031		4.64
7.5	0.150	0.118	0.135	0.043	0.474	4.60
10.0	0.068	0.084	0.230	0.037		4.57
15.0	0.010	0.011	0.333	0.006		4.54
20.0	0.004	0.000	0.269	0.001	0.359	4.63
25.0	0.003	0.000	0.200	0.002		4.73
30.0	0.004	0.000	0.143	0.002		4.83
35.0	0.003	0.000	0.095	0.001	0.280	4.93
40.0	0.004	0.000	0.062	0.002		5.03
45.1	0.004	0.000	0.035	0.001		5.11
50.3	0.003	0.000	0.017	0.001	0.246	5.18
55.0	0.002	0.000	0.007	0.001		5.22
59.9	0.003	0.000	0.000	0.001		5.26
65.0	0.003	0.000	0.000	0.001	0.261	5.26
70.0	0.002	0.000	0.000	0.001		5.27
75.1	0.003	0.000	0.000	0.002		5.27
80.0	0.002	0.000	0.000	0.002	0.243	5.27
85.3	0.003	0.000	0.000	0.001		5.28
90.0	0.002	0.000	0.000	0.001	0.221	5.28

Table D4. Experimental Results of $H_3C_2O_3^{\cdot}$ Photodecomposition in DIW (C_0 = 2.242 × 10^{-5} M, I_a = 2.60 × 10^{-6} E L^{-1} s^{-1}, T = 17°C).

Time (min)	$H_3C_2O_3^{\cdot}$ (mg/L as C)	$HC_2O_3^{-}$ (mg/L as C)	$C_2O_4^{2-}$ (mg/L as C)	HCO_2^{-} (mg/L as C)	pH
0.0	0.538	0.000	0.000	0.000	4.57
0.5	0.537	0.013	0.000	0.000	4.56
1.0	0.515	0.033	0.000	0.000	4.56
1.5	0.489	0.055	0.003	0.000	4.55
2.0	0.460	0.077	0.006	0.000	4.55
2.5	0.429	0.097	0.010	0.005	4.54
3.0	0.396	0.111	0.016	0.010	4.54
3.6	0.364	0.124	0.025	0.014	4.53
4.0	0.338	0.133	0.034	0.017	4.53
4.5	0.308	0.140	0.044	0.021	4.52
5.0	0.277	0.143	0.057	0.024	4.52
5.5	0.249	0.143	0.071	0.029	4.51
5.9	0.226	0.143	0.084	0.031	4.51
7.0	0.176	0.135	0.121	0.038	4.49
8.0	0.128	0.123	0.160	0.036	4.48
9.0	0.091	0.107	0.201	0.034	4.47
10.0	0.069	0.086	0.241	0.030	4.45
11.0	0.034	0.063	0.280	0.020	4.45
12.0	0.020	0.041	0.311	0.013	4.44
13.0	0.016	0.022	0.327	0.016	4.44
14.0	0.008	0.009	0.331	0.004	4.45
15.0	0.000	0.002	0.319	0.006	4.46
16.0	0.000	0.000	0.303	0.002	4.48
17.0	0.000	0.000	0.280	0.002	4.51
18.0	0.000	0.000	0.262	0.002	4.53
19.0	0.000	0.000	0.243	0.003	4.55
20.0	0.000	0.000	0.226	0.006	4.57
22.0	0.000	0.000	0.191	0.002	4.62
24.0	0.000	0.000	0.158	0.001	4.68
26.0	0.000	0.000	0.128	0.003	4.73
28.0	0.000	0.000	0.103	0.001	4.78
30.0	0.000	0.000	0.078	0.004	4.84
35.0	0.000	0.000	0.036	0.002	4.96
40.0	0.000	0.000	0.010	0.003	5.06
45.0	0.000	0.000	0.000	0.004	5.10
50.0	0.000	0.000	0.000	0.002	5.11

Table D5. Experimental Results of $H_3C_2O_3^-$ Photodecomposition in DIW (C_0 = 2.121 × 10^{-5} M, I_a = 2.60 × 10^{-6} E L^{-1} s^{-1}, T = 25°C).

Time (min)	$H_3C_2O_3^-$ (mg/L as C)	$HC_2O_3^-$ (mg/L as C)	$C_2O_4^{2-}$ (mg/L as C)	HCO_2^- (mg/L as C)	NPOC (mg/L as C)	pH
0.0	0.509	0.000	0.000	0.000		4.63
1.4	0.420	0.050	0.007	0.003	0.680	4.65
2.7	0.337	0.104	0.022	0.017	0.634	4.61
5.0	0.192	0.116	0.089	0.040	0.636	4.58
7.5	0.076	0.085	0.192	0.035	0.601	4.56
10.0	0.015	0.036	0.282	0.015	0.515	4.63
15.0	0.000	0.000	0.259	0.001	0.482	4.73
19.1	0.000	0.000	0.191	0.002	0.465	4.87
25.0	0.000	0.000	0.111	0.001	0.447	5.03
30.0	0.000	0.000	0.063	0.001	0.378	5.14
35.0	0.000	0.000	0.030	0.001	0.376	5.20
40.0	0.000	0.000	0.011	0.001	0.306	5.25
45.0	0.000	0.000	0.001	0.001	0.289	5.27
50.0	0.000	0.000	0.000	0.001	0.359	5.27
55.0	0.000	0.000	0.000	0.001	0.360	5.27
60.0	0.000	0.000	0.000	0.001	0.400	5.27
65.0	0.000	0.000	0.000	0.001	0.388	5.28
70.3	0.000	0.000	0.000	0.002	0.266	5.28
75.0	0.000	0.000	0.000	0.001	0.216	5.28
80.2	0.000	0.000	0.000	0.001	0.337	5.28

Table D6. Experimental Results of $H_3C_2O_3^-$ Photodecomposition in DIW (C_0 = 2.371 × 10^{-5} M, I_a = 2.60 × 10^{-6} E L^{-1} s^{-1}, T = 25°C).

Time (min)	$H_3C_2O_3^-$ (mg/L as C)	$HC_2O_3^-$ (mg/L as C)	$C_2O_4^{2-}$ (mg/L as C)	HCO_2^- (mg/L as C)	NPOC (mg/L as C)	pH
0.0	0.569	0.000	0.006	0.000	0.561	4.57
1.0	0.532	0.045	0.004	0.000	0.553	4.55
2.0	0.457	0.091	0.008	0.004		4.55
3.0	0.383	0.119	0.016	0.010	0.482	4.54
4.0	0.318	0.133	0.029	0.019		4.54
5.0	0.253	0.137	0.046	0.028		4.53
6.0	0.196	0.132	0.067	0.032	0.428	4.53
7.0	0.149	0.121	0.092	0.036		4.53
8.0	0.104	0.105	0.119	0.035		4.53
9.2	0.060	0.083	0.151	0.027	0.365	4.53
10.0	0.040	0.065	0.173	0.024		4.53
12.0	0.013	0.023	0.199	0.009		4.55
14.0	0.000	0.003	0.168	0.003	0.208	4.62
16.0	0.000	0.000	0.114	0.002		4.73
20.0	0.000	0.000	0.029	0.002		4.94
25.0	0.000	0.000	0.000	0.002	0.016	5.07
30.4	0.000	0.000	0.000	0.005		5.10
36.0	0.000	0.000	0.000	0.004		5.11
40.0	0.000	0.000	0.000	0.001	0.043	5.11
50.0	0.000	0.000	0.000	0.001		5.13
60.1	0.000	0.000	0.000	1.000e-3	0.040	5.14

Table D7. Experimental Results of $H_3C_2O_3^-$ Photodecomposition in DIW Containing $NaHCO_3$ = 25 mg/L as $CaCO_3$ ($C_0 = 1.996 \times 10^{-5}$ M, $I_a = 2.60 \times 10^{-6}$ E L^{-1} s^{-1}, T = 25°C).

Time (min)	$H_3C_2O_3^-$ (mg/L as C)	$HC_2O_3^-$ (mg/L as C)	$C_2O_4^{2-}$ (mg/L as C)	HCO_2^- (mg/L as C)	pH
0.0	0.479	0.000	0.000	0.000	7.36
0.5	0.467	0.013	0.000	0.000	7.37
1.0	0.446	0.030	0.000	0.000	7.37
1.5	0.428	0.047	0.002	0.000	7.37
2.0	0.399	0.062	0.004	0.000	7.36
3.0	0.354	0.086	0.011	0.009	7.36
4.0	0.315	0.098	0.019	0.016	7.35
5.0	0.276	0.104	0.032	0.024	7.35
6.0	0.236	0.105	0.048	0.035	7.32
7.0	0.204	0.103	0.065	0.043	7.32
8.0	0.173	0.097	0.085	0.049	7.29
9.0	0.144	0.083	0.107	0.057	7.29
10.0	0.118	0.074	0.131	0.059	7.28
11.0	0.098	0.064	0.157	0.063	7.26
12.0	0.077	0.053	0.177	0.061	7.25
13.0	0.060	0.045	0.200	0.057	7.24
14.0	0.046	0.032	0.221	0.056	7.23
15.1	0.034	0.025	0.242	0.050	7.21
16.0	0.025	0.020	0.261	0.043	7.20
17.0	0.019	0.016	0.276	0.036	7.19
18.0	0.013	0.012	0.291	0.029	7.19
19.0	0.010	0.009	0.301	0.023	7.18
20.0	0.006	0.005	0.308	0.019	7.18
21.0	0.000	0.003	0.314	0.014	7.17
22.0	0.000	0.000	0.316	0.010	7.18
23.0	0.000	0.000	0.322	0.010	7.18
24.0	0.000	0.000	0.318	0.005	7.18
26.0	0.000	0.000	0.313	0.003	7.19
28.0	0.000	0.000	0.306	0.001	7.20
30.0	0.000	0.000	0.296	0.001	7.21
35.1	0.000	0.000	0.273	0.001	7.23
40.0	0.000	0.000	0.252	0.001	7.25
50.1	0.000	0.000	0.213	0.000	7.30
60.0	0.000	0.000	0.179	0.000	7.34
80.0	0.000	0.000	0.126	0.000	7.43
100.4	0.000	0.000	0.085	0.000	7.50

Table D8. Experimental Results of $H_3C_2O_3^-$ Photodecomposition in DIW at Initial pH Adjusted to 6.98 with Concentrated NaOH ($C_0 = 2.271 \times 10^{-5}$ M, $I_a = 2.60 \times 10^{-6}$ E L^{-1} s^{-1}, T = 25°C).

Time (min)	$H_3C_2O_3^-$ (mg/L as C)	$HC_2O_3^-$ (mg/L as C)	$C_2O_4^{2-}$ (mg/L as C)	HCO_2^- (mg/L as C)	pH
0.0	0.545	0.000	0.000	0.000	6.98
0.4	0.518	0.000	0.000	0.000	6.96
1.0	0.484	0.039	0.000	0.000	6.96
1.6	0.453	0.059	0.003	0.000	6.92
2.2	0.416	0.078	0.008	0.006	6.89
2.6	0.387	0.089	0.012	0.012	6.85
3.0	0.364	0.095	0.017	0.015	6.81
3.5	0.336	0.104	0.025	0.021	6.77
4.0	0.308	0.107	0.034	0.027	6.73
4.5	0.282	0.110	0.043	0.034	6.69
5.0	0.255	0.108	0.055	0.039	6.64
6.0	0.207	0.106	0.082	0.048	6.56
7.0	0.165	0.099	0.111	0.053	6.46
8.0	0.126	0.092	0.148	0.055	6.38
9.0	0.094	0.080	0.180	0.053	6.32
10.0	0.063	0.065	0.218	0.048	6.25
11.0	0.044	0.052	0.252	0.041	6.19
12.1	0.026	0.038	0.287	0.031	6.13
13.0	0.016	0.027	0.312	0.023	6.08
14.0	0.009	0.017	0.331	0.015	6.06
15.0	0.007	0.009	0.341	0.008	6.04
16.0	0.000	0.005	0.343	0.004	6.05
17.0	0.000	0.002	0.341	0.002	6.05
18.0	0.000	0.000	0.331	0.001	6.06
19.0	0.000	0.000	0.321	0.001	6.07
20.0	0.000	0.000	0.311	0.001	6.09
22.0	0.000	0.000	0.289	0.001	6.12
24.0	0.000	0.000	0.266	0.000	6.14
30.0	0.000	0.000	0.210	0.000	6.20
35.0	0.000	0.000	0.168	0.000	6.25
40.0	0.000	0.000	0.133	0.000	6.28
45.0	0.000	0.000	0.104	0.000	6.31
50.0	0.000	0.000	0.081	0.000	6.34
60.3	0.000	0.000	0.047	0.000	6.38
70.0	0.000	0.000	0.027	0.000	6.41
80.2	0.000	0.000	0.014	0.000	6.44
90.0	0.000	0.000	0.007	0.000	6.45

Table D9. Experimental Results of $H_3C_2O_3^-$ Photodecomposition in DIW at Initial pH Adjusted to 8.20 with Concentrated NaOH ($C_0 = 2.258 \times 10^{-5}$ M, $I_a = 2.60 \times 10^{-6}$ E L^{-1} s^{-1}, T = 25°C).

Time (min)	$H_3C_2O_3^-$ (mg/L as C)	$HC_2O_3^-$ (mg/L as C)	$C_2O_4^{2-}$ (mg/L as C)	HCO_2^- (mg/L as C)	pH
0.0	0.542	0.000	0.000	0.000	8.20
0.5	0.555	0.017	0.000	0.000	8.15
1.0	0.533	0.040	0.002	0.000	8.13
1.5	0.505	0.065	0.004	0.000	8.08
2.0	0.478	0.087	0.007	0.000	8.02
2.5	0.449	0.106	0.011	0.005	7.93
3.0	0.417	0.123	0.018	0.010	7.80
3.5	0.391	0.134	0.026	0.015	7.62
4.0	0.358	0.144	0.035	0.144	7.40
4.5	0.330	0.151	0.046	0.024	7.20
5.0	0.306	0.158	0.059	0.028	7.00
6.0	0.242	0.157	0.089	0.035	6.73
7.0	0.191	0.154	0.125	0.040	6.50
8.0	0.150	0.144	0.166	0.042	6.32
9.0	0.111	0.130	0.210	0.040	6.17
10.0	0.083	0.108	0.254	0.039	6.05
11.0	0.050	0.086	0.301	0.029	5.93
12.0	0.032	0.063	0.338	0.022	5.84
13.1	0.021	0.039	0.372	0.014	5.78
14.0	0.012	0.022	0.388	0.008	5.75
15.0	0.006	0.009	0.399	0.006	5.75
16.0	0.001	0.003	0.396	0.004	5.78
17.1	0.000	0.001	0.383	0.003	5.82
18.1	0.000	0.000	0.370	0.005	5.86
20.0	0.000	0.000	0.341	0.007	5.93
22.0	0.000	0.000	0.310	0.002	5.99
24.0	0.000	0.000	0.288	0.002	6.04
26.0	0.000	0.000	0.262	0.004	6.08
30.0	0.000	0.000	0.219	0.003	6.14
35.0	0.000	0.000	0.170	0.003	6.21
40.0	0.000	0.000	0.129	0.004	6.25
45.0	0.000	0.000	0.098	0.001	6.29
50.2	0.000	0.000	0.071	0.001	6.32
63.0	0.000	0.000	0.033	0.002	6.35
70.0	0.000	0.000	0.020	0.001	6.36
81.4	0.000	0.000	0.009	0.002	6.37

Table D10. Experimental Results of $H_3C_2O_3^-$ Photodecomposition in DIW at Initial pH Adjusted to 9.12 with Concentrated NaOH ($C_0 = 2.279 \times 10^{-5}$ M, $I_a = 2.60 \times 10^{-6}$ E L^{-1} s^{-1}, T = 25°C).

Time (min)	$H_3C_2O_3^-$ (mg/L as C)	$HC_2O_3^-$ (mg/L as C)	$C_2O_4^{2-}$ (mg/L as C)	HCO_2^- (mg/L as C)	pH
0.0	0.547	0.000	0.000	0.000	9.12
0.5	0.507	0.018	0.000	0.000	9.11
1.0	0.489	0.035	0.001	0.000	9.09
1.5	0.466	0.051	0.003	0.000	9.08
2.0	0.442	0.066	0.005	0.004	9.08
2.5	0.416	0.078	0.009	0.009	9.06
3.0	0.394	0.085	0.013	0.016	9.04
3.5	0.372	0.091	0.018	0.022	9.04
4.0	0.349	0.095	0.024	0.029	9.04
4.5	0.329	0.097	0.031	0.035	9.02
5.0	0.305	0.096	0.039	0.043	9.02
6.0	0.265	0.090	0.057	0.058	8.99
7.0	0.230	0.085	0.076	0.068	8.95
8.0	0.197	0.076	0.102	0.078	8.91
9.0	0.166	0.067	0.123	0.084	8.86
10.0	0.139	0.058	0.147	0.086	8.82
11.0	0.113	0.044	0.172	0.090	8.76
12.0	0.092	0.036	0.196	0.089	8.70
13.0	0.073	0.030	0.221	0.083	8.62
14.0	0.057	0.025	0.245	0.077	8.53
15.0	0.044	0.021	0.269	0.069	8.42
16.0	0.032	0.017	0.289	0.059	8.30
17.0	0.024	0.012	0.309	0.051	8.15
18.1	0.016	0.010	0.327	0.039	7.93
19.0	0.011	0.009	0.339	0.029	7.71
20.0	0.008	0.008	0.353	0.020	7.41
22.0	0.005	0.003	0.361	0.007	7.06
24.0	0.002	0.000	0.351	0.002	6.95
30.0	0.000	0.000	0.302	0.001	6.85
35.0	0.000	0.000	0.220	0.000	6.81
40.0	0.000	0.000	0.184	0.000	6.79
45.0	0.000	0.000	0.154	0.000	6.77
50.0	0.000	0.000	0.104	0.000	6.75
60.0	0.000	0.000	0.068	0.000	6.73
70.0	0.000	0.000	0.044	0.000	6.71
80.0	0.000	0.000	0.027	0.000	6.68
90.3	0.000	0.000	0.017	0.000	6.65

Table D11. Experimental Results of $H_3C_2O_3^-$ Photodecomposition in DIW ($C_0 = 4.892 \times 10^{-5}$ M, $I_a = 2.60 \times 10^{-6}$ E L^{-1} s^{-1}, T = 25°C).

Time (min)	$H_3C_2O_3^-$ (mg/L as C)	$HC_2O_3^-$ (mg/L as C)	$C_2O_4^{2-}$ (mg/L as C)	HCO_2^- (mg/L as C)	pH
0.0	1.174	0.000	0.000	0.000	4.38
0.5	1.165	0.026	0.002	0.000	4.37
1.0	1.121	0.050	0.002	0.000	4.37
1.6	1.066	0.084	0.005	0.000	4.36
2.0	1.027	0.101	0.008	0.000	4.36
2.6	0.977	0.124	0.011	0.000	4.35
3.0	0.934	0.142	0.017	0.007	4.35
3.5	0.918	0.150	0.019	0.008	4.35
4.0	0.867	0.168	0.025	0.013	4.35
5.0	0.799	0.182	0.038	0.022	4.35
6.0	0.695	0.196	0.059	0.034	4.35
7.0	0.621	0.204	0.082	0.043	4.35
8.0	0.559	0.206	0.104	0.054	4.34
9.0	0.495	0.209	0.137	0.065	4.33
10.0	0.436	0.200	0.166	0.071	4.33
11.0	0.361	0.189	0.210	0.076	4.31
12.0	0.313	0.182	0.243	0.078	4.31
13.0	0.265	0.171	0.282	0.080	4.30
14.0	0.220	0.159	0.322	0.077	4.30
15.0	0.179	0.141	0.367	0.087	4.30
16.0	0.138	0.130	0.405	0.066	4.29
17.0	0.105	0.113	0.448	0.058	4.29
18.0	0.082	0.096	0.489	0.050	4.28
19.0	0.055	0.076	0.526	0.038	4.28
20.0	0.039	0.060	0.553	0.027	4.28
21.0	0.023	0.041	0.570	0.018	4.29
22.0	0.015	0.032	0.582	0.019	4.29
23.0	0.005	0.018	0.577	0.008	4.31
24.0	0.000	0.009	0.564	0.006	4.32
26.0	0.000	0.002	0.513	0.006	4.35
30.0	0.000	0.000	0.405	0.003	4.44
35.0	0.000	0.000	0.270	0.004	4.57
40.1	0.000	0.000	0.169	0.002	4.70
45.3	0.000	0.000	0.088	0.006	4.84
50.0	0.000	0.000	0.041	0.002	4.96
60.0	0.000	0.000	0.003	0.001	5.09
70.1	0.000	0.000	0.000	0.001	5.12
80.0	0.000	0.000	0.000	0.001	5.13

Table D12. Experimental Results of $H_3C_2O_3^-$ Photodecomposition in DIW ($C_0 = 1.092 \times 10^{-4}$ M, $I_a = 2.60 \times 10^{-6}$ E L^{-1} s^{-1}, T = 25°C).

Time (min)	$H_3C_2O_3^-$ (mg/L as C)	$HC_2O_3^-$ (mg/L as C)	$C_2O_4^{2-}$ (mg/L as C)	HCO_2^- (mg/L as C)	pH
0.0	2.621	0.000	0.000	0.000	4.06
1.0	2.352	0.047	0.001	0.000	4.05
2.0	2.288	0.114	0.003	0.000	4.04
3.0	2.145	0.168	0.008	0.000	4.04
4.0	2.032	0.210	0.014	0.000	4.03
5.0	1.886	0.248	0.024	0.015	4.03
6.0	1.765	0.276	0.036	0.022	4.02
7.0	1.649	0.299	0.051	0.034	4.02
8.0	1.527	0.315	0.071	0.048	4.02
9.0	1.427	0.326	0.093	0.064	4.01
10.0	1.320	0.335	0.119	0.077	4.00
11.1	1.212	0.337	0.151	0.098	4.00
12.4	1.069	0.329	0.198	0.119	3.99
13.0	1.025	0.333	0.224	0.130	3.98
14.0	0.922	0.321	0.263	0.144	3.98
15.0	0.845	0.313	0.303	0.155	3.97
16.0	0.760	0.301	0.351	0.166	3.97
17.1	0.674	0.288	0.403	0.176	3.96
18.0	0.598	0.275	0.453	0.182	3.95
19.1	0.532	0.263	0.505	0.182	3.95
20.1	0.467	0.247	0.561	0.186	3.94
21.1	0.403	0.231	0.624	0.184	3.94
22.0	0.348	0.219	0.683	0.179	3.93
23.0	0.295	0.205	0.747	0.172	3.93
24.0	0.245	0.183	0.809	0.165	3.92
25.1	0.203	0.167	0.874	0.149	3.92
26.0	0.167	0.156	0.929	0.138	3.92
27.1	0.129	0.137	1.002	0.119	3.91
28.3	0.095	0.119	1.073	0.098	3.91
30.0	0.057	0.090	1.164	0.068	3.91
35.1	0.008	0.020	1.243	0.011	3.93
40.3	0.003	0.000	1.017	0.000	4.00
45.0	0.000	0.000	0.787	0.000	4.08
50.0	0.000	0.000	0.570	0.000	4.18
60.0	0.000	0.000	0.269	0.000	4.40
70.2	0.000	0.000	0.073	0.000	4.68
80.0	0.000	0.000	0.005	0.000	4.87
90.2	0.000	0.000	0.000	0.000	4.91

Table D13. Experimental Results of $H_3C_2O_3^-$ Photodecomposition in DIW (C_0 = 2.188 × 10^{-5} M, I_a = 2.60 × 10^{-6} E L^{-1} s^{-1}, T = 35°C).

Time (min)	$H_3C_2O_3^-$ (mg/L as C)	$HC_2O_3^-$ (mg/L as C)	$C_2O_4^{2-}$ (mg/L as C)	HCO_2^- (mg/L as C)	pH
0.0	0.525	0.000	0.004	0.000	4.50
0.5	0.504	0.029	0.002	0.000	4.49
1.0	0.467	0.058	0.003	0.000	4.49
1.6	0.429	0.084	0.007	0.006	4.49
2.0	0.395	0.100	0.011	0.005	4.48
2.5	0.365	0.114	0.017	0.013	4.48
3.0	0.328	0.124	0.025	0.014	4.48
3.5	0.301	0.134	0.034	0.024	4.48
4.0	0.270	0.137	0.044	0.027	4.48
4.5	0.238	0.139	0.055	0.029	4.48
5.0	0.212	0.135	0.069	0.034	4.47
5.5	0.185	0.132	0.083	0.036	4.46
6.0	0.155	0.129	0.099	0.034	4.46
7.0	0.116	0.115	0.130	0.036	4.45
8.0	0.077	0.095	0.164	0.032	4.45
10.0	0.026	0.052	0.222	0.017	4.46
12.0	0.010	0.015	0.240	0.006	4.48
14.0	0.005	0.002	0.207	0.005	4.54
16.2	0.002	0.000	0.155	0.001	4.62
20.0	0.000	0.000	0.077	0.000	4.79
25.0	0.000	0.000	0.021	0.000	4.96
30.1	0.000	0.000	0.002	0.000	5.06

Table D14. Experimental Results of $H_3C_2O_3^{\cdot}$ Photodecomposition in DIW (C_0 = 2.004 × 10^{-5} M, I_a = 3.99 × 10^{-6} E L^{-1} s^{-1}, T = 25°C).

Time (min)	$H_3C_2O_3^{\cdot}$ (mg/L as C)	$HC_2O_3^{-}$ (mg/L as C)	$C_2O_4^{2-}$ (mg/L as C)	HCO_2^{-} (mg/L as C)	NPOC (mg/L as C)	pH
0.0	0.481	0.000	0.002	0.000	0.510	4.61
1.0	0.416	0.057	0.004	0.005	0.500	4.61
2.0	0.338	0.100	0.021	0.020		4.58
3.0	0.235	0.116	0.056	0.031	0.520	4.57
3.9	0.168	0.110	0.104	0.042		4.55
5.0	0.102	0.093	0.164	0.041		4.54
6.0	0.049	0.067	0.222	0.028	0.473	4.51
7.0	0.020	0.040	0.277	0.016		4.49
8.0	0.011	0.016	0.305	0.008		4.48
9.0	0.000	0.003	0.298	0.002	0.399	4.49
10.0	0.000	0.000	0.282	0.002		4.51
12.0	0.000	0.000	0.235	0.002		4.59
14.0	0.000	0.000	0.189	0.002	0.375	4.63
16.0	0.000	0.000	0.155	0.002		4.70
20.0	0.000	0.000	0.102	0.003		4.81
25.0	0.000	0.000	0.047	0.001	0.267	4.94
29.9	0.000	0.000	0.021	0.002		5.04
35.0	0.000	0.000	0.006	0.002		5.10
40.0	0.000	0.000	0.000	0.001	0.266	5.12
46.8	0.000	0.000	0.000	0.001		5.12
50.0	0.000	0.000	0.000	1.000e-3	0.250	5.13
60.6	0.000	0.000	0.000	1.000e-3	0.235	5.14

Table D15. Experimental Results of $H_3C_2O_3^-$ Photodecomposition in DIW (C_0 = 2.308 × 10^{-5} M, I_a = 3.99 × 10^{-6} E L^{-1} s^{-1}, T = 25°C).

Time (min)	$H_3C_2O_3^-$ (mg/L as C)	$HC_2O_3^-$ (mg/L as C)	$C_2O_4^{2-}$ (mg/L as C)	HCO_2^- (mg/L as C)	pH
0.0	0.554	0.000	0.000	0.000	4.58
0.5	0.513	0.026	0.000	0.000	4.58
1.0	0.465	0.062	0.003	0.000	4.58
1.5	0.418	0.091	0.008	0.005	4.57
2.0	0.366	0.113	0.016	0.010	4.57
2.5	0.324	0.127	0.027	0.015	4.56
3.0	0.284	0.136	0.037	0.022	4.55
3.5	0.239	0.137	0.058	0.027	4.54
4.0	0.202	0.136	0.080	0.033	4.54
4.5	0.166	0.130	0.101	0.034	4.53
5.0	0.129	0.118	0.127	0.034	4.52
5.5	0.100	0.107	0.153	0.034	4.51
6.0	0.074	0.094	0.180	0.030	4.51
7.0	0.034	0.062	0.225	0.020	4.50
8.0	0.015	0.031	0.252	0.011	4.51
10.0	0.000	0.002	0.214	0.005	4.60
12.0	0.000	0.000	0.122	0.001	4.76
14.0	0.000	0.000	0.050	0.004	4.93
16.0	0.000	0.000	0.010	0.001	5.06
18.0	0.000	0.000	0.000	0.001	5.10
20.0	0.000	0.000	0.000	0.002	5.11
25.0	0.000	0.000	0.000	0.002	5.12
30.0	0.000	0.000	0.000	0.000	5.14

Table D16. Experimental Results of $H_3C_2O_3^{\cdot}$ Photodecomposition in DIW (C_0 = 2.188 × 10^{-5} M, I_a = 5.27 × 10^{-6} E L^{-1} s^{-1}, T = 25°C).

Time (min)	$H_3C_2O_3^{\cdot}$ (mg/L as C)	$HC_2O_3^{-}$ (mg/L as C)	$C_2O_4^{2-}$ (mg/L as C)	HCO_2^{-} (mg/L as C)	NPOC (mg/L as C)	pH
0.0	0.525	0.000	0.002	0.000	0.461	4.58
0.5	0.505	0.034	0.001	0.000		4.57
1.0	0.441	0.078	0.005	0.000	0.470	4.56
1.5	0.379	0.108	0.014	0.004		4.55
2.0	0.315	0.128	0.028	0.010	0.488	4.54
2.5	0.258	0.134	0.047	0.019		4.53
3.0	0.203	0.134	0.071	0.028	0.420	4.53
3.5	0.157	0.125	0.101	0.032		4.52
4.0	0.115	0.110	0.132	0.036		4.51
4.5	0.075	0.092	0.166	0.035	0.482	4.50
5.0	0.048	0.073	0.197	0.027		4.50
5.5	0.031	0.050	0.224	0.024		4.51
6.0	0.013	0.029	0.241	0.009	0.277	4.52
7.0	0.008	0.005	0.228	0.003		4.56
9.0	0.06	0.000	0.177	0.002		4.63
12.0	0.000	0.000	0.015	0.002	0.052	5.01
14.0	0.000	0.000	0.001	0.002		5.07
16.0	0.000	0.000	0.000	0.005		5.08
20.1	0.000	0.000	0.000	0.004	0.029	5.08
25.1	0.000	0.000	0.000	0.001	0.096	5.09
30.0	0.000	0.000	0.000	0.003	0.045	5.09

Table D17. Experimental Results of $H_3C_2O_3^-$ Photodecomposition in DIW (C_0 = 1.887 × 10^{-4} M, I_a = 2.60 × 10^{-6} E $L^{-1}s^{-1}$, T = 25°C).

Time (min)	$H_3C_2O_3^-$ (mg/L as C)	$HC_2O_3^-$ (mg/L as C)	$C_2O_4^{2-}$ (mg/L as C)	HCO_2^- (mg/L as C)	NPOC (mg/L as C)	TC (mg/L as C)	O_2 (M)	pH
0.0	4.528	0.001	0.006	0.000	4.715	4.698	2.719×10^{-4}	7.07
5.0	4.291	0.192	0.007	0.000			2.580×10^{-4}	7.00
10.0	3.919	0.303	0.032	0.008	4.490	4.700	2.414×10^{-4}	6.79
15.0	3.616	0.351	0.079	0.402			2.239×10^{-4}	6.56
20.0	3.122	0.372	0.156	0.443	4.288	4.608	2.063×10^{-4}	6.36
30.0	2.339	0.375	0.384	0.565			1.725×10^{-4}	6.02
41.0	1.524	0.318	0.779	0.627	3.845	4.408	1.350×10^{-4}	5.68
50.0	0.949	0.271	1.180	0.578			1.066×10^{-4}	5.43
60.3	0.406	0.190	1.774	0.390	3.394	4.255	8.134×10^{-4}	5.18
71.1	0.068	0.087	2.402	0.098	3.091	3.824	6.946×10^{-4}	5.03
86.2	0.002	0.020	2.287	0.000			1.059×10^{-4}	5.54
101.4	0.000	0.000	1.647	0.000	1.782	3.334	1.570×10^{-4}	5.98
120.5	0.000	0.000	1.086	0.000			1.947×10^{-4}	6.22
140.0	0.000	0.000	0.628	0.000	0.730	3.209	2.166×10^{-4}	6.37
160.1	0.000	0.000	0.352	0.000			2.303×10^{-4}	6.46
180.0	0.000	0.000	0.173	0.000	0.237	3.018	2.386×10^{-4}	6.53
210.2	0.000	0.000	0.069	0.000	0.050		2.453×10^{-4}	6.61
240.0	0.000	0.000	0.016	0.000			2.481×10^{-4}	6.67
270.0	0.000	0.000	0.003	0.000	0.014	2.875	2.500×10^{-4}	6.71

Table D18. Observed Rate Constants for $H_3C_2O_3^-$ Photodecomposition

$C_0 \times 10^5$ (M)	NaHCO3 Alk. (mg L^{-1} as $CaCO_3$)	T (°C)	$I_a \times 10^6$ ($E\,L^{-1}s^{-1}$)	pH				Maximum Glyoxalate		Maximum Oxalate		Maximum Formate		Observed Rate Constants				
				pH_0	t where pH↑ (min)	pH_{max}	pH_f	t (min)	$C \times 10^6$ (M)	t (min)	$C \times 10^5$ (M)	t (min)	$C \times 10^6$ (M)	$k_1 \times 10^6$ ($Mmin^{-1}$)	$k_2 \times 10^6$ ($Mmin^{-1}$)	k_1/k_2	Rate switch	
																	t(min)	% conv.
2.121	-	25	1.38	-	-	-	-	7.5	4.33	*20*	1.20	**10**	3.67	1.451	-	-	**10**	67
2.175	-	25	1.38	4.57	*23*	4.44	5.11	10	6.08	*24*	1.37	**13**	3.50	1.380	0.955	1.45	**10**	56
2.129	-	15	2.60	4.67	*15*	4.54	5.26	5	5.21	*15*	1.39	**7.5**	3.58	2.183	-		**7.5**	71
2.242	-	17	2.60	4.57	*13*	4.44	5.10	5.5	5.96	*14*	1.38	**7**	3.17	2.449	1.429	1.71	**6**	58
2.121	-	25	2.60	4.63	*7.5*	4.56	5.27	5	4.83	*10*	1.18	**5**	3.33	2.647	-	-	**5**	62
2.371	-	25	2.60	4.57	*7.5*	4.53	5.10	5	5.71	*12*	0.83	**7**	3.00	2.702	1.680	1.61	**6**	66
2.271	-	25	2.60	6.96	*15*	6.04	6.45	4.5	4.58	*16*	1.43	**8**	4.58	2.335	1.408	1.66	**6**	61
2.258	-	25	2.60	8.20	*15*	5.75	6.37	5	6.58	*15*	1.66	**8**	3.50	2.381	1.353	1.76	**7**	65
2.183	-	25	2.60	9.12	-	-	6.63	4.5	4.04	*22*	1.50	**11**	7.5	1.814	1.096	1.66	**7**	56
4.892	-	25	2.60	4.38	*22*	4.28	5.13	9	8.71	*22*	2.43	**13**	6.67	3.313	2.187	1.52	**9**	58
9.825	-	25	2.60	4.06	*35*	3.91	4.91	11	14.04	*35*	5.18	**20**	15.5	4.908	3.429	1.43	**11**	49
18.87	-	25	2.60	7.07	*71*	5.03	6.71	30	15.63	*71*	10.01	**41**	52.25	3.142	1.736	1.81	**41**	66
2.188	-	35	2.60	4.50	*12*	4.45	5.07	4.5	5.79	*12*	1.00	**6**	2.83	2.769	2.000	1.38	**4.5**	55
2.004	-	25	3.99	4.61	*8*	4.48	5.12	3	4.83	*8*	1.27	**4**	3.5	3.593	-	-	**4**	65
2.308	-	25	3.99	4.58	*8*	4.50	5.10	3.5	5.71	*8*	1.05	**5**	2.83	3.731	2.542	1.45	**4**	64
2.188	-	25	5.27	4.58	*6*	4.5	5.08	3	5.58	*6*	1.00	**4**	3	5.055	3.417	1.48	**3**	61
1.996	25	25	2.599	7.36	*21*	7.17	7.50	6	4.38	*23*	1.34	**11**	5.25	1.704	0.992	1.72	**7**	57

APPENDIX E

TABLES OF EXPERIMENTAL DATA FOR PYRUVATE

Table E1. Experimental Results of $H_3C_3O_3^-$ Photodecomposition in DIW (C_0 = 1.447 × 10^{-5} M, I_a = 2.60 × 10^{-6} E $L^{-1}s^{-1}$, T = 25°C).

Time (min)	$H_3C_3O_3^-$ (mg/L as C)	$H_2C_3O_3^-$ (mg/L as C)	$HC_2O_3^-$ (mg/L as C)	$C_2O_4^{2-}$ (mg/L as C)	TC (mg/L as C)	UP1 Peak Height	UP2 Peak Height	pH
0	0.521	7.000e-3	0.000	0.000	0.589	0	0	5.43
1	0.478	0.010	0.000	0.003	0.596	591	309	5.42
2	0.435	0.015	0.001	0.006		914	1142	5.39
3	0.395	0.014	0.001	0.011	0.555	1591	2713	5.34
4	0.355	0.019	0.002	0.016		1814	4256	5.30
5	0.325	0.019	0.002	0.020		1923	6112	5.25
6	0.301	0.017	0.002	0.024	0.539	2004	8164	5.22
7	0.268	0.020	0.002	0.030		1890	9769	5.18
8	0.243	0.020	0.002	0.033		1803	11748	5.15
9	0.212	0.017	0.002	0.039	0.532	1626	13400	5.12
10	0.198	0.018	0.002	0.044		1462	14810	5.10
12	0.150	0.020	0.001	0.052		1133	17232	5.06
14	0.120	0.014	0.001	0.060	0.503	896	19324	5.05
16	0.093	0.014	0.001	0.067		642	20592	5.03
20	0.058	0.011	0.001	0.076		0	21190	5.04
25	0.014	0.006	0.000	0.084	0.405	0	17491	5.08
30	0.006	0.005	0.000	0.083		0	13935	5.15
35	0.003	0.000	0.000	0.077		0	10646	5.24
40	0.000	0.000	0.000	0.070	0.416	0	7889	5.33
45	0.000	0.000	0.000	0.059		0	5875	5.41
50	0.000	0.000	0.000	0.040		0	2603	5.48
60	0.000	0.000	0.000	0.010	0.363	0	193	5.59
80	0.000	0.000	0.000	0.011	0.425	0	0	5.72

Table E2. Experimental Results of $H_3C_3O_3^-$ Photodecomposition in DIW (C_0 = 1.433 × 10^{-4} M, I_a = 2.60 × 10^{-6} E $L^{-1}s^{-1}$, T = 25°C).

Time (min)	$H_3C_3O_3^-$ (mg/L as C)	$H_2C_3O_3^-$ (mg/L as C)	$HC_2O_3^-$ (mg/L as C)	$C_2O_4^{2-}$ (mg/L as C)	NPOC (mg/L as C)	TC (mg/L as C)	UP1 Peak Height	UP2 Peak Height	$O_2 \times 10^4$ (M)	pH
0	5.159	0.000	0.000	0.000	4.863	4.765	0	0	2.766	5.60
5	4.623	0.041	0.006	0.022			7433	3462	2.593	5.65
10	4.161	0.080	0.013	0.057	4.822	4.540	11028	10240	2.409	5.56
15	3.655	0.108	0.019	0.106			12792	20940	2.200	5.45
20	3.306	0.122	0.021	0.146	4.575	3.966	13054	30598	2.068	5.39
30	2.653	0.140	0.023	0.252			11672	52164	1.753	5.24
40	2.124	0.143	0.021	0.362			9246	71958	1.503	5.16
60	1.219	0.122	0.015	0.560	3.261	3.353	4756	97757	1.092	5.13
80	0.636	0.085	0.010	0.677			2402	103296	0.997	5.27
100	0.252	0.042	0.005	0.703	1.952	2.807	802	91412	1.190	5.50
121	0.096	0.016	0.003	0.625			0	70978	1.500	5.72
150	0.014	0.002	0.000	0.421	0.922	2.341	0	32251	1.921	5.96
180	0.002	0.000	0.000	0.211			0	8360	2.210	6.13
213	0.000	0.000	0.000	0.053	0.164	2.048	0	434	2.383	6.27
231	0.000	0.000	0.000	0.015	0.072	1.940	0	0	2.438	6.32
258	0.000	0.000	0.000	0.000	0.081	1.946	0	0	2.487	6.39
295	0.000	0.000	0.000	0.000	0.064	4.765	0	0	2.523	6.47

APPENDIX F

TABLES OF EXPERIMENTAL DATA FOR MIXTURE PHOTODECOMPOSITION

Table F1. Experimental Results for Photodecomposition of $HCO_2^-/C_2O_4^{2-}$ Mixture in DIW ($[HCO_2^-]_0 = 4.067 \times 10^{-5}$ M, $[C_2O_4^{2-}]_0 = 2.188 \times 10^{-5}$ M, $I_a = 2.60 \times 10^{-6}$ E L^{-1} s^{-1}, T = 25°C).

Time (min)	HCO_2^- (mg/L as C)	$C_2O_4^{2-}$ (mg/L as C)	NPOC (mg/L as C)	pH
0.0	0.488	0.525	0.980	5.54
0.5	0.503	0.525		5.63
1.0	0.486	0.524		5.75
1.5	0.465	0.523	0.900	5.87
2.0	0.453	0.522		5.98
2.5	0.428	0.519		6.07
3.0	0.401	0.508	0.898	6.15
4.0	0.355	0.514		6.29
5.0	0.302	0.509		6.39
6.0	0.238	0.502	0.682	6.47
8.0	0.141	0.490		6.60
10.0	0.029	0.478		6.67
12.1	0.001	0.458	0.530	6.68
14.0	0.000	0.439		6.69
20.0	0.000	0.381		6.71
25.0	0.000	0.334	0.391	6.73
30.0	0.000	0.295		6.74
40.0	0.000	0.225		6.76
50.7	0.000	0.161	0.208	6.77
70.0	0.000	0.093		6.79
100.0	0.000	0.033		6.79
120.0	0.000	0.016	0.133	6.79

Table F2. Experimental Results for Photodecomposition of $C_2O_4^{2-}$/ $H_3C_2O_3^-$ Mixture in DIW ($[C_2O_4^{2-}]_0 = 2.050 \times 10^{-5}$ M, $[H_3C_2O_3^-]_0 = 2.175 \times 10^{-5}$ M, $I_a = 2.60 \times 10^{-6}$ E L^{-1} s^{-1}, T = 25°C).

Time (min)	$H_3C_2O_3^-$ (mg/L as C)	$HC_2O_3^-$ (mg/L as C)	$C_2O_4^{2-}$ (mg/L as C)	HCO_2^- (mg/L as C)	NPOC (mg/L as C)	pH
0.0	0.522	0.007	0.492	0.000	1.080	4.61
0.5	0.494	0.031	0.491	0.000	1.091	4.61
1.0	0.445	0.069	0.490	0.000		4.61
1.5	0.384	0.103	0.495	0.005	1.049	4.62
2.0	0.331	0.126	0.503	0.011		4.62
3.0	0.231	0.143	0.526	0.022		4.62
4.0	0.139	0.131	0.566	0.027	0.958	4.61
5.0	0.074	0.101	0.609	0.026		4.61
6.0	0.030	0.059	0.650	0.015		4.61
7.0			0.665			4.63
8.0	0.000	0.004	0.639	0.002	0.770	4.71
10.0	0.000	0.000	0.554	0.001		4.95
12.0	0.000	0.000	0.474	0.000		5.23
14.0	0.000	0.000	0.395	0.000	0.451	5.43
16.0	0.000	0.000	0.332	0.000		5.57
20.0	0.000	0.000	0.230	0.000		5.74
25.0	0.000	0.000	0.131	0.000	0.236	5.88
30.0	0.000	0.000	0.075	0.000		5.95
35.0	0.000	0.000	0.030	0.000		6.00
40.0	0.000	0.000	0.010	0.000	0.147	6.03
45.8	0.000	0.000	0.000	0.000		6.06
50.0	0.000	0.000	0.000	0.000		6.08
55.0	0.000	0.000	0.000	0.000		6.10
60.0	0.000	0.000	0.000	0.000	0.139	6.12

APPENDIX G

ABSORBANCE PROFILES

Table G1. Absorbance Profiles for Photodecomposition of HCO_2^- in DIW ($C_0 = 4.145 \times 10^{-4}$ M, $I_a = 3.99 \times 10^{-6}$ E L^{-1} s^{-1}, T = 25°C).

Time (min)	Absorbance at 190 nm	Absorbance at 200 nm	Absorbance at 220nm	Absorbance at 253.7 nm
0.0	0.187	0.034	0.006	0.001
10.0	0.188	0.048	0.014	0.003
20.0	0.170	0.053	0.018	0.005
27.0	0.152	0.053	0.019	0.005
30.0	0.141	0.052	0.020	0.005
35.0	0.128	0.053	0.022	0.006
40.0	0.105	0.048	0.021	0.005
45.0	0.097	0.042	0.018	0.005
55.5	0.093	0.035	0.014	0.005
65.2	0.083	0.026	0.009	0.004
75.0	0.083	0.026	0.008	0.004
90.0	0.077	0.023	0.008	0.005
106.1	0.077	0.020	0.006	0.003

Table G2. Absorbance Profiles for Photodecomposition of HCO_2^- in DIW in the Absence of DO ($C_0 = 4.051 \times 10^{-4}$ M, $I_a = 3.99 \times 10^{-6}$ E L^{-1} s^{-1}, T = 25°C).

Time (min)	Absorbance at 190 nm	Absorbance at 200 nm	Absorbance at 220nm	Absorbance at 253.7 nm
0.0	0.163	0.034	0.009	0.003
10.0	0.348	0.119	0.017	0.003
19.0	0.491	0.183	0.022	0.005
30.0	0.637	0.249	0.027	0.004
39.7	0.750	0.301	0.032	0.006
45.5	0.803	0.324	0.034	0.006
50.0	0.843	0.344	0.036	0.007
55.0	0.882	0.361	0.037	0.007
60.0	0.905	0.376	0.042	0.010
65.0	0.914	0.379	0.041	0.008
70.0	0.902	0.367	0.033	0.001
80.0	0.843	0.347	0.037	0.006
90.0	0.786	0.323	0.035	0.006
100.0	0.731	0.299	0.032	0.005
110.0	0.605	0.184		

Table G3. Absorbance Profiles for $C_2O_4^{2-}$ Photodecomposition in DIW ($C_0 = 2.111 \times 10^{-4}$ M, $I_a = 2.60 \times 10^{-6}$ E $L^{-1}s^{-1}$, T = 25°C).

Time (min)	Absorbance at 190 nm	Absorbance at 200 nm	Absorbance at 220nm	Absorbance at 253.7 nm
0.0	1.129	0.465	0.041	0.007
10.3	1.052	0.434	0.041	0.007
20.0	0.981	0.403	0.039	0.006
30.1	0.905	0.370	0.037	0.006
40.0	0.824	0.337	0.034	0.006
60.0	0.683	0.276	0.028	0.005
80.0	0.551	0.221	0.023	0.004
100.0	0.447	0.175	0.019	0.004
150.0	0.273	0.097	0.010	0.002
180.0	0.206	0.068	0.007	0.002
230.0	0.142	0.040	0.005	0.002
275.0	0.113	0.028	0.004	0.002
300.0	0.106	0.024	0.030	0.001
345.1	0.091	0.020	0.003	0.001
380.2	0.087	0.015	0.002	0.001

Table G4. Absorbance Profiles for $HC_2O_3^-$ Photodecomposition in DIW (C_0=2.051×10^{-4} M, I_a = 2.60 × 10^{-6} E $L^{-1}s^{-1}$, T = 25°C).

Time (min)	Absorbance at 190 nm	Absorbance at 200 nm	Absorbance at 220nm	Absorbance at 253.7 nm
3.0	0.312	0.065	0.021	0.003
10.0	0.381	0.103	0.024	0.004
20.0	0.462	0.164	0.033	0.004
40.0	0.628	0.283	0.051	0.008
60.0	0.638	0.290	0.044	0.008
100.3	0.311	0.130	0.002	0.004
150.0	0.122	0.043	0.007	0.002
180.0	0.080	0.024	0.004	0.002
210.3	0.062	0.017	0.004	0.002
240.0	0.054	0.013	0.003	0.002
270.0	0.056	0.014	0.004	0.002

Table G5. Absorbance Profiles for $H_3C_2O_3^{\cdot}$ Photodecomposition in DIW (C_0 = 1.887 × 10^{-4} M, I_a = 2.60 × 10^{-6} E $L^{-1}s^{-1}$, T = 25°C).

Time (min)	Absorbance at 190 nm	Absorbance at 200 nm	Absorbance at 220nm	Absorbance at 253.7 nm
0.0	0.206	0.048	0.003	0.001
10.0	0.226	0.057	0.010	0.002
20.0	0.265	0.073	0.015	0.003
41.0	0.379	0.132	0.027	0.005
60.3	0.553	0.219	0.034	
71.1	0.626	0.277	0.046	0.008
101.4	0.443	0.191	0.029	0.006
140.0	0.207	0.082	0.013	0.004
180.0	0.096	0.031	0.006	0.002
210.2	0.069	0.018	0.004	0.002
270.0	0.056	0.012	0.003	0.002

Table G6. Absorbance Profiles for $H_3C_3O_3^-$ Photodecomposition in DIW (C_0 = 1.433 × 10^{-4} M, I_a = 2.60 × 10^{-6} E $L^{-1}s^{-1}$, T = 25°C).

Time (min)	Absorbance at 190 nm	Absorbance at 200 nm	Absorbance at 220nm	Absorbance at 253.7 nm
0.0	0.319	0.276	0.171	0.013
10.0	0.307	0.244	0.149	0.012
40.0	0.290	0.192	0.105	0.011
60.0	0.293	0.170	0.084	0.010
100.4	0.258	0.127	0.048	0.007
180.0	0.090	0.035	0.009	0.003
213.0	0.053	0.016	0.004	0.002
231.0	0.044	0.011	0.004	0.002
258.0	0.032	0.006	0.005	0.001
295.3	0.039	0.009	0.003	0.001

APPENDIX H

QUALITY ASSURANCE AND QUALITY CONTROL IN LABORATORY ANALYSES

APPENDIX H

QUALITY ASSURANCE AND QUALITY CONTROL IN LABORATORY ANALYSES

H.1. Determination of Anionic Species by Ion Chromatograph

Ion chromatography was calibrated each time it was used and fresh calibration standards were prepared daily from stock solution. Sample calibration curves for HCO_2^-, $C_2O_4^{2-}$, $HC_2O_3^-$, $H_3C_2O_3^-$ and $H_3C_3O_3^-$ are given in Figures H.1.1, H.1.2, H.1.3, H.1.4 and H.1.5 with r^2 of 1.0000, 0.9999, 0.9997, 0.9984 and 0.9995, respectively.

H.2. Measurements of NPOC and TC by TOC Analyzer

The calibration curve for TOC analyzer was updated each time it was used with fresh calibration standards. A sample calibration curve for TOC analyzer is given in Figure H.2.1. The measured concentrations of the samples were obtained by quantitative calculation based on measured peak area using the calibration curve developed. In either measurement of standard solutions or measurements of samples, mean value (MN), standard deviation (SD) and coefficient of variation (CV) were calculated and displayed on the screen by the software. SD and CV were used to check for repeatability. Standard solutions and samples were measured repetitively, any value with large fluctuation (with large SD and CV) was deleted, additional measurements were conducted and MN, SD and CV were calculated automatically. The reported NPOC and TC concentrations were

the average of 4 different injections. A maximum of 8 injections were carried out as seen in Figure H.2.1.

H.3. Determination of Absorbed Light Intensity

Absorbed light intensity was determined for each lamp configuration and it was performed 4 times for 2 UV lamps and 3 times for the other lamp configurations. The average absorbed light intensities with standard deviations are given in Table H.3.1.

Component: **Formate;** Fit Type: Linear
Method: c:\peaknet\method\gonca\as11.met; Updated: 8/19/103 5:37:13 PM
r^2 = 0.999962
C = 1.417e-6 * Area + 0
Standard: External
Calibration: Area

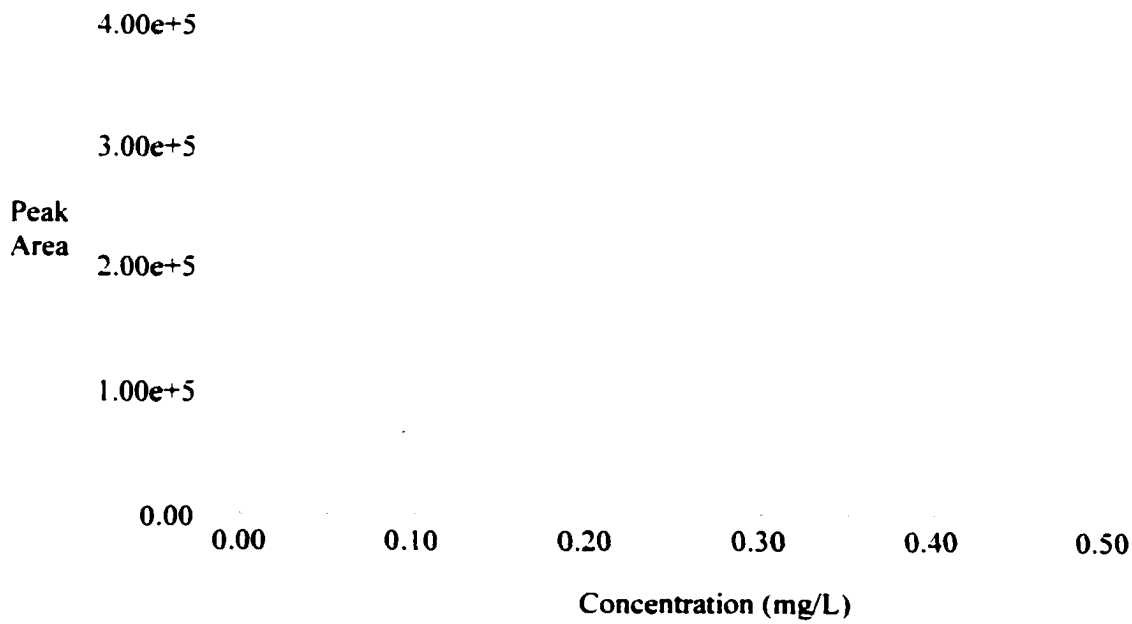

Figure H.1.1. A Sample Calibration Curve for HCO_2^-.

Component: **Oxalate;** Fit Type: Linear
Method: c:\peaknet\method\gonca\as11.met; Updated: 8/19/103 5:29:47 PM
$r^2 = 0.999851$
C = 4.786e-6 * Height + 0
Standard: External
Calibration: Height

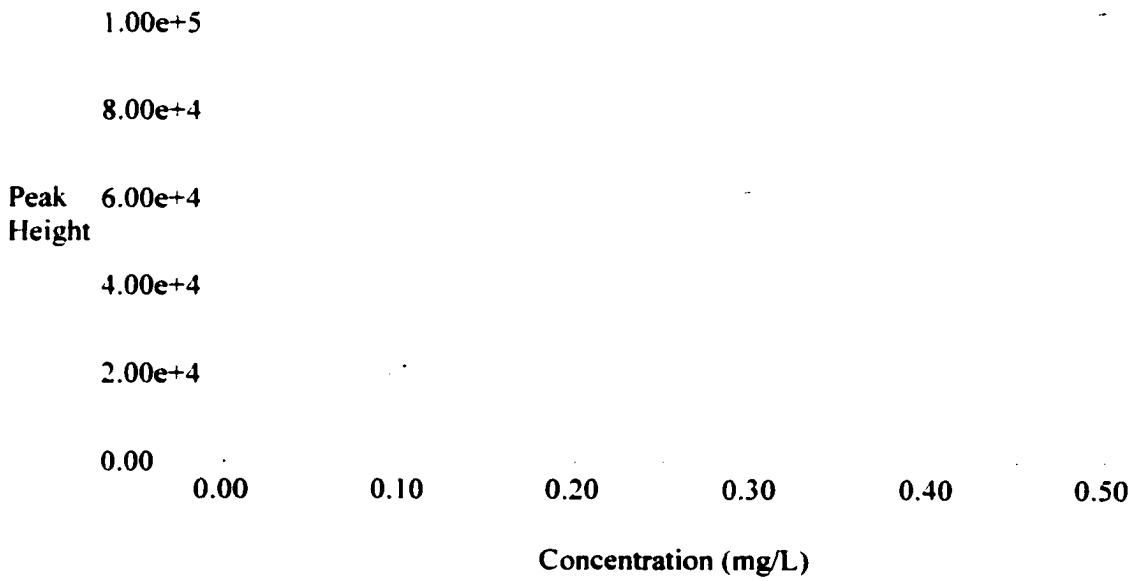

Figure H.1.2. A Sample Calibration Curve for $C_2O_4^{2-}$.

Component: **Glyoxalate;** Fit Type: Linear
Method: c:\peaknet\method\gonca\as11.met; Updated: 8/19/103 5:08:14 PM
r^2 = 0.999716
C = 9.62e-6 * Height + 0
Standard: External
Calibration: Height

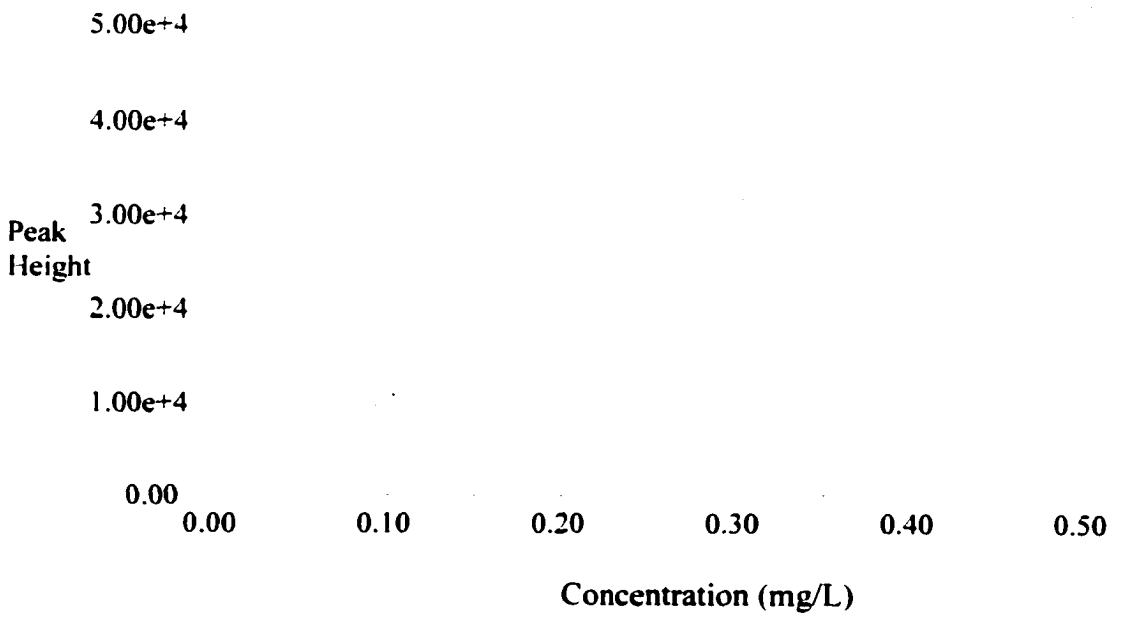

Figure H.1.3. A Sample Calibration Curve for $HC_2O_3^-$.

Component: **Glycolate;** Fit Type: Linear
Method: c:\peaknet\method\gonca\as11.met; Updated: 8/19/103 4:52:12 PM
r^2 = 0.998408
C= 8.483e-6 * Height + 0
Standard: External
Calibration: Height

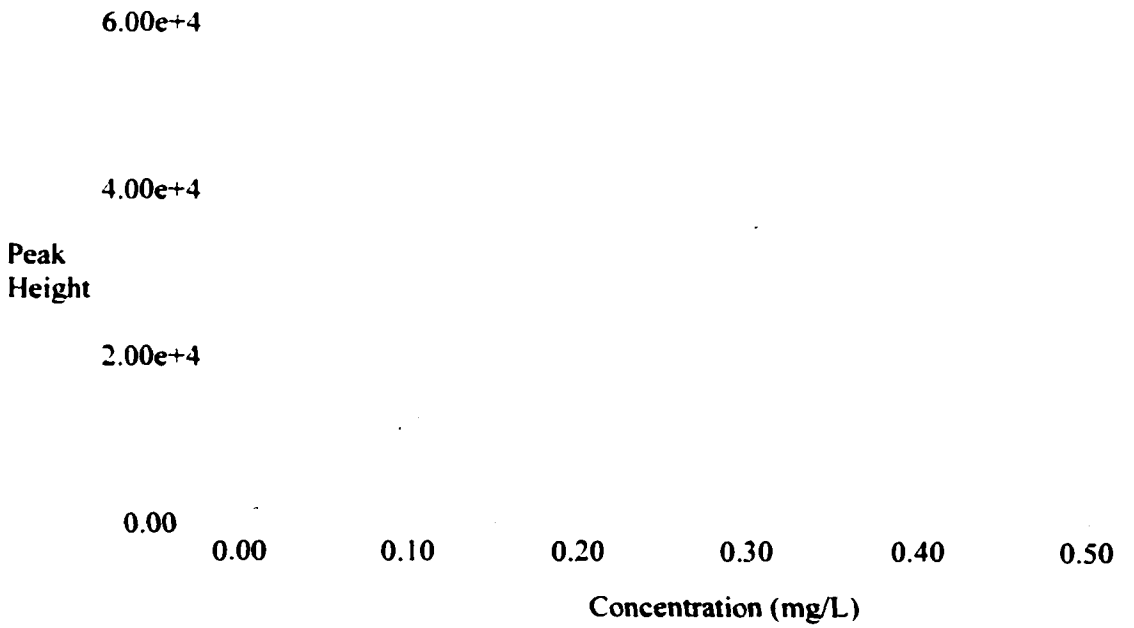

Figure H.1.4. A Sample Calibration Curve for $H_3C_2O_3^-$.

Component: **Pyruvate;** Fit Type: Linear
Method: c:\peaknet\method\gonca\as11.met: Updated: 8/19/103 5:46:19 PM
r^2 = 0.999534
C = 1.007e-5 * Height + 0
Standard: External
Calibration: Height

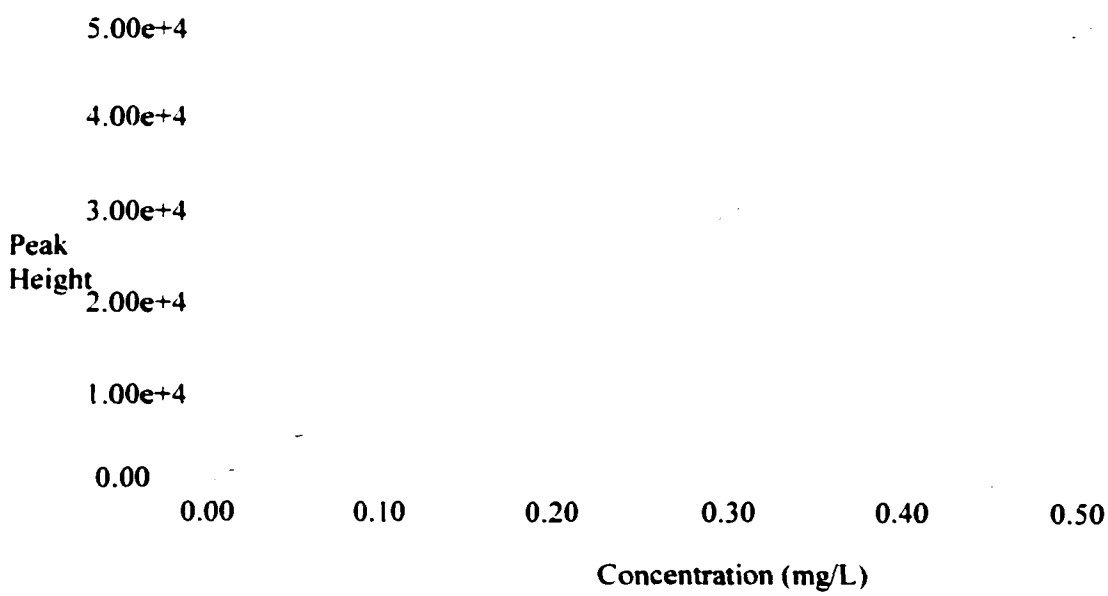

Figure H.1.5. A Sample Calibration Curve for $H_3C_3O_3^-$.

TOC-Control

Slope: 25424.9
Intercept: 1679.8
R^2: 0.999816

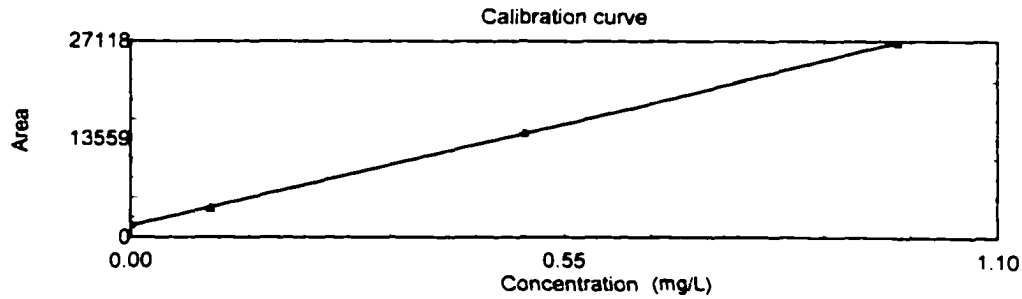

Samples

Sample Name: 120 min
Sample ID: sample8
Remark:
Comment:
Method: c:\toccntr\method\gonca\gonca.met
Cal Curve: 1: c:\toccntr\calibr\gonca\cal.cal

Type	Analysis	Acid Add	Dilution	Sparge Time	Date/Time	SD Max	CV Max
Unknown	NPOC	0	1.000	0	11/29/2001 16.16.18	200	2.000

Mean Area	Conc	Result	No. Of Washes	SD	CV	Modified
7956	0.2469 +/- 0.02384 ppm		1	293	3.69%	

No	Vial	Range	Inj Vol.	Area	Conc	Excl.	Notes	Date/Time	Cal Curve
1	8	1	533	30006	1.1141	E	******	11/29/2001 15.51.15	c:\toccntr\calibr\gonca\cal.cal
2	8	1	533	13041	0.44685	E	******	11/29/2001 15.55.05	c:\toccntr\calibr\gonca\cal.cal
3	8	1	533	9233	0.29708	E	******	11/29/2001 15.59.16	c:\toccntr\calibr\gonca\cal.cal
4	8	1	533	8319	0.26113		******	11/29/2001 16.03.44	c:\toccntr\calibr\gonca\cal.cal
5	8	1	533	7989	0.24815		******	11/29/2001 16.07.55	c:\toccntr\calibr\gonca\cal.cal
6	8	1	533	7913	0.24516		******	11/29/2001 16.12.05	c:\toccntr\calibr\gonca\cal.cal
7	8	1	533	7605	0.23305		******	11/29/2001 16.16.18	c:\toccntr\calibr\gonca\cal.cal

Figure H.2.1. A Sample Calibration Curve and a Sample Analysis for TOC Analyzer.

Iron measurements were also duplicated by analyzing same sample twice and analyzing different dilutions (Table H.3.2).

Table H.3.1. I_a Measurements During the Course of Study.

Number of UV Lamp	I_a (1) $\times 10^6$ ($EL^{-1}s^{-1}$)	I_a (2) $\times 10^6$ ($EL^{-1}s^{-1}$)	I_a (3) $\times 10^6$ ($EL^{-1}s^{-1}$)	I_a (4) $\times 10^6$ ($EL^{-1}s^{-1}$)	I_a (Average) ($EL^{-1}s^{-1}$)
1	1.39	1.39	1.37	-	1.38 ± 0.01
2	2.66	2.61	2.55	2.56	2.60 ± 0.05
3	4.05	3.95	3.96	-	3.99 ± 0.06
4	5.27	5.29	5.23	-	5.27 ± 0.03

Table H.3.2. Fe^{2+} Measurements During I_a Determinations.

Intensity Measurement	Fe^{2+} (mg/L)				
	1	2	3	4	Average
3 UV Lamps	91.7 (1:50 Dilution)	90.9 (1:50 Dilution)	95.1 (1:100 Dilution)	91.8 (1:100 Dilution)	92.4 ± 1.9
4 UV Lamps	111.3 (1:100 Dilution)	111.0 (1:100 Dilution)	110.0 (1:200 Dilution)	111.2 (1:200 Dilution)	110.9 ± 0.6

BIBLIOGRAPHY

American Water Works Association (AWWA) Research Foundation, (1991). *Ozone in Water Treatment Application and Engineering Cooperative Research Report.* Langlais, B., Reckhow, D.A. and Brink, D.R. editors. Lewis Publishers, New York.

Baboukas, E.D., Kanakidou, M. and Mihalopoulos, N. (2000). *Carboxylic Acids in Gas and Particulate Phase above the Atlantic Ocean.* J. Geophys. Res. Vol. 105, pp. 14459-14471.

Bangun, J. and Adesina, A.A. (1998). *The photodegradation Kinetics of Aqueous Sodium Oxalate Solution Using TiO_2 Catalyst.* Applied Catalysis A: General. Vol. 175, pp. 221-235.

Bertilsson, S. and Tranvik, L.J. (2000). *Photochemical Transformation of Dissolved Organic Matter in Lakes.* Limnology and Oceanography. Vol. 45, No.4, pp. 753-762.

Bolton, J.R. (2000). *Terms and Definitions in Ultraviolet Disinfection.* Conference Proceedings, Disinfection 2000: Disinfection of Wastes in the New Millennium. Water Environment Federation. New Orleans, Louisiana U.S.A. March 2000.

Bolton, J.R. and Cater, S.R. (1994). *Homogenous Photodegradation of Pollutants in Contaminated Water: An Introduction.* In Aquatic and Surface Photochemistry, Chapter 33. Helz, G.R., Zepp, R.G. and Crosby, D.G. Eds. Lewis Publishers, New York.

Buckingham, J. and Donaghy, S.M. Eds. *Dictionary of Organic Compounds.* Chapman and Hall, Fifth ed, 1982.

Clancy, J.L., Bukhari, Z., Hargy, T.M., Bolton, J.R., Dussert, B., Marshall, M.M. (2000). *Using UV to Inactivate Cryptosporidium.* J.Am. Water Work Assoc. 92(9), pp. 97-104.

Coyle, J.D. *Introduction to Organic Photochemistry.* John Wiley & Sons, Great Britain, 1986.

Glaze, H.W. and Weinberg, H.S. Eds. *Identification and Occurrence of Ozonation By-Products in Drinking Water.* AWWA Research Foundation and American Water Work Association, U.S.A., 1993.

Gorden, R. and Ausloos, P. (1961). *Vapor-PhasePhotolysis of Formic Acid.* J. Phys.Chem. Vol.65, pp. 1033-1037.

Hatchard, C.G. and Parker, C.A. (1956). *A New Sensitive Chemical Actinometer II. Potassium Ferrioxalate as a Standard Chemical Actinometer.* Proceed. Royal Soc. London, A235, pp. 518-536.

Heilbron, I. and Bunbury, H.M. Eds. *Dictionary of Organic Compounds*. Oxford University Press, New York, 1953.

Hoigné, J. and Bader, H. (1983). *Rate Constants of Reactions of Ozone with Organic and Inorganic Compounds in Water II*. Wat. Res. Vol. 17, pp. 185-194.

Hosmani, S.P., Kumar, L.V. and Partha, S. (1999). *Ecological Significance of Biochemical Parameters in Certain Fresh Water Lakes of Mysore*. Journal of Environmental Biology. 20(2), pp 121-124.

Ikemizu, K., Orita, M. Sagiike, M., Morooka, S. and Kato, Y. (1987). *Ozonation of Organic Refractory Compounds in Water in Combination with UV Radiation*. J.Chem. Eng. Japan. Vol. 20, No. 4, pp. 369-374.

Karpel Vel Leitner, N. and Doré, M. (1994). *Rôle de l'oxygène dissous dans le mécanisme de décomposition de l'acide formique en solution aqueuse par irradiation UV en présence de peroxide d'hydrogène*. J. Chim. Phys. Vol. 91, pp.503-518.

Karpel Vel Leitner, N. and Doré, M. (1996). *Hydroxyl Radical Induced Decomposition of Aliphatic Acids in Oxygenated and Deoxygenated Aqueous Solutions*. Journal of Photochemistry and Photobiology A: Chemistry. Vol. 99, pp. 137-143.

Karpel Vel Leitner, N. and Doré, M. (1997). *Mechanism of the Reaction Between Hydroxyl Radicals and Glycolic, Glyoxalic, Acetic and Oxalic Acids in Aqueous Solutions: Consequence on Hydrogen Peroxide Consumption in the H_2O_2/UV and O^3/H_2O_2 Systems*. Wat. Res. Vol. 31, No. 6, pp. 1383-1397.

Khwaja, H.A. (1995). *Atmospheric Concentrations of Carboxylic Acids and Related Compounds at a Semiurban Site*. Atmos. Environ. Vol. 29, pp. 127-139.

Krasnov, B.P., Pakul, D.L. and Kirillova, T.V. (1974). *Use of Ozone for Treatment of Industrial Wastewaters*. Int. Chem. Eng. Vol. 14, No. 4, pp. 747-750.

Krýsa, J., Vodehnal, L. and Jirkovsky, J. (1999). *Photocatalytic Degradation Rate of Oxalic Acid on a Semiconductive Layer of n-TiO_2 Particles in a Batch Mode Plate Photoreactor Part II: Light Intensity Limit*. Journal of Applied Electrochemistry Vol. 29, No. 4, pp 429-435.

Kumar, N., Kulshrestha, U.C., Saxena, A., Kumari, K.M. and Srivastava, S.S. (1993). *Formate and Acetate in Monsoon Rainwater of Agra, India*. J. Geophys. Res. Vol. 98, pp. 5135-5137.

Kusakabe, K., Aso, S., Hayashi, J., Isomura, K. and Morooka, S. (1990). Decomposition of Humic Acid and Reduction of Trihalomethane Formation Potential in Water by Ozone with UV Irradiation. Wat. Res. Vol. 24, No. 6, pp. 781-785.

Li, S.M. and Winchester, J.W. (1993). *Water Soluble Organic Constituents in Arctic Aerosols and Snow Pack.* Geophys. Res. Lett. Vol. 20, pp. 45-48.

Li, W. L., Yu, Z., Gao, M., Zhang, L., Cai, X. and Chao, F. (1996). *Effect of Ultraviolet Irradiation on the Characteristics and Trihalomethanes Formation potential of Humic Acid.* Wat. Res. Vol.30, No. 2, pp. 347-350.

Mazzarino, I., Piccinini, P. and Spinelli, L. (1999). *Degradation of Organic Pollutants in Water by Photochemical Reactors.* Catalysis Today, vol. 48, pp 315-321.

Miller, W.L. (1994). *Recent Advances in the Photochemistry of Natural Dissolved Organic Matter.* In Aquatic and Surface Photochemistry, Chapter 7. Helz, G.R., Zepp, R.G. and Crosby, D.G. Eds. Lewis Publishers, New York.

Neta, P. Simic, M. and Hayon, E. (1969). *Pulse radiolysis of Aliphatic Acids in Aqueous Solutions. I. Simple Monocarboxylic Acids.* The J. Phys.Chem. Vol.73, No. 12, pp. 4207-4213.

Ogata, Y., Tomizawa, K. and Takagi, K. (1981). *Photo-Oxidation of Formic, Acetic, and Propionic Acids with Aqueous Hydrogen Peroxide.* Can. J. Chem. Vol. 59, pp. 14-18.

Ramsperger, H.C. and Porter, C.W. (1926). *The Ultraviolet Absorption Spectrum of Formic Acid.* J. Am. Chem. Soc. Vol.48, No.5, pp. 1267-1273.

Sakugawa, H., Kaplan, I.R. and Shepard, L.S. (1993). Measurements of H_2O_2, Aldehydes and Organic Acids in Los Angeles Rainwater: Their Sources and Deposition Rates. Atmospheric Environment. Part B, Urban Atmosphere, Vol. 27B, pp. 203-219.

Sayato, Y., Nakamuro, K. and Ueno, H. (1989). *Mutagenicity on Chlorination of Products Formed by Ozonation of Naphthoresorcinol in Water.* Mutation Res. Vol. 226, No. 3, pp. 151-155.

Schwarzenbach, R.P., Gschwend, P.M. and Imboden, D.M. *Environmental Organic Chemistry.* Wiley-Interscience, New York, 1993.

Sempéré, R. and Kawamura, R. (1994). *Comparative Distribution of Dicarboxylic Acids and Related Polar Compounds in Snow, Rain and Aerosols from Urban Atmosphere.* Atmos. Environ. Vol. 28, pp. 449-459.

Smithies, D. and Hart, E.J. (1960). *Radiation Chemistry of Aqueous Formic Acid Solutions. Effect of Concentration.* J. Am. Chem. Soc. Vol. 82, pp. 4775-4779.

Souza, S.R., Vasconcellos, P.C. and Carvalho, L.R.F. (1999). *Low Molecular Weight Carboxylic Acids in an Urban Atmosphere: Winter Measurements in São Paulo City, Brazil.* Atmos. Environ. Vol. 33, pp. 2563-2574.

Talbot, R.W., Vijgen, A.S. and Harris, R.C. (1992). *Soluble Species in the Arctic Summer Troposphere: Acidic gases, aerosols and precipitation.* J. Geophys. Res. Vol. 97, pp. 16531-16543.

Wang, H. and Adesina, A.A. (1997). *Photocatalytic Causticization of Sodium Oxalate Using Commercial TiO_2 Particles.* Applied Catalysis B: Environmental 14, pp. 241-247.

Yamamoto, S. and Back, A. (1985). *The Gas-Phase Photochemistry of Oxalic Acid.* J. Phys. Chem. Vol. 89, pp. 622-625.

Zuo, Y. and Hoigné, J. (1992). *Formation of Hydrogen Peroxide and Depletion of Oxalic Acid in Atmospheric Water by Photolysis of Iron (III)-Oxalato Complexes.* Envir. Si. Technol. Vol. 26, No.5, pp. 1014-1022.

Zuo, Y. and Hoigné, J. (1994). *Photochemical Decomposition of Oxalic, Glyoxalic and Pyruvic Acid Catalysed by Iron in Atmospheric Waters.* Atmos. Environ. Vol. 28, pp. 1231-1239.